THE UNIVERSITY
of EDINBURGH

Manganese-Catalysed Hydrofunctionalisation of Alkenes

Jonathan R. Carney

A thesis submitted for the degree of

Doctor of Philosophy

2018

Abstract

The development of new first-row transition metal catalysts as both replacements for precious metals catalysts and in the search for novel reactivity is a crucial evolution for catalysis. Manganese is a non-toxic, inexpensive and Earth-abundant metal, making it a perfect candidate for catalysis. Despite this, manganese catalysis has not undergone the same development as for other Earth-abundant metals.

The manganese-catalysed hydrosilylation and hydroboration of alkenes has been developed to give hydrofunctionalisation products in typically good yields (up to >95%) with control of regio- and chemo-selectivity. This work uses a bench-stable pre-catalyst/activator manifold allowing for a simple methodology, ideal for the non-specialist.

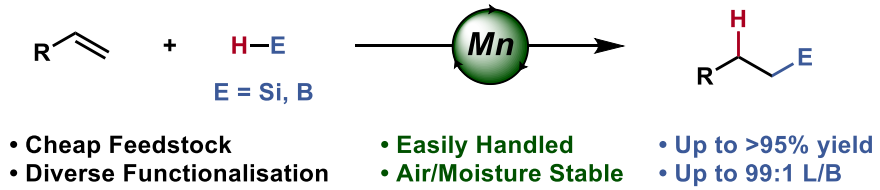

Scheme A1: Manganese-catalysed hydrofunctionalisation of alkenes.

This represents the first example of a developed methodology for the manganese-catalysed hydrosilylation of alkenes. This methodology uses a bis(imino)pyridine manganese(II) pre-catalyst which has previously been unreactive in related reactions. The critical discovery has been in the use of an alkoxide activation system which enables the generation of a catalytically-active manganese species.

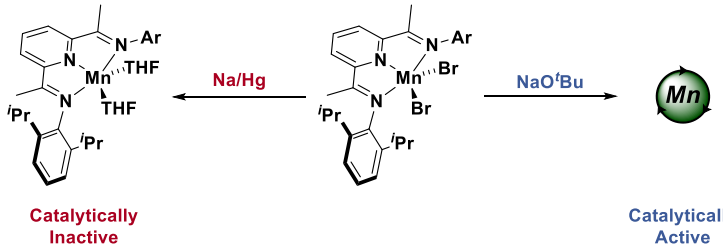

Scheme A2: Effect of activation method on the catalytically ability of the generated manganese species.

Lay Summary

A catalyst is a substance that facilitates the controlled transformation of one chemical species into another species. Crucially, the transformation would not occur under the same conditions were the catalyst not present. At the end of the transformation, the catalyst will remain unchanged from its original form, allowing for potentially limitless repetition of the process.

Catalysts are ubiquitous in modern day life; the original catalysts are found in biological systems (enzymes) but man-made (and natural) catalysts are now crucial in the production of bulk and fine chemicals (pharmaceuticals, plastics, agrochemicals) and are essential tools in sustaining our environment (catalytic converters in motor vehicles). However, precious metal catalysts (e.g. platinum, rhodium, palladium) tend to dominate in the fine chemical sector. These metals are highly efficient however they are rare, expensive and toxic to biological systems. Catalysis is widely used in dispersive technologies catalysis which renders the recapture and recycling of these metals impossible.

Therefore, the ideal catalyst consists of elements which are Earth-abundant and consequentially are inexpensive and non-toxic. Manganese is a key rock-forming element; it has been utilised by humans since Palaeolithic humankind used manganese ore as a pigment in cave paintings. The development and implementation of a broad range of selective and efficient manganese catalysts would help make chemical manufacture more sustainable and affordable. To this end we have developed manganese compounds capable of catalysing a range of transformations from which high-value products can be obtained. These discoveries will hopefully provide an entry point for future research and the development of sustainable processes that will allow for a more sustainable future.

Declaration

I certify:

a) that the thesis has been composed by myself, and

b) either that the work is my own, or, where I have been a member of a research group, that I have made a substantial contribution to the work, such contribution being clearly indicated, and

c) that the work has not been submitted for any other degree or professional qualification except as specified.

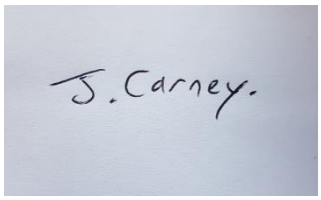

Jonathan Carney

Acknowledgements

Thanks to:

Steve: For the opportunity, for your time, patience and advice but most of all for making it such a joy.

The Group: Somewhat for enduring my mess and for always lending a hand but mostly for the gossip, the hype and the bantz.

Technical Staff: For the unthanked hours spent making my life easier. And for running the fantasy football league.

Barry/Leonie: For all your help regarding everything AZ related and beyond.

AZ Case Students: For making those winter days less bleak.

AZ/University of Edinburgh: For funding my PhD.

Mum, Dad, Beth: For 22 years of support, encouragement and nourishment that made the last 4 possible.

Elsa: For moving with me and making memories. For enduring the many highs and lows that are inevitable when ~~supporting Liverpool~~ doing a PhD.

Table of Contents

Abbreviations

Ac	Acetyl
acac	Acetylacetonate
API	Active Pharmaceutical Ingredient
Ar	Aryl
BAr^F_3	tris(3,5-bis(trifluoromethyl)-phenyl)borane
BIP	Bis(imino)pyridine
Bn	Benzyl
Bpin	4,4,5,5-Tetramethyl-1,3,2-dioxaborolane
Box	Bis(oxazoline)
Bu	Butyl
COD	1,5-Cyclooctadiene
COT	1,3,5,7-Cyclooctatetraene
COE	Cyclooctene
COSY	Correlation spectroscopy
Cp	Cyclopentadienyl
Cy	Cyclohexyl
DCT	Dibenzo[*a,e*]cyclooctatetraene
DIPP	Di*iso*propylphenyl
DMAP	4-Dimethylaminopyridine
DMF	*N*,*N*-Dimethylformamide
DMSO	Dimethyl sulfoxide
dpm	tris(2,2,6,6-tetramethyl-3,5-heptanedionato)
dppe	1,2-Bis(diphenylphosphino)ethane
dr	Diastereomeric ratio
E	Element
ee	Enantiomeric excess
equiv.	Equivalents
ESI	Electrospray ionisation
Et	Ethyl
EWG	Electron-withdrawing group
GCMS	Gas chromatography mass spectrometry
HAT	Hydrogen Atom Transfer
HMDS	Bis(trimethylsilyl)amide

HPLC	High performance liquid chromatography
HRMS	High resolution mass spectrometry
HSQC	Heteronuclear single quantum coherence
ICP-MS	inductively coupled plasma mass spectroscopy
IR	Infrared
IP	Imino(pyridine)
J	Coupling constant in Hz
L	Ligand
m.p.	Melting point
M	Metal
MD'M	1,1,1,3,5,5,5-heptamethyltrisiloxane
Me	Methyl
Mes	Mesityl
NHC	*N*-heterocyclic carbene
NMP	*N*-methylpyrrolidine
NMR	Nuclear magnetic resonance
Ph	Phenyl
Pr	Propyl
py	Pyridine
Rf	Retention factor
r.t.	Room temperature
TBAF	Tetrabutylammonium fluoride
TEMPO	2,2,6,6-tetramethylpiperidin-1-yl)oxyl
Terpy	Terpyridine
Tf	Trifluoromethanesulfonyl
THF	Tetrahydrofuran
TMEDA	*N*,*N*,*N*',*N*'-Tetramethylethylenediamine
TOF	Turnover frequency
TON	Turnover number
Ts	*para*-Toluenesulfonyl
UV	Ultraviolet

1. Introduction

The use of catalysts is a cornerstone in the movement towards greener and more sustainable synthesis. To achieve sustainable synthesis, chemists must address the prevention of waste by using highly atom-economic and selective processes.[1] In this respect, hydrofunctionalisation is an ideal reaction. It is, theoretically, a 100% atom-economic approach to the formation of carbon–heteroatom (e.g. hydrosilylation, hydroboration) and carbon–carbon bonds (hydroformylation, hydrovinylation). Hydrofunctionalisation has been reported using a variety of transition-metal catalysts but has most commonly used platinum group metal catalysts. In particular, the hydrofunctionalisation of olefins is a highly useful reaction, as olefins are readily available, diversely functionalised and the construction of carbon–carbon bonds has always been highly prized.[2,3]

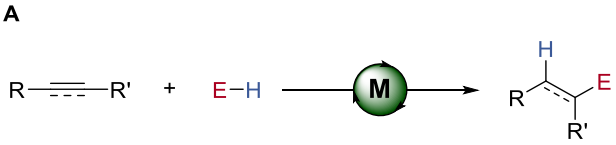

Scheme 1.1 Overview of the hydrofunctionalisation of olefins.

A hydrofunctionalisation reaction is defined by the addition of a hydrogen atom and another moiety, 'E' which can be either electrophilic or nucleophilic, across an unsaturated bond (Scheme 1.1 A). The nature of 'E' defines the type of hydrofunctionalisation reaction. The most versatile type of hydrofunctionalisation is when 'E' is electrophilic (e.g. hydrosilylation, hydroacylation, hydroboration). Hydrofunctionalisation reactions typically use a precious metal catalyst. This somewhat negates the sustainability of the hydrofunctionalisation process and is an area which can be improved. Whilst developments have been made towards recycling precious metal catalysts, an ideal solution would be the use of abundant, cheap and low-toxicity metals.

Hydrofunctionalisation have many important industrial applications. Hydroformylation is a vital reaction for the conversion of low-value hydrocarbons into aldehydes which are valuable chemical precursors.[4] Hydrosilylation is one of the largest uses of homogeneous catalysis and is particularly important for the synthesis of cross-linked silicone polymer chains.[5,6] The synthesis of Nylon 66 (the second most common Nylon polymer) requires consecutive hydrocyanation reactions which are catalysed by a nickel compound.[7,8]

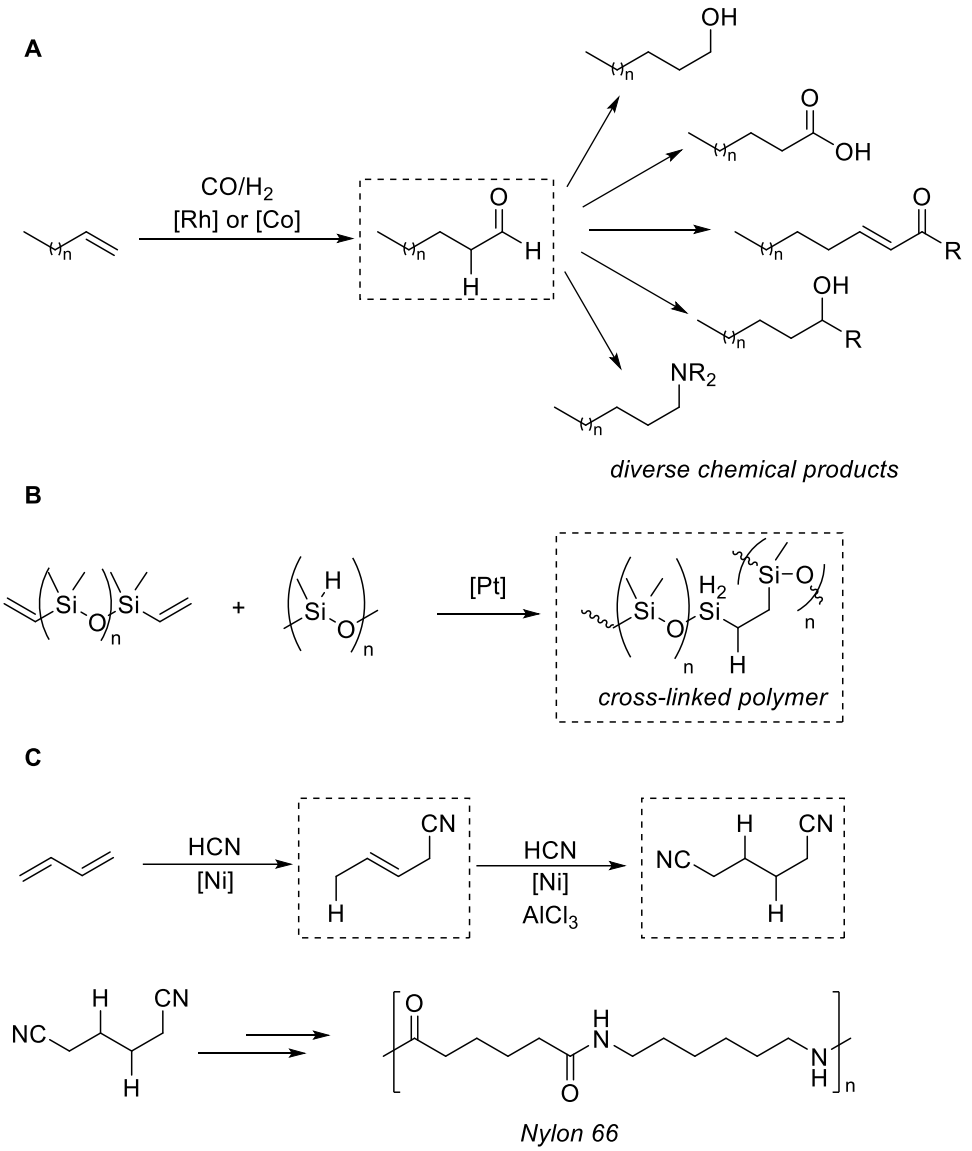

Scheme 1.2 The utility of a range of hydrofunctionalisation reactions. A) Hydroformylation to form an aldehyde from low-value hydrocarbons. B) Hydrosilylation to form cross-linked silicone polymers. C) The use of hydrocyanation in the synthesis of Nylon 66.

1.1 Alkene Hydrosilylation

The hydrosilylation of olefins is essential in a myriad of sectors such as healthcare,[9] construction,[5] cosmetics[10,11] and agriculture.[12] Platinum is widely used to catalyse the hydrosilylation of olefins on industrial scale. [5,6,12,13] The first significant platinum catalyst was hexachloroplatinic acid (Speier's catalyst) which was found to be highly active and selective.[14] A second generation platinum catalyst was reported by Karstedt which displayed improved activity and selectivity and has been an industry benchmark since.[6,15] However, in 2008 it was estimated that the hydrosilylation industry consumes 5.6 tonnes of platinum a year.[13] Recycling of the platinum catalyst is non-trivial. In the production of silicone polymers, the catalyst can become immobilised within the crosslinked product and as this is a dispersive technology the waste is impossible to collect.[6] Therefore, the discovery of inexpensive, low-toxicity catalysts is an important challenge for the hydrosilylation industry.

The minimisation of waste by-products (for instance regio and stereoisomers) is a crucial aspect of sustainable synthesis. Highly selective processes eliminate waste and can make energy intensive purification methods simpler. Platinum-catalysed hydrosilylation reactions typically generate a range of side products.[16] Regioselectivity of the hydrosilylation product can vary between the *anti*-Markovnikov product and the Markovnikov product but platinum-catalysed hydrosilylation reactions typically exhibit *anti*-Markovnikov selectivity. Additional by-products can originate from dehydrogenative silylation, alkene isomerisation, hydrogenation and over-addition processes (Scheme 1.3).

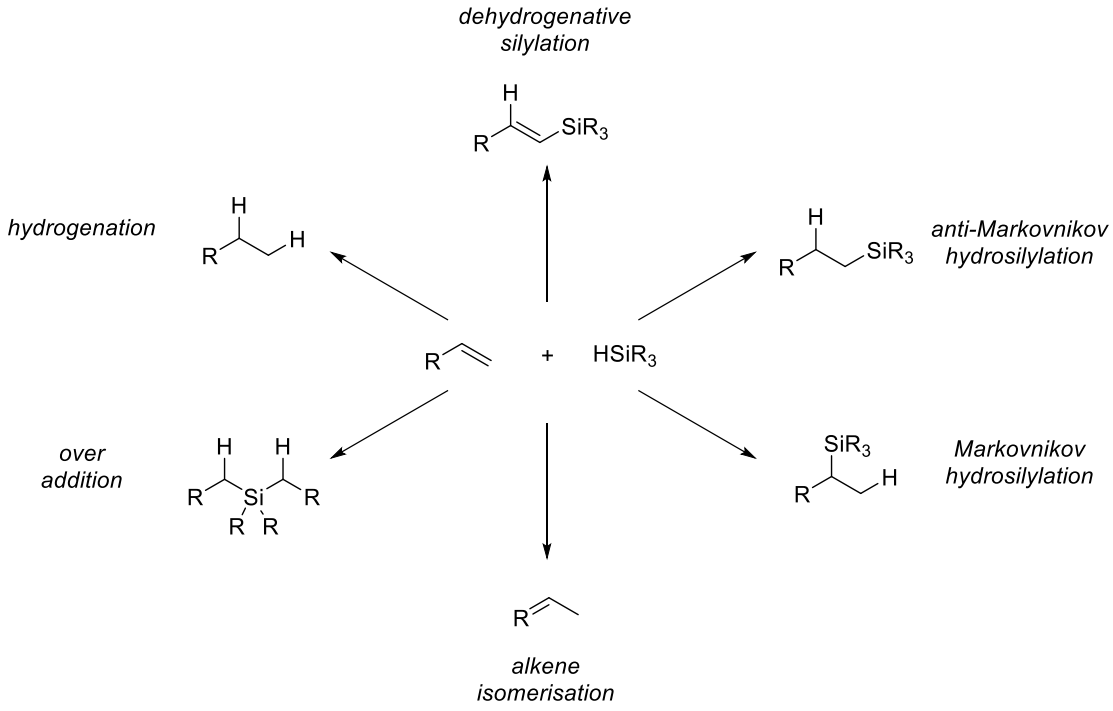

Scheme 1.3 An overview of the potential products and by-products from the hydrosilylation of alkenes

The first detailed mechanistic report into the hydrosilylation of alkenes was described by Chalk and Harrod in 1965,[17] in which the mechanism of olefin hydrosilylation using a range of preformed platinum(II) and iridium(I) complexes was investigated. The proposed mechanism, known as the 'Chalk-Harrod' mechanism, has long been accepted to be correct (Scheme 1.4).[18] It was proposed that silane oxidative addition would be followed by alkene coordination to the metal centre to give the metal-olefin complex **C**. This would be followed by hydrometallation of the alkene to give the alkyl-metal species **D** and then carbon-silicon bond forming reductive elimination. An alternative mechanism also exists, known as the 'modified Chalk-Harrod' mechanism.[19] In this mechanism upon formation of intermediate **C**, insertion of the alkene into the M–[Si] bond occurs, a process known as silylmetalation to give intermediate **F**. This is followed by carbon–hydrogen bond forming reductive elimination.

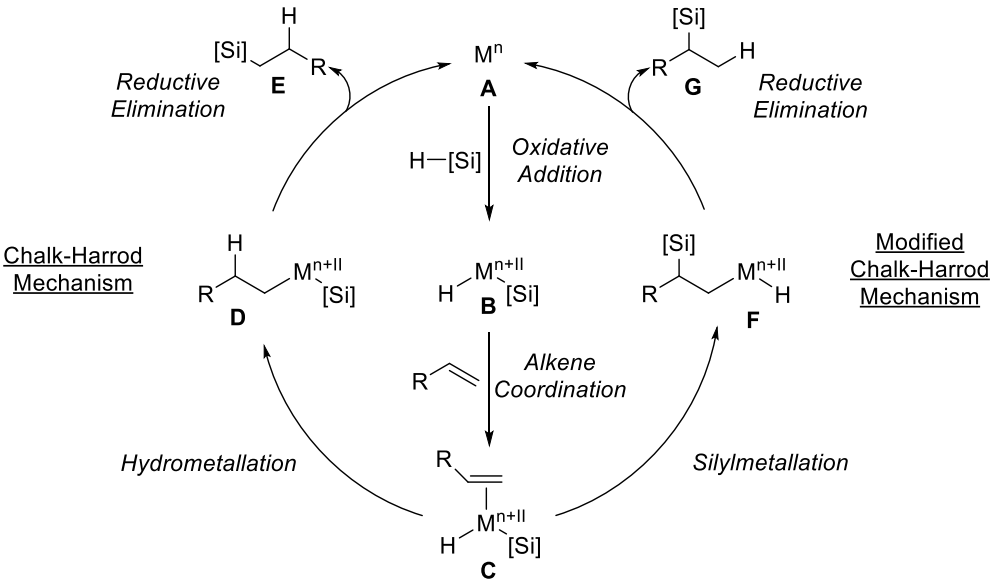

Scheme 1.4 The Chalk-Harrod and Modified Chalk-Harrod mechanisms.

1.1.1 Development of Platinum Catalysts for Hydrosilylation of Alkenes and Alkynes

Platinum-catalysed hydrosilylation was first reported in a patent by Wagner and co-workers.[20] It showed that platinum deposited on powdered charcoal could catalyse the hydrosilylation of acetylene **1** at high pressures and temperatures to give the vinylsilane product **2** and the bis hydrosilylation product **3** (Table 1.1, Entry 1).

Table 1.1 Discovery of solid-supported platinum catalysts in the hydrosilylation of acetylene

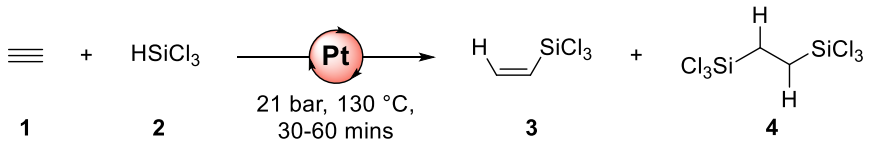

1 **2** **3** **4**

Entry	Catalyst	Catalyst Loading (mol%)	Yield of H-Si (%)	Yield of Bis H-Si (%)
1	5% Pt on powdered charcoal **5**	0.004	75	25
2	0.77% Pt on powdered charcoal **6**	$6x10^{-4}$	60	12.5
3	5% Pt on powdered $CaCO_3$ **7**	0.004	Trace	Trace
4	5% Pt on powdered asbestos **8**	0.004	Trace	Trace

This was followed by Speier's report that H_2PtCl_6 **14** was a highly active catalyst for the hydrosilylation of alkenes.[14] It showed that very small loadings of platinum would catalyse the hydrosilylation of 1-pentene, 2-pentene and cyclohexene in high yields over short reaction times (Table 1.2, Entry 4).

Table 1.2 The hydrosilylation of pentene by different platinum species

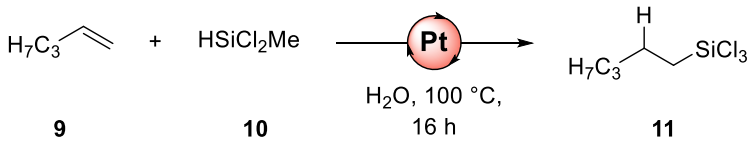

9 **10** **11**

Entry	Catalyst	Catalyst Loading (mol%)	Yield of H-Si (%)
1	K_2PtCl_4 **12**	0.05	65
2	K_2PtCl_4 **12**	2.5	>95
3	Pt-black **13**	12.5	92
4	H_2PtCl_6 **14**	0.0005	93[a]
5	0.06% Pt/C **15**	0.002	84

[a]Reaction time is 30 minutes.

Whilst Speier's catalyst revolutionised the hydrosilylation industry, providing access to a range of poly(siloxane) products, it suffered from catalyst-poisoning, which led to the formation of by-products.[15] Therefore, a range of methods designed to stabilise the low-valent platinum centre were developed. Ashby reported a platinum-olefin complex[21] whilst Lamoreaux reported that when hexachloroplatinic acid was reacted with alcohols, ethers or aldehydes the resulting, undefined platinum catalyst was more catalytically active and more easily recycled than hexachloroplatinic acid.[22] Karstedt's report of a platinum-siloxane catalyst was a major advance for catalyst activity and it remains the benchmark for catalyst activity.[6,15] Karstedt's original report was of a catalytically active solution rather than of a defined catalyst (Scheme 1.5A). Hitchcock *et al.* synthesised platinum species **17** from $Pt(cod)_2$ **18** and 1.5 equivalents of tetramethyldivinylsiloxane **16** and were able to determine the structure by X-ray crystallography (Scheme 1.5B).[23] An NMR comparison between this isolated species and the catalytically active solution (formed from Speier's catalyst) indicated the two species were similar enough to assume that platinum species **17** is largely responsible for the catalytic activity of the solution reported by Karstedt.

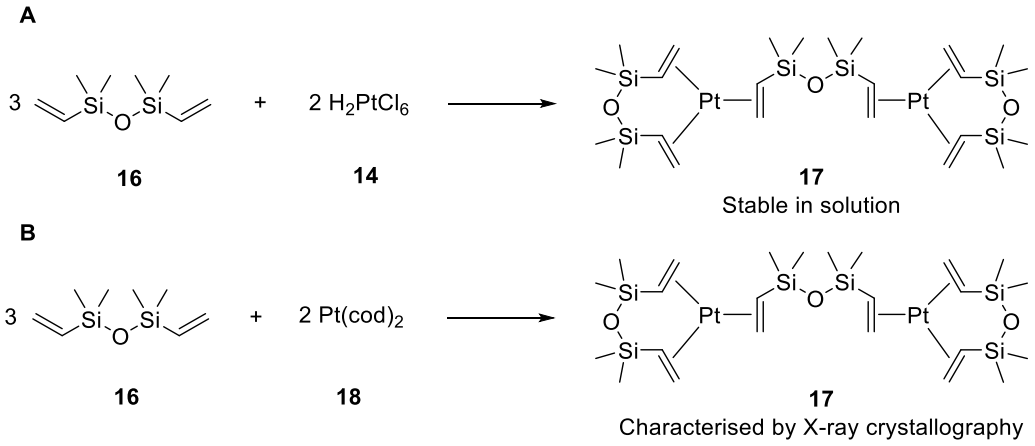

Scheme 1.5 Synthesis of Karstedt's catalyst **17** from different precursors

Mechanistic studies suggest that Karstedt's catalyst operates by a Chalk-Harrod mechanism. Despite the high amounts of platinum black formed in the reaction and a long induction period, sufficient evidence exists to suggest that Karstedt's catalyst operates in a homogeneous manner.[24] The degradation of Karstedt's catalyst to platinum black is thought to be responsible for the high proportion of side products observed in the reaction.[25,26] The incorporation of oxygen into the reaction mixture is known to aid catalysis as oxygen disrupts the formation of platinum colloids and therefore allows for the hydrosilylation of poorly-coordinating olefins.[24] The induction period exists because the vinyl siloxane ligands coordinated to the pre-catalyst are required to undergo hydrosilylation and/or ligand exchange with the substrate prior to catalysis. Steffanut *et al.* reported that the substitution of one of the vinyl siloxane ligands in Karstedt's catalyst with an electron-deficient napthoquinone ligand led to rate enhancements and increased catalyst stability (Scheme 1.6A).[27]

A final development was the replacement of a vinyl siloxane ligand with a σ-donor type ligand such as a phosphine or a carbene.[25] The carbene ligated complexes were found to be extremely stable and gave increased selectivity for the hydrosilylation product **25**. The hydrosilylation product of octene was isolated in a 96% yield when catalysed by platinum carbene complex **24**, whilst Karstedt's catalyst **17** only gave a 78% yield due to the formation of unwanted by-products. Increased functional group tolerance was also reported, particularly for alcohols and epoxides.

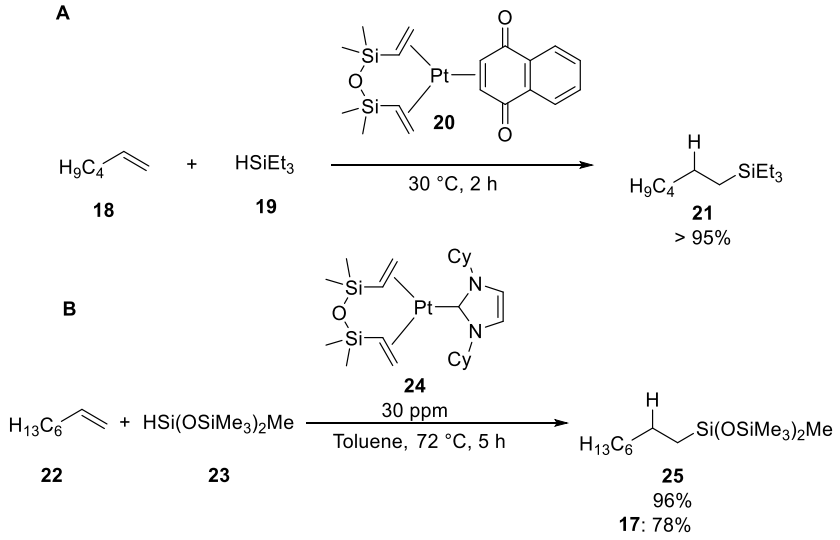

Scheme 1.6: A) The utilisation of a napthoquinone ligated platinum catalyst **20** to increase the selectivity of alkene-hydrosilylation. B) A comparison of the hydrosilylation of 1-octene catalysed by Karstedt's catalyst **17** and a carbene derivative **24**.

1.1.2 First-row Transition Metals as Catalysts for Alkene Hydrosilylation

In a society increasingly conscious of its own impact on the environment, sustainable approaches to existing technologies are urgently required. Within the context of hydrosilylation, this desire for change is heightened by the high and volatile price of platinum and immobilisation of the catalyst within cross-linked products. Platinum group metals are sourced in only a few locations meaning supply can be unreliable.[28,29] Consequently, the replacement of rare, toxic and expensive metals by inexpensive, benign and readily available alternatives in catalysis has been a rapidly developing area of research since the turn of the millennium.

The first-row of the transition metals contains elements that are up to one million times more abundant than the precious metals of the second- and third-row.[30] The abundance of these metals has meant that in many cases, nature has evolved to utilise them in its biological functions. A key step in photosynthesis utilises a manganese photocatalyst[31] and iron-heme complexes are essential for human life.[32] Accordingly, residual iron traces allowed in active pharmaceutical ingredients (API's) are one hundred times greater than for that of the platinum group metals.[33]

Some of the most studied first-row transition metals for catalysis are nickel and cobalt. Nickel has been used extensively as a more abundant replacement for palladium in cross-coupling reactions.[34–38] Similarly, cobalt has been used as an alternative to rhodium for hydroformylation.[4,39] Cobalt catalysts have displayed a diverse range of reactivity in olefin hydrosilylation reactions.[40] There have been numerous reports of cobalt-catalysed *anti*-Markovnikov hydrosilylation,[41–48] Markovnikov hydrosilylation[41,49–52] and dehydrosilylation of alkenes.[53] Additionally, the cobalt-catalysed hydrosilylation of alkynes to give (*E)*-vinylsilanes,[54,55] (*Z)*-vinylsilanes[56,57] and α-vinyl silanes[58,59] is well established. Likewise, there are multiple reports investigating the nickel-catalysed *anti*-Markovnikov hydrosilylation,[60–67] Markovnikov hydrosilylation[68,69] and dehydrosilylation of alkenes.[70] However, nickel and cobalt are significantly less abundant than other first row metals such as iron, titanium and manganese and are significantly more toxic than iron, manganese and copper.[30,71,72] They therefore do not present a complete solution to the issues created by platinum.

1.1.3 Iron-Catalysed Alkene Hydrosilylation

Iron is the most abundant transition-metal and is incorporated in many biological systems. It is therefore viewed as an excellent candidate for sustainable catalysis. Accordingly, iron has undergone a renaissance in use as a catalyst.[73,74] In addition to cross-coupling and hydrogenation, a significant portion of this research has been dedicated towards the iron-catalysed hydrosilylation of carbonyls and olefins.

Nesmeyanov *et al.* demonstrated that iron pentacarbonyl could catalyse the hydrosilylation of alkenes at high temperatures to make alkyl silane and alkenyl silane products.[75] The selectivity between the two products was poor and unpredictable. Additionally, it was proposed that the alkene of the substrate was also acting as a hydrogen acceptor to give the alkane product (as a byproduct of dehydrogenative silylation). This methodology was further investigated by Wrighton and Schroeder who used UV irradiation to force dissociation of carbonyl ligands and create co-ordinately unsaturated iron species.[19,76]

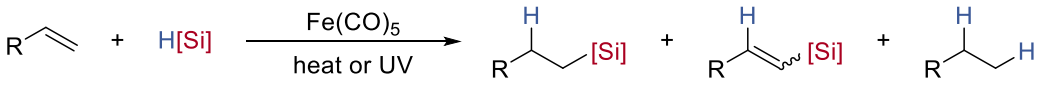

Scheme 1.7 General overview of iron carbonyl-catalysed hydrosilylation of alkenes.

The formation of alkneyl silane products led Wrighton to propose the modified Chalk-Harrod mechanism (Scheme 1.8). [19,77–80] The formation of an active catalyst **G** was proposed to occur by the liberation of two molecules of carbon monoxide from iron pentacarbonyl **A**. This would then undergo silylmetallation to give intermediate **H**. At this point C–H reductive elimination could occur to give intermediate **L**. Alternatively, β-hydride elimination could occur from the alkyl silane to give an iron dihydride intermediate **I**. Ligand exchange of the olefinic ligand would give alkenyl silane, the dehydrosilylation product. Hydrometallation of the newly coordinated alkene (from intermediate **J**), followed by a metathesis-type reaction with another hydrosilane molecule would give an alkane, the hydrogenation product, and iron hydride species **L**.

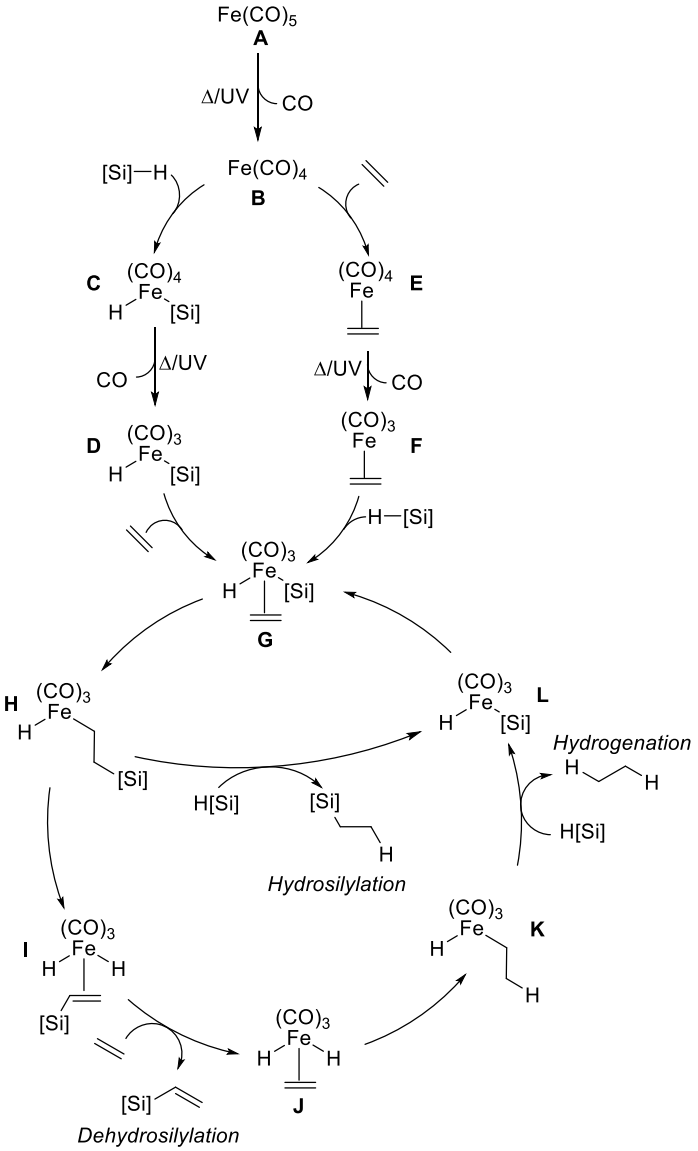

Scheme 1.8 Wrighton's proposed activation of $Fe(CO)_5$ and the modified Chalk-Harrod mechanism that leads to the production of dehydrosilylation and hydrogenation products.

Iron carbonyl clusters have also been used to catalyse olefin hydrosilylation. Kakiuchi *et al.* reported the use of $Fe_2(CO)_9$ **28** and $Fe_3(CO)_{12}$ **29** to selectively give the dehydrosilylation product in the hydrosilylation of styrenes (Scheme 1.9A).[81] This reaction occurred at lower temperatures than previous reports using $Fe(CO)_5$, which was inactive under the reported conditions. Naumov *et al.* reported that the iron carbonyl compound $CpFe(CO)_2Me$ **31** would catalyse the dehydrosilylation of divinylsiloxanes using a range of hydrosilanes at 80 °C (Scheme 1.9B).[82] Nagashima and co-workers

reported that the hydrogenation and hydrosilylation of alkenes was catalysed by an iron disilyl dicarbonyl compound.[83]

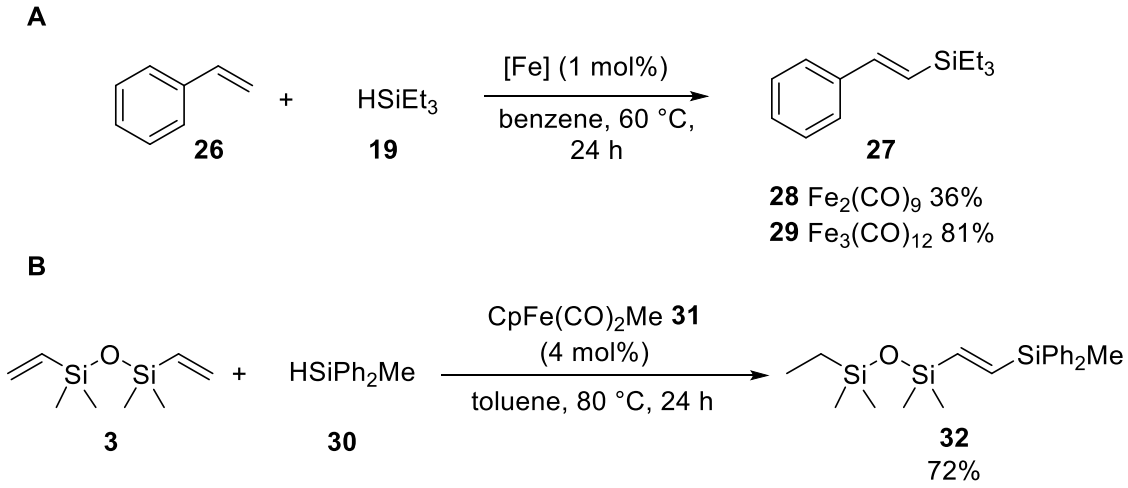

Scheme 1.9 A) Hydrosilylation of styrene **26** catalysed by iron carbonyl cluster compounds. B) Hydrosilylation of divinylsiloxane catalysed by $CpFe(CO)_2Me$ **31**

Using strong field carbonyl ligands results in the formation of catalytically-active low-spin iron species. However, these methodologies are limited by the need for high temperatures or near-constant photoirradiation to generate active catalyst. The use of multiple carbonyl ligands leads to saturation of the metal coordination sphere, limiting the addition of ligands that can exert an influence on the selectivity and reactivity of the catalyst. Additionally, the liberation of carbon monoxide makes these methodologies undesirable. Alternative methods of controlling the spin-state of iron would allow for the design of more sophisticated catalysts. In particular, the use of redox non-innocent ligands allows stabilisation of low oxidation-state iron centres.

Chirik and co-workers reported that reduced iron bis(imino)pyridine (BIP) complexes were highly active for the hydrogenation and hydrosilylation of a range of olefins.[84] The complexes were synthesised by reduction of iron(II) chloride and bromide precursors using a sodium/mercury amalgam to give the formally Fe(0) complexes (Scheme 1.10A). The reduced species were found to bear a diradical on the ligand which was antiferromagnetically coupled to the metal center.[85–87] The hydrosilylation of monosubstituted and 1,2-disubstituted alkenes occurred rapidly at room temperate with as little as 0.3 mol% of catalyst **34** (Scheme 1.10B). The hydrosilylation of an

internal alkyne, diphenylacetylene gave the alkenyl silane product also proceeded in a quantitative yield.

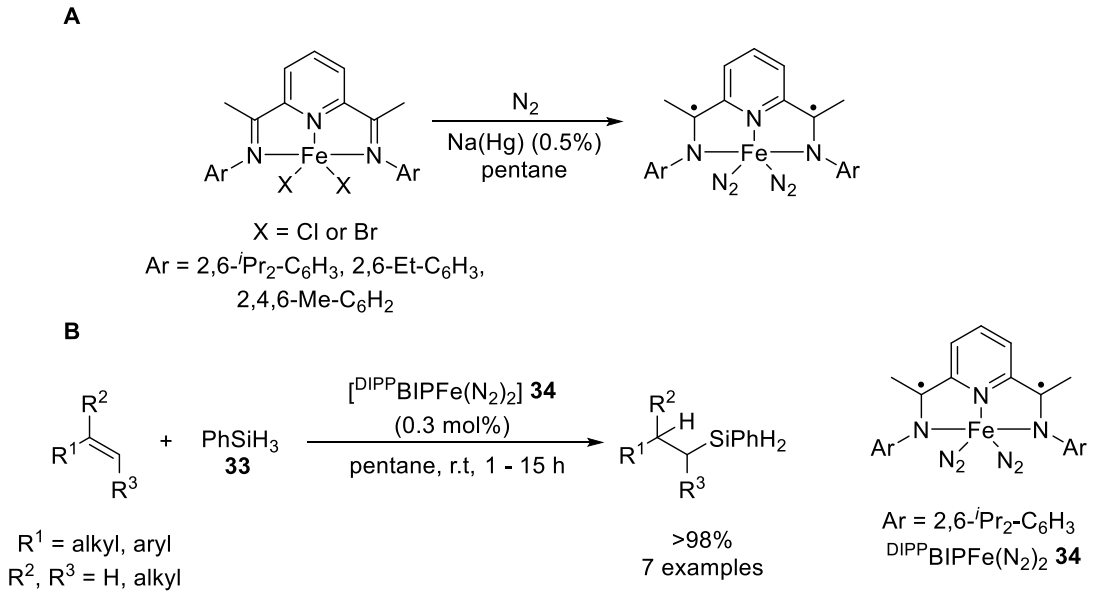

Scheme 1.10 A) The reduction of bis(imino)pyridine iron(II) precursors B) The hydrosilylation of a range of alkenes catalysed by the reduced bis(imino)pyridine iron species.

Attempts to synthesise related compounds bearing smaller *N*-aryl substituents (for instance 2,6-dimethylphenyl) led to the formation of $^{Me}BIP_2Fe$ **36** which was catalytically inactive (Scheme 1.10A). Using sodium napthalenide as the reductant led to the formation of iron dimers, bridged by a μ_2-N_2 ligand **37**.[88] It was found that BIP complexes bearing sterically smaller *N*-aryl substituents were more active for the hydrosilylation of alkenes and $(^{Me}BIPFe)_2N_2$ was capable of operating with a turnover number (TON) up to 100 000 mol h^{-1} (Scheme 1.10B).[89] Notably, these catalysts were also compatible with tertiary silanes, allowing access to a range of industrially important products. These reactions were also highly regioselective for the *anti*-Markovnikov product.

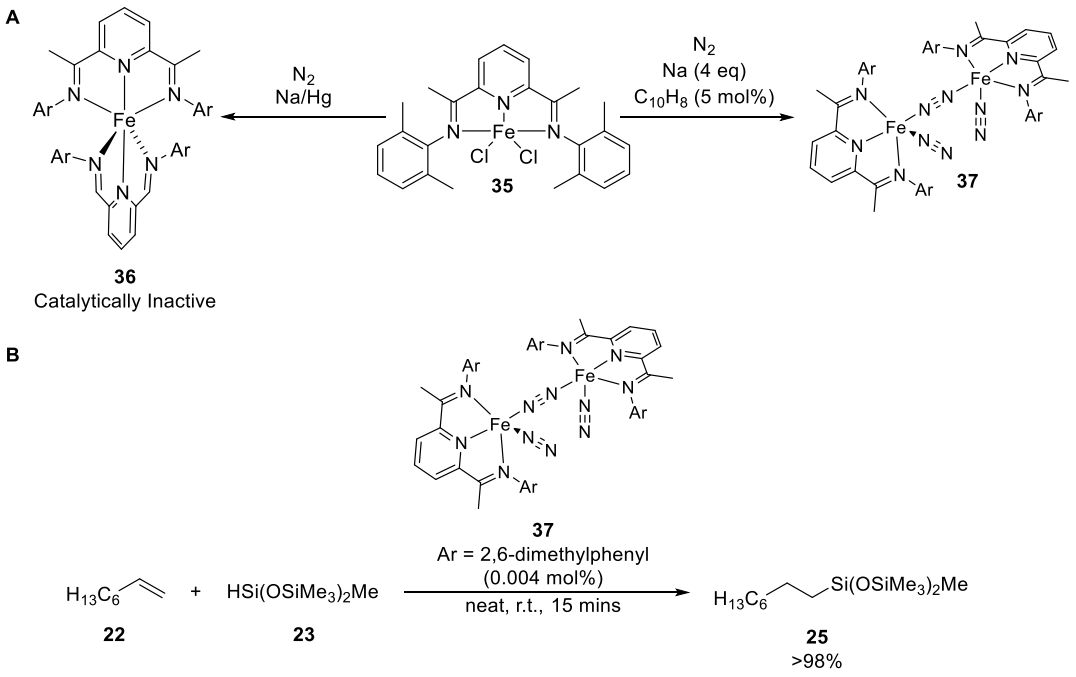

Scheme 1.11 A) Reduction of bis(imino)pyridine iron(II) precursors **35** with different reducing agents. B) hydrosilylation of octene **22** catalysed by highly active iron dimer species **37**.

Despite the high activity and selectivity of the pre-formed iron(0) bis(imino)pyridine complexes they are highly air- and moisture-sensitive. This makes them unsuitable for large-scale use and the synthesis is beyond the capabilities of a non-expert. As a result, substantial work has gone into the exploration of *in situ* activation of bench-stable iron(II) precursors. This typically involved the addition of stoichiometric, with respect to catalyst, quantities of an organometallic reagent which can act as a hydride source.

The Thomas group have reported the hydrosilylation of alkenes using ^{Et}BIPFeCl$_2$ **38** as a pre-catalyst (Scheme 1.12A).[90,91] The pre-catalyst was formed *in* situ from the free ligand and $FeCl_2$ and the complex was then activated *in situ* using EtMgBr. This is proposed to occur by transmetalation of the ethyl group, from magnesium to iron, to give an iron(II) dialkyl intermediate **39**. This intermediate can then undergo β-hydride elimination, to eliminate ethene and give an iron(II) hydride ethyl intermediate **40**. This was proposed to reductively eliminate ethane and form a reduced iron species **41** (Scheme 1.12B). The use of tolylmagnesium bromide, which cannot undergo β-hydride elimination, still gave an active catalyst occurring by direct reductive elimination of bitolyl **43**. The amount of bitolyl formed was equivalent to the formation of an iron(I) active catalyst (Scheme

1.12C). Additionally, the most thorough substrate-scope of iron bis(imino)pyridine catalysed hydrosilylation at the time was reported. This found the reaction conditions were tolerant of amine, amido, imino, pyridine, ester and ketone functionalities.

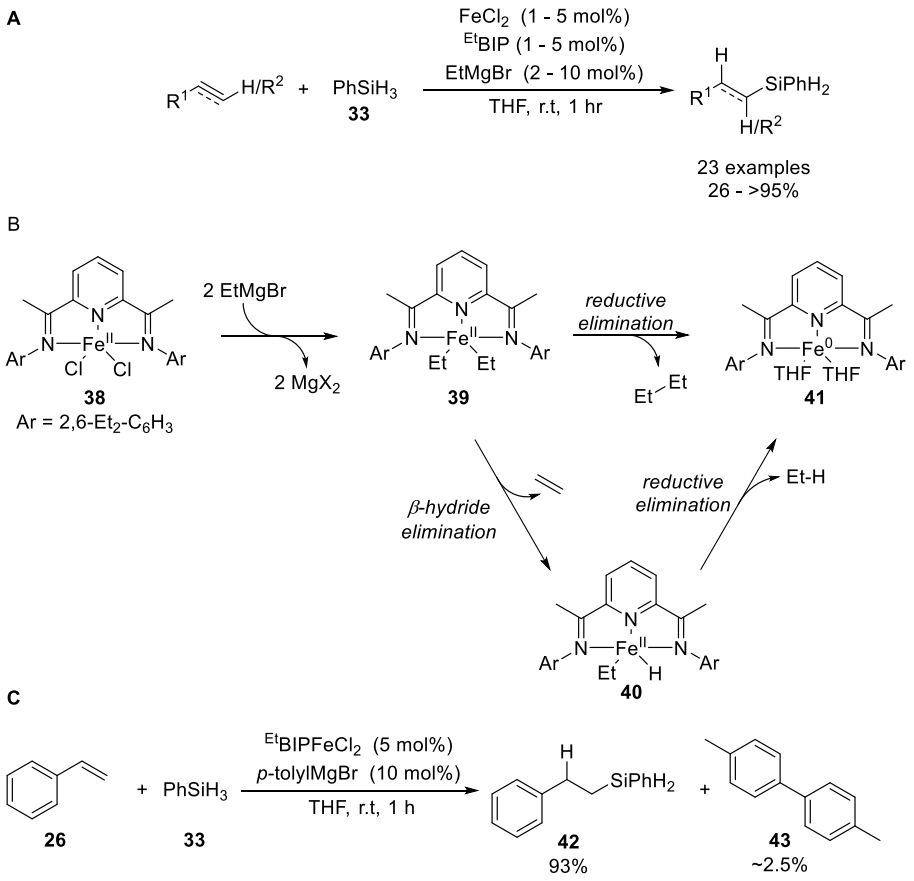

Scheme 1.12 A) General overview of the hydrosilylation of olefins catalysed by an air-stable iron(II) pre-catalyst. B) Proposed route of iron(II) reduction. C) Reduction using tolylmagnesiumbromide

This work was developed further by the discovery of air- and moisture-stable activation platforms to assist the easy implementation of iron-catalysed olefin hydrosilylation. Challinor *et al.* reported that ^{Et}BIPFe(OTf)$_2$ **44** with the tertiary amine Hunig's base **45**, was capable of catalysing alkene hydrosilylation (Scheme 1.13A).[92] The use of the weakly coordinating triflate counterion was shown to be crucial for catalysis to occur. Notably the bench-stable reagents, paired with the high catalyst activity, allowed for the hydrosilylation of octene **22** to occur under air. More recently, Thomas and co-workers reported the use of the bench-stable alkoxide salt NaO^tBu **49** as a generic activation platform for a range of Earth-abundant metals used to catalyse a range of

transformations, including hydrosilylation and hydroboration (Scheme 1.13B).[42] The activation was proposed to proceed through the *in situ* generation of hypervalent siliconate and boronate species. The transmetalation of hydrides to the transition metal would then lead to a reductive elimination event and the production of a formally reduced, low oxidation-state species (Scheme 1.13C).

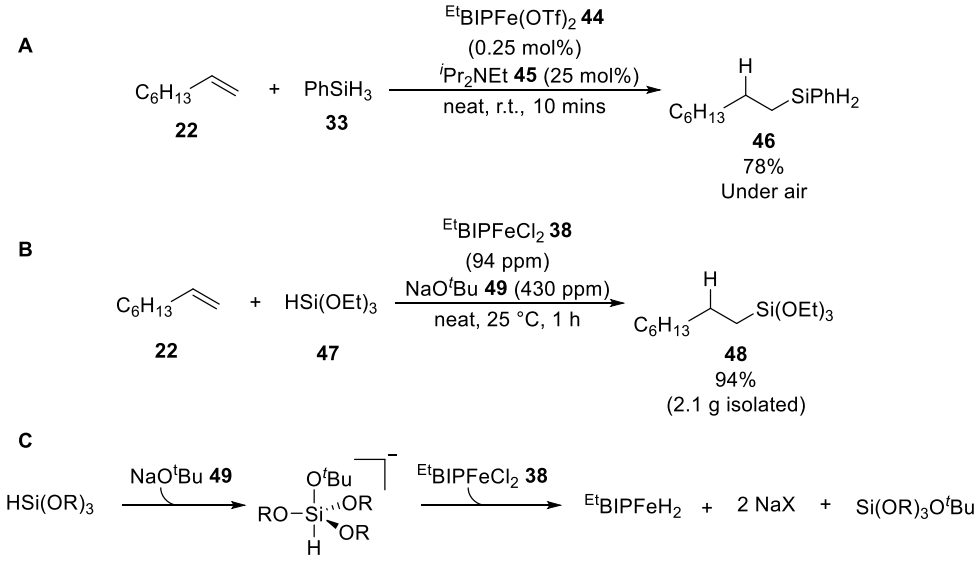

Scheme 1.13 A) The use of an amine to activate an iron(II) triflate precatalyst. B) The use of NaO*t*Bu to activate ^{Et}BIPFeCl$_2$ to catalyse the hydrosilylation of octene. C) The proposed activation route for NaO*t*Bu.

Lam *et al.* published a computational analysis of the iron bis(imino)pyridine hydrosilylation of alkenes.[93] They proposed a modified Chalk-Harrod mechanism in which the rate-determining step was hydride transfer directly from the hydrosilane into the coordinated alkene.

Bis(imino)pyridine ligands have led to the development of a range of bi-, tri- and tetradentate ligands being used in hydrosilylation processes. Nakazawa and co-workers reported that iron terpyridine complexes, activated *in situ* by NaHBEt$_3$, were active for the hydrosilylation of unfunctionalized aliphatic alkenes (Scheme 1.14A).[94] This was swiftly followed by the Chirik group reporting that terpyridine and bis(imino)pyridine iron dialkyl species were active for the hydrosilylation of alkenes.[95] Notably, the high-spin terpyridine iron(II) alkyl species was used to catalyse the hydrosilylation of industrially relevant vinylcyclohexene oxide **51** by MD'M **23** giving high yields and

complete control of selectivity (Scheme 1.14B). This is analogous to the carbene-substituted derivatives of Karstedts catalyst (see section 1.1.1).[25]

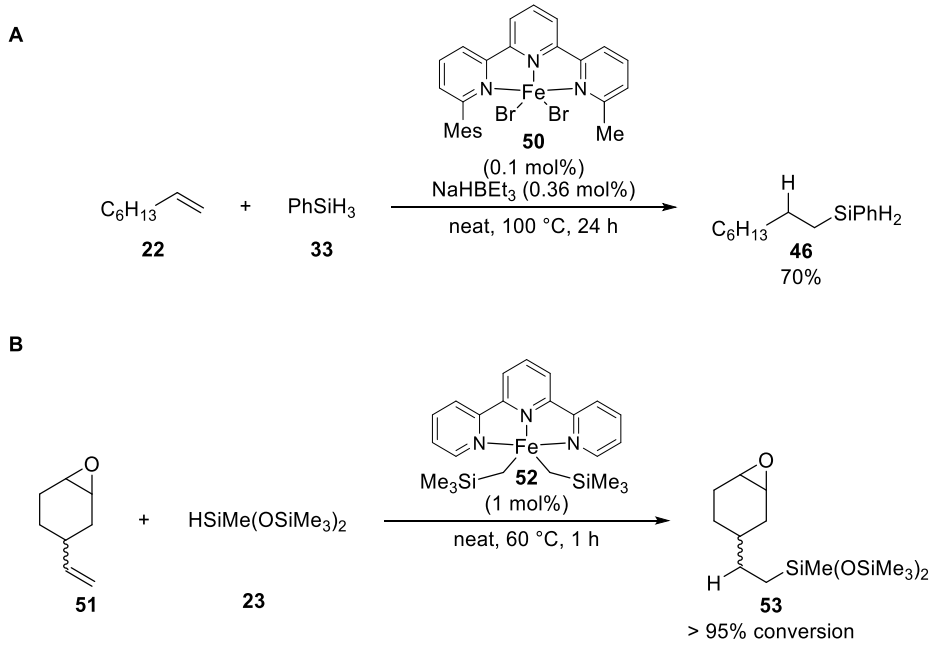

Scheme 1.14 A) Hydrosilylation of heptene catalysed by an *in situ* activated terpyridine iron catalyst B) Hydrosilylation of vinylcyclohexene oxide catalysed by a terpyridine iron dialkyl species.

Huang and Walter reported a highly chemoselective iron-catalysed methodology for the hydrosilylation of alkenes (Scheme 1.15).[96] This used a phosphinite-iminopyridine (PNN) iron complex **54** that was activated *in situ* at -37 °C by sodium triethylborohydride. Notably they reported the hydrosilylation of the alkene functionality of 1-hexen-5-one **61** by diphenyl silane **62** with complete control of chemoselectivity. Previous reports by Chirik[97] using ^{DIPP}BIPFe$(CH_2SiMe_3)_2$ **59** and Tilley[98] using $Fe(HMDS)_2$ **58** had shown chemoselectivity for reduction of the carbonyl **63**. Thomas had previously reported that the hydrosilylation of 5-hexen-2-one **61** by phenylsilane **33** gave a mixture of both products but predominately the alkylsilane product **64**.[90] Huang demonstrated that a crucial parameter for the chemoselectivity of both the BIP and PNN iron catalysts was the steric bulk of the catalyst as ligands substituted with smaller *N*-aryl substituents demonstrated more chemoselectivity for alkene hydrosilylation over carbonyl hydrosilylation. Additionally, spectroscopic measurements showed that the phosphinite-iminopyridine iron complex was more electron-rich than the iron complex ligated by bis(imino)pyridine. It was proposed that

the increased electron density of PNNFe would give a larger binding affinity to the olefin functionality due to more favourable π-backbonding interactions, explaining the high chemoselectivity of PNNFe.

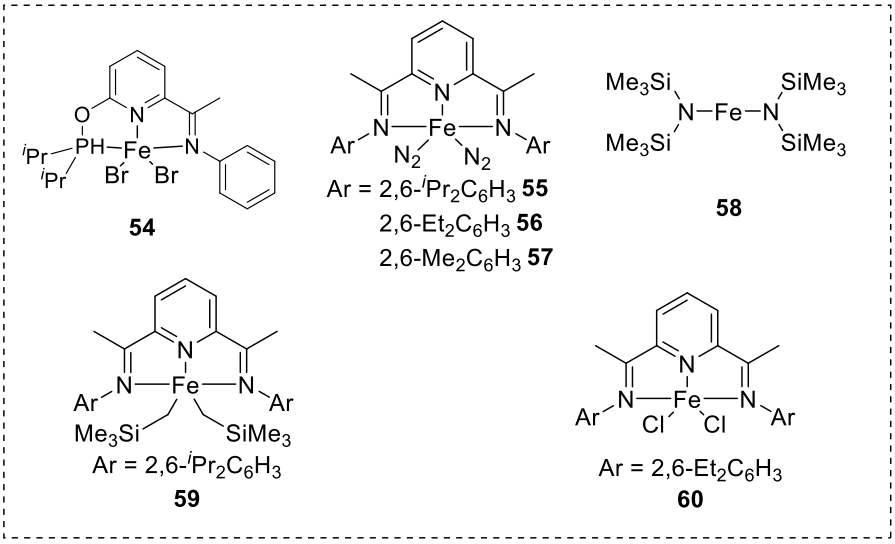

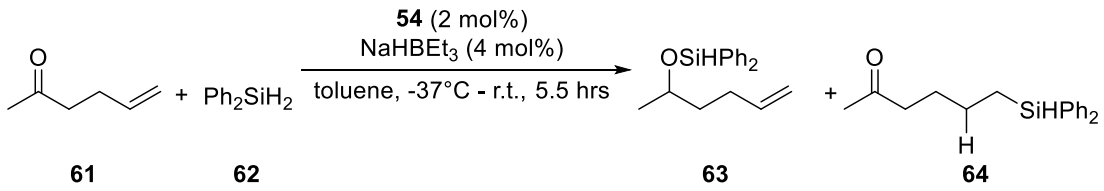

	63	64
54	0%	86%
55	<5%	23%
56	<5%	16%
57	50%	12%

Literature Precendents

Tilley **58** (1 mol%):	95%	0%
Chirik **59** (1 mol%):	75%[a]	0%
Thomas **60** (3 mol%) + EtMgBr:	14%[a]	57%[b]

Scheme 1.15 The hydrosilylation of 1-hexen-5-one by a range of catalysts. [a] Alcohol product isolated. [b] Using phenylsilane

Huang and co-workers developed a phosphine-iminopyridine ligand system which displayed regiodivergence for alkene hydrosilylation depending on the metal used.[51] Iron pre-catalysts **67** selectively gave the *anti*-Markovnikov product **46** whilst cobalt pre-catalysts **66** gave the Markovnikov product **65** (Scheme 1.16). By replacing the oxygen tether in the phosphinite-iminopyridine iron complex **54** with a carbon atom, the active catalyst was found to have greater stability which was demonstrated by a higher

TON. It was proposed that the iron-catalysed method proceeded by a Chalk-Harrod mechanism. They propose the regiodivergence stems from the cobalt-catalysed reaction following a deviation from the modified Chalk-Harrod mechanism. The suggested mechanism includes silylmetalation of the alkene, followed by a σ-bond metathesis-type interaction between hydrosilane and the alkylcobalt intermediate.

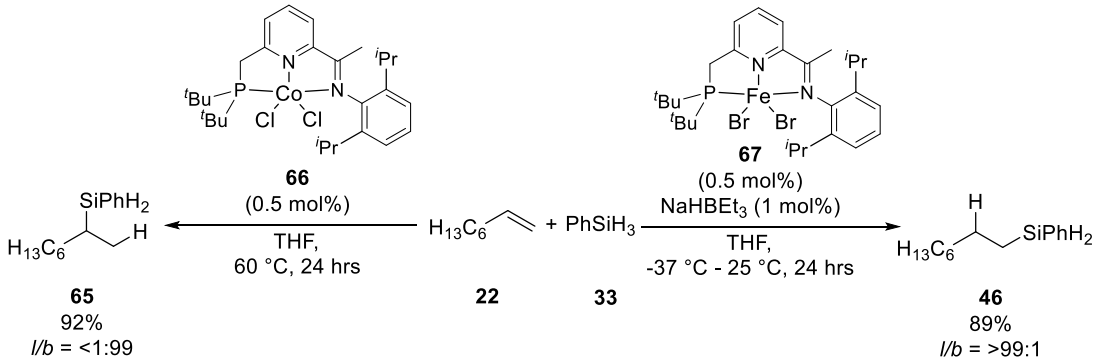

Scheme 1.16 Regiodivergent hydrosilylation of alkenes.

The Lu Group have undertaken pioneering studies towards the asymmetric iron-catalysed hydrosilylation of alkenes using iminopyridine oxazoline ligands.[99] Initially they reported the asymmetric hydrosilylation of 1,1-disubstituted alkenes. The hydrosilylation of 1,1-disubstituted styrene derivatives gave high yields and enantiomeric excess (*ee)* (Scheme 1.17A).[52] The methodology was limited as the hydrosilylation of aliphatic alkenes proceeded with very little stereocontrol. This work was followed by a report into the asymmetric, Markovnikov hydrosilylation of alkenes (Scheme 1.17B). This was remarkable as during the preparation of the manuscript there was no precedent for an iron-catalysed, Markovnikov selective methodology for the hydrosilylation of alkenes. This work used an iminopyridine oxazoline ligand possessing extremely bulky *N*-aryl substituents **69**. Contrary to the previous work, this methodology gave excellent yields and control of the stereochemistry for aliphatic alkenes, while no styrene derivatives were reported. When $PhSiD_3$ **33'** was incorporated into the reaction, no deuterium scrambling from β-hydride elimination product was observed **71** (Scheme 1.17C). Therefore, it was assumed that an iron(I)–silyl species was the active catalyst and silylmetaltion of the alkene was the key mechanistic step.

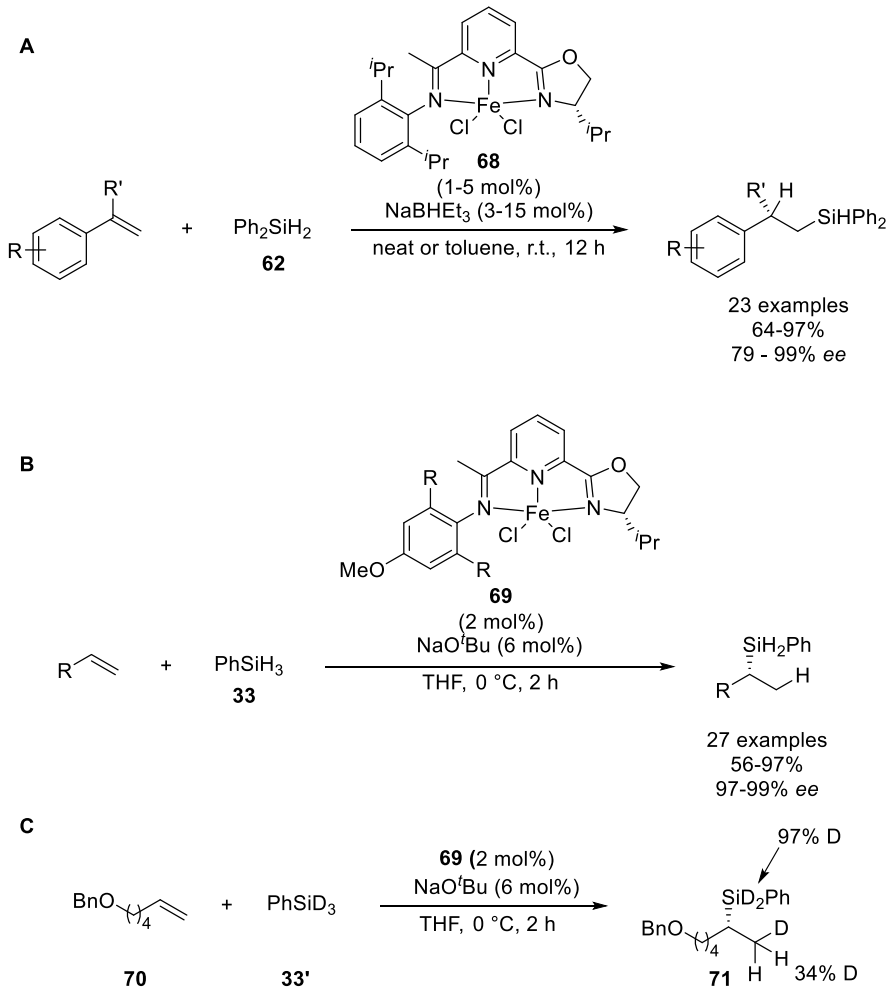

Scheme 1.17 A) An overview of the asymmetric hydrosilylation of 1,1-disubstituted alkenes catalysed by an iron catalyst bearing an iminopyridine oxazoline ligand. B) Asymmetric Makovnikov selective hydrosilylation of alkenes. C) Mechanistic insight showing deuterium incorporation using $PhSiD_3$.

An alternative ligand system for Markovnikov selective iron-catalysed hydrosilylation was reported by Hu *et al.*[100] This system used an iron(II) pre-catalyst bearing a bidentate 1,10-phenanthroline ligand **72** which gave Markovnikov selectivity for a range of terminal and 1,2-disubstituted styrenes (Scheme 1.17A). Terminal, aliphatic alkenes would also undergo hydrosilylation in high yields, but the *anti*-Markovnikov product was formed selectively (Scheme 1.17B).

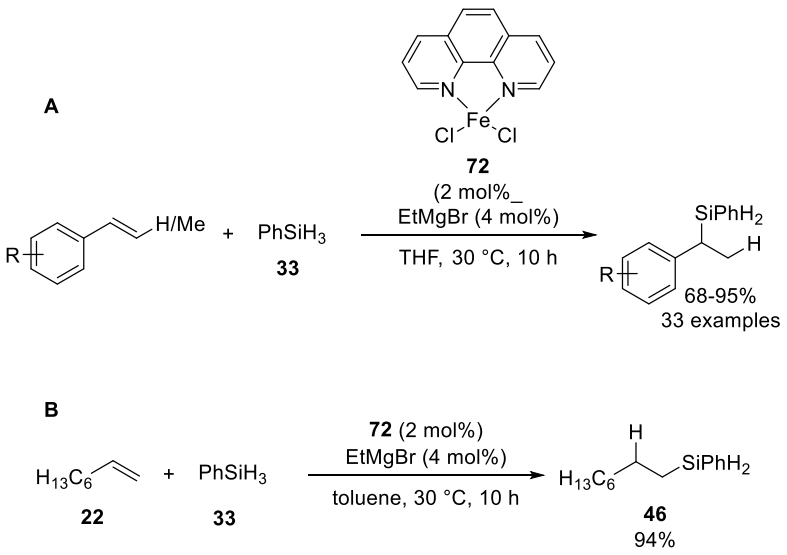

Scheme 1.18 A) Markovnikov hydrosilylation of styrenes. B) *anti*-Markovnikov hydrosilylation of octene.

The Ritter group reported that *in situ* formed imino(pyridine) iron species **74** could catalyse the hydrosilylation of 1,3 dienes.[101] The increase in available coordination sites, through using bidentate ligand **75** instead of a tridentate ligand, is a plausible explanation for the reactivity with dienes in preference to alkenes.

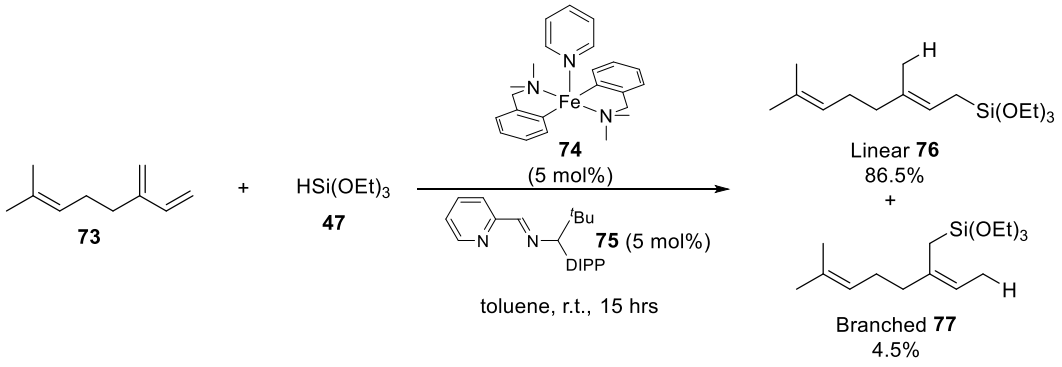

Scheme 1.19 Iron-catalysed hydrosilylation of 1,3-dienes

Nagashima and co-workers reported an activator free iron(II)-catalysed methodology for the hydrosilylation of alkenes using hydroalkoxysilanes and hydrosiloxanes.[102] This work built on previous work using iron(0) (1,3,5,7-cyclotetraene) compounds and adamantyl isocyanide **80** ligands.[103] By using iron(II) pivolate **79** pre-catalysts a range of styrene derivatives underwent hydrosilylation in high yields. It was shown that the hydrosilane used in the reaction acts as the reductant and the reagent.

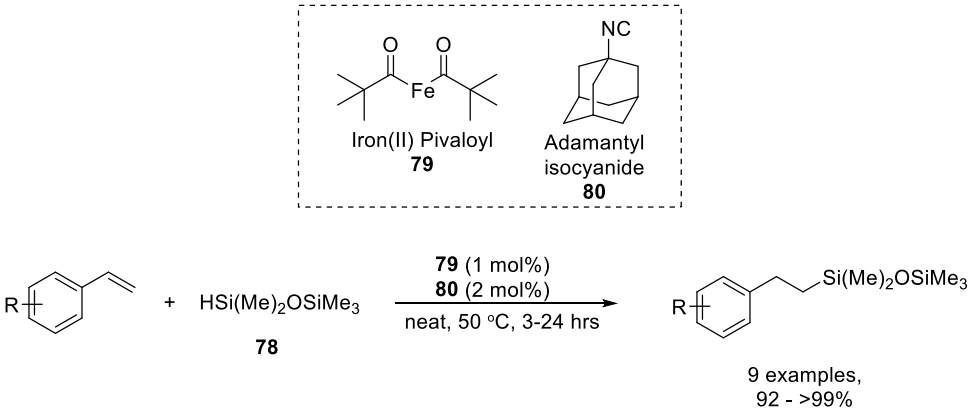

Scheme 1.20 Iron(II) pivolate catalysed hydrosilylation of styrenes

1.2 Manganese Catalysis

Manganese is the third most abundant transition-metal and is crucial to life, as the photosystem II uses a Mn(II) oxidation catalyst. Humans have a long association with manganese species with manganese oxides being used in cave paintings by Paleolithic humankind and in the production of glass by the Romans.[104]

Manganese has access to a wide number of oxidation states (-3 to +7) but is most stable as manganese(II).[30] Manganese(II) has 5 *d*-electrons and therefore has a half-filled shell. Therefore, manganese is more electron-positive than vanadium and chromium (despite it possessing more valence electrons) and manganese(II) alkyl species are known to possess more ionic character than is typical for a transition metal alkyl species.[105,106] Manganese is most well-known for oxidation chemistry with potassium permanganate and manganese dioxide being common laboratory oxidants.[107,108]

1.2.1. Oxidative Manganese Catalysis

In catalysis manganese has predominately been used in oxidative transformations. Most notably, the Jacobson-Katsuki asymmetric epoxidation of alkenes uses a manganese salen catalyst **83** (Scheme 1.21).[109,110]

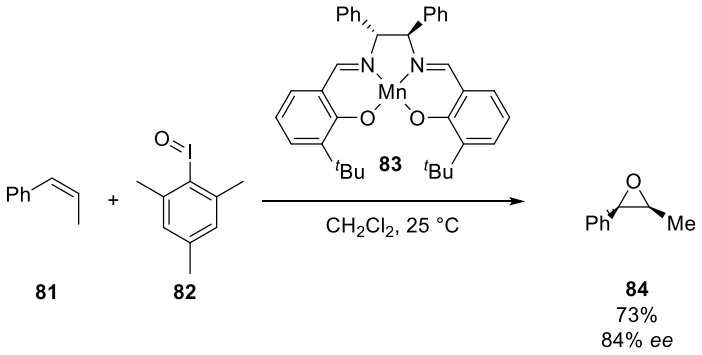

Scheme 1.21: Jacobsen-Katsuki epoxidation of alkenes.

Groves and co-workers have developed the manganese porphyrin-catalysed oxidation of aliphatic C–H bonds (Scheme 1.22A).[111] Whilst chemoselectivity is generally driven by the stability of the resulting alkyl radical (tertiary > secondary > primary), it is possible to bias the catalyst selectivity by using bulky porphyrin ligands. This methodology proceeds by oxidation of the manganese catalyst from manganese(III) **A** to a oxomanganese(V) species **B**. The oxomanganese species can then perform a radical abstraction from the alkyl species to generate a hydroxomanganese(IV) species **C**. This is followed by hydroxyl recombination with the alkyl radical to give the alcohol product (Scheme 1.22B). The use of hypochlorite allows for chlorination of C–H bonds.[112] The replacement of hypochlorite with silver fluoride or sodium azide allowed for fluorination or azidation transformations to occur instead (Scheme 1.22C).[113–115]

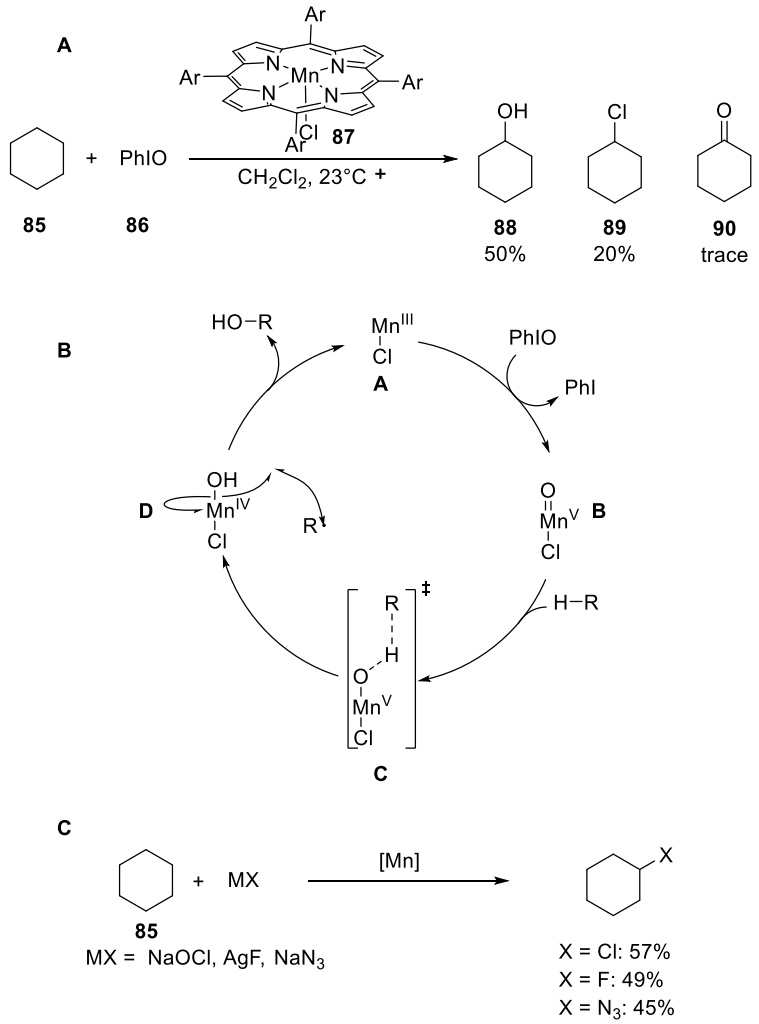

Scheme 1.22 A) Manganese-catalysed C–H oxidation of cyclohexane. B) Heteroatom rebound mechanism for C–H oxidation. C) The chlorination, fluorination and azidation of cyclohexane enabled by the addition of a corresponding metal salt.

1.2.2 Reductive Manganese Catalysis

Despite these successes manganese catalysis has not received the same attention as other first-row transition metals, particularly in hot-topic research areas such as cross-coupling, hydrogenation and hydrofunctionalisation. However, since 2016 major advances have been made in manganese-catalysis, particularly in hydrogenation-type reactions.[116,117]

The hydrogenation of ketones has been reported using a range of manganese(I) compounds bearing PNP ligands. Beller and co-workers reported the hydrogenation of nitriles, ketones and aldehydes using hydrogen gas.[118] The PNPMn(I) pre-catalyst **93** is activated by NaO^{t}Bu and was shown to tolerate a range of other reducible functionalities such as esters, alkenes, alkynes, amides as well as coordinating groups such as pyridine and amines. A manganese(II) compound ligated by the PNP ligand **94** was not catalytically active and neither were manganese(I) species which did not bear the PNP ligand (**95** and **96**. Scheme 1.23A). Beller proposed a mechanism for the reaction where the pre-catalyst **93** was activated by NaO^{t}Bu to form a Mn(I) amido intermediate **94** which can then activate H_2. From there hydrogenation of the substrate can occur in an outer-sphere mechanism (Scheme 1.23C). The group of Kempe reported a similar methodology which used a PNP ligand with a 1,3,5-triazine backbone **99** and Sortais reported the use of a manganese complex bearing a PNP ligand with a pyridine backbone **100** would catalyse the hydrogenation of ketones. (Scheme 1.23B).[119,120]

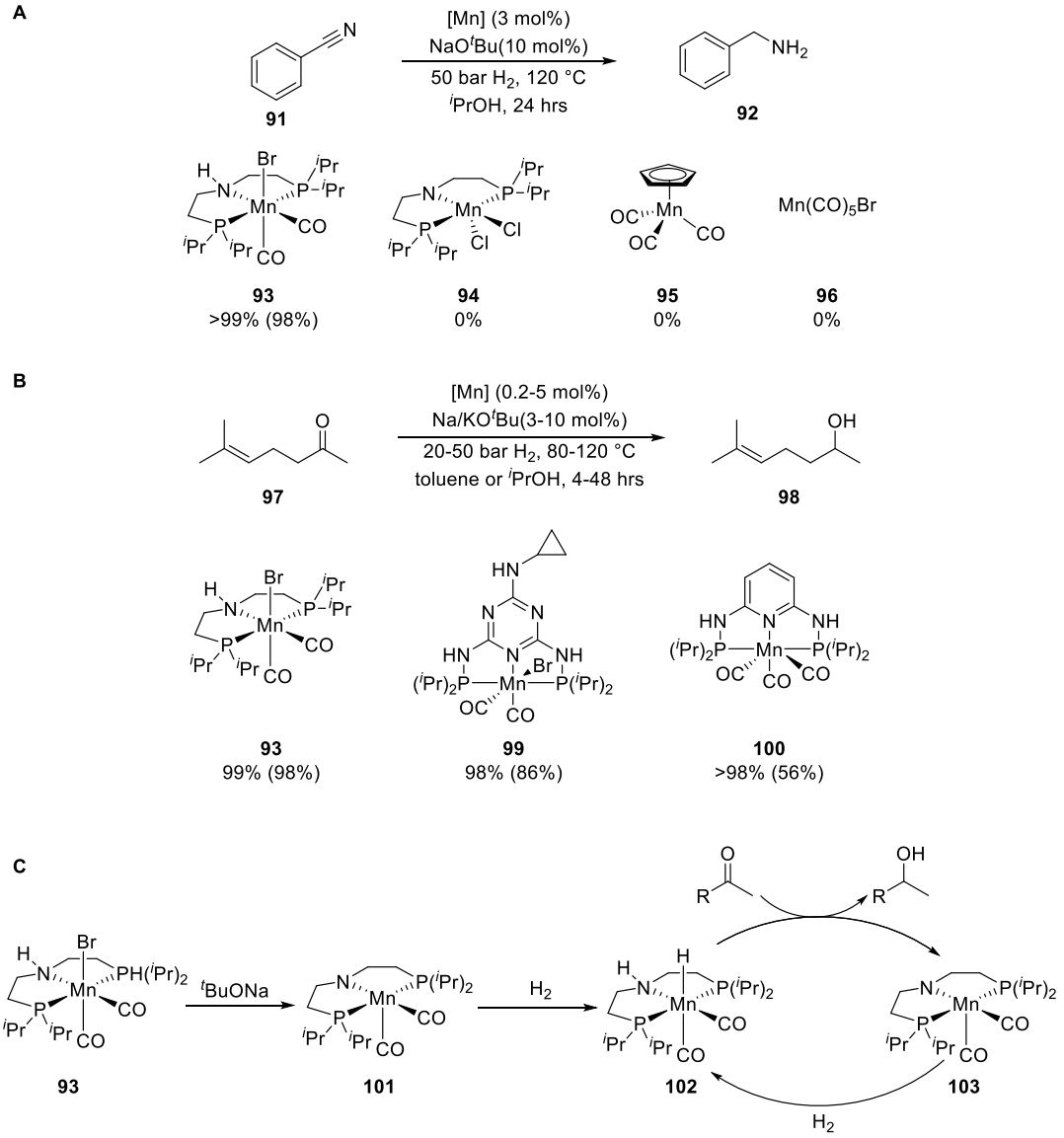

Scheme 1.23 A) Activity of a range of manganese compounds in the hydrogenation of benzonitrile. B) Overview of the Beller, Kempe and Sortais catalyst systems in ketone hydrogenation. C) Proposed outer-sphere mechanism for ketone hydrogenation.

Clarke and co-workers advanced the field by reporting the asymmetric hydrogenation of ketones catalysed by a cationic Mn(I) species ligated by a facially coordinating PNP ligand **104**. The hydrogenation of a range of aryl ketones was performed in high yields and enantiomeric excess (*ee)* (Scheme 1.24A). Beller and co-workers reported the asymmetric hydrogenation of ketones catalysed by chiral PNPMn(I) complex **105**, which was also tolerant of aliphatic ketones in addition to aryl ketones (Scheme 1.24B).

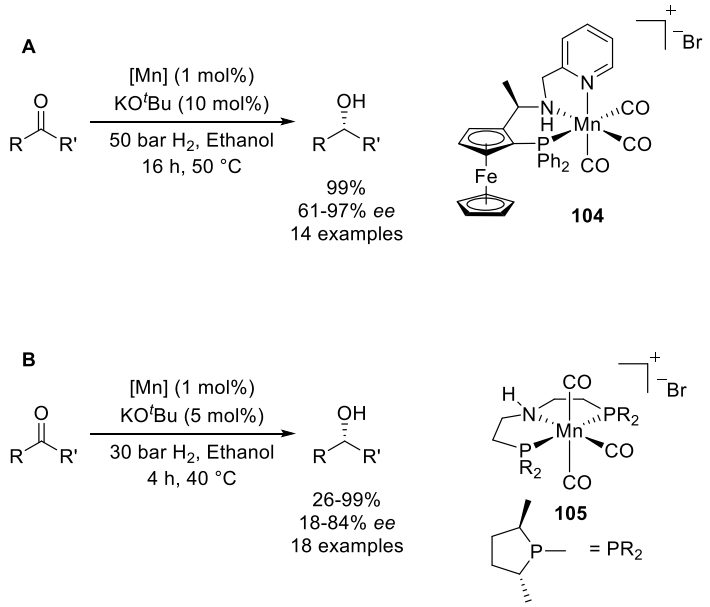

Scheme 1.24 A) Asymmetric hydrogenation of ketones by cationic *fac*-PNN manganese species **104** B) Asymmetric hydrogenation of ketones by cationic PNP manganese species **105**.

The hydrogenation of esters is more challenging than ketones and aldehydes due to the decreased electrophilicity of the carbon atom. Elangovan, Garbe *et al.* reported the first manganese-catalysed hydrogenation of esters by hydrogen gas (Scheme 1.25A). A range of aliphatic and aryl esters underwent hydrogenation, catalysed by a cationic manganese(I) species with a PNP ligand **106**.[121] The Clarke group demonstrated the hydrogenation of esters could be performed using a similar system to that used for the asymmetric hydrogenation of ketones.[122] This work would be extended to the hydrogenation of enantioenriched α-chiral esters, which proceeded without loss of stereochemistry (Scheme 1.25B).[123] Espinosa-Jalapa *et al.* reported a PNNMn(I) compound **107** which was capable of catalysed hydrogenation of esters.[124] The report also showed the isolation of two key intermediates in the hydrogenation: the Mn(I) amido species **108** created by base-activation of the pre-catalyst and the subsequent manganese(I) hydride intermediate **109** (Scheme 1.25C). Pidko and co-workers reported a manganese(I) catalyst bearing a simple bidentate aminophosphine ligand **112**.[125] The methodology's substrate scope was slightly hampered by the substantial amount of KO^{t}Bu (75 mol%) used but this was necessary due to catalyst deactivation (Scheme 1.25D).

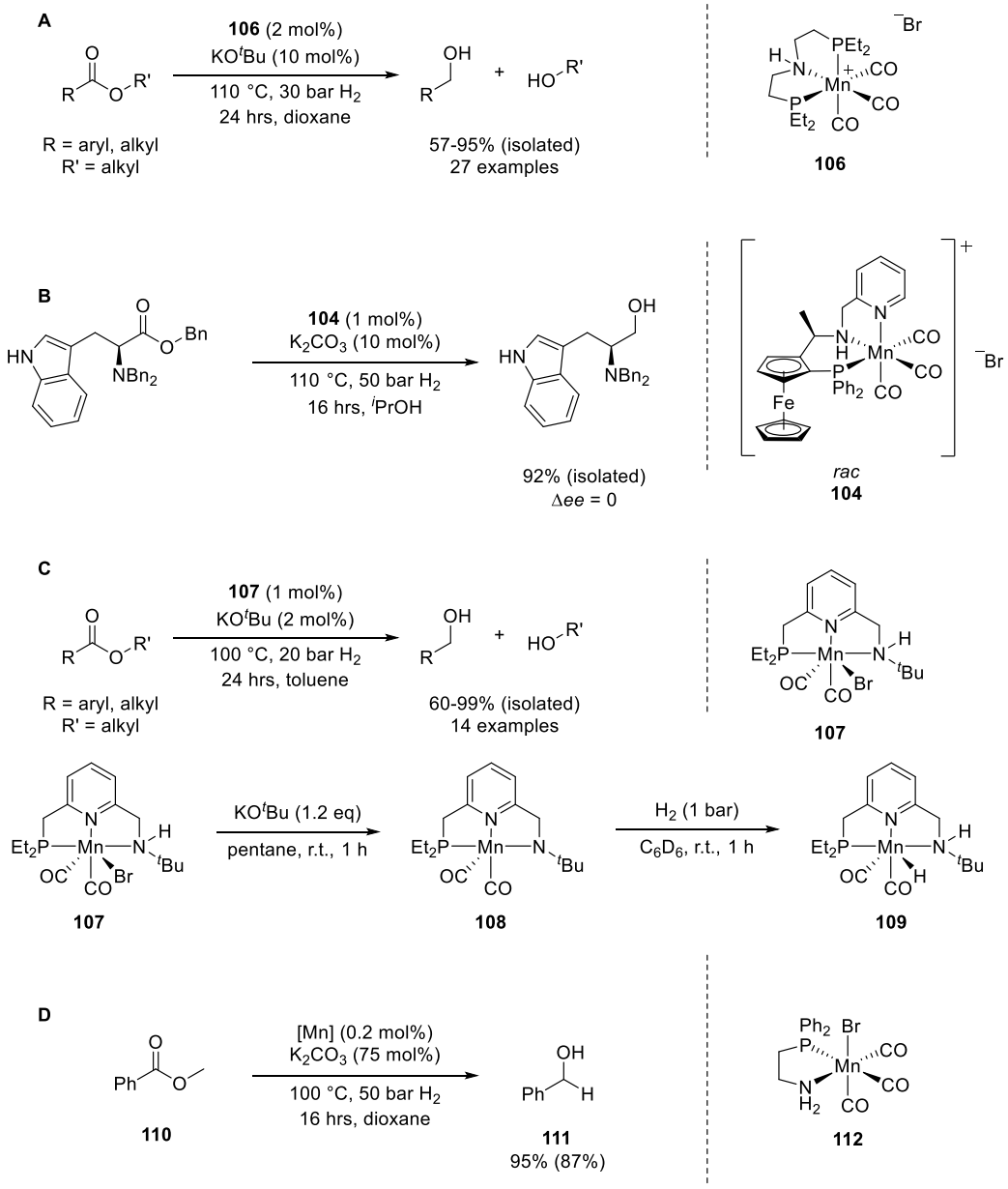

Scheme 1.25 A) Hydrogenation of esters by a PNP manganese catalyst **106** B) Hydrogenation of esters with α-chiral groups, proceeding with retention of stereochemistry. C) Hydrogenation of esters catalysed by PNN manganese species **107** The three manganese structures were all isolated and proposed to be part of any mechanism. D) Hydrogenation of esters by a bidentate iminopyridine manganese species **112**

Many of these complexes have also been used as dehydrogenation catalysts too, for instance in the conversion of alcohols to aldehydes or ketones. The addition of external nucleophiles can lead to a range of reactions with the intermediate carbonyl species. The manganese-catalysed dehydrogenation of alcohols can be used to form a range of

nitrogen-containing heterocycles,[126–129] amines,[130–132] alkylated ketones[133] and alcohols[134].

Whilst many advances have been made in manganese-catalysis, especially in the last two years, there remains huge amounts to explore. Currently manganese catalysts do not show the activity of cobalt and iron analogues. However, excellent functional group tolerance is displayed even in the presence of terminal alkenes. This demonstrates the difficulty in developing manganese catalysts which are reactive with olefins. This is an area which is hugely underdeveloped in manganese-catalysed hydrogenation, hydrosilylation and hydroboration methodologies.

2. Manganese-Catalysed Hydrosilylation of Alkenes

2.1 State-of-the-Art at the Outset of the Project

2.1.1 Manganese-Catalysed Hydrosilylation of Carbonyls

2.1.1.1 Manganese Carbonyls as Catalysts for Carbonyl Hydrosilylation

The first reports of carbonyl hydrosilylation facilitated by a manganese species focussed on the use of stoichiometric amounts of a manganese-silyl or manganese-acyl species. Gladysz reported the insertion of benzaldehyde **113** into the manganese–silyl bond of $(CO)_5MnSiMe_3$ **114** (Scheme 2.1. A).[135] This reaction was very slow, taking over two weeks. The analogous reaction between a manganese-acyl species **117** and a hydrosilane **33** was reported by Cutler and co-workers (Scheme 2.1. B).[136] Despite giving the same product **116**, the reactions are mechanistically distinct. When using the manganese silyl complex **114** it was proposed that the benzaldehyde oxygen would first add to the silyl group in a nucleophilic fashion before addition of the manganese centre to the acyl carbon. This was proposed not to be in a concerted manner with the formation of an intermediate ion pair **115**. The manganese-acyl species reacted by oxidative addition of the hydrosilane to give Manganese(III) hydride **118**, before a 1,3-silatropic shift to give alkenyl manganese species **119** and then a 1,2-hydride shift to give the hydrosilylation product **116**.

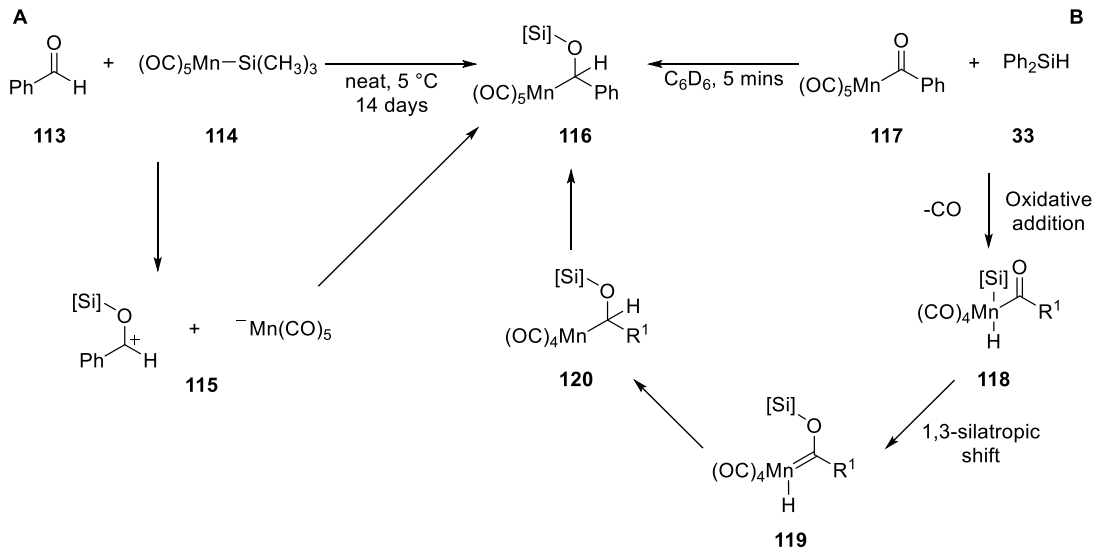

Scheme 2.1 Formation of $(CO)_4MnCH(O[Si])C_6H_5$ from either A) a manganese silyl precursor or B) manganese acyl precursor.

When an external ketone, either as a non-labile organometallic acyl complex or as an organic carbonyl, was added to sub-stoichiometric quantities of manganese acyl species **121**, the reaction proceeded to give silyl ether products in high yields (Scheme 2.2 A).[136,137] It was proposed that the active catalyst was $PPh_3(CO)_3MnSiR_3$ **129** which was generated by the addition of excess hydrosilane to the pre-catalyst. The use of triphenylphosphine as a ligand led to increased rates of reaction, compared to other σ-donor ligands. The same pre-catalyst could also be used to catalyse the hydrosilylation of esters to give the ether and silyl acetate products *by* a similar mechanism to that of ketone reduction (Scheme 2.2 B).

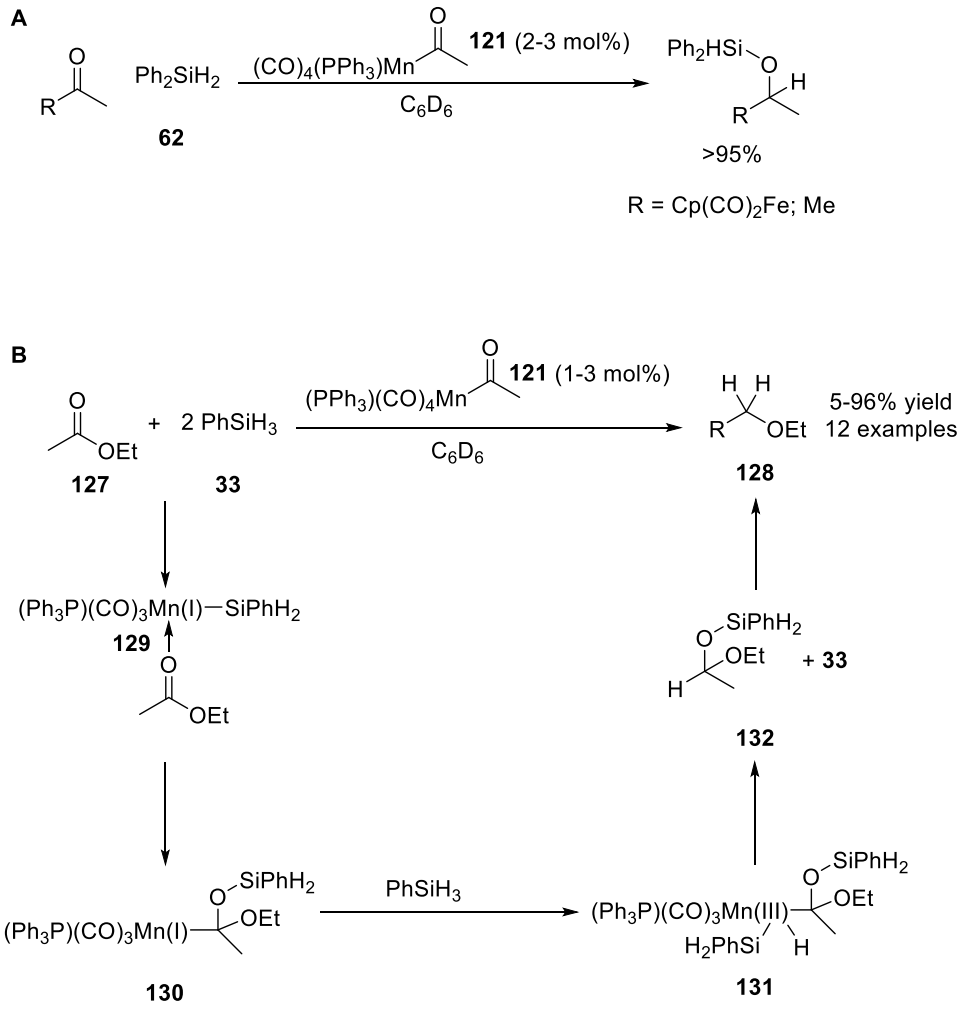

Scheme 2.2 Reduction of carbonyl functionalities by sub-stoichiometric manganese compounds A) Reduction of ketones and B) Reduction of esters to ethers

Lavigne *et al.* showed that a *N*-heterocyclic carbene (NHC) manganese carbonyl complex **135** would catalyse the reduction aldehydes and ketones under UV irradiation (Scheme 2.3).[138] The use of the related cymantrene compound **137** showed no activity as did the use of poor σ-donor type ligands such as triphenylphosphine **138**.

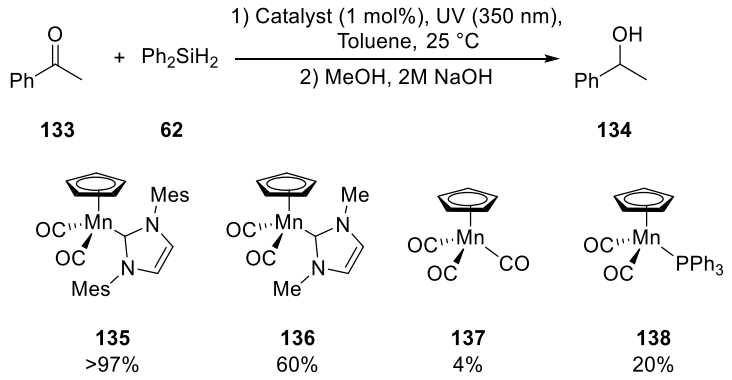

Scheme 2.3 Hydrosilylation of carbonyls with a manganese carbene complex

Manganese carbonyl compounds have been shown to catalyse the hydrosilylation of formamides, amides and carboxylic acids. The photolytic reduction of formamides in the presence of silane by $CpMn(CO)_3$ **137** gave the disiloxane **141** and amine **142** product in high yields (Scheme 2.4 A).[139] The reduction of *N*-acetylpiperidine **143** by triethylsilane **19** is catalysed by $Mn_2(CO)_{10}$ **144** and diethylamine to give 1-ethylpiperidine **145** in a 90% isolated yield (Scheme 2.4 B).[140] The reduction of carboxylic acids can be catalysed by $Mn_2(CO)_{10}$ and upon acidic workup the aldehyde product is formed in high yields (Scheme 2.5 C).[141] The process is dependent on the use of UV irradiation to form coordinatively unsaturated manganese species. Notably when a pendant terminal alkene **146** is used as a substrate, 32% of the 'trisilylated' product **148** was formed.

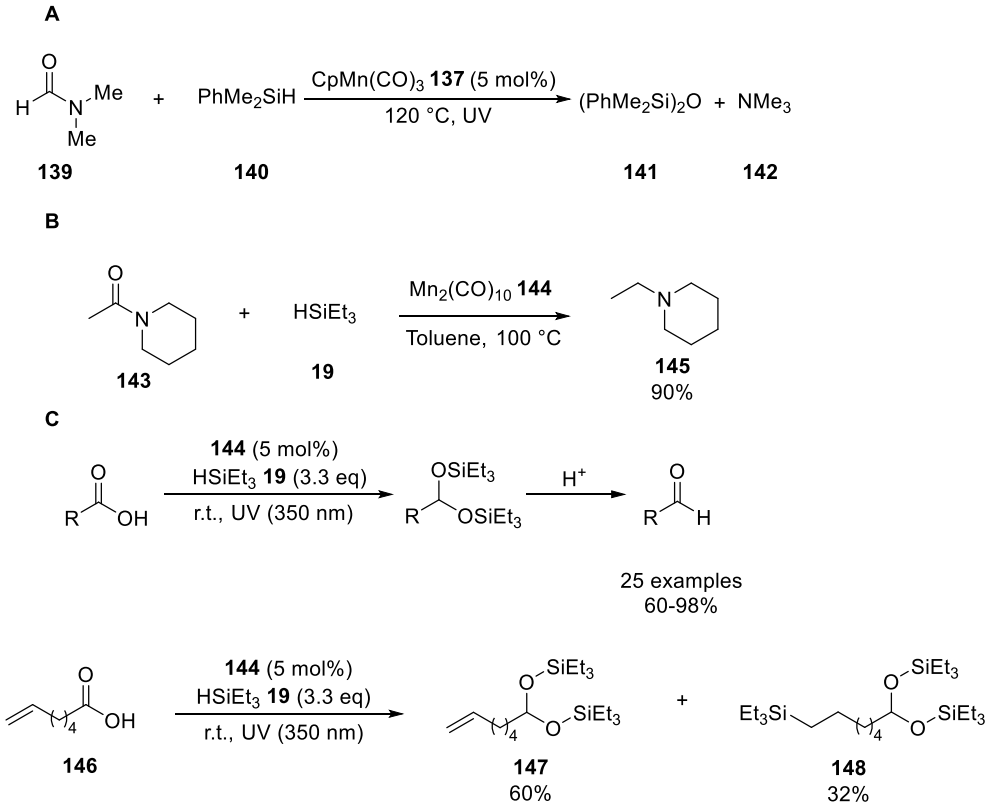

Scheme 2.4 A) Reduction of dimethylformamide to trimethylamine and a disilylether. B) Hydrosilylation of *N*-acetylpiperidine to give the amine product. C) Hydrosilylation of carboxylic acids to give the aldehyde product.

A novel approach to the formation of a co-ordinately unsaturated manganese species was taken by Chung and co-workers (Scheme 2.5.).[142] The use of a η^5-1-hydronaphthalene ligand allowed for a haptotropic shift between the η^5- (**149**) and η^3-coordination modes (**151**). This allows for manganese-catalysed hydrosilylation of ketones using diphenylsilane.

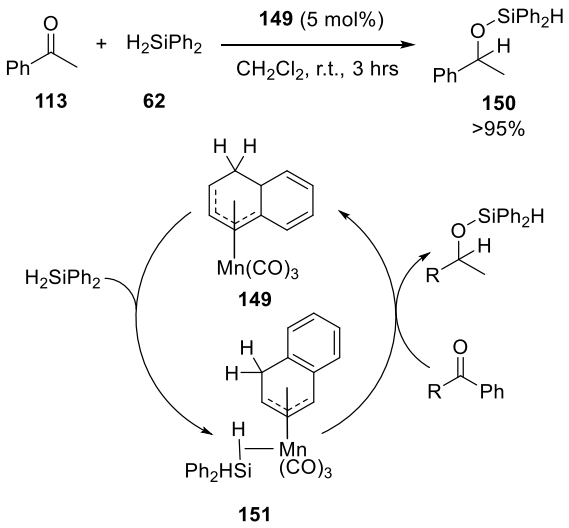

Scheme 2.5 Hydrosilylation of ketones using a manganese hydronapthalene complex.

2.1.1.2 Manganese Complexes as Catalysts for Carbonyl Hydrosilylation

Chidara and Du reported the hydrosilylation of aldehydes and ketones catalysed by a salen Mn(V) nitride pre-catalyst **152** (Scheme 2.6.).[143] The pre-catalyst was proposed to be reduced in the presence of an arylsilane, potentially to a (salen)Mn–H **153** or (salen)Mn–SiR_3 species, which could then undergo a carbonyl insertion process.

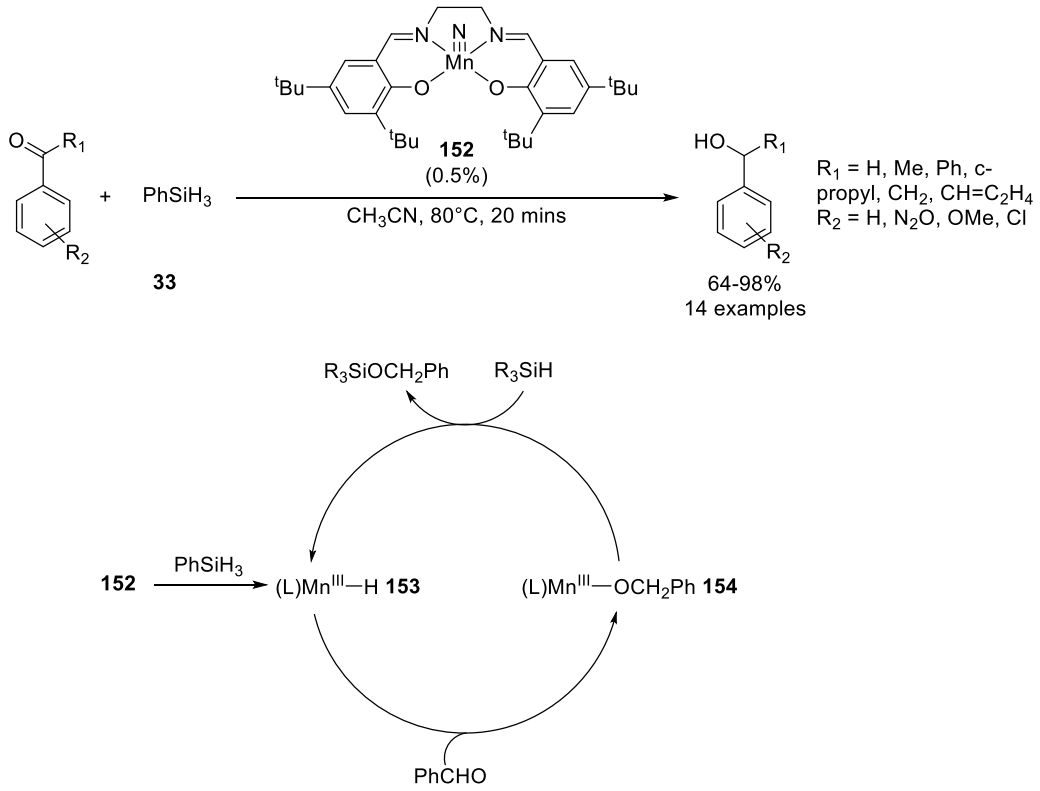

Scheme 2.6 Hydrosilylation of carbonyls with a manganese(salen) nitride complex, detailing the substrate scope and the mechanism.

Trovitch *et. al.* reported the hydrosilylation of aldehydes, ketones, esters and formates catalysed by a pentadentate bis(imino)pyridine complex bearing pendant σ-donor phosphine groups **155** (Scheme 2.7 A-B).[144–147] Complex **155** gave a TOF of 76,800 h^{-1} for the hydrosilylation of ketones which exceeds that of other first row transition metals. The mechanism of hydrosilylation using complex **155** was reported to proceed by a modified Ojima mechanism whereby a hydrosilane would undergo oxidative addition at the manganese centre **156** (Scheme 2.7 C).[145] This would be followed by hydrometallation of the carbonyl and reductive elimination to form the O–Si bond. A modified pre-catalyst, a hexacoordinate manganese hydride **159**, was proposed to

undergo a different mechanism (Scheme 2.7 D). Initial carbonyl coordination to the pre-catalyst to generate an alkoxide intermediate **161** was followed by a metathesis-type interaction with the silane to give the alkoxysilane product.

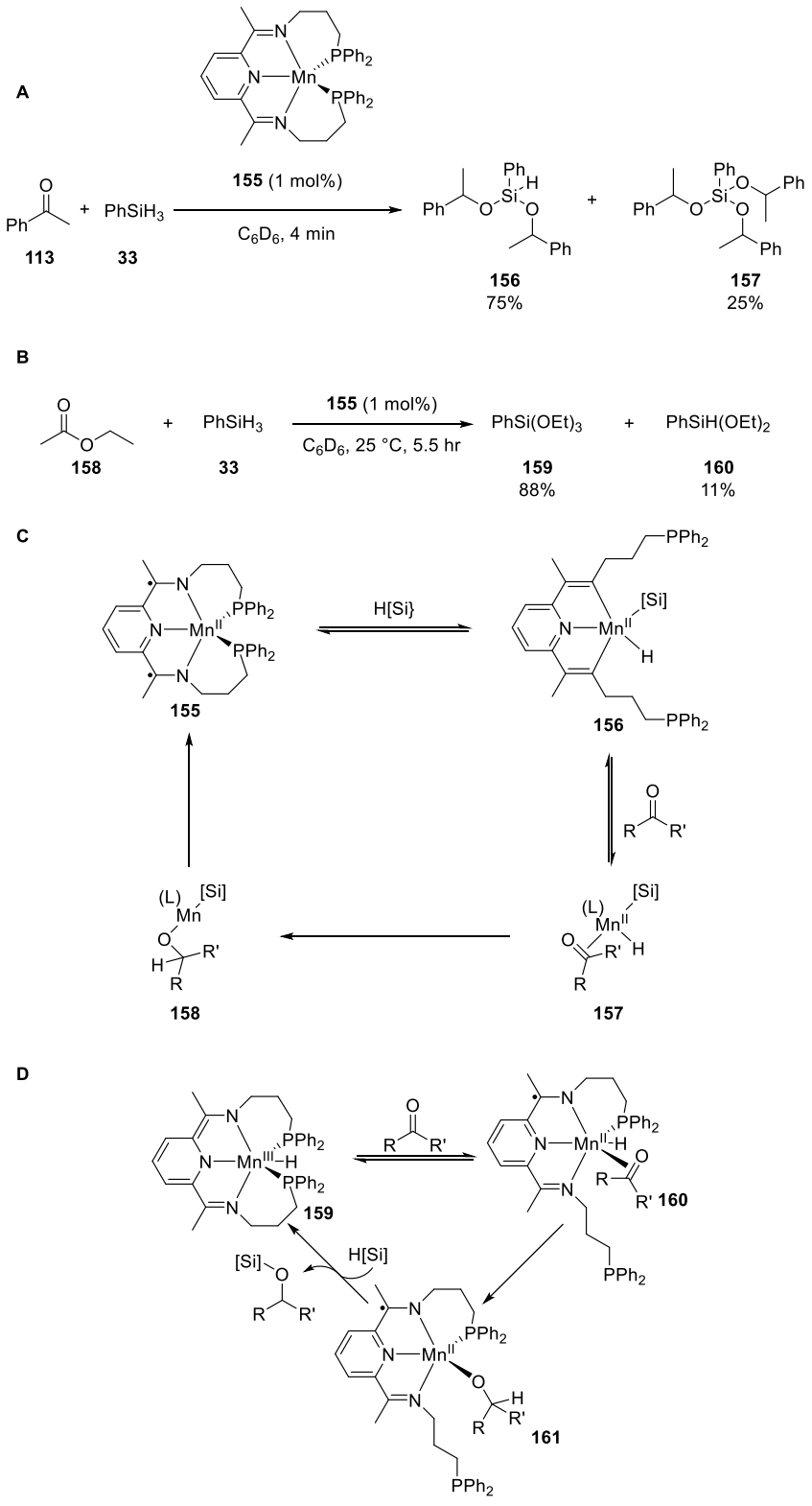

Scheme 2.7 A) Hydrosilylation of ketones with a manganese bisiminopyridine complex. B) Hydrosilylation of esters. C) Mechanism of carbonyl hydrosilylation using a Mn(II) pre-catalyst. D) Mechanism of carbonyl hydrosilylation using a Mn(III) pre-catalyst.

Turculet *et. al.* reported a (*N*-phosphinoamidinate)manganese complex **163** that could catalyse the hydrosilylation of a range of carbonyl groups (Scheme 2.8).[148] Amides were reduced to the amine whereas ketones, aldehydes and esters were reduced to the silyl ether.

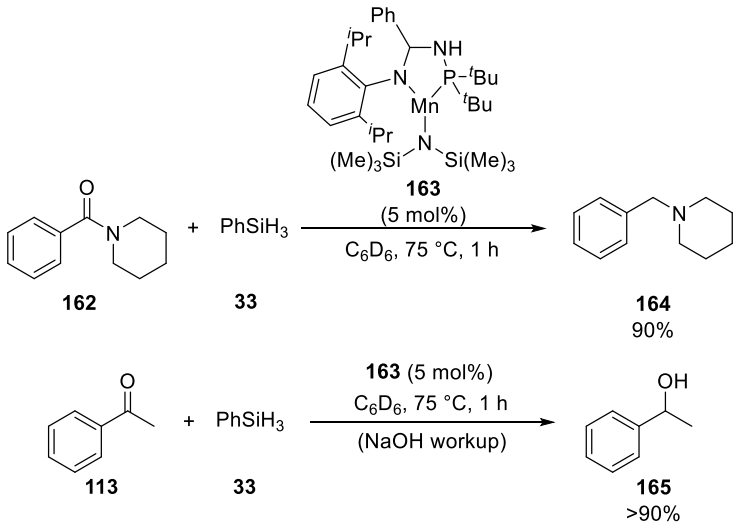

Scheme 2.8 Hydrosilylation of amides and ketones by a (*N*-phosphinoamidinate)manganese complex.

The first report of an asymmetric hydrosilylation of aryl ketones using a manganese catalyst was reported by Huang and co-workers (Scheme 2.9).[149] Using a manganese-complex bearing an enantiopure iminopyridine oxazoline ligand **167**, the reduction of ketones was carried out with an enantiomeric excess (e.e.) of up to 92%.

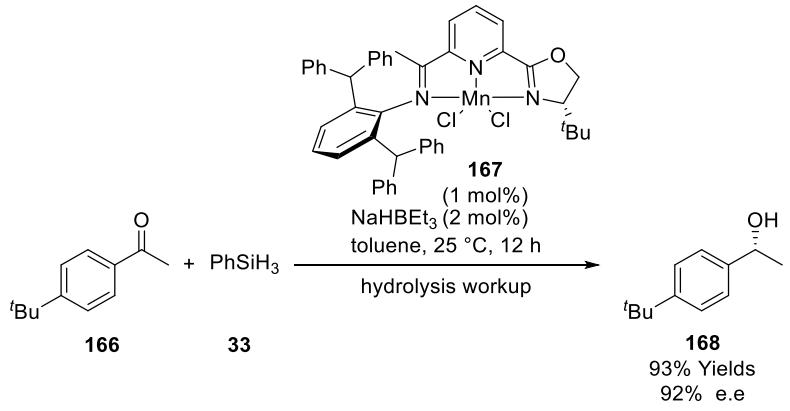

Scheme 2.9 Asymmetric hydrosilylation of ketones catalysed by a manganese(II) iminopyridine oxazoline complex.

2.1.2 Manganese-Catalysed Alkene Hydrosilylation

The very first reports of manganese-catalysed hydrosilylation were performed using alkene substrates. Despite an increasing number of reported manganese catalysts for the hydrosilylation of carbonyl groups; the field of alkene hydrosilylation has remained sparse. In 1983 Faltynek and Pratt explored the hydrosilylation of pentene **9** using $(CO)_5MnSiPh_3$ **170** which was activated either thermally or by photoirradiation (Scheme 2.10).[150] Thermal activation was unselective, giving alkene hydrosilylation **171**, dehydrosilylation **172** and alkene isomerisation **173 & 174** products. Photoirradiation gave solely the hydrosilylation product.

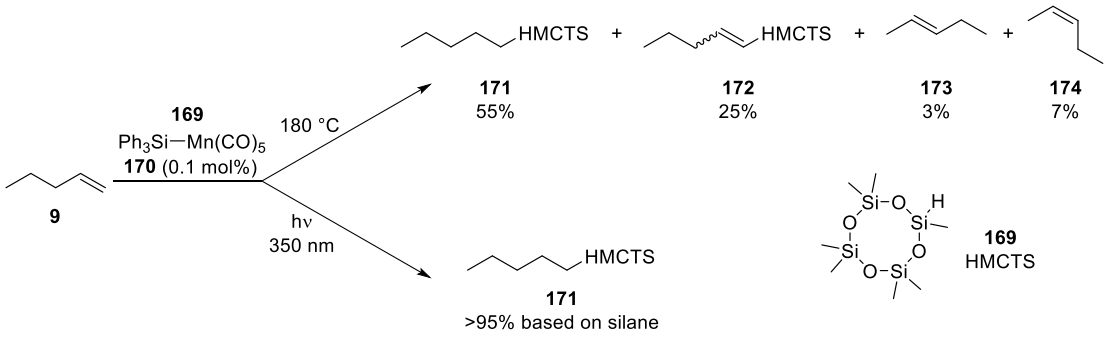

Scheme 2.10 Hydrosilylation of alkenes using a manganese carbonyl compound

Hilal *et. al.* then reported the hydrosilylation of 1-hexene **18** using triethylsilane **19** catalysed by $Mn_2(CO)_{10}$ **144** (Scheme 2.11 A).[151] Both alkene hydrosilylation and alkene isomerisation products were obtained. By adding $Mn_2(CO)_{10}$ **144** to a poly(siloxane) surface a polymer-supported manganese pre-catalyst **177** was obtained (Scheme 2.11 B).[152] This enabled the catalyst to still perform well after recycling. Furthermore, the addition of the polymer support improved the selectivity of the reaction, exclusively giving the hydrosilylation product. More recently, Hilal *et. al.* reported the hydrosilylation of 1-octene **22** by a manganese porphyrin catalyst **178** intercalated into micro- and nano-scale clay particles obtained from the Palestinian Territories (Scheme 2.11 C).[153] The support was found to increase the regioselectivity for the linear hydrosilylation product **48**, but the catalyst was not able to be recycled efficiently with even the first repeat showing significantly decreased catalyst activity.

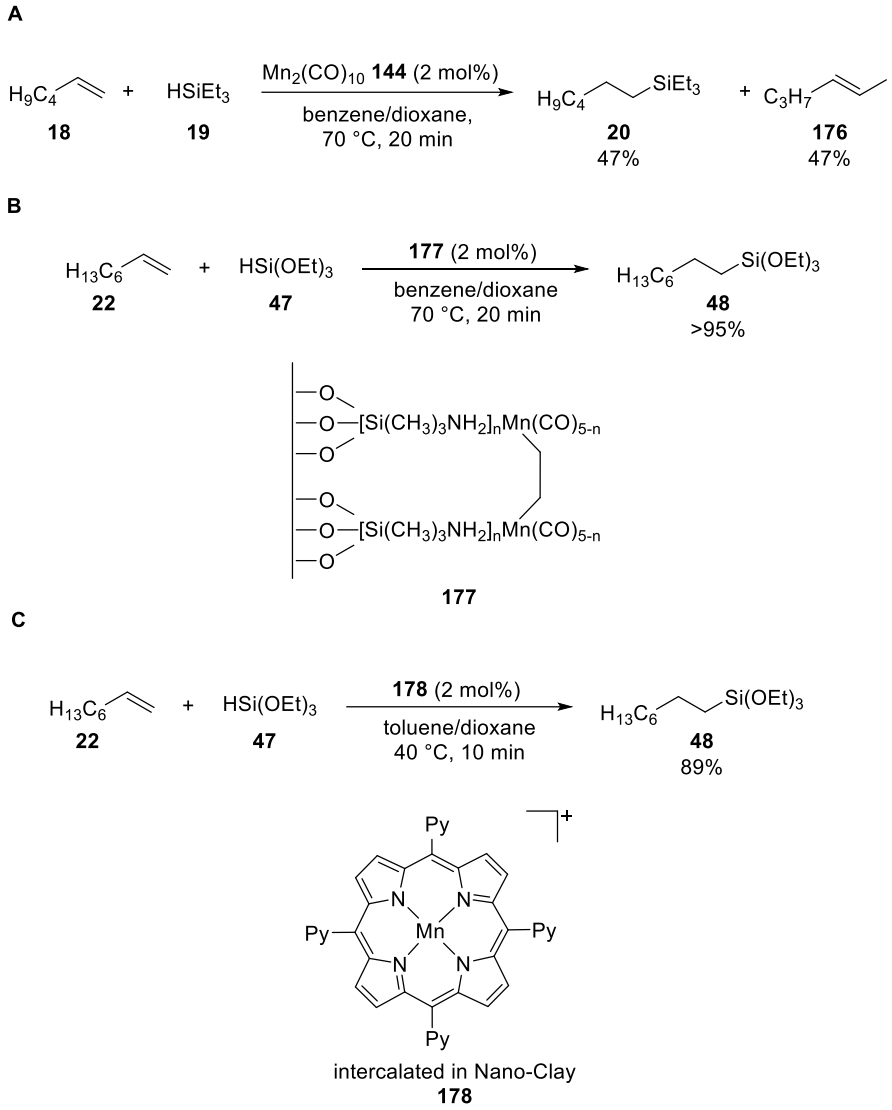

Scheme 2.11 Hydrosilylation of alkenes using a manganese carbonyl compound.

Shenvi *et. al.* reported the formal hydrosilylation of 1-*tert*butyl-4-methylenecyclohexane **179** catalysed by tris(2,2,6,6-tetramethyl-3,5-heptanedionato)manganese(III) ($Mn(dpm)_3$) **180** (Scheme 2.12.).[154] It was proposed that the reaction proceeded by a radical mechanism with hydrogen atom transfer (HAT) being the initial step.

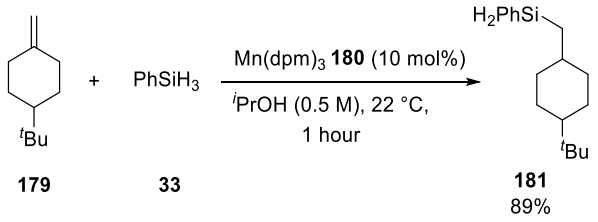

Scheme 2.12 Hydrosilylation of a 1,1-disubstituted alkene using $Mn(dpm)_3$.

2.1.3 Bis(imino)pyridine Manganese Complexes

Bis(imino)pyridine complexes have been developed to be highly active and selective catalysts for a range of transformations but most prominently: polymerisation, hydrofunctionalisation and hydrogenation.[12,155–157] Whilst the ligand has been used in combination with many metals, it has been most successful when paired with iron or cobalt. The highly conjugated nature of the ligand allows for acceptance of up to three-electrons from the central metal atom (Scheme 2.13).[158] This allows for stabilisation of low oxidation-state metal centres. In the case of iron, this allows for access to unstable, co-ordinately unsaturated formally Fe(0) species which are highly reactive.[159]

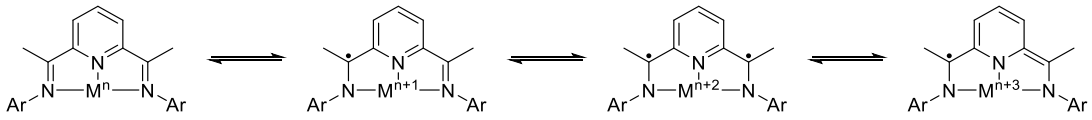

Scheme 2.13 Stabilisation of low-oxidation state iron species by a bis(imino)pyridine ligand.

Despite the catalytic capabilities of iron- and cobalt-analogues, manganese bis(imino)pyridine complexes have not yet been shown to be catalytically active. In fact there are only a handful of reports of their synthesis. The first manganese bis(imino)pyridine to be characterised by single crystal X-ray crystallography was ^{H}BIPMnBr$_2$ as reported by Walton and co-workers.[160] This was followed by the characterisation of $^{4\text{-OMe}}$BIPMn(PF$_6$)$_2$.[161]

The first detailed analysis of the catalytic potential of a manganese bis(imino)pyridine complex was performed by Gambarotta and co-workers.[162] They synthesised ^{DIPP}BIPMnCl$_2$ **182** (a direct analogue of highly successful iron and cobalt polymerisation catalysts[163–165]) but attempts to perform olefin polymerisation were unsuccessful. This was attributed to the high spin, $S = \frac{5}{2}$ manganese(II) center (Scheme 2.14. A). Britovsek and co-workers attempted alkane oxidation using ^{Mes}BIPMn(OTf)$_2$ **184** and ^{DIPP}BIPMn(OTf)$_2$ **185** but were also found to be inactive (Scheme 2.14 B).[166] Chirik and co-workers synthesised the manganese(II) complex ^{DIPP}BIPMn(THF)$_2$ **187** by stirring ^{DIPP}BIPMnCl$_2$ **182** in the presence of sodium and sub-stoichiometric amounts of naphthalene.[167] Attempts to catalyse the hydrogenation of hexene **18** and cyclohexene were unsuccessful, as were attempts to catalyse the [2+2] cycloaddition of dienes

(Scheme 2.14 C).[168] Iron and Cobalt bis(imino)pyridine complexes have been shown to be highly successful in these reactions.[84,88,159,169–171]

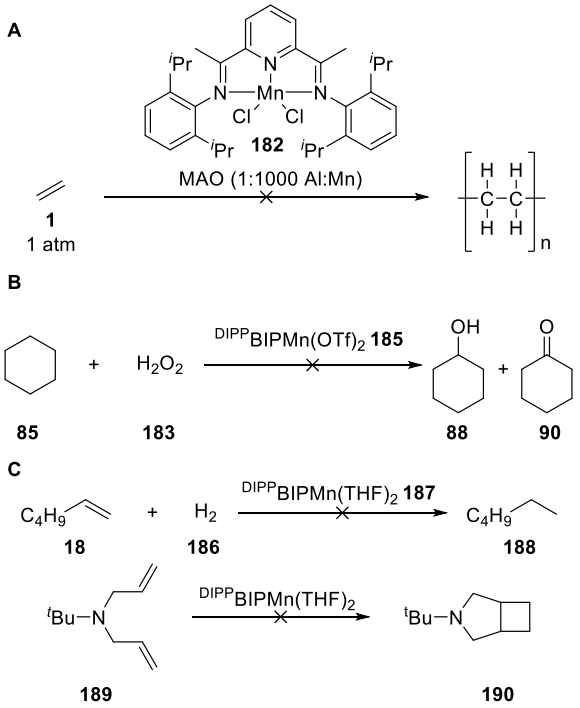

Scheme 2.14 A) Attempted ethylene polymerization catalysed by a Mn(II) bis(imino) pyridine pre-catalyst. B) Attempted alkane oxidation catakysed by a Mn(II) bis(imino)pyridine pre-catalyst. C) Attempted hydrogenation and [2+2] cycloaddition catalysed by Mn(II) pre-catalyst.

2.2 Project Aims

The objective of the project was to discover a methodology for the manganese-catalysed hydrosilylation of alkenes. This would then be thoroughly optimised and applied to a number of substrates to demonstrate the generality of the methodology. Ideally the system would tolerate tertiary silanes as they are most important in industry. If a methodology was developed, it would be important to focus on the mechanism of the reaction and the key factor which has generated reactivity to allow further work to be done in the area.

State-of-the-Art

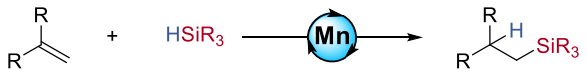

Report	Number of Examples	Substrate	Catalyst
Faltynek 1983	1	1-Pentene	$Mn^{I}Br(CO)_5$
Shenvi 2016	1	1-^{t}Bu-4-methylene cyclohexane	$Mn^{III}(dpm)_3$
Hilal 1986	1	1-Hexene	$Mn^{0}{}_2(CO)_{10}$
Hilal 2016	1	1-Octene	$Mn^{III}TPyP^{+}$@Nano-Clay

Project Aim

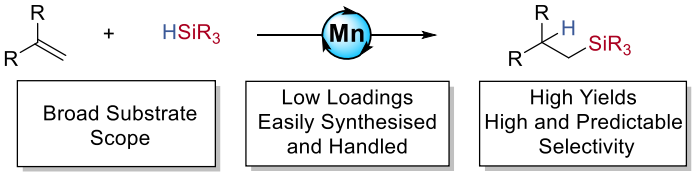

Scheme 2.15 State-of-the-Art at the outset of the project and the aims of this project.

2.3 Methodology Development

2.3.1 Ligand and Pre-Catalyst Synthesis

Given the success of bis(imino)pyridine (BIP) ligands in iron- and cobalt-catalysed hydrofunctionalisation, the synthesis of a range of bis(imino)pyridine ligands and bis(imino)pyridine manganese complexes was a natural starting point for the project. Bis(imino)pyridines are synthesised in a one-step imine-condensation between 2,6-diacetylpyridine and an aniline (Scheme 2.16 A). The bis(imino)pyridine manganese complexes were prepared by stirring the bis(imino)pyridine ligand and the respective manganese salt (Scheme 2.16 B).

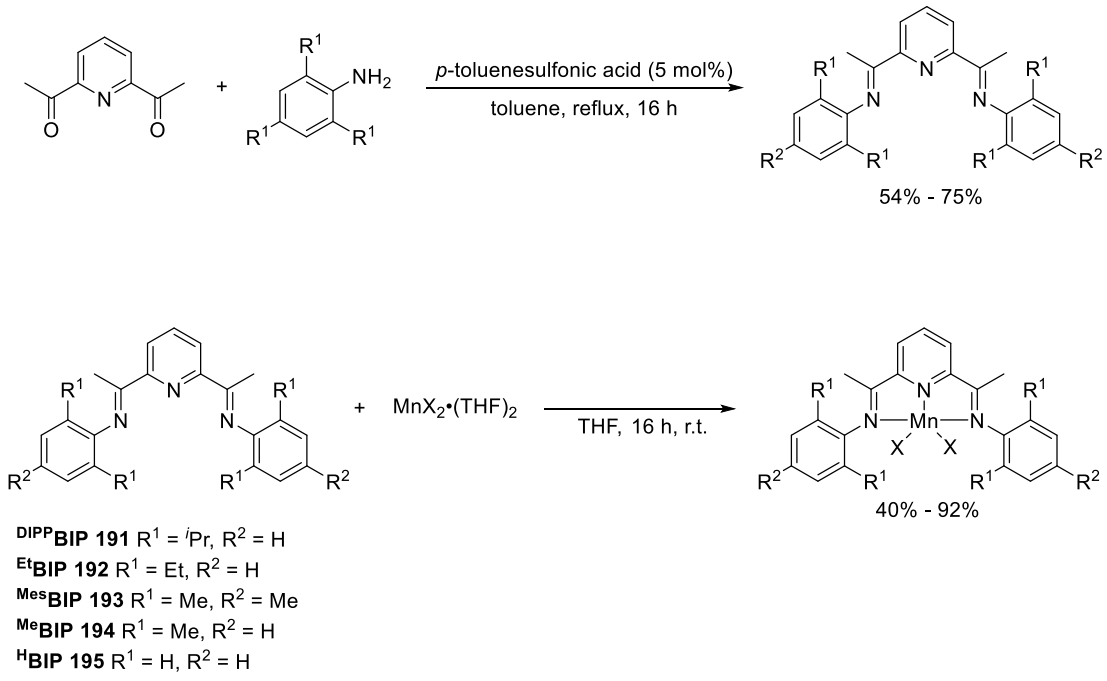

Scheme 2.16 A) Synthesis of bis(imino)pyridine ligands. B) Synthesis of bis(imino) pyridine manganese(II) complexes.

These complexes were predominately air- and moisture-stable and were benchtop stable for weeks. Characterisation of these species was not trivial as the complexes are paramagnetic, so NMR studies were not possible. A number of the complexes were highly sensitive under mass spectrometry conditions and rapidly decomposed to free ligand and the metal salt. Crystallisation of the complexes was possible and single crystal x-ray structures of ^{Et}BIPMnBr$_2$ **196** and ^{DIPP}BipMnBr$_2$ **197** were obtained by cooling solutions of the complex in dichloromethane (Figure 1). The complexes both displayed distorted

square pyramidial geometry, similar to that previously reported for manganese bis(imino)pyridine compounds.

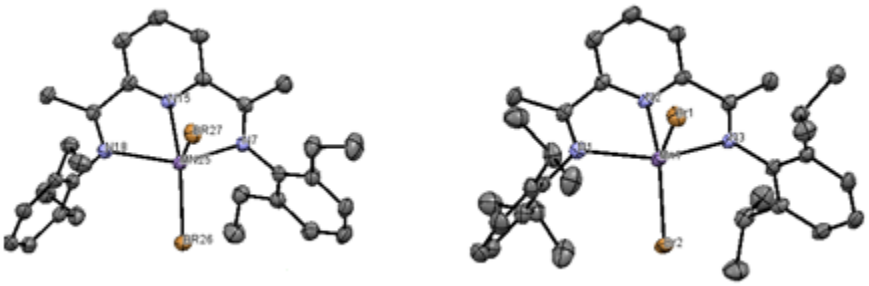

Figure 1: Molecular structures of ^{Et}BIPMnBr$_2$ **196** (left) and ^{DIPP}BIPMnBr$_2$ **197** (right) precatalysts. 50% probability of ellipsoids; hydrogen atoms and solvent molecules omitted for clarity; Grey = C, Blue = N, Orange = Br, Purple = Mn.

Two other ligand systems were also synthesised by simple coordination reactions between the ligand and the metal. The synthesis of ^{DIPP}IPMnBr$_2$ (made by Jamie Doherty), terpyridinemanganesedichloride and terpyridinemanganesedibromide were all completed in high yield (Scheme 2.17).

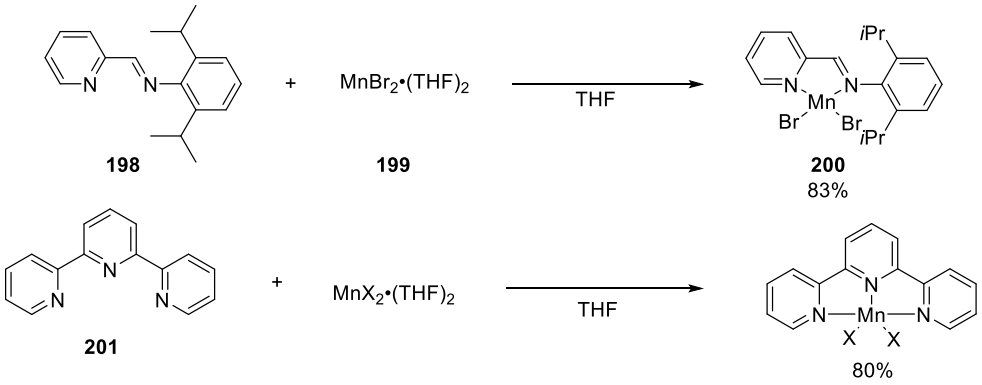

Scheme 2.17 Synthesis of imino(pyridine) manganese(II) bromide and terpyridine manganese(II) pre-catalysts.

2.3.2 Reaction Discovery and Control Reactions

Initial investigations of the manganese-catalysed alkene hydrosilylation were performed using 1-octene **22** as a model alkene, ^{Et}BIPMnBr$_2$ **196** (catalyst), sodium *tert*-butoxide (activator), and phenylsilane **33** (Scheme 2.18). The reaction occurred under *neat* conditions and was left to stir at 25 °C for 20 hours. The average yield of the linear hydrosilylation product **46** over 3 reactions was 32% with >99% selectivity for the linear regioisomer (work done by Jamie Docherty).[42]

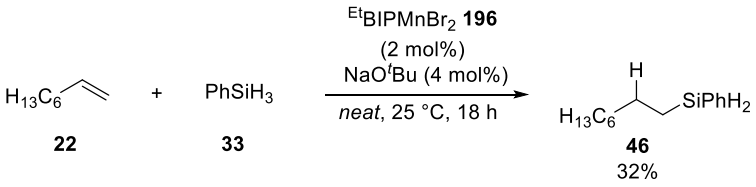

22 **33** **46** 32%

Scheme 2.18 Initial hits for the manganese-catalysed hydrosilylation of alkenes.

Initial optimisation looked at increasing the reactivity of this catalyst/activator system by changing the temperature and solvent. Repeating the original conditions led to a small increase in the yield, 55% over two reactions but with a high of a 90% yield (Table 2.1., entry 1). Results of individual reactions were observed to be quite inconsistent, so every reaction was performed twice in parallel to allow for an average to be taken. Increasing the temperature to 60 °C gave a decreased yield of 18%, possibly because of catalyst decomposition at higher temperatures (entry 2). The addition of solvent, in this case THF, led to no reactivity being observed (entry 3). By reducing the catalyst loading to 1 mol% the yield was also reduced to 41%. Increasing the catalyst loading to 5 mol% had only a small impact on the yield, with a 57% yield of linear hydrosilylation product **46** being obtained. The system was tested with a range of other alkenes to quantify the generality of the methodology. Using 4-phenyl-1-butene **202** as the substrate gave a reduced reaction yield of 42% (entry 6) compared to 55% for 1-octene. Subjecting different classes of alkenes beyond aliphatic, terminal alkenes to the developed reaction conditions, such as styrenes (*tert*-butylstyrene **203** entry 7), 1,2-disubstituted alkenes (cyclooctene **204** entry 8) and 1,1 disubstituted alkenes (α-methylstyrene **205** entry 9), gave no conversion of starting material in all cases. Based on these findings the reaction needed substantially more optimisation and refinement.

Table 2.1. Initial screening of reaction conditions

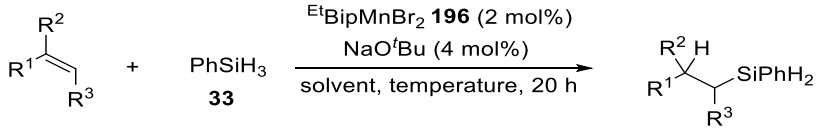

Entry	Substrate	t (°C)	Catalyst Loading (mol%)	Solvent	Yield (%)[a]
1	1-Octene **22**	25	2	*Neat*	55
2	1-Octene **22**	60	2	*Neat*	18
3	1-Octene **22**	25	1	*Neat*	41
4	1-Octene **22**	25	5	*Neat*	57
5	1-Octene **22**	25	2	THF	0
6	4-phenyl-1-butene **202**	25	2	*Neat*	42
7	^{t}Butylstyrene **203**	25	2	*Neat*	0
8	Cyclooctene **204**	25	2	*Neat*	0
9	α-Methylstyrene **205**	25	2	*Neat*	0

Reaction conditions: Alkene (0.5 mmol), $HSiR_3$ (0.63 mmol), catalyst (0.01 mmol), $NaO^{t}Bu$ (0.03 mmol), *neat*, 25 °C, 18 h. a) Yield determined by ^1H NMR of the crude reaction mixture, using 1,3,5-trimethoxybenzene as an internal standard, as an average of two runs. Selectivity for the linear hydrosilylation product is >95%

Control reactions were carried out to ensure the validity of the methodology. By removing the individual components of the reaction, it was shown that each component was essential for reactivity. The reaction was trialled with only $NaO^{t}Bu$ **49** and no transition metal catalyst or ligand but there was no observed reactivity (Table 2.2., entry 1). Using $MnBr_2$ either with or without $NaO^{t}Bu$ **49**, gave no catalyst activity (entries 2 &

3). Adding only the ligand with or without NaO^{t}Bu **49** gave no observed reactivity. Finally, running the reaction under air also gave no yield of hydrosilylation product.

Table 2.2. Control Reactions

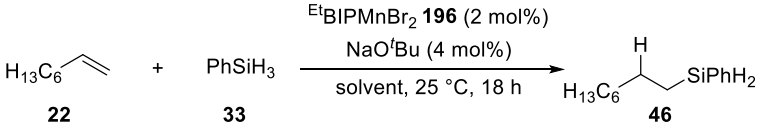

Entry	Deviation from standard conditions	Yield %[a]
1	Only NaO^{t}Bu	0
2	$MnBr_2 \cdot (THF)_2$ + NaO^{t}Bu	0
3	$MnBr_2 \cdot (THF)_2$	0
4	Only ^{Et}BIP	0
5	^{Et}BIP + NaO^{t}Bu	0
6	Under air	0

Reaction conditions: Alkene (0.5 mmol), $HSiR_3$ (0.63 mmol), catalyst (0.01 mmol), NaO^{t}Bu (0.03 mmol), solvent, 25 °C, 18 h. a) Yield determined by ^{1}H NMR of the crude reaction mixture, using 1,3,5-trimethoxybenzene as an internal standard, as an average of two runs. Selectivity for the linear hydrosilylation product is >95%.

2.3.3 Catalyst Optimisation

Variation of the steric parameters on bis(imino)pyridine components of the catalyst have been shown to have dramatic effects on the reactivity of these systems. For instance, Chirik *et. al.* showed that alternating between sterically bulky 2,6-di*iso*propyl (DIPP) substituted aryl imines and unsusbstituted aryl imines would change the chemoselectivity of the hydrosilylation of 5-hexen-2-one **61** from the ketone (bulky ligand) to the alkene (smaller ligand).[96,169] The choice of counterion can also have an influence on the activity and selectivity of the catalytic system. For instance, more coordinating counter-ions (Cl^-) on iron bis(imino)pyridine species have been shown to have a higher reduction potential than less coordinating counter-ions (^-OTf).[92]

The hydrosilylation of 3 different alkenes with phenylsilane **33** was attempted using a range of sterically differentiated bis(imino)pyridine catalysts and several manganese salts. The three alkenes (1-octene **22**, 4-phenyl-1-butene **202** and *t*butylstyrene **203**) were chosen as they had been shown to be highly reactive, moderately reactive and not active, respectively, under the established conditions. The use of the sterically bulky complexes $^{DIPP}BIPMnBr_2$ **197** (Table 2.3. entry 1) and $^{DIPP}BIPMnCl_2$ **208** (entry 5) gave low hydrosilylation yields. As above, $^{Et}BIPMnBr_2$ **196** gave good yields over 18 hours for 1-octene (90%), moderate activity for 4-phenyl-1-butene (41%) and low activity for *t*butylstyrene (1%). However, and uniquely in the series of $BIPMnX_2$ complexes synthesised for this project, the $^{Et}BIPMnCl_2$ analogue was extremely unstable and would spontaneously decompose in the solid state under inert conditions. Using a catalyst with a trisubstituted *N*-aryl group, $^{Mes}BIPMnBr_2$ **206** (Entry 3) and $^{Mes}BIPMnCl_2$ **209** (Entry 6) gave lower yields than the disubstituted ethyl analogue. In this case, the chloride analogue was significantly more active than the bromide analogue. The second highest yield was obtained with $^{Me}BIPMnCl_2$ **210** giving a 32% yield for the hydrosilylation of 1-octene and 4-phenyl-1-butene (Entry 7). The least-sterically hindered ligand ^{H}Bip gave poor yields for both the bromide salt **207** (Entry 4) and chloride salt **211** (Entry 8). The use of a less coordinating triflate counterion **212** gave no catalyst activity for the hydrosilylation of 1-octene. These results showed that both sterically hindered, and less-sterically hindered ligands gave poor reactivity but mid-sized bis(imino) pyridine ligands were optimal. Likewise, counterion variation did not give a consistent pattern, with only $^{Mes}BIPMnCl_2$ **209** being significantly more active than $^{Mes}BIPMnBr_2$ **206**.

Mono(imino) pyridine manganese compounds have been reported to catalyse ethane polymerization.[172] However, under the developed conditions, di*iso*propylphenyl imino(pyridine) (^{DIPP}IP, **200**), (Entry 10) gave no conversion to the hydrosilylation products. Terpyridine manganese(II) alkyl complexes have been reported to catalyse the hydroboration of alkenes.[173] We prepared terpyridine manganese dibromide **213** and terpyridine manganese dichloride **214** complexes however both gave only trace reactivity. The terpyridine complexes were also tested using THF as a solvent but still gave no reactivity. Finally, we used (trimethylsilyl)methylenelithium as an *in-situ* activator, in an attempt to mimic the conditions used by Zheng *et. al.* more closely but this still gave no reactivity. The highest yields for hydrosilylation were still found using ^{Et}BIPMnBr_2 as the catalyst, therefore to increase the substrate tolerance of our system further optimisation was required.

Table 2.3. Screening of catalysts for the hydrosilylation of 1-octene with phenylsilane.

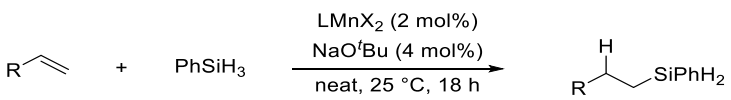

Entry	Substrate	Catalyst	Yield %[a]
1a	1-Octene	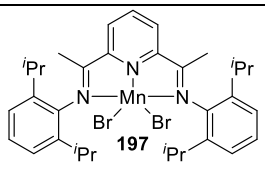 **197**	8
1b	4-Phenyl-1-butene		2
1c	^{t}Butylstyrene		0
2a	1-Octene	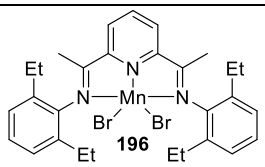 **196**	90
2b	4-Phenyl-1-butene		41
2c	^{t}Butylstyrene		1
3a	1-Octene	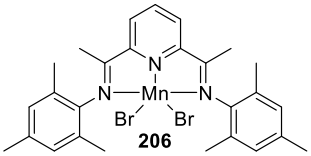 **206**	5
3b	4-Phenyl-1-butene		0
3c	^{t}Butylstyrene		0
4a	1-Octene	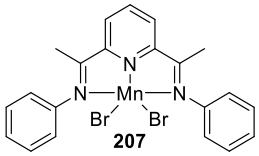 **207**	8
4b	4-Phenyl-1-butene		6
4c	^{t}Butylstyrene		0
5a	1-Octene	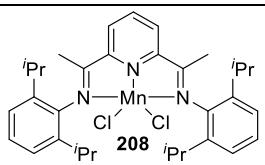 **208**	0
5b	4-Phenyl-1-butene		5
5c	^{t}Butylstyrene		0
6a	1-Octene	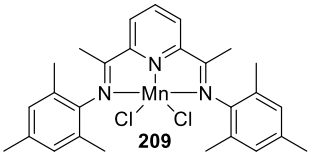 **209**	31
6b	4-Phenyl-1-butene		26
6c	^{t}Butylstyrene		0
7a	1-Octene		32

7b	4-Phenyl-1-butene	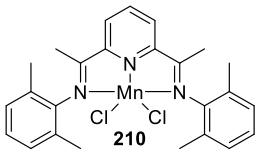 **210**	26
7c	^{t}Butylstyrene		0
8a	1-Octene	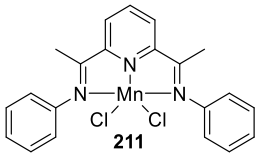 **211**	5
8b	4-Phenyl-1-butene		8
8c	^{t}Butylstyrene		0
9	1-Octene	^{DIPP}BIPMn(OTf)$_2$ **212**	0
10	1-Octene	^{DIPP}IPMnBr$_2$ **200**	0
11	1-Octene	TerpyMnBr$_2$ **213**	Trace
12	1-Octene	TerpyMnCl$_2$ **214**	Trace
13	1-Octene	TerpyMnBr$_2$ **213**	Trace[b]
14	1-Octene	TerpyMnCl$_2$ **214**	Trace[b]
15	1-Octene	TerpyMnBr$_2$ **213**	Trace[c]
16	1-Octene	TerpyMnCl$_2$ **214**	Trace[c]

Reaction conditions: Alkene (0.5 mmol), $HSiR_3$ (0.63 mmol), catalyst (0.01 mmol), NaO^tBu (0.03 mmol), *neat*, 25 °C, 18 h. a) Yield determined by ^{1}H NMR of the crude reaction mixture, using 1,3,5-trimethoxybenzene as an internal standard, as an average of two runs. Selectivity for the linear hydrosilylation product is >95%. b) Reaction performed in THF. c) reaction performed with $LiCH_2SiMe_3$ as reductant.

2.3.4 Further Optimisation using ^{Et}BIPMnBr$_2$ and Discovery of ^{DIPP}BIPMnBr$_2$

The reaction gave highly variable results when subjected to temperatures above and below room temperature. Raising the temperature to 60 °C led to greatly decreased yields, presumably because of degradation of the active catalyst (Table 2.4. entry 2). Even increasing the temperature to only 40 °C caused the yield to be reduced to 42% (entry 3). Leaving the reaction temperature unregulated (room temperature approximately 18 °C) led to no reaction (entry 4). Changing the catalyst to ^{Mes}BIPMnCl$_2$ **209** gave improved consistency as at both 25 °C and 40 °C the yield was similar (31% and 33% respectively) (entry 5-6). However, the yield was significantly lower than with ^{Et}BIPMnBr$_2$ **33** so this was not investigated further.

Table 2.4: Optimisation of temperature

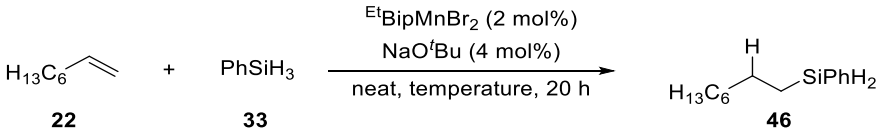

22 **33** **46**

Entry	Catalyst	Temperature (°C)	Yield (%)[a]
1	^{Et}BIPMnBr$_2$	25	90
2	^{Et}BIPMnBr$_2$	60	18
3	^{Et}BIPMnBr$_2$	40	42
4	^{Et}BIPMnBr$_2$	r.t. (~18 °C)	0
5	^{Mes}BIPMnCl$_2$	25	31
6	^{Mes}BIPMnCl$_2$	40	33

Reaction conditions: Alkene (0.5 mmol), $HSiR_3$ (0.63 mmol), catalyst (0.01 mmol), NaO^{t}Bu (0.03 mmol), *neat*, 25 °C, 18 h. a) Yield determined by ^{1}H NMR of the crude reaction mixture, using 1,3,5-trimethoxybenzene as an internal standard, as an average of two runs. Selectivity for the linear hydrosilylation product is >95%

The use of NaO^{t}Bu **49** as an activator is preferable as it is an easily handled, bench stable reagent. However, conventionally organometallic reagents such as Grignard

reagents,[90,174] borohydrides and lithium alkyl species[173] have been used to reduce first-row transition metal pre-catalysts to low oxidation-state active catalysts. A selection of these organometallic reductants was applied in the reaction but none of the organometallics gave more than trace hydrosilylation product (table 2.5. entries 1-3). The amount of NaO^{t}Bu **49** required to trigger catalysis was also screened (entries 4-8). A minimum of two equivalents of NaO^{t}Bu, with respect to catalyst, was required for any catalysis to occur. Raising the number of equivalents to three allowed for an improved yield. Other alkoxide activators were tested in this system but without success. Whilst this reactivity is somewhat surprising, Stoltz and Grubbs have observed similar reactivity in the silylation of heteroaromatics where the choice of metal alkoxide was limited to KO^{t}Bu.[175–177]

Table 2.5. Screening of different activators

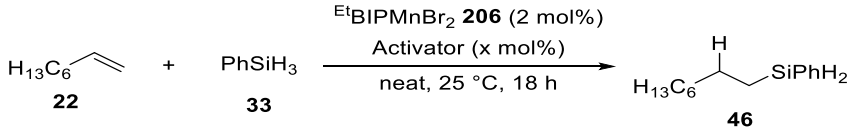

Entry	Activators	Mol%	Yield (%)[a]
1	EtMgBr[b]	4	4
2	$NaHBEt_3$[c]	4	2
3	$LiAlH_4$[d]	4	0
4	NaO^{t}Bu	2	Trace
5	NaO^{t}Bu	3	5
6	NaO^{t}Bu	4	40
7	NaO^{t}Bu	5	22
8	NaO^{t}Bu	6	45
9	KO^{t}Bu	4	0
10	NaOMe	4	0
11	NaO^{i}Pr	4	0

Reaction conditions: Alkene (0.5 mmol), $HSiR_3$ (0.63 mmol), catalyst (0.01 mmol), activator (0.03 mmol), *neat*, 25 °C, 18 h. a) Yield determined by ^{1}H NMR of the crude reaction mixture, using 1,3,5-trimethoxybenzene as an internal standard, as an average of two runs. Selectivity for the linear hydrosilylation product is >95%**.** b) 3M in Et_2O. c) 1M in THF. d) 1M in THF.

As the organometallic reagents were all added in solution, an investigation into various solvents was carried out to determine if this was the cause of reaction inhibition with organometallic activators. All solvents tested were obtained from a solvent purification system. 4-Phenyl-1-butene **202** was chosen as the substrate so an improvement in reactivity could be seen. THF gave a slight increase to the yield compared to *neat* conditions (Table 2.6 entry 1-2), whilst diethylether showed no improvement (entry 3). The other solvents tested all inhibited reactivity with only trace product being observed (entries 4-6).

Table 2.6 Screening of Solvent

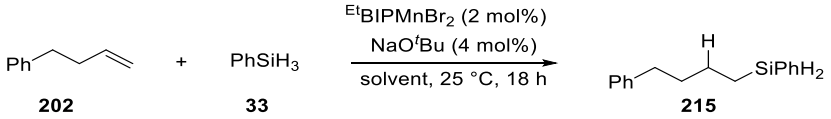

202 33 215

Entry	Solvent	Yield %[a]
1	*Neat*	42
2	Tetrahydrofuran	69
3	Diethylether	41
4	Toluene	2
5	Dichloromethane	1
6	Acetonitrile	0

Reaction conditions: Alkene (0.5 mmol), $HSiR_3$ (0.63 mmol), catalyst (0.01 mmol), NaO^tBu (0.03 mmol), solvent (0.5 mL), 25 °C, 18 h. a) Yield determined by ^1H NMR of the crude reaction mixture, using 1,3,5-trimethoxybenzene as an internal standard, as an average of two runs. Selectivity for the linear hydrosilylation product is >95%

Whilst phenylsilane **33** had been shown to work well with aliphatic alkenes, the hydrosilylation products are not particularly synthetically or industrially useful so other silanes were tested to gauge reactivity. Given the twofold role of the silane, as an activator and as a reagent, the silane choice would be important. Silanes would need to be capable of forming a silicon-ate species **F** able to transfer hydride to the pre-catalyst **A** in addition to participating in the oxidative addition **B-C** and reductive elimination **D-B** steps of the catalytic cycle of a typical hydrosilylation reaction (Scheme 2.19).

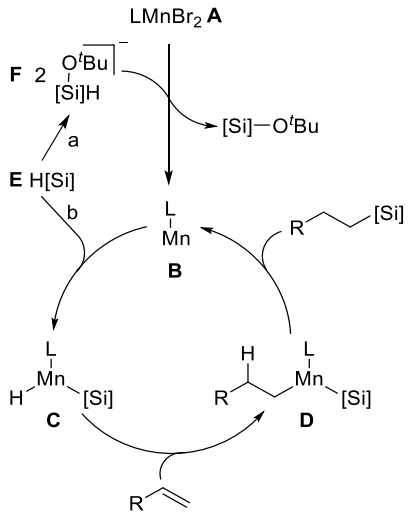

Scheme 2.19 The dual role of silane in the hydrosilylation of alkene. a) as an activator for the manganese pre-catalyst and b) as a silane reagent.

Hexylsilane **216** gave a moderate yield of 31% but this was significantly less than phenylsilane **33** (Table 2.7. entry 1-2). A secondary silane, diphenylsilane **62** only gave trace hydrosilylation product (entry 3). A range of tertiary silanes were tested: triethylsilane **19** (entry 4) and siloxane $HSiMe(OSiMe_3)_2$ **23** (MD'M) (entry 5) gave no conversion to the hydrosilylation product. When triethoxysilane **47** was used (entry 6) the reaction proceeded with quantitative conversion. Dimethoxymethylsilane **217**, which is a safe alternative to triethoxysilane (due to the inert $Si–CH_3$ bond being unable to disproportionate) was able to undergo hydrosilylation in a 37% yield (entry 7).

Table 2.7. Screening of Silane

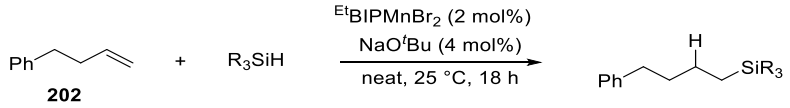

Entry	Silane	Yield %[a]
1	$PhSiH_3$ **33**	85
2	$H_{13}C_6SiH_3$ **216**	31
3	Ph_2SiH_2 **62**	5
4	$HSiEt_3$ **19**	0
5	$HSiMe(OSiMe_3)_2$ **23**	0
6	$HSi(OEt)_3$ **47**	>95
7	$HSiMe(OMe)_2$ **217**	37

Reaction conditions: Alkene (0.5 mmol), $HSiR_3$ (0.63 mmol), catalyst (0.01 mmol), reductant (0.03 mmol), solvent, 25 °C, 18 h. a) Yield determined by ^1H NMR of the crude reaction mixture, using 1,3,5-trimethoxybenzene as an internal standard, as an average of two runs. Selectivity for the linear hydrosilylation product is >95%

Notably, upon addition of $HSi(OEt)_3$ **47** to the reaction mixture, the reaction instantly effervesced as a gas was formed. The reaction rapidly changed from orange to brown suggesting activation of the catalyst. Alkoxy hydrosilane compounds are known to rapidly disproportionate when mixed with alkoxide salts to the tetraalkoxysilane and SiH_4.[178] SiH_4 is a highly flammable gas which can spontaneously ignite when exposed to air. The mechanism for the catalyst activation proposes the formation of a pentavalent siliconate **218** intermediate. In the absence of a hydride acceptor this intermediate would disproportionate with another molecule of triethoxysilane **47** to give a dihydrosilane **219** and tetraethoxysilane **220** (Scheme 2.20 A).[64] Assuming the manganese pre-catalyst intercepts the siliconate species then the facile nature of alkoxysilane disproportionation could explain why triethoxysilane is a more active silane for the reaction (Scheme 2.20 B). Importantly as manganese acts as a hydride acceptor the disproportionation of the silane is surpressed and only trace $R–SiH_3$ is typically observed by ^1H NMR of the crude reaction mixture. Additionally, silanes more electron-withdrawing substituents tend to undergo faster oxidative addition due to

greater polarisation of the Si–H bond.[179] Therefore, triethoxysilane is likely to also undergo faster oxidative addition to the manganese centre than alkylsilanes or monosubstituted silanes such as phenylsilane.

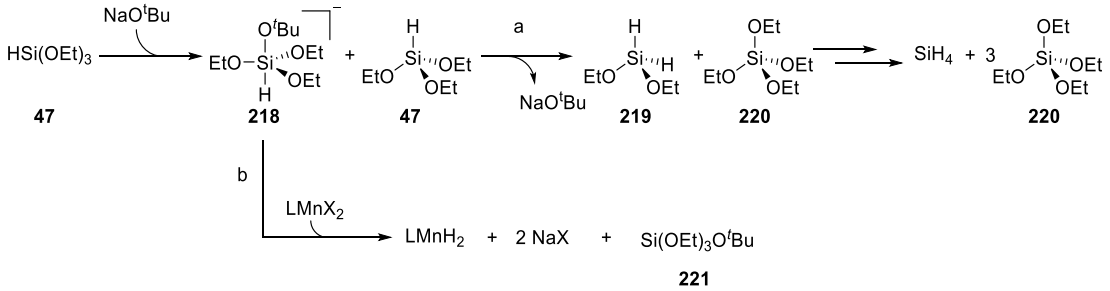

Scheme 2.20 The potential fates of the silicon-'ate' intermediate in the reaction. A) disproportionation to SiH_4 and $Si(OR)_4$. B) interception of the 'ate' intermediate by $LMnX_2$ to form MnH_2, NaX and $Si(OR)_3O^tBu$.

As triethoxysilane **47** gave significantly increased product yield compared to phenylsilane, a screen of substrates and solvent choice were tested with the newly established conditions. The hydrosilylation of 4-phenyl-1-butene **202** proceeded in high yields with all trialled solvents, but not to quantitative conversion as was the case using *neat* conditions (Table 2.8. entries 1-4). 1-Octene **22** underwent hydrosilylation under the conditions in quantitative yield, as expected (entry 5). When using triethoxysilane, 4-*t*butylstyrene **203** yielded 27% of hydrosilylation product, the first time in this project that the hydrosilylation of styrenes proceeded above trace yield (entry 6). The hydrosilylation of cyclooctene only proceeded with trace yield (entry 7).

Table 2.8. Screening with $HSi(OEt)_3$

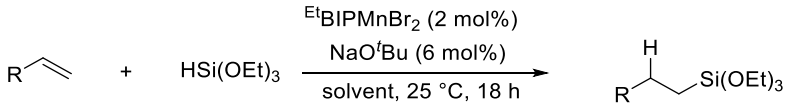

Entry	Substrate	Solvent	Yield %[a]
1	4-Phenyl-1-butene	*neat*	>95
2	4-Phenyl-1-butene	THF	93
3	4-Phenyl-1-butene	Et_2O	81
4	4-Phenyl-1-butene	C_7H_8	88
5	1-Octene	*Neat*	>95
6	4-*t*Butylstyrene	*Neat*	27
7	Cyclooctene	*Neat*	trace

Reaction conditions: Alkene (0.5 mmol), $HSiR_3$ (0.63 mmol), catalyst (0.01 mmol), reductant (0.03 mmol), *neat*, 25 °C, 18 h. a) Yield determined by ^1H NMR of the crude reaction mixture, using 1,3,5-trimethoxybenzene as an internal standard, as an average of two runs. Selectivity for the linear hydrosilylation product is >95%.

As styrene derivatives are an important class of alkenes, we decided to optimise for the hydrosilylation of styrenes using triethoxysilane **47**. A range of catalysts were screened in tetrahydrofuran and *neat* conditions. In all cases, the screened catalysts performed worse in solvent than under *neat* conditions. It appeared that bis(imino)pyridine ligands with bulkier *N*-aryl substituents were most active (Table 2.9. Entry 1a and 2a). This is somewhat atypical as for iron and cobalt bis(imino)pyridine catalysts smaller *N*-aryl substituents generally give more active catalysts.[12,42,84,157] Additionally, iron and cobalt analogues, tend to show a higher TOF and TON than displayed here.[42,89] Therefore, it is plausible that the larger substituents on the imine side-arm are stabilising the catalyst and preventing catalyst degradation rather than facilitating the generation of a more active catalyst. The activity of $^{DIPP}BIPMnBr_2$ **197** here highly contrasts with previous results (table 2.3. entry 1a-c) using phenyl silane **33**. The choice of silane clearly has a major effect on catalyst reactivity. The ability of triethoxysilane **47** to rapidly form the siliconate species and its comparably facile oxidative-addition are likely reasons for the observed reactivity with $^{DIPP}BIPMnBr_2$ **197**. To further exploit this further we heated the

reaction to 60 °C (entry 2c and 4c). This led to higher conversion of starting material but to a mixture of linear and branched hydrosilylation products. With ^{DIPP}BIPMnBr$_2$ **197** the branched hydrosilylation product was formed in a 2:3 ratio to the linear product, along with a significant proportion of the hydrogenation product. When trialling ^{DIPP}BIPMnCl$_2$ **208** at 60 °C, we obtained the highest yield of the linear hydrosilylation product of ^{t}butylstyrene (57%). However, 18% of the branched hydrosilylation product and 14% of the hydrogenation product were also observed. The increased activity of the bromide analogue over the chloride analogue, at 25 °C, led us to synthesise ^{DIPP}BIPMnI$_2$ **223**. However, while this gave comparatively good yields, it was still inferior to that of ^{DIPP}BIPMnBr$_2$ **197**.

Table 2.9. Catalyst and solvent screening of ^{t}butylstyrene with triethoxysilane

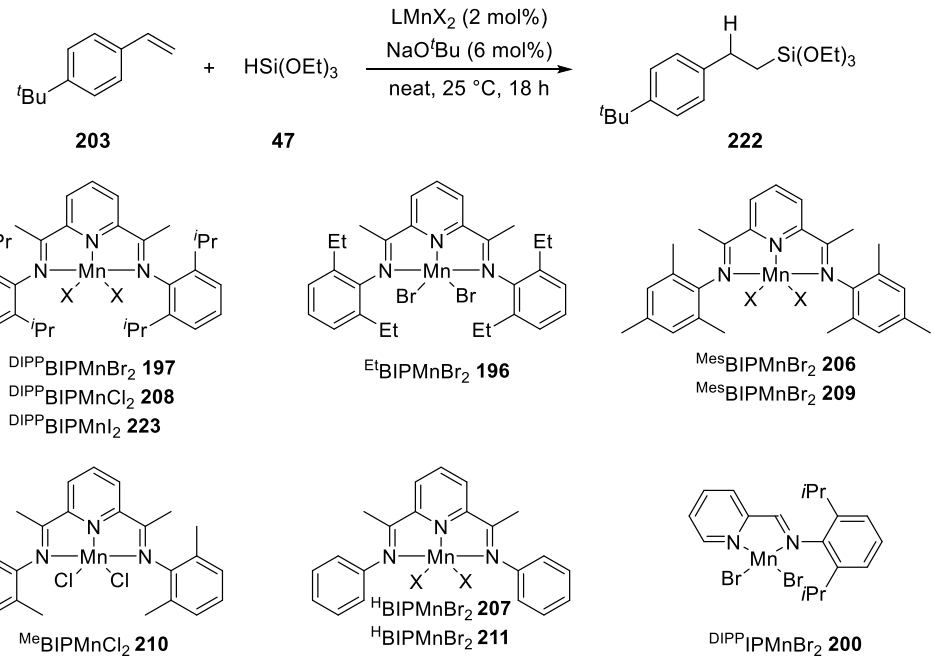

Entry	Catalyst	Solvent	Yield %[a]
1a	^{Et}BIPMnBr$_2$ **196**	*neat*	27
1b		THF	4
2a		*neat*	37[b]
2b	^{DIPP}BIPMnBr$_2$ **197**	THF	3

2c		*neat*	30[b]
3a	^{Mes}BIPMnBr$_2$ **206**	*neat*	16
3b		THF	trace
4a		*neat*	13[c]
4b	^{DIPP}BIPMnCl$_2$ **208**	THF	8
4c		*neat*	57[c]
5a	^{Mes}BIPMnCl$_2$ **209**	*neat*	trace
5b		THF	trace
6a	^{Me}BIPMnCl$_2$ **210**	*neat*	3
6b		THF	trace
7a	^{H}BIPMnCl$_2$ **211**	*neat*	0
7b		THF	0
8a	^{DIPP}BIPMnI$_2$ **223**	*neat*	19

Reaction conditions: Alkene (0.5 mmol), $HSiR_3$ (0.63 mmol), catalyst (0.01 mmol), NaO^{t}Bu (0.03 mmol), *neat*, 25 °C, 18 h. a) Yield determined by ^{1}H NMR of the crude reaction mixture, using 1,3,5-trimethoxybenzene as an internal standard, as an average of two runs. Selectivity for the linear hydrosilylation product is >95%. b) reaction was heated to 60 °C and also yielded 7% of the hydrogenation product and 20% of the branched hydrosilylation product. c) reaction was heated to 60 °C and also yielded 14% of the hydrogenation product and 18% of the branched hydrosilylation product.

A range of activators were tested for hydrosilylation using triethoxysilane **47** and ^{Dipp}BIPMnBr$_2$ **197** as a catalyst. Organometallic activators were still inactive under the conditions (Table 2.10. entries 1 and 2) but under these conditions a range of alkoxide salts were effective (entries 3-5), in contrast to the conditions using $PhSiH_3$ and ^{Et}BIPMnBr$_2$. KO^{t}Bu was almost as effective as NaO^{t}Bu with near quantitative conversion of starting material. NaOMe was also capable of facilitating the formation of the active catalyst, however the yield of hydrosilylation product was significantly below that when using bulkier alkoxides.

Table 2.10. Screening of different activators

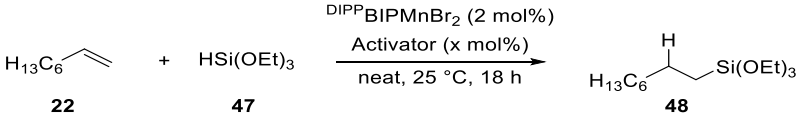

22 **47** **48**

Entry	Activators	Mol %	Yield %[a]
1	EtMgBr[b]	4	0
2	$NaHBEt_3$[c]	4	0
3	NaO*t*Bu	6	>95
4	KO*t*Bu	6	94
5	NaOMe	6	48

Reaction conditions: Alkene (0.5 mmol), $HSiR_3$ (0.63 mmol), catalyst (0.01 mmol), activator (0.03 mmol), *neat*, 25 °C, 18 h. a) Yield determined by ^1H NMR of the crude reaction mixture, using 1,3,5-trimethoxybenzene as an internal standard, as an average of two runs. Selectivity for the linear hydrosilylation product is >95%**.** b) 3M in Et_2O. c) 1M in THF.

2.4 Substrate Scope

2.4.1 Scope of Alkene

With optimised conditions in hand, a screen of different substrates was carried out. Firstly, a range of alkenes were tested. The number and type of substituent on the alkene was investigated (Scheme 2.21). During the optimisation of this methodology, monosubstituted terminal alkenes were shown to work in high yield. However, increasing substituents to di-substituted alkenes led to decreased catalytic activity. 1,1-Disubstituted alkenes (α-methylstyrene **205**, limonene **224**) and 1,2-disubstituted alkenes (*trans*-oct-4-ene **225**) were both unreactive. The use of a strained 1,2-disubstituted alkene, norbornene **226**, gave a 22% yield of hydrosilylation product. Trisubstituted 2-methyl-2-butenenitrile **227** was unreactive however the presence of a nitrile functional group, which can coordinate to metal centres, could also impact on the reactivity in addition to the sterically hindered alkene. Conjugated 1,4 dienes, myrcene **73**, were also tested and they too proved to be unreactive under the reaction conditions.

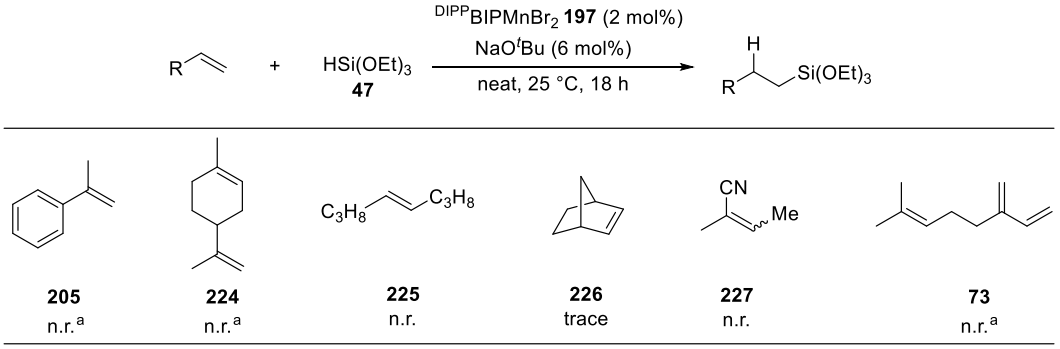

Reaction conditions: Alkene (0.5 mmol), $HSiR_3$ (0.63 mmol), catalyst (0.01 mmol), NaO^tBu (0.03 mmol), *neat*, 25 °C, 18 h. a) Yield determined by ^1H NMR of the crude reaction mixture, using 1,3,5-trimethoxybenzene as an internal standard, as an average of two runs. Also tested using $^{Et}BIPMnBr_2$ and $PhSiH_3$ to give the same result.

Scheme 2.21 Attempted substrates containing di- and trisubstituted alkenes

A range of terminal alkenes were trialled and, in all cases, the linear hydrosilylation product was obtained in high yields and with excellent regioselectivity. Isolated products were purified by vacuum distillation as the triethoxysilane motif is unstable to silica gel column chromatography. As shown during optimisation, simple alkenes underwent hydrosilylation in high yields (Scheme 2.22 5a – 5c). The hydrosilylation of allylbenzene **230** proceeded in an 81% yield, with no isomerisation to the alkene being observed. The methodology was entirely chemoselective for the reduction of a terminal alkene over an

internal alkene **231**. Terminal amines were tolerated with a morpholine derived alkene giving high yield of the hydrosilylation product **232**. The trifluoromethyl functional group **233** was well tolerated in the reaction, as were derivatives containing aryl C–F **234** and C–Cl **235** bonds. However, aryl C–Br **236** bonds lead to reduced yields (41%). Whilst the protodehalogenated product was not observed, it is feasible that metal insertion into the C–X bond caused catalyst deactivation and therefore reduces the yield. Alternatively, Nakamura *et al.* have recently shown that hydrosilicate intermediates are capable of reacting with aryl-bromides to give the silylated aryl product.[180] 4-*tert*-Butylstyrene **237**, 4-methoxystyrene **238** and styrene **239** all underwent hydrosilylation with a moderate yield of product. Notably the branched product was also observed for all three styrenes, with an 81:19 ratio of linear product to branched product observed when styrene was the substrate. The presence of alkenyl α-heteroatoms caused the reaction to stop working. Vinyl ether **242** gave trace reaction product, while the commercially significant alkene **241** gave no reaction. Vinyltrimethoxysilane **240** displayed no reactivity which contrasted to the related compound allyltriethoxysilane **229** with the only significant difference being the proximity of the silicon heteroatom (in this instance, vinylic) to the alkene.

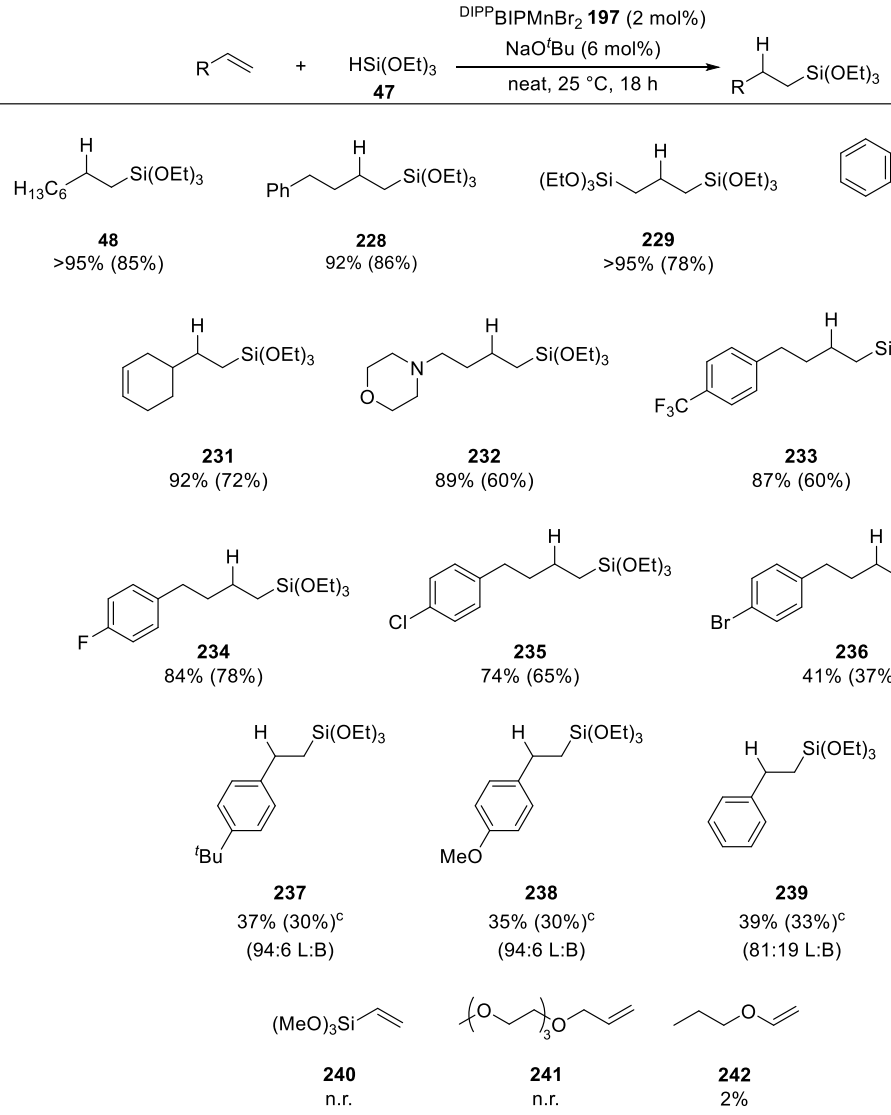

Reaction conditions: Alkene (0.5 mmol), $HSiR_3$ (0.63 mmol), catalyst (0.01 mmol), NaO^tBu (0.03 mmol), *neat*, 25 °C, 18 h. a) Yield determined by ^1H NMR of the crude reaction mixture, using 1,3,5-trimethoxybenzene as an internal standard, as an average of two runs.

Scheme 2.22 Substrate screen of terminal alkenes containing a range of functionality.

The incorporation of substrates bearing reducible functionalities was difficult in this methodology as triethoxysilane **47** has been previously reported to reduce aldehydes, ketones and esters in the presence of fluoride or alkoxide salts to give the silyl ether product (Scheme 2.23 A).[181–183] This has been proposed to occur through siliconate formation. Corriu and co-workers showed that the direct addition of a range of hydrosilicate species (including potassium tetraethoxysilicate **244**) would reduce aldehydes, ketones, esters and alkyl halides (Scheme 2.23 B+C).[184] The hydrosilicate species can also deprotonate alkynes, with phenylacetylene **247** being deprotonated in

4 hours by potassium tetraethoxysilicate **244** (Scheme 2.23 D).[184] It has also been shown that the use of sub-stoichiometric quantities of metal alkoxides are sufficient to catalyse the asymmetric reduction of carbonyl compounds using triethoxysilane **47** (Scheme 2.23 E). This methodology utilises a chiral lithium alkoxide catalyst **250** in low loadings (0.4 mol%) to give the alcohol in good yields and moderate enantiomeric excess (ee).[185]

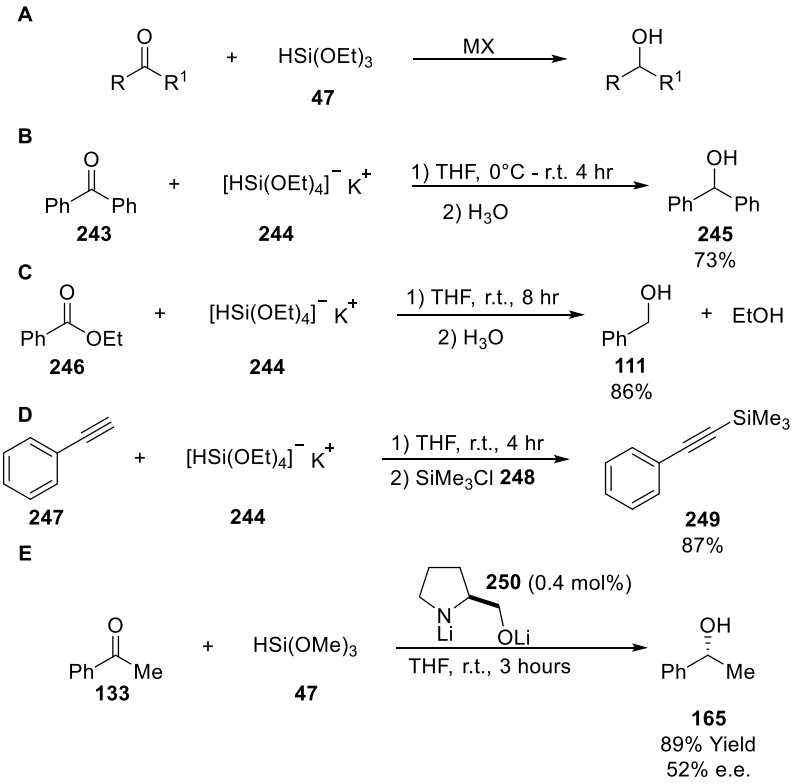

Scheme 2.23 Reactivity of hypervalent hydrosilane species with different functionalities. A) The reaction of triethoxysilane and carbonyl compounds in the presence of a fluoride or alkoxide salt B) Ketone reduction by a pre-formed hydrosiliconate species. C) Ester reduction by a pre-formed hydrosiliconate species. D) Alkyne deprotonation by a pre-formed hydrosiliconate species. E) Enantioselective reduction of acetophenone using a hydrosilane and a chiral amino alkoxide.

This reactivity offers an explanation for the limitations in functional group tolerance for this methodology. The methodology used an excess, with respect to catalyst, of NaO*t*Bu. The excess NaO*t*Bu can catalyse hydrosilicate formation which can then react with carbonyl functionalities outside of the catalytic process. 5-Hexen-2-one **61** saw both functionalities reduced when 3 equivalents of triethoxysilane **47** was used in the reaction (Table 2.11. Entry 1). However, when 1.25 equivalents of triethoxysilane **47** was used only the carbonyl functionality was reduced. The methodology was tested with two

different substrates with pendant ester groups. When methyl 4-(3-buten-1-yl)benzoate **252** was used as the substrate only the ester was reduced, in quantitative yields to the alcohol product **253** (Table 2.11. Entry 2). When methyl 10-undecenoate **254** was subjected to the conditions, some alkene hydrosilylation **255** was observed but only in low yields and the ester functionality remained intact (Table 2.11. Entry 3). 1-(4-Morpholinyl)-3-buten-1-one **256** gave a complex mixture of intractable products when subjected to the hydrosilylation conditions (Table 2.11. Entry 4). Allyl bromide **257** gave no observed hydrosilylation product, with protodebromination by the siliconate a potential deactivation pathway (Table 2.11. Entry 5; Scheme 2.24).

Table 2.11. Reaction of substrates containing reducible functionalities

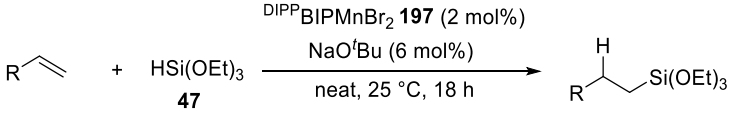

Entry	Substrate	Product	Yield %[a]
1	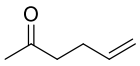 **61**	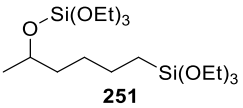 **251**	>95 (81)
2	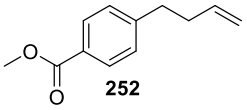 **252**	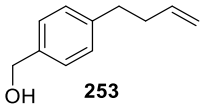 **253**	>95%
3	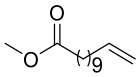 **254**	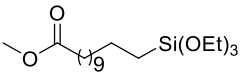 **255**	27%
4	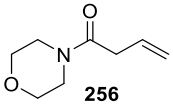 **256**	Complex mixture of starting material and reduction products	-
5	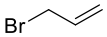 **257**	n.r.	-

Reaction conditions: Alkene (1 mmol), $HSiR_3$ (3 mmol), catalyst (0.02 mmol), reductant (0.06 mmol), *neat*, 25 °C, 18 h. a) Yield determined by ^1H NMR of the crude reaction mixture, using 1,3,5-trimethoxybenzene as an internal standard, as an average of two runs. Selectivity for the linear hydrosilylation product is >95%**.** Isolated yield in parenthesis.

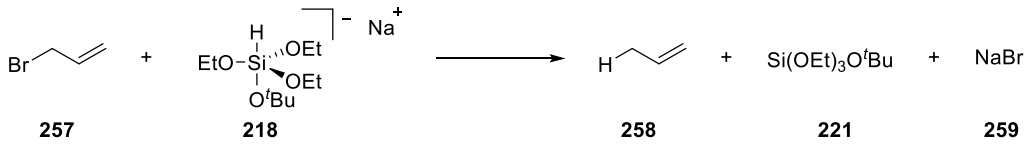

257 **218** **258** **221** **259**

Scheme 2.24 A potential deactivation pathway of a siliconate species in the presence of an alkyl bromide

A potential work around to the side reactions associated with the hydrosilicate reactivity would be to allow a pre-stirring period before the addition of substrate. This would allow for complete reaction of the hydrosilicate species with pre-catalyst before the substrate was introduced. However, bis(imino)pyridine species in the presence of NaO^{t}Bu can undergo ligand decomplexation making this approach unviable.

2.4.2 Scope of Silane

Although triethoxysilane **47** is an industrially important silane, its high reactivity in conjugation with alkoxide salts has limited the functional group tolerance of the system. A screening of other silanes would not only demonstrate the tolerance of the system but could potentially allow us to generate a system with increased functional group tolerance.

However, the silane screen using ^{DIPP}BIPMnBr$_2$ **197** was unproductive, with only triethoxysilane **47** giving any alkene hydrosilylation (Scheme 2.25). Even related alkoxysilanes such as methyldiethoxysilane **260** were unreactive. When the conditions were altered to use ^{Et}BIPMnBr$_2$ **196** the silane scope was broader. As previously discussed phenylsilane **46** would undergo hydrosilylation of octene **22** in quantitative yield. The yield of methyldiethoxysilane **260** was improved compared to earlier testing and full conversion and an 88% isolated yield of product was observed. Both these silanes retained the high regioselectivity seen with triethoxysilane **47**, however, diphenylsilane **261**, triethylsilane **262** and 1,1,1,3,5,5,5-heptamethyltrisiloxane **263** (MD'M) remained unreactive.

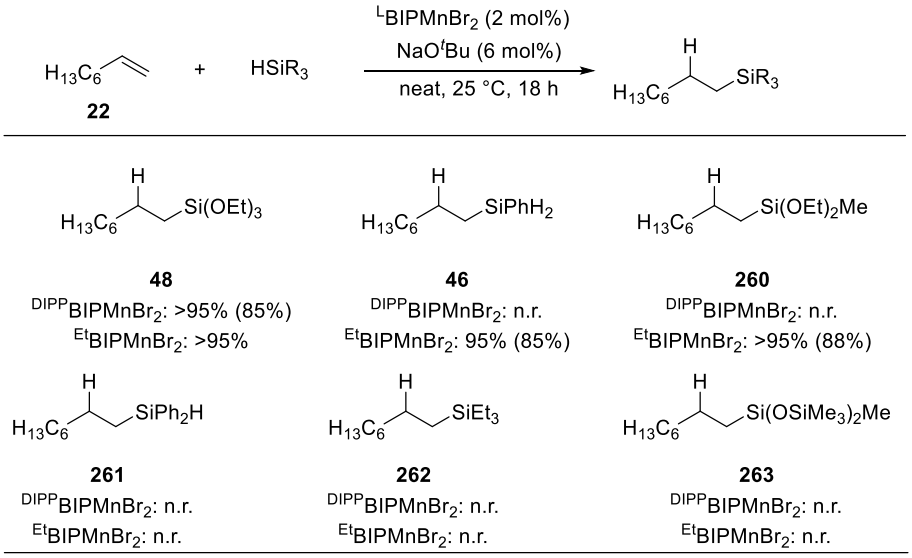

22

48
^{DIPP}BIPMnBr$_2$: >95% (85%)
^{Et}BIPMnBr$_2$: >95%

46
^{DIPP}BIPMnBr$_2$: n.r.
^{Et}BIPMnBr$_2$: 95% (85%)

260
^{DIPP}BIPMnBr$_2$: n.r.
^{Et}BIPMnBr$_2$: >95% (88%)

261
^{DIPP}BIPMnBr$_2$: n.r.
^{Et}BIPMnBr$_2$: n.r.

262
^{DIPP}BIPMnBr$_2$: n.r.
^{Et}BIPMnBr$_2$: n.r.

263
^{DIPP}BIPMnBr$_2$: n.r.
^{Et}BIPMnBr$_2$: n.r.

Reaction conditions: Alkene (0.5 mmol), HSiR$_3$ (0.63 mmol), catalyst (0.01 mmol), NaO^{t}Bu (0.03 mmol), *neat*, 25 °C, 18 h. a) Yield determined by ^{1}H NMR of the crude reaction mixture, using 1,3,5-trimethoxybenzene as an internal standard, as an average of two runs. Also tested using ^{Et}BIPMnBr$_2$ and PhSiH$_3$ to give the same result.

Scheme 2.25 Substrate screen of silanes

2.5 Gram-Scale Hydrosilylation of Octene

Hydrosilylation of 1-octene **22** typically had been carried out on a 0.5 mmol or 1.0 mmol scale. As the reaction was exothermic, under *neat* conditions and the formation of a gas presumed to be SiH_4 had been observed in the initial phase of the reaction, we envisioned the scale-up of the reaction could be difficult. The safety concerns led to the reaction to be carried-out in a sealed system, in an inert atmosphere as silane is only spontaneously flammable above a 10:1 SiH_4:O_2 ratio.[186] As triethoxy(octyl)silane **48** is a commercially important chemical and was made in high yields under our conditions we decided to fully optimise this reaction.[5] It was hoped that by increasing the reaction scale a lower catalyst loading could be used and therefore increasing the TON (turnover number) and TOF (turnover frequency) of the catalyst.

Gradually scaling-up by 4 times saw no impact on the yield (Table 2.13 entries 1-3). However, when the scale was increased to 4 mmol the reaction yield fell to 35% (entry 4). The increase of pressure in a sealed system on this scale, as well as the greater temperatures being reached by the reaction mixture could lead to catalyst decomposition, causing the lower yield. A potential solution to this was the lowering the catalyst concentration and therefore the activator concentration which would make the disproportionation of $HSi(OEt)_3$ **47** less rapid and give more controlled conditions. This worked to an extent as the yield rose when using 1 mol% of $^{DIPP}BIPMnBr_2$ **197** to 46% (entry 5) and to 67% when using 0.5 mol% of catalyst (entry 6). Further decreasing the catalyst loading led to lower yields and the formation of the branched regioisomer (entry 7 and 8).

Another potential issue is that the reaction vessel was unchanged from the small-scale experiments (6 mL reaction vessel) and to be able to perform the reaction on gram-scale an alternative vessel would need to be used. Initial testing on gram-scale (8.9 mmol) used a 25 mL round bottom flask and a catalyst loading of 0.2 mol %. The reaction was poorly yielding for the hydrosilylation of 1-octene **22** and the selectivity was poor compared to the small-scale reaction (entry 9). By adding alkene before the silane, it was hoped that the production of silane gas would be suppressed, and the reaction temperature would be more consistent. However, this led to lower conversions to hydrosilylation product (entry 10), potentially because siliconate formation would be less rapid in a more dilute mixture enabling residual NaO^tBu **49** to demetallate the pre-catalyst before activation could occur. Increasing the catalyst loading to 0.5 mol% led to increased yields of 49%

(entry 11). Switching from a 25 mL roundbottom flask to a small Schlenk tube (appox 12 mL volume, 1.5 cm internal diameter) led to the reaction to occur with a quantitative conversion (entry 12). The product was isolated by distillation to give 2.3 g of triethoxy(octyl)silane **48** in a 95% yield. Decreasing the catalyst loading to 0.1 mol% gave a conversion of 65% (entry 13). This result gave the highest obtained TON for this methodology with a TON of 650 being obtained. The highest TON for iron bis(imino)pyridine catalysed hydrosilylation is 2000 obtained by Chirik *et. al*.[42,89] Optimisation attempts in a larger Schlenk tube (~ 20 ml and 2.5 cm internal diameter) gave lower yields and poor regioselectivity (entry 14).

Table 2.13. Screening for the gram-scale hydrosilylation of 1-octene.

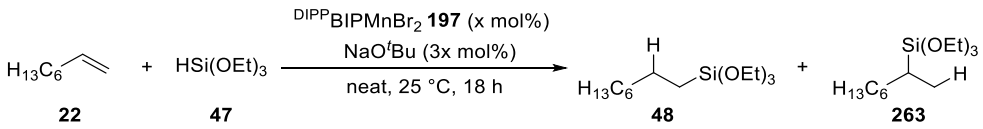

Entry	Scale (mmol)	Catalyst Loading (mol %)	Activator Loading (mol %)	Yield **48**	Yield **263**
1	.5[a]	2	6	85[b]	0[b]
2	1[a]	2	6	>95[b]	0[b]
3	2[a]	2	6	85[b]	0[b]
4	4[a]	2	6	35[b]	0[b]
5	4[a]	1	3	46[b]	0[b]
6	4[a]	.5	1.5	67[b]	0[b]
7	4[a]	.1	.3	55[b]	11[b]
8	4[a]	.01	.03	4[b]	7[b]
9	8.9[c]	0.2	0.6	20[d]	4[d]
10	8.9[c]	0.2	0.6	15[d]	Trace[d]
11	8.9[c]	0.5	1.5	49[d]	0[d]
12	8.9[e]	0.5	1.5	>95[d] (95)[f]	0[d]
13	8.9[e]	0.1	0.3	65[d]	0[d]
14	8.9[g]	0.5	1.5	25[d]	29[d]

Reaction conditions: Alkene, $HSiR_3$, catalyst, NaO^tBu, *neat*, 25 °C, 18 h. a) reaction performed in a 6 mL sealed tube. b) Yield determined by ^1H NMR of the crude reaction mixture, using 1,3,5-trimethoxybenzene as an internal standard, as an average of two runs. c) reaction performed in a 25 mL round bottom flask. d) Conversion determined by the ratio of products to starting material in an NMR of the crude reaction mixture, as an average of 2 runs. e) reaction performed in a 12 mL Schlenk tube. f) isolated yield obtained by distillation. g) reaction performed in a 25 mL Schlenk tube.

2.6 Mechanistic Investigations

During the reaction screening for the manganese-catalysed hydrosilylation of alkenes it was found that the *in situ* activation of the pre-catalyst would only give an active catalyst when a siliconate species was used as an activator. The use of related hydride species as activators such as $NaHBEt_3$ and $LiAlH_4$, failed to give an active catalyst. Previously, $BIPMn(II)X_2$ species have been reduced using a range of organometallic reagents. Gambarotta *et al.* had reduced $^{DIPP}BIPMnCl_2$ **196** using methyl lithium to give a formally manganese(I) reduction product **264** (Scheme 2.26).[162] It was proposed that a methyl radical elimination mechanism was responsible for reducing the manganese by one electron. By changing the reductant to $LiCH_2SiMe_3$, $^{DIPP}BIPMnCl_2$ **196** was reduced to a formally manganese(0) species **265**. The difference in observed reactivity is rationalised by the participation of the ligand when using $LiCH_2SiMe_3$ as a reductant. Bis(imino) pyridine ligands can accept electron density from the bound metal. This occurs when the metal becomes antiferromagnetically coupled to the bis(imino)pyridine triplet. Gambarotta and co-workers found that when this happened in their manganese species that the ligand could reductively couple with another molecule of pre-catalyst to give a dimeric species **267**.[187] This species was isolated and characterised by x-ray crystallography.

Chirik *et al.* had shown that the reduction of $^{DIPP}BIPMnCl_2$ using sodium naphthalene, in THF gave $^{DIPP}BIPMn(THF)_2$ **268** (Scheme 2.26).[167] The structural, electronic and spectroscopic properties of the complex were studied. These studies concluded that the high-spin manganese(II) centre was antiferromagnetically coupled to the bis(imino) pyridine triplet diradical ligand. The species was inactive in [2+2] cycloaddition and hydrogenation processes.

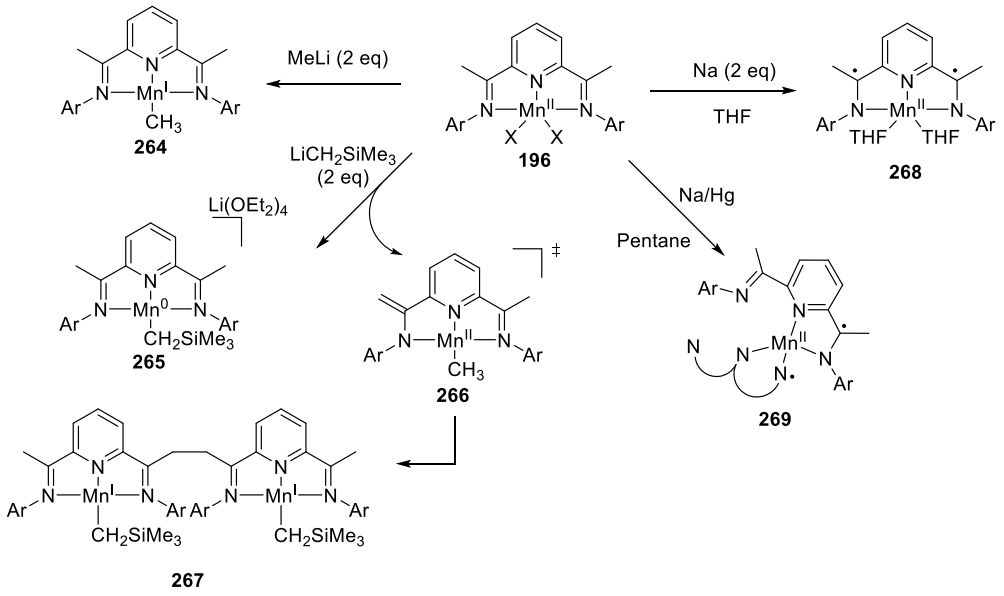

Scheme 2.26 Reductions of Manganese(II) complexes.

In order to ascertain insight into the reaction mechanism, attempts were made to isolate the reduction product of the manganese(II) pre-catalyst. Adding ^{DIPP}BIPMnBr$_2$ **197** to a THF solution of HSi(OEt)$_3$ **47** and NaO^{t}Bu **49** led to a rapid colour change from orange to purple. The order of addition was important as the addition of HSi(OEt)$_3$ **33** or THF after the introduction of ^{DIPP}BIPMnBr$_2$ **197** led to the formation of a pink solid, presumed to be manganese(II) dibromide. Filtering the purple solution through celite, washing with pentane and removing the solvent gave a purple solid. ^{1}H NMR analysis of the solid was uninformative. Many attempts were made to grow crystals of this solid however none of these attempts were successful. The solid was stirred with CH_3OD to probe if deuterium incorporation into the ligand would occur upon decomplexation however, no deuterium signals were present by NMR analysis.

The identity of the activating agent was also investigated. By mixing alkoxide and HSi(OEt)$_3$ in an NMR tube we were able to observe the formation of siliconate species *in situ* (scheme 2.27). The addition of KOEt to a solution of HSi(OEt)$_3$ **197** in d_8-tetrahydrofuran gave two peaks in the ^{29}Si NMR. The peak at -77.6 ppm was attributed to the formation of the siliconate species tetraethoxyhydrosilane **270**. The peak at -82.3 ppm is for tetraethyl orthosilicate, a decomposition product of HSi(OEt)$_3$ disproportionation. The addition of 0.5 equivalents with respect to of ^{DIPP}BIPMnBr$_2$ led to the complete removal of the siliconate peak from the spectra.

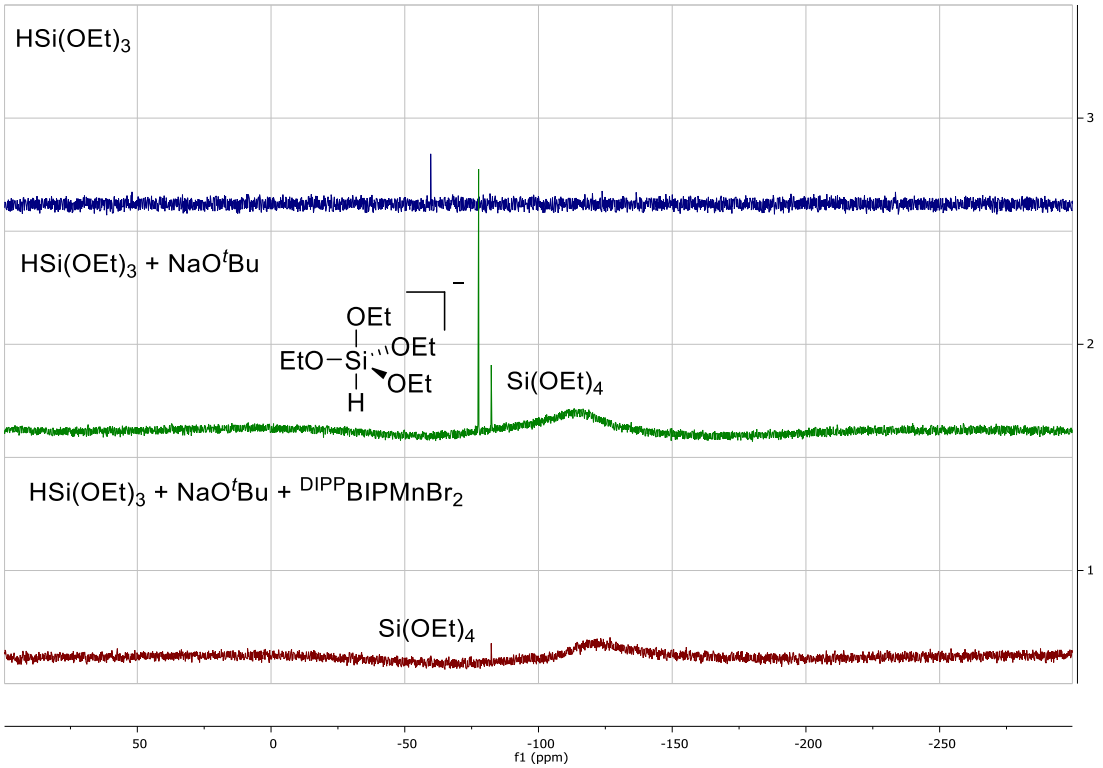

Scheme 2.27 ^{29}Si NMR spectra of siliconate formation and then quenching with ^{DIPP}BIPMnBr$_2$.

Deuterium labelling experiments were performed to test for reversible hydrometallation. 1,1,2-Trideutero-4-phenylbutene **273** was synthesised from 4-phenyl-1-butyne **271** by deprotonation with ^{t}BuLi and quenching with MeOD followed by alkyne semi-hydrogenation using D_2 gas and Lindlar's catalyst (Scheme 2.28).

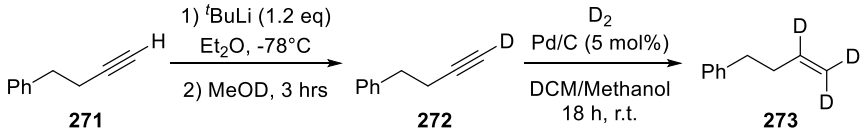

Scheme 2.28 Synthesis of d$_3$-4-phenyl-1-butene **273** from 4-phenyl-1-butyne **271**.

The hydrosilylation of 1,1,2-trideuterophenylbutene gave a distribution of products. The expected product **274** with a single hydrogen atom incorporated at the internal position of the alkene was the major product obtained (Scheme 2.29). Products containing two hydrogens **275** and two deuteriums **276** in the internal alkene position were also found. There was no evidence of deuterium incorporation α- to the silane.

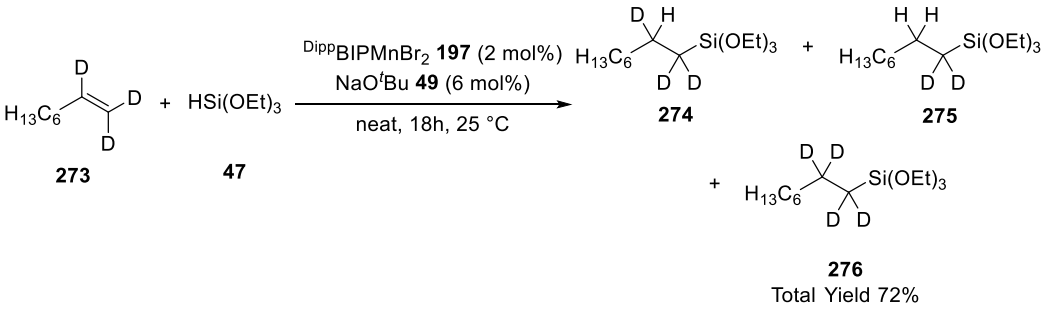

Scheme 2.29 Hydrosilylation of d_3-4-phenyl-1-butene.

The incorporation of multiple hydrogens or deuteriums in the C2 position is presumably due to reversible hydrometalation/β-hydride elimination steps in the mechanism (Scheme 2.30). Insertion of the d_3-alkene into a manganese–hydride bond (formed by oxidative addition of the hydrosilane would give an organomanganese intermediate. This intermediate could either undergo silicon-carbon reductive elimination, to give the major hydrosilylation product, or undergo β-hydride elimination to give 1,1-dideuterooctene. If this d_2-alkene then inserts into a second manganese–hydride bond and undergoes reductive elimination it would give the product bearing 2 hydrogen atoms in the C2-position. The absence of deuterium scrambling in the C1 position agrees with the observed regioselectivity of the hydrosilylation of 1-octene under standard reaction conditions.

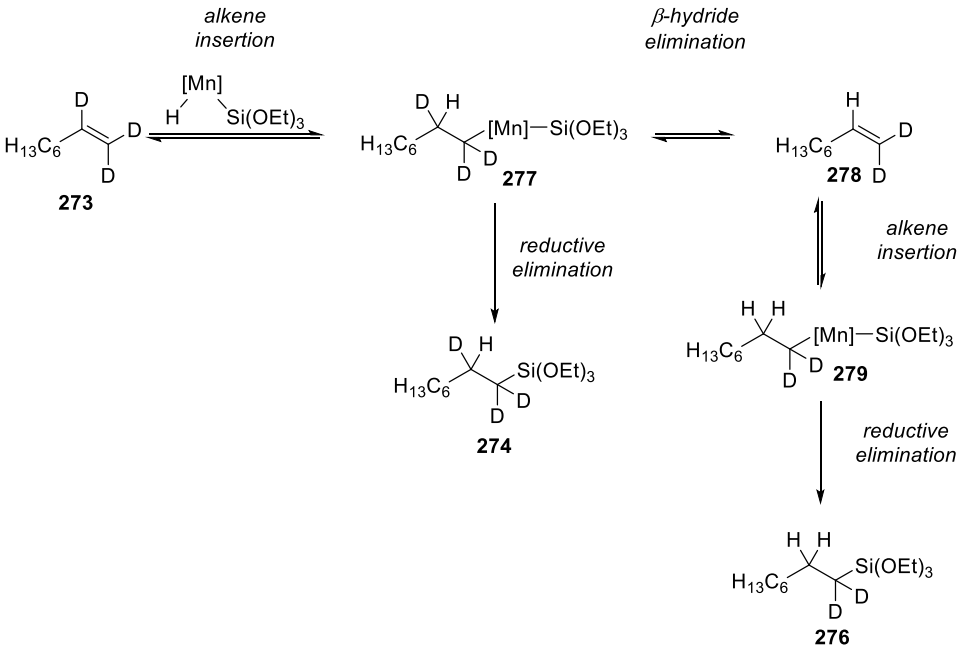

Scheme 2.30 Reversible hydrometallation/β-hydride elimination pathway for deuterium scrambling at the alkene.

In order to probe a potential radical mechanism, the addition of radical traps to the reaction were investigated. When low quantities of 2,2,6,6-tetramethylpiperidin-1-yl)oxyl (TEMPO, **277**, 1-2 mol%) were added to the standard reaction conditions there was no effect on yield (Table 2.14 entries 2 and 3). When the amount added was increased to 10 mol% and above, the yield of reaction started to decrease (entry 4 and 5). However, even when 100 mol% of TEMPO **277** was added to the reaction, there was still some observed reactivity (entry 6). There was no observed TEMPO-octene adduct or TEMPO-catalyst adduct so it is unlikely the reaction was inhibited due to radical trapping. Instead, radical traps have been reported to interact with metal-hydrides even in reactions which are known to operate by two-electron processes.[188] The use of further radical traps such as 3-carboyl-PROXYL **278** (entries 7-9) and Galvinoxyl **279** (entries 10-12) led to complete inhibition of catalyst activity. However, these radical traps bear amide groups which could either coordinate to the catalyst or act as a hydride acceptor for the siliconate species and prohibit catalyst activation. As a result, no reactivity was observed in these trials.

Table 2.14 Screening of radical traps and their impact on catalysis

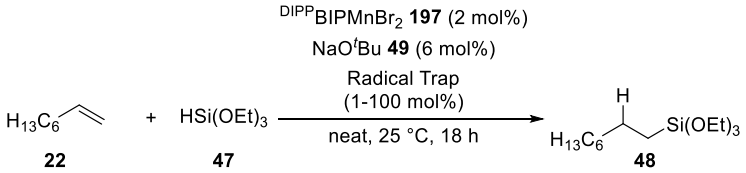

22 47 48

Entry	Radical Trap	Mol %	Yield %[a]
1	-	-	>95%
2		1	>95
3	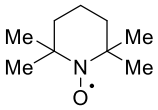 277	2	71
4		10	69
5		50	36
6		100	6
7		10	0
8	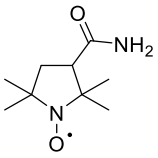 278	50	0
9		100	0
10		10	0
11	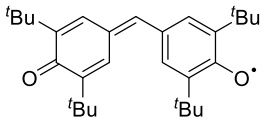 279	50	0
12		100	0

Reaction conditions: Alkene (0.5 mmol), $HSiR_3$ (0.63 mmol), catalyst (0.01 mmol), NaO^tBu (0.03 mmol), *neat*, 25 °C, 18 h. a) Yield determined by ^1H NMR of the crude reaction mixture,

using 1,3,5-trimethoxybenzene as an internal standard, as an average of four runs. Selectivity for the linear hydrosilylation product is >95%.

Dibenzo[*a,e*]cyclooctatetraene **283** (DCT) has been shown to be a selective poison of homogenous catalysts.[189] Given the use of strong reducing agents in the reaction, it is not inconceivable that manganese colloids or nanoparticles are formed in the reaction. For instance, Jacobi von Wangelin and co-workers had reduced a Mn(II) precursor to a Mn_6 cluster that was an active catalyst in hydrogenation reactions.[190] Whilst this test has not been applied to manganese, the test has proved indicative in examples with iron catalysts.[191,192] When DCT was added 10 minutes into the reaction it caused a decrease in the yield of the octene hydrosilylation product (table 2.15. entry 3+4) suggesting a homogeneous catalyst.

Trityl cations have been shown to accept hydrides from organometallic compounds.[193,194] If a manganese–hydride is on the catalytic cycle, the addition of trityl cation should inhibit catalysis. It should be noted that two potential hydride sources are present under reaction conditions: the *in situ* generated siliconate species and a potential manganese–hydride species (Scheme 2.31).

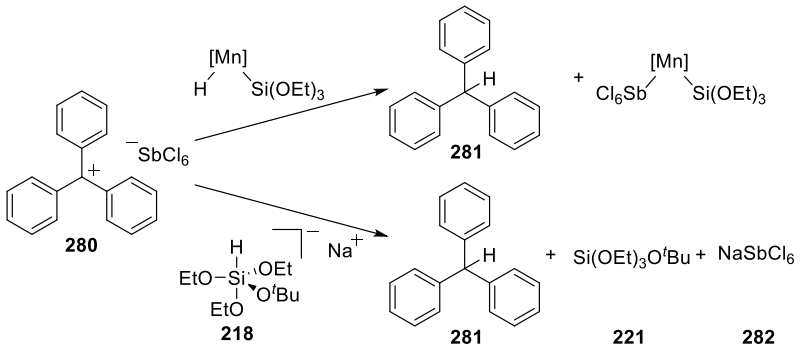

Scheme 2.31 Proposed quenching of manganese hydride and a hydrosiliconate by trityl cation.

When trityl hexachloroantimonate **280** is added before the reaction, no catalytic activity was observed. However, this was likely due to the hydride abstraction from the *in-situ* generated siliconate species **218**. The addition of trityl cation **280** 10 minutes after the

activation of the catalyst by siliconate should rule out inhibition of catalyst activation. The addition of stoichiometric amounts, with respect to catalyst, of trityl hexachloroantimonate **280** to a reaction after 10 minutes still led to complete inhibition of the reaction (Table 2.15, entry 5) equal to the quench by aqueous acid. The addition of 1 mol% and 0.5 mol% of trityl led to proportional increases in reactivity (entry 6 + 7). The addition of superstoichiometric quantities of trityl cation gave unclear results, as the diagnostic hydrosilylation peak in the NMR was broadened. This was presumed to be caused by the formation of trityl–OH upon reaction quenching with aqueous hydrochloric acid. This could interact with the hydrosilylation product and cause peak broadening.

Table 2.15 The impact of additives on the hydrosilylation of 1-octene

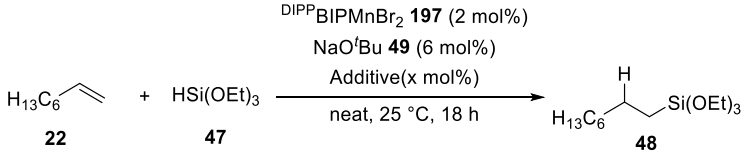

22 47 48

Entry	Additive	Mol %	Yield %[a]
1	-	-	>95%
2	HCl	Excess	12
3	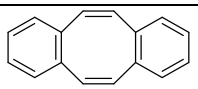 **283**	10	36
4		2	46
5	 **280**	2	11
6		1	44
7		0.5	47

Reaction conditions: Alkene (0.5 mmol), $HSiR_3$ (0.63 mmol), catalyst (0.01 mmol), NaO^tBu (0.03 mmol), *neat*, 25 °C, 4 h. Additive added after 10 mins from substrate addition. a) Yield determined by ^1H NMR of the crude reaction mixture, using 1,3,5-trimethoxybenzene as an internal standard, as an average of four runs. Selectivity for the linear hydrosilylation product is >95%.

The regioselectivity of the reaction also offers an insight into the mechanism (Scheme 2.32.). The regioselectivity is dictated by the hydrometalation step. Hydrometalation

could occur to give either a primary organometallic **285** or a secondary organometallic **286**. If a secondary organomanganese intermediate **286** was formed it would give the branched product **290**, whilst the primary organomanganese intermediate **285** would give the linear product **289**. Alternatively, if silylmetalation (alkene insertion into the manganese–silane bond) was to occur instead of hydrometalation, the secondary organomanganese intermediate **287** would give the linear product **289** and the primary organomanganese intermediate **288** would give the branched product **290**. Given the high regioselectivity observed for the linear product **289**, it is likely that the primary organometallic **285**, formed from hydrometallation, or the secondary organometallic intermediate **287**, formed from silylmetallation, would be predominately formed as the key intermediate. The increased inductive effect from an additional neighbouring carbon centre and the increased steric bulk would make the formation of the branched silylmetaltion intermediate **287** disfavoured. The formation of a primary organomanganese intermediate **285** would be thermodynamically favoured. This would give the predominate formation of the linear product **289**, as has been observed in experiments.

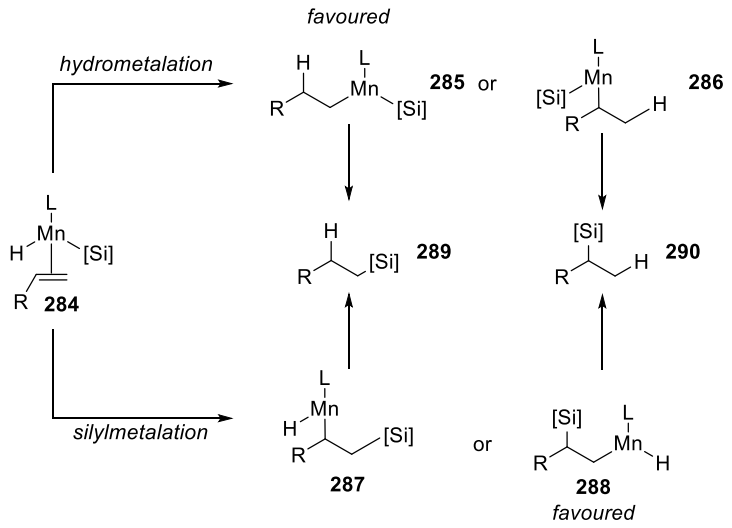

Scheme 2.32. Rationale for the regioselectivity based on the intermediate formed by hydro- and silylmetalation.

Using all these experiments, a mechanism was proposed (Scheme 2.33.). The manganese(II) pre-catalyst **A** is reduced by hydride transfer from an *in-situ* generated hydrosiliconate species. The manganese(II) dihydride complex **B** would then eliminate H_2 gas to give a formally low-oxidation state species **C**. The oxidation addition of silane would produce manganese–hydride **D**. Coordination of the alkene followed by alkene

insertion into the manganese–hydride bond would give organomanganese **F**. This would be followed by reductive elimination to form a carbon–silyl bond and regenerate the formally low oxidation-state manganese species.

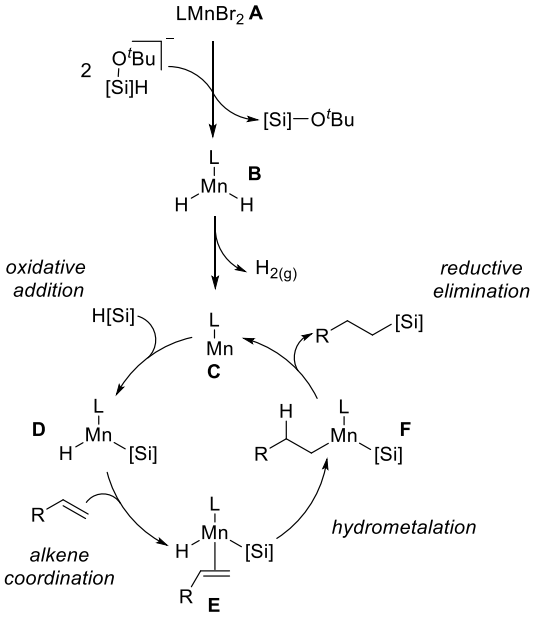

Scheme 2.33. Proposed mechanism for the hydrosilylation of alkenes.

2.7 Future Work and Conclusions

The manganese-catalysed hydrosilylation of alkenes has been developed, with broad substrate scope. The reaction is operationally simple and uses a bench-stable manganese pre-catalyst and activator.

A thorough optimisation of the methodology was performed. In particular, a range of bis(imino)pyridine ligands were comprehensively tested. Terpyridine and an imino(pyridine) ligand were also trialled however a comprehensive ligand screen has not been performed. There are numerous redox-active ligands known and by investigating manganese complexes bearing these ligands it may become possible to develop methodologies that give differing selectivity or are more active.

The methodology was applied to a range of substrates. Terminal, aliphatic alkenes were well tolerated, undergoing hydrosilylation in excellent yields with total control of regioselectivity. Whilst styrenes proceeded in lower yields, di- and tri-substituted alkenes were unreactive. When using ^{DIPP}BIPMnBr$_2$ only triethoxysilane was reactive but the closely related catalyst ^{Et}BIPMnBr$_2$ was capable of tolerating phenylsilane and diethoxymethylsilane.

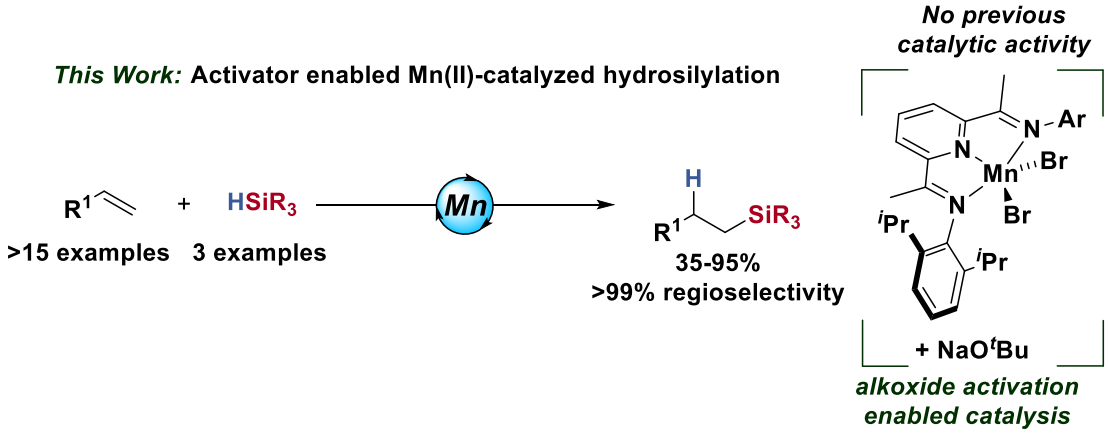

Scheme 2.34 Overview of the manganese-catalysed hydrosilylation of alkenes.

It was found that catalyst activation by sodium *tert*-butoxide was crucial for the catalysis to occur. Whilst attempts were made to isolate the reduced manganese species they were unsuccessful. If this key species could be characterised it would offer a key insight into the activation mechanism and help determine what makes the sodium *tert*-butoxide activation methodology so potent in this system.

A mechanistic investigation using 1,1,2-trideuterooct-1-ene showed deuterium scrambling suggesting that a reversible hydrometalation/β-hydride elimination step is key to the reaction mechanism. Quenching studies with trityl cation indicated that a manganese–hydride is probably generated in the reaction pathway. These experiments strongly suggest a Chalk-Harrod type mechanism is being followed in this methodology.

3. Manganese-Catalysed Hydroboration of Alkenes

3.1. State-of-the-Art at the Outset of the Project

Hydroboration is the addition of hydrogen and boron across an unsaturated bond. Unlike most other hydrofunctionalisations, hydroboration can proceed without a catalyst. Alkyl borane (9-BBN) or borane species (BH_3 **291**, B_2H_6) are capable of undergoing alkene hydroboration without a catalyst. However, the resulting products are unstable and are usually oxidised to the alcohol without being isolated. The synthesis of isolable hydroboration products necessitates the use of boronic ester reagents (catechol borane, pinacol borane **292**). These species are less electrophilic and require a catalyst for hydroboration to occur. Catalysed hydroboration reactions potentially possess a greater control of selectivity, allowing for chemo-, regio- or stereoisomers to be selectively formed.

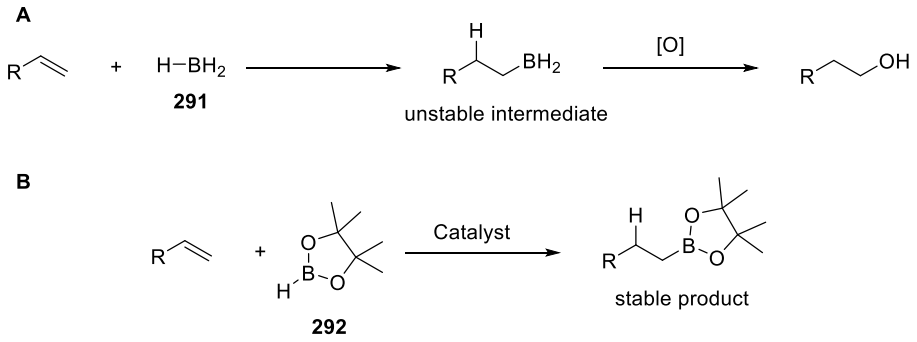

Scheme 3.1: A) Uncatalysed hydroboration of an alkene by BH_3 followed by an oxidation to form the primary alcohol. B) The catalysed hydroboration of an alkene using pinacol borane which gives a stable boronic ester product.

3.1.1 Catalysed Hydroboration Reactions

Männig and Nöth used Wilkinson's catalyst, $Rh(PPh_3)_3Cl$ **294**, to catalyse the hydroboration of 5-hexen-2-one **61** with catechol borane **293**.[195] When no catalyst was added, the hydroboration of the ketone **295** was observed, but the addition of Wilkinson's catalyst **294** gave complete selectivity for the alkene hydroboration product **296**. Additionally, it was shown that unfunctionalized alkenes would undergo uncatalyzed hydroboration by catechol borane at high temperatures. Meanwhile, the use of Wilkinson's catalyst allowed for the hydroboration of alkenes at room temperature. Whilst catechol borane **293** is more stable than alkyl boranes, it is still not easily isolated. Pinacol borane (HBPin) **292** is the most commonly used reagent which can provide access to bench-stable hydroboration products. Pereira and Srebnik used Wilkinson's catalyst **294** to catalyse the addition of pinacol borane **292** to a range of alkenes.[196] Mechanistic investigations suggests that the rhodium-catalysed reaction proceeds akin to the Chalk-Harrod mechanisms for hydrosilylation reactions.[197–201]

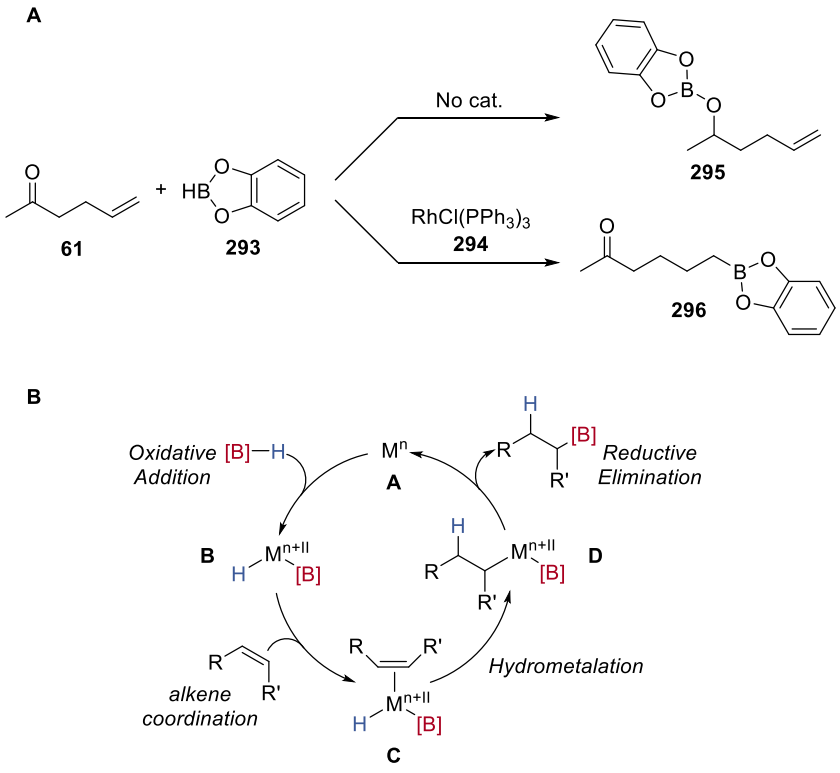

Scheme 3.2: A) The effect of adding a rhodium catalyst **294** on the hydroboration of 5-hexen-2-one **293**. B) The proposed mechanism for a catalysed hydroboration reaction.

Recently, efforts have gone into developing new hydroboration methodologies. Significant amounts of this research has focussed on the development of enantioselective hydroboration catalysts. This area has been previously reviewed[202] but a notable recent example was the development of a Markovnikov hydroboration of terminal alkenes that proceeded with good yields, high regioselectivity and good *ee* (Scheme 3.3).[203]

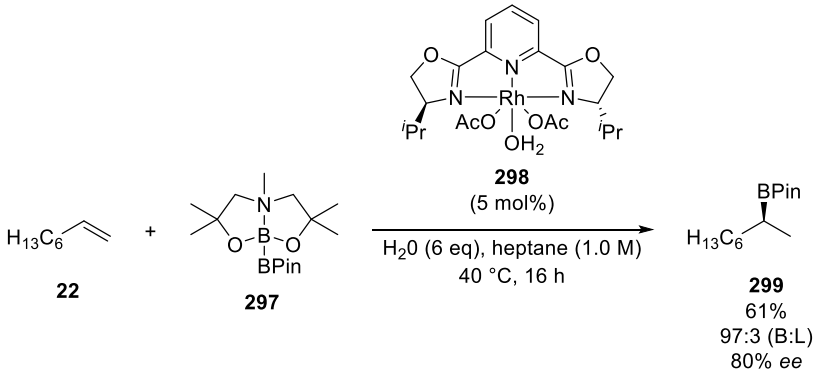

Scheme 3.3: An example of a Markovnikov-selective, enantioselective hydroboration of terminal alkenes by Aggarwal and co-workers.

Developments have also focused on the use of non-precious metals as catalysts in hydroboration, particularly iron and cobalt.[12,204] Notably, Zhang *et. al.* reported the first manganese-catalysed hydroboration of alkenes.[173] This methodology used a well-defined manganese(II) dialkyl catalyst bearing a terpyridine ligand **300**. The reaction was regiodivergent, with the regioselectivity dictated by the substrate. The hydroboration of styrene proceeded with Markovnikov selectivity **301** (Scheme 3.4A) whilst aliphatic alkenes underwent hydroboration in an anti-Markovnikov fashion **302** (Scheme 3.4B). The selectivity is presumably dictated by the formation of the thermodynamically favoured organomanganese intermediate (see structure D in Scheme 3.2). For aliphatic alkenes, the primary organometallic is favoured whilst for styrenes the secondary, benzylic organometallic is thermodynamically more stable.

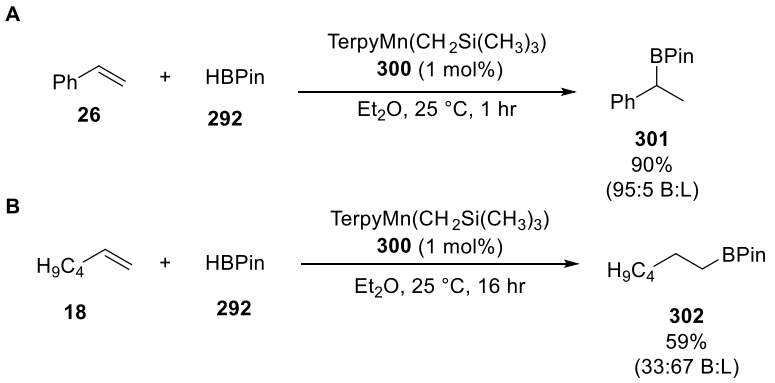

Scheme 3.4: A) Hydroboration of styrenes using a manganese(II) pre-catalyst **300** to give the Markovnikov hydroboration product **301**. B) Hydroboration of octene using a manganese(II) pre-catalyst **300** to give the *anti*-Markovnikov product **302**.

Recently, main group elements have been used as catalysts for hydroboration, particularly the metals in group 13.[205–212] Ingleson and co-workers reported the *trans*-hydroboration of alkynes which was mediated by a borenium cation **304** and $B(C_6F_5)_3$ **305** (Scheme 3.5A).[207] This was followed by a report by Stephan and co-workers of the hydroboration of alkynes using substoichiometric amounts of Piers' borane ($HB(C_6F_5)_2$ **307**) as an initiator for catalysis (Scheme 3.5B).[209] The boron-catalysed hydroboration of alkenes was reported by Oestreich and co-workers who used tris(3,5-bis(trifluoromethyl)-phenyl)borane, BAr^{F}_3 **309**, as a catalyst (Scheme 3.5C).[210] This work was also extended to the hydroboration of alkynes, ketones and imines.[211]

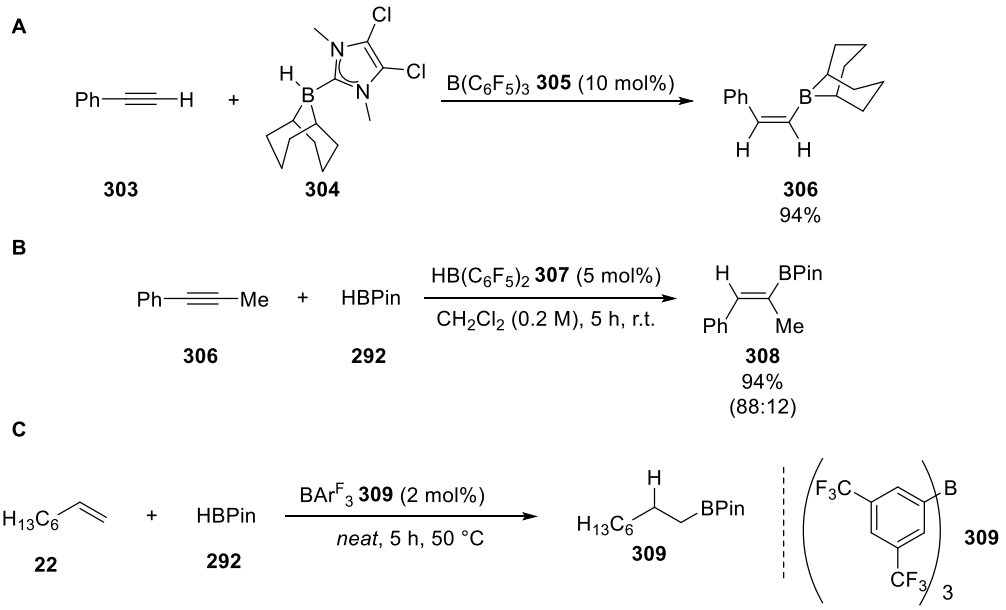

Scheme 3.5 A) Hydroboration of alkynes mediated by a borenium cation and $B(C_6F_5)_3$. B) Hydroboration of internal alkynes catalysed by Piers' borane. C) Alkene hydroboration catalysed by Bar^{F}_3.

Of the most relevance to this chapter, is the borane-catalysed hydroboration of alkynes and alkenes reported by Thomas and co-workers.[213] Here the formation of boronic esters by hydroboration was catalysed by BH_3 **291** (Scheme 3.6A). The reaction is proposed to proceed initially by BH_3 **291** hydroboration of the alkene **22** (akin to the uncatalyzed hydroboration methodology). The resulting alkylboron species **310** can then undergo either a transborylation or a ligand exchange to give the boronic ester product **309** (Scheme 3.6B).

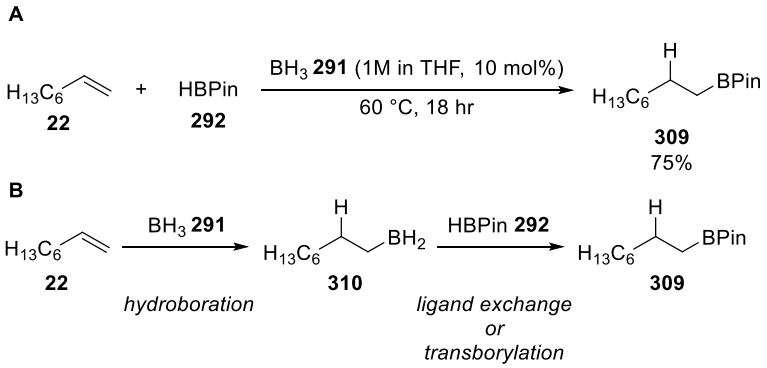

Scheme 3.6 A) Synthesis of alkyl boronic esters using BH_3 **291** as a catalyst. B) Proposed mechanism for the formation of boronic ester product **303**.

3.2 Project Aims

At the outset of the project there was no precedent for the manganese-catalyzed hydroboration of alkenes. Therefore, the project aimed to build upon the previously developed manganese-catalysed hydrosilylation of alkenes methodology (Chapter 2) and develop a methodology for the manganese-catalysed hydroboration of alkenes. Following the publication by Zhang *et. al.,*[173] shortly after the start of the project, we focused on exploring the differences between the methodologies. Particularly with styrenes derivatives, we observed a different regioselectivity, so this area was explored with a more thorough substrate scope than with aliphatic alkenes.

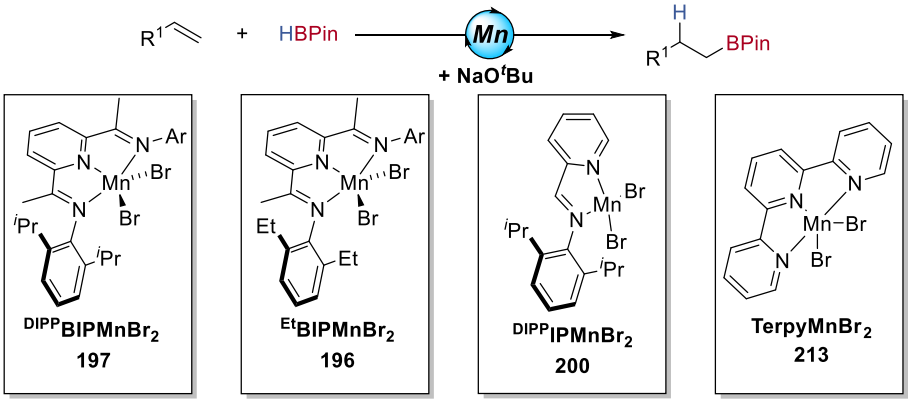

Scheme 3.7 Overview of the manganese-catalysed hydroboration of alkenes with potential catalysts.

3.3 Methodology Development

3.3.1 Reaction Discovery and Control Reactions

Whilst optimising the manganese-catalysed hydrosilylation of alkenes, several attempts to perform a similar hydroboration reaction were attempted by replacing the silane with pinacol borane **292**. Pinacol borane **292** also had precedent at being capable of the activation of first-row transition metals when mixed with sodium *tert*-butoxide **49**.[42]

Initial attempts focussed on modifying the procedure used for the hydrosilylation of alkenes by replacing the silane reagent with pinacol borane **292**. As attempts made using bis(imino)pyridine manganese pre-catalysts were initially unsuccessful. Investigations turned to other manganese catalysts. For instance, Sood *et. al.* had reported the use of an iminopyridine manganese(II) complex successfully catalysing ethene polymerisation at 60 °C.[172] In an effort to replicate these conditions the reaction temperature was raised to 60 °C. Under these increased temperatures $^{DIPP}IPMnBr_2$ **200** catalysed the hydroboration of octene **22** in a moderate yield (entry 7). By increasing the amount of pinacol borane **292** to 1.5 equivalents the reaction yield increased to 75% (Entry 8). When using $^{DIPP}BIPMnBr_2$ **197** as a pre-catalyst at 60 °C, the hydroboration of octene **22** proceeded in a comparable yield to $^{DIPP}IPMnBr_2$ **200** (Entry 9). Due to the simplicity of using the same catalyst for both hydrosilylation and hydroboration methodologies it was decided that the studies would focus on the bis(imino)pyridine catalyst.

Table 3.1 Initial screening reactions and discovery of the manganese-catalysed hydroboration of alkenes.

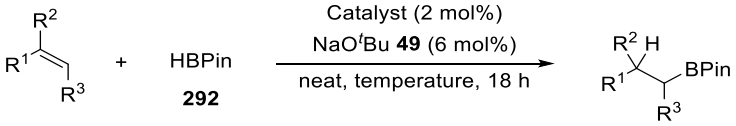

Entry	Substrate	t (°C)	Catalyst	Eq of HBPin	Yield (%)[a]
1	Octene	r.t.	^{Et}BIPMnBr$_2$	1.25	0
2	Octene	25	^{Et}BIPMnBr$_2$	1.25	0
3	Octene	25	^{DIPP}BIPMnBr$_2$	1.25	0
4	Octene	25	^{IP}BIPMnBr$_2$	1.25	0
5	Myrcene	25	^{IP}BIPMnBr$_2$	1.25	0
6	Myrcene	60	^{IP}BIPMnBr$_2$	1.25	0
7	Octene	60	^{IP}BIPMnBr$_2$	1.25	43
8	Octene	60	^{IP}BIPMnBr$_2$	1.50	75
9	Octene	60	^{DIPP}BIPMnBr$_2$	1.50	67

Reaction conditions: Alkene (0.5 mmol), HBPin (0.63 mmol), catalyst (0.01 mmol), NaOtBu (0.03 mmol), neat, 25 °C, 18 h. a) Yield determined by ^{1}H NMR of the crude reaction mixture, using 1,3,5-trimethoxybenzene as an internal standard, as an average of two runs. Selectivity for the linear hydroboration product is >95%

Control reactions showed that whilst ligand, metal salt and activator were all crucial for the highest yields to be obtained, there was a relatively high degree of background reactivity. In particular, running the reaction with only the activator, NaO^{t}Bu, present gave moderate amounts of the linear boronic ester (Table 3.2, entry 1). Using the manganese dibromide salt in conjunction with the alkoxide gave similar reactivity (entry 2) and using just the metal salt gave lower reactivity than only the alkoxide (entry 3). Free bis(imino)pyridine ligand gave no conversion of starting material to the hydroboration product (entry 4). Running the reaction with standard conditions but in air gave low yields of hydroboration (entry 5).

Table 3.2: Control reactions for the manganese-catalysed hydroboration of alkenes.

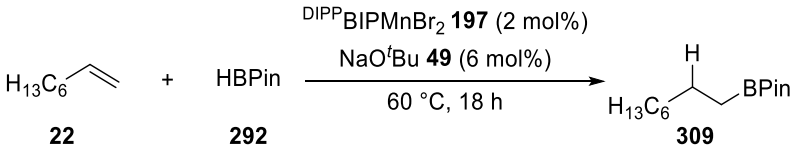

Entry	Alteration to standard conditions	Yield %[a]
1	Only NaO^tBu	41
2	$MnBr_2{\cdot}(THF)_2$ + NaO^tBu	44
3	$MnBr_2{\cdot}(THF)_2$	21
4	Only ^{DIPP}BIP	0
5	Ran in air	12

Reaction conditions: Alkene (0.5 mmol), HBPin (0.75 mmol), catalyst (0.01 mmol), NaO^tBu (0.03 mmol), neat, 25 °C, 18 h. a) Yield determined by 1H NMR of the crude reaction mixture, using 1,3,5-trimethoxybenzene as an internal standard, as an average of two runs. Selectivity for the linear hydroboration product is >95%

3.3.2 Methodology Optimisation

Initial attempts at optimising the reaction focussed on changing the temperature. Increasing the temperature of the reaction to 80°C did significantly increase the reaction yield (Table 3.3, entry 2) but decreasing the temperature below 60°C (entry 3) led to decreased yields even at higher loadings of HBPin **292** (entry 3).

Table 3.3: Optimisation of temperature

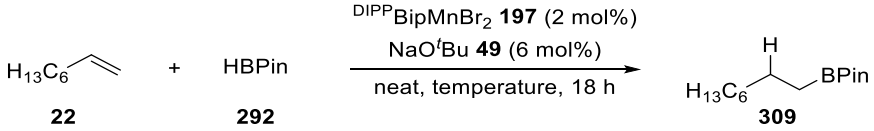

Entry	Amount of HBPin	Temperature (°C)	Yield (%)[a]
1	1.5	60	67
2	1.5	80	74
3	1.5	40	6
4	2.0	40	6

Reaction conditions: Alkene (0.5 mmol), HBPin (0.75/1 mmol), catalyst (0.01 mmol), NaO^{t}Bu (0.03 mmol), neat, 25 °C, 18 h. a) Yield determined by ^{1}H NMR of the crude reaction mixture, using 1,3,5-trimethoxybenzene as an internal standard, as an average of two runs. Selectivity for the linear hydroboration product is >95%

In general, the addition of solvent led to decreased yields. Ethereal solvents gave some activity but significantly inferior yields to neat conditions (Table 3.4, entries 1-3). Using toluene as the solvent gave a small improvement on the yield but dichloroethane, acetonitrile, ethyl acetate and dimethyl carbonate all gave no reaction or very low boronic ester yields (Table 3.4, entries 4-8).

Table 3.4. Screening of Solvent

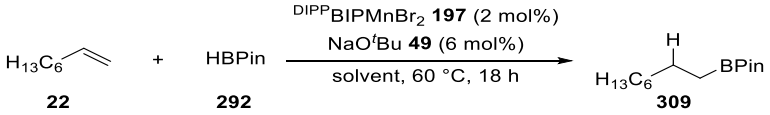

Entry	Solvent	Yield %[a]
1	Neat	67
2	Tetrahydrofuran	21
3	Diethylether	18
4	Toluene	28
5	Dichloroethane	6
6	Acetonitrile	0
7	Ethyl Acetate	0
8	Dimethyl carbonate	0

Reaction conditions: Alkene (0.5 mmol), $HSiR_3$ (0.75 mmol), catalyst (0.01 mmol), NaO^tBu (0.03 mmol), solvent (0.5 mL), 25 °C, 18 h. a) Yield determined by ^1H NMR of the crude reaction mixture, using 1,3,5-trimethoxybenzene as an internal standard, as an average of two runs. Selectivity for the linear hydroboration product is >95%

A range of bis(imino)pyridine ligands with sterically differentiated *N*-aryl groups were tested under the developed hydroboration conditions. These ligands were trialled in conjunction with both manganese bromide and manganese chloride salts (Table 3.4). $^{DIPP}BIPMnBr_2$ **197** (entry 1) and $^{DIPP}BIPMnCl_2$ **208** (entry 2) were the most active catalysts and the remaining catalysts all gave moderate to good yields. There was not a strong trend with respect to ligand size or the choice of counter-ion. It is notable how each catalyst was active for hydroboration, apart from $^{Mes}BIPMnX_2$ which only gave background reactivity (see Table 3.2). This contrasts with the previously developed manganese-catalysed hydrosilylation methodology where changing the steric properties of the bis(imino)pyridine ligand could lead to a large variation in reactivity.

Table 3.4. Screening of catalyst

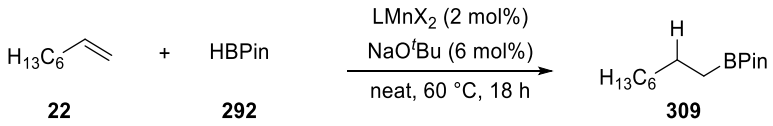

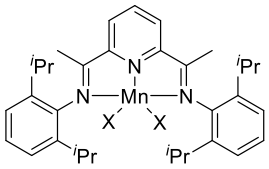

DIPPBIPMnBr2 197
DIPPBIPMnCl2 208

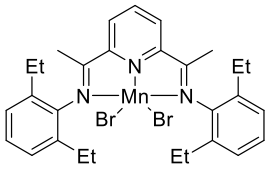

EtBIPMnBr2 196

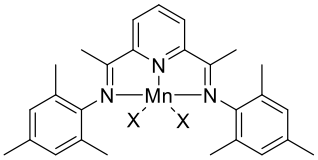

MesBIPMnBr2 206
MesBIPMnBr2 210

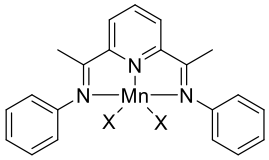

HBIPMnBr2 207
HBIPMnCl2 211

Entry	Catalyst	Yield %[a]
1	^{DIPP}BIPMnBr$_2$ **197**	67
2	^{DIPP}BIPMnCl$_2$ **208**	68
3	^{Et}BIPMnBr$_2$ **196**	61
4	^{Mes}BIPMnBr$_2$ **206**	44
5	^{Mes}BIPMnCl$_2$ **210**	47
6	^{H}BIPMnBr$_2$ **207**	52
7	^{H}BIPMnCl$_2$ **211**	60

Reaction conditions: Alkene (0.5 mmol), HBPin (0.75 mmol), catalyst (0.01 mmol), NaO^{t}Bu (0.03 mmol), neat, 25 °C, 18 h. a) Yield determined by ^{1}H NMR of the crude reaction mixture, using 1,3,5-trimethoxybenzene as an internal standard, as an average of two runs. Selectivity for the linear hydroboration product is >95%.

3.4 Substrate Scope

The generality and selectivity of the methodology was explored using HBPin **292** and a range of alkenes. Initial attempts were undertaken using ^{DIPP}BIPMnBr$_2$ **197** , NaO^{t}Bu **49** (in a 1:3 ratio) and 1.5 eq of HBPin **292**. Whilst consumption of the starting materials was in many cases quantitative, product yield determined by ^{1}H NMR of the crude reaction mixture using an internal standard showed that only moderate-good amounts of hydroboration product were formed. Attempts to purify the hydroboration products by distillation and flash column chromatography were difficult and led to poor yields. The resulting products were often yellow amorphous solids despite precedent identifying them as colourless oils. This suggested a competing polymerization reaction was taking place, consuming starting material and making purification non-trivial. As a result, the amount of HBPin **292** was increased from 1.5 to 3 equivalents giving increased yields of hydroboration and supressing polymerisation. The products were then easily purified by flash column chromatography with good retention of isolated yields compared to NMR analysis of the crude reaction.

A range of electronically and sterically differentiated styrene derivatives were subjected to the hydroboration conditions (Scheme 3.8). 4-*tert*-Butylstyrene underwent hydroboration in excellent yield (96%) with predominant formation of the *anti*-Markovnikov product **311** (90:10). The use of styrene derivatives bearing electron-withdrawing groups containing trifluoromethyl- **312**, fluoro- **313** and bromo-groups **314** proceeded in good yields (64%-74%) and high selectivity. 3-Methoxystyrene **315** underwent hydroboration in an excellent yield (99%) with slightly improved selectivity (93:7). A highly sterically hindered substrate, 2,4,6-trimethylstyrene was converted to the hydroboration product **316** in a significantly lower yield (31%) but with excellent control of regioselectivity (97:3). Hydroboration of 1,1-disusbtituted styrene, α-methylstyrene gave a 33% of the boronic ester product **317** but with excellent selectivity (>99:1). Aliphatic alkenes underwent hydroboration in high yields and with essentially complete control of regioselectivity.

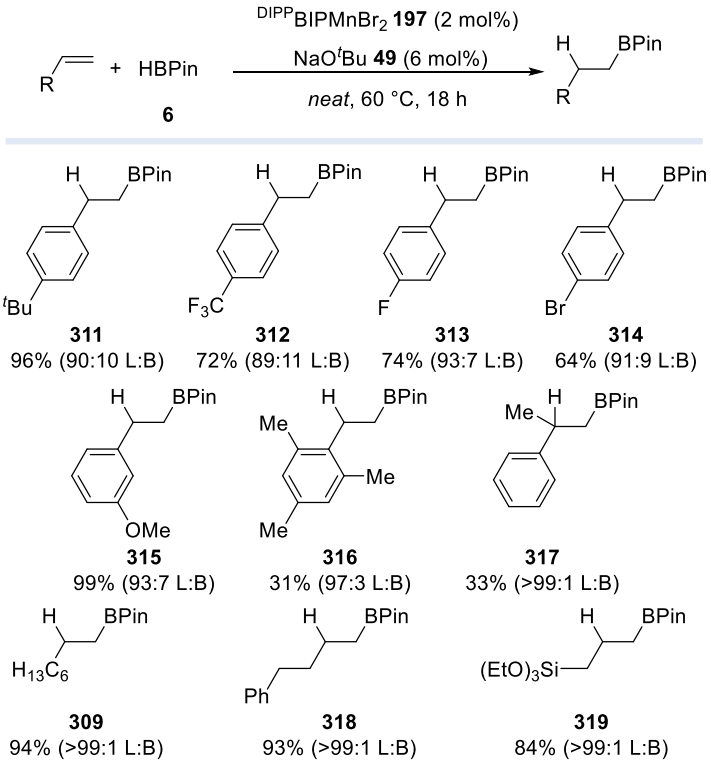

Scheme 3.8 Substrate scope for the manganese-catalysed hydroboration of alkenes.

When compared to the substrate scope of the previously developed hydrosilylation methodology there are some stark contrasts. Most noticeably in the hydroboration methodology is that styrene derivatives gave excellent yields of linear boronic esters. Substrates such as 2,4,6-trimethylstyrene and α-methylstyrene, which were unreactive under hydrosilylation conditions, exhibited some reactivity. If this method is compared to that of Zhang *et al.* there are also considerable differences. The terpyridine based system displayed *anti*-Markovnikov selectivity (although with significant Markovnikov product in some cases) for aliphatic alkenes and Markovnikov selectivity for styrene derivatives. It also was unreactive for α-methylstyrene. The method developed here is consistently selective for the *anti*-Markovnikov position across styrenes and aliphatic alkenes. In the case of aliphatic alkenes there was no observation of the Markovnikov product.

A range of alkenes were tested which were not reactive under the developed conditions including highly substituted alkenes, limonene **224**, (1,1-disubstituted alkene), oct-4-ene **225** (1,2-disubstituted) and myrcene **73** (1,4-disubstituted diene). Styrene derivatives bearing strongly electron-withdrawing groups were consumed under reaction conditions but did not convert to the hydroboration product. Given the broad

NMR spectra and viscosity of the resulting product, it was presumed a polymer was formed.

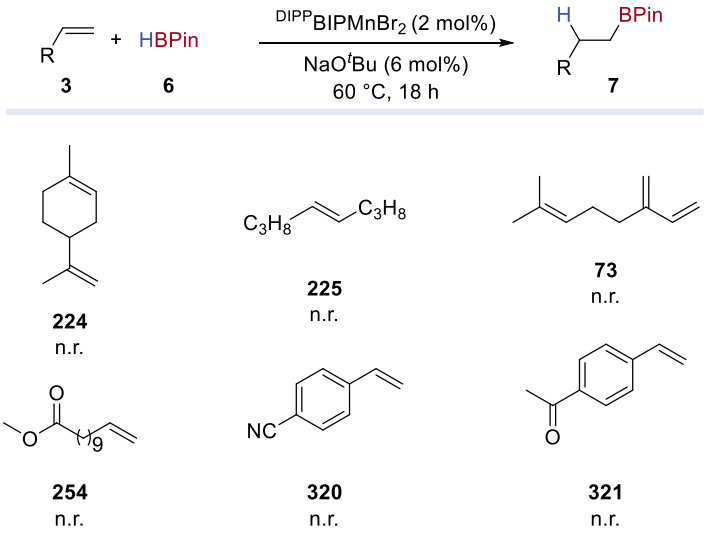

Scheme 3.9 Unreactive substrates for the manganese-catalysed hydroboration of substrates.

3.5 Mechanistic Investigations

3.5.1 Activation

The first step in the activation process is the *in situ* generation of a hypervalent borohydride species by alkoxide addition to pinacol borane. Presumably the hydride then undergoes transmetalation to the manganese(II) pre-catalyst to form a manganese(II) dihydride intermediate which can then undergo reductive elimination to form hydrogen gas and a reduced manganese-species. Notably, sodium triethylborohydride was not a successful activator in the hydrosilylation methodology which is conducted at room temperature (see Chapter 2). This indicates that boronate complexes are not as powerful activators as siliconate species and might explain why the manganese-catalysed hydroboration of alkenes required higher temperatures than the manganese-catalysed hydrosilylation of alkenes.

3.5.2 Identity of the Active Catalyst

It has been shown that reacting alkoxide salts with pinacol borane **292** leads not only to the boronate species **316**, but also to BH_3 **49** which is formed by disproportionation of the boronate species.[42] Further studies by Thomas and co-workers showed that BH_3 would catalyse the hydroboration of alkynes and alkenes at 60 °C.[213] Therefore, it is plausible that the method demonstrated here is merely an extension of the BH_3-catalysed methodology.

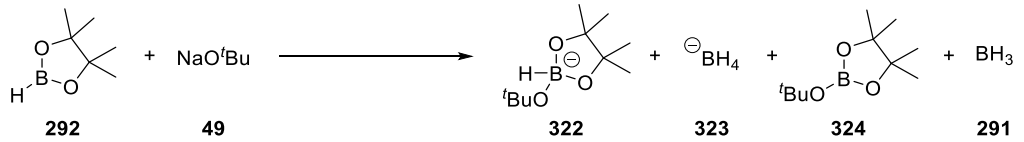

Scheme 3.10 Formation of BH_3 **291** when pinacol borane **292** and an alkoxide salt **49** are mixed as reported by Docherty *et al.*[42]

There is evidence that supports a boron-based active catalyst. The control reaction without a manganese-species demonstrated moderate activity (41%, see Table 3.2, entry 1). Whilst adding a manganese-species had a clear impact on the overall reactivity, it may assist the alkoxide-mediated decomposition of pinacol borane **292** to BH_3 **291**. Additionally, the choice of ligand seems to have a limited effect on the activity of the system (see Table 3.4). This could possibly indicate that the coordination sphere around the metal is not influential in the mechanism. Finally, the substrate scope contrasts strongly with that of the manganese-catalysed hydrosilylation of alkenes (Scheme 3.11). If the methodology was to follow a similar mechanism (i.e. hydrometallation) then it would be presumed that similar classes of substrate would demonstrate similar activities across both methodologies. However, the high activity this method demonstrates with styrene derivatives contrasts with manganese-catalysed hydrosilylation.

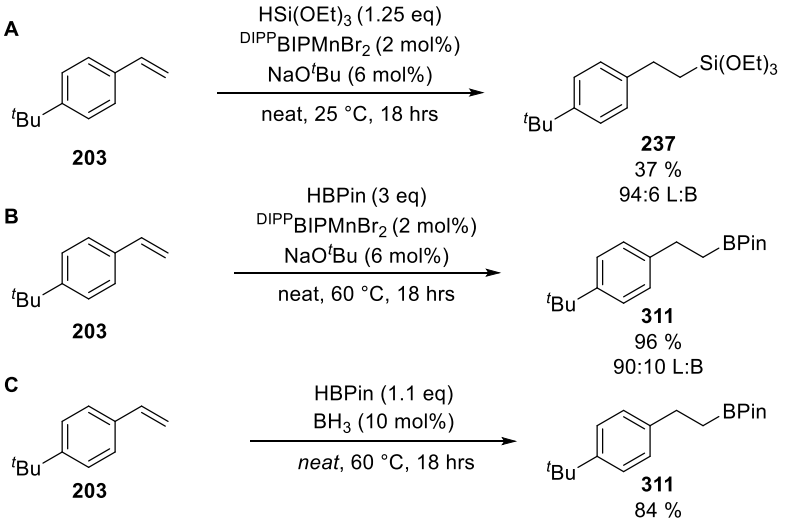

Scheme 3.11 Comparison of *tert*-butylstyrene hydrofunctionalisation. A) manganese-catalysed hydrosilylation of *tert*-butylstyrene. B) manganese-catalysed hydroboration of *tert*-butylstyrene. C) BH_3-catalysed hydroboration of *tert*-butylstyrene.

However, there is evidence that supports a manganese-based catalyst. Previously, $^{DIPP}BIPMnBr_2$ had been reacted with NaO^{t}Bu and $HSi(OEt)_3$ to give an activated manganese-species. This amorphous, purple solid was isolated and although it was not characterised, a small quantity of the activated manganese species was used as a catalyst in a test hydroboration reaction. When mixed with HBPin and octene at room temperature and left for 18 hours, a 35% yield of hydroboration product was observed. Considering the limitations of this approach (not using exact proportions of catalyst and possible contaminants), this represents a reasonable yield and is evidence that this transformation is catalysed by a manganese-based catalyst.

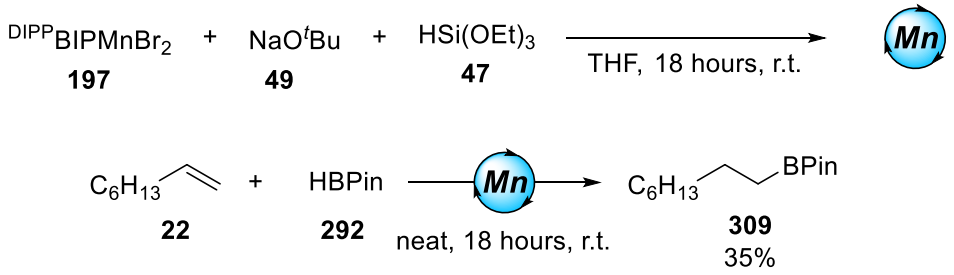

A) the solution was stirred for 18 hours at room temperature before the crude mixture was filtered through celite and the volatiles removed *in vacuo*. The purple substance was then washed with pentane to give a purple solid. B) The reduced manganese species (5mg) was added to a reaction vessel. Octene and pinacol borane were added and the reaction left to stir at room temperature for 18 hours.

Scheme 3.12: A) Synthesis of an undefined manganese species through activation with $HSi(OEt)_3$ **47** and NaO^tBu **49**. B) The use of this species to catalyse a hydroboration reaction at room temperature.

There is sufficient evidence to propose that there are two active catalysts in the reaction. It is plausible that depending on the substrate class, the predominant catalyst could change (for instance BH_3 could be the major catalytic species in the hydroboration of styrenes). It is unknown whether the BH_3 methodology proceeds by a ligand exchange or a transborylation event. Likewise, the manganese-catalysed pathway could follow an oxidative addition or σ-bond metathesis of the B–H bond.

3.6 Conclusions and Future Work

The *anti*-Markovnikov manganese-catalysed hydroboration of alkenes has been developed. The method shows consistent regioselectivity for the linear product for both styrenes and aliphatic alkenes, in contrast to previous methods. There is evidence to suggest that there may be two different mechanisms occurring under the reaction conditions. The most significant is likely to be a manganese-catalysed pathway, reminiscent of the Chalk-Harrod mechanism for hydrosilylation. The minor pathway is likely to be BH_3-catalysed hydroboration. BH_3 was formed by alkoxide decomposition of HBPin as reported by Docherty *et. al.* in 2017.[42]

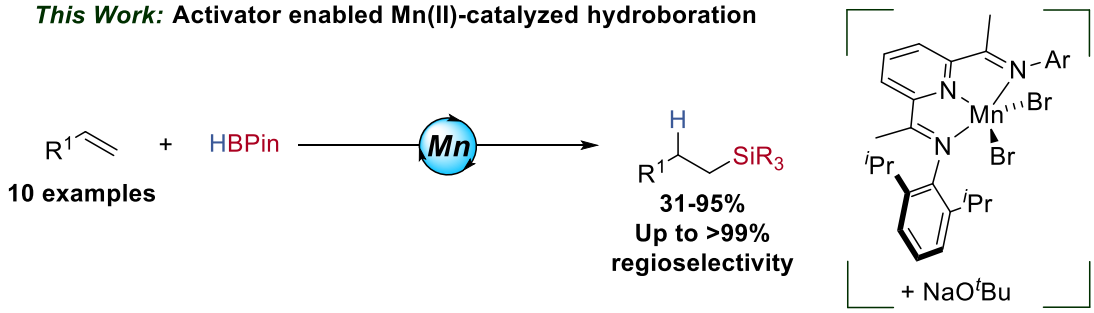

Scheme 3.13 Overview of the manganese-catalysed hydroboration of alkenes

Future work should be carried out on the necessity of the transition metal. Investigating the activation process would allow a greater understanding of the role of the manganese catalyst. For instance investigating the use of $NaHBEt_3$ as an activator in hydrosilylation methodologies at increased temperatures would confirm that boronate species are capable of activating the manganese(II) bromide pre-catalyst. Ideally, isolation and characterisation of the activated manganese species would also enable it to be used directly in hydroboration reactions and avoid the use of sodium *tert*-butoxide.

A kinetic analysis of two model reactions, one with an aryl and one with an aliphatic alkene, would show if the two reactions are significantly different. Comparison with the kinetic profile of the equivalent reactions catalysed by BH_3 would allow for comparisons to be made. Possibly the most important information would be determining the order of the reaction with respect to catalyst and substrate.

4. Iron-Catalysed Reductive Cyclisation

4.1 Project Aim

The use of iron catalysts for the hydrogenation of alkenes has been an important development in replacing precious metal catalysts with sustainable alternatives.[74,214] The rate-determining step for the iron-catalysed hydrogenation of alkenes is reductive-elimination to form a C–H bond. Due to the slow reductive-elimination, the alkyl iron intermediate **326** has a longer lifetime than is typical. Thus, it was proposed that an intramolecular nucleophile could intercept the alkyl iron species **326** to give the product of reductive cyclisation **327** (Scheme 4.1).

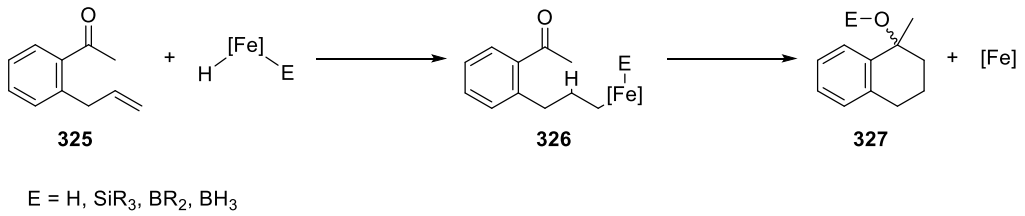

Scheme 4.1 Proposed mechanism of iron-catalysed reductive cyclisation.

The main challenge of this methodology would lie in finding a catalyst which is chemoselective for hydrometallation of an alkene over a carbonyl. Additionally, the reductive elimination could compete with reductive cyclisation, and a mixture of products would be formed (Scheme 4.2).

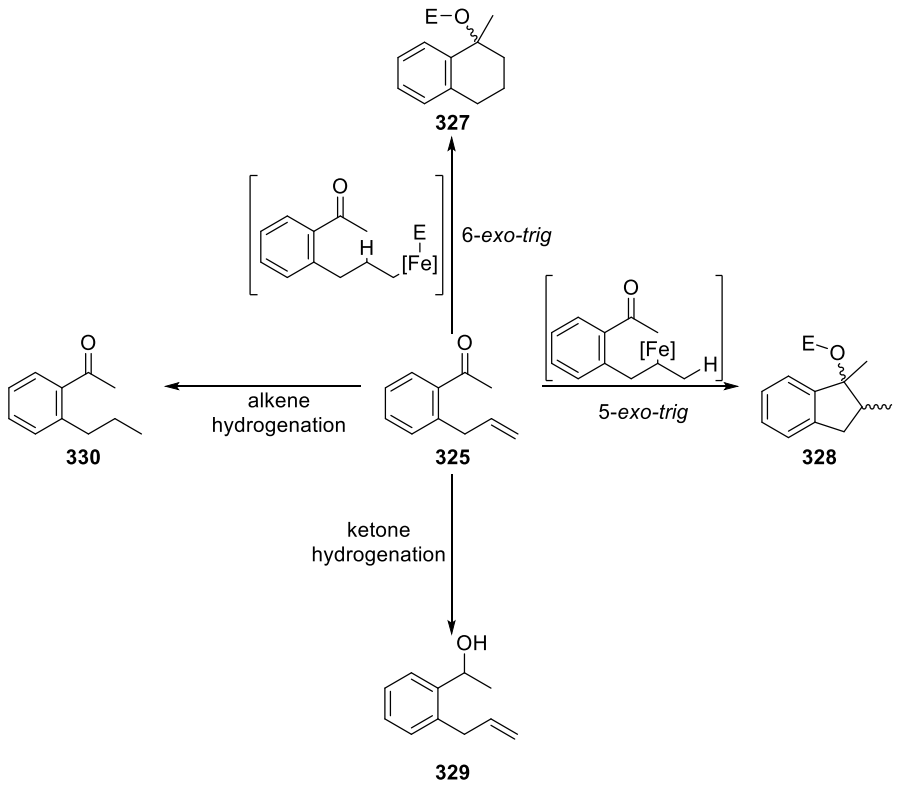

Scheme 4.2 Potential products of iron-catalysed reductive cyclisation

The choice of catalyst was dictated by the need for chemoselective hydrogenation of the alkene in preference to the nucleophilic group. At the outset of the project there were no reports of iron-compounds chemoselectively catalysing the hydrogenation of unactivated alkenes in preference to ketones.[156] However, Carter *et al.* reported the iron-catalysed hydrogenation of 1-cyclopenten-1-ylacetonitrile **331** to give cyclopentyl acetonitrile **333** (Scheme 4.3A).[215] This process used a simple iron salt, $Fe(OTf)_2$ **44**, and sodium triethylborohydride as a hydride source. Additionally, there are examples of iron-catalysed alkene hydrosilylation processes which are selective for the alkene group in the presence of a ketone. Huang and co-workers reported an iron-compound **54** which was capable of catalysing the hydrosilylation of alkenes in the presence of a ketone (Scheme 4.3B).[96] In addition, they showed that bis(imino)pyridine catalysts bearing small *N*-aryl substituents were also chemoselective for alkene hydrosilylation when using the unactivated alkene 5-hexen-2-one **61** (Scheme 4.3C).

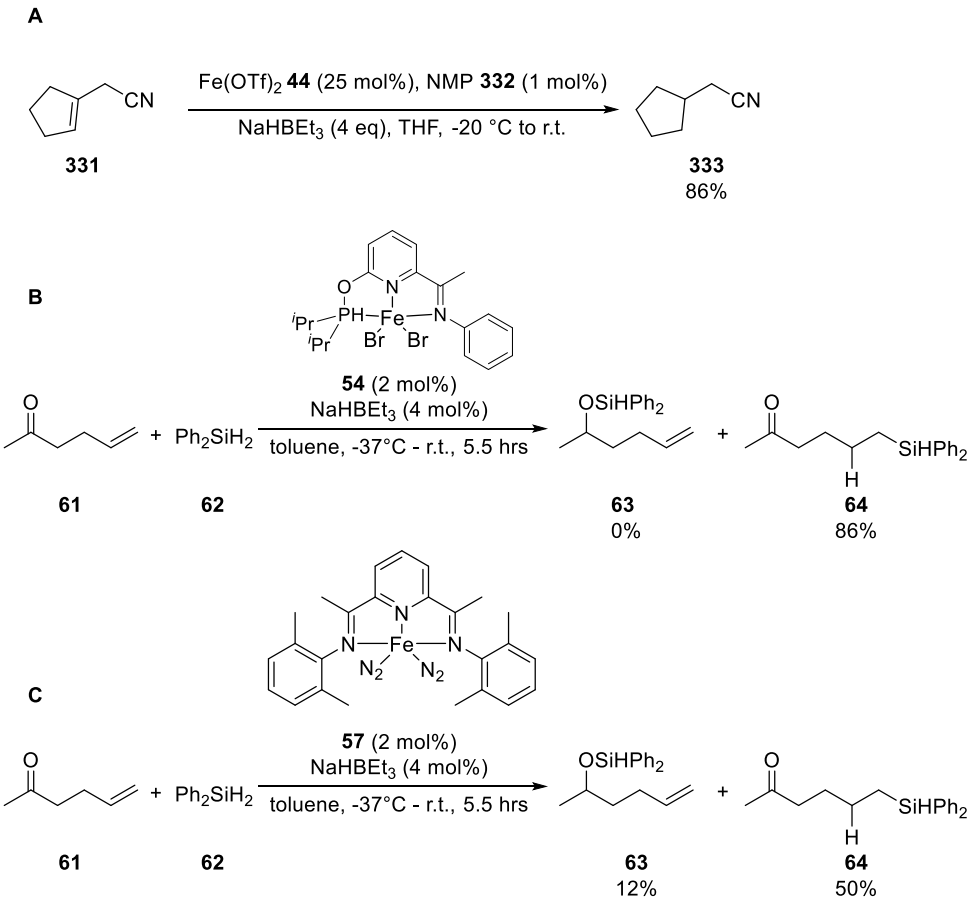

Scheme 4.3 Chemoselective alkene reduction in the presence of other reducible functional groups A) Iron-catalysed alkene hydrogenation in the presence of a nitrile group using a simple iron(II) salt **44**.[215] B) Iron-catalysed alkene hydrosilylation in the presence of a ketone using an iron catalyst bearing an imino(pyridine)phosphinite ligand **54**.[96] C) Iron-catalysed alkene hydrosilylation in the presence of a ketone using an iron-catalyst bearing a bisimino(pyridine) ligand **57**.[169]

4.2 Starting Materials Synthesis

2'-Allylacetophenone **325** was chosen as the model substrate which would allow for a 5- or 6-membered ring to be formed depending on if hydrometallation formed a primary or secondary organoferrate intermediate. This substrate was synthesised by Stille cross-coupling from 2'-bromoacetophenone **334** and allyltributylstannane **335** in a 72% isolated yield. Whilst this method was simple, removal of the residual tin proved difficult.[216] Therefore, 2'-allylacetophenone was also synthesised from 2'-bromoacetophenone by acetal protection, Grignard formation and nucleophilic addition to allyl bromide **257** and subsequent deprotection. 2-Allylbenzonitrile **344**, 2-allylbenzaldehyde **345** and 1-(2-Allylphenyl)propan-2-one **346** were synthesised by Stille cross-coupling.

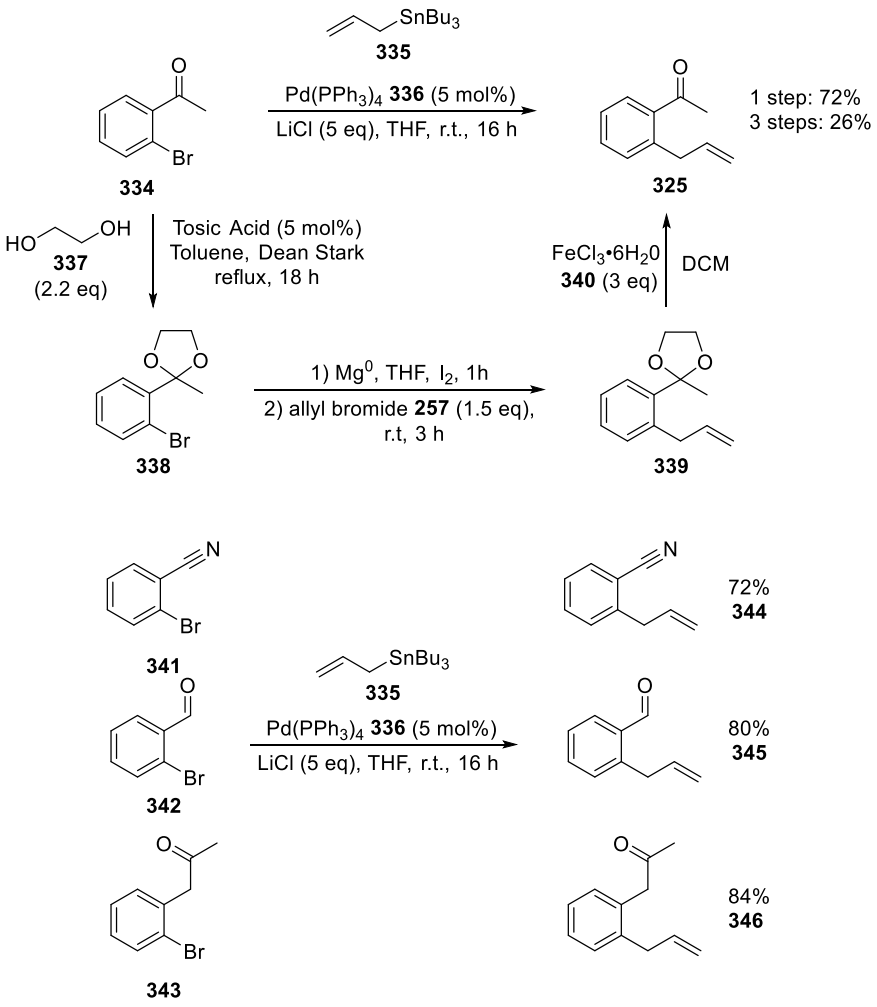

Scheme 4.4 Synthesis of 2'allylacetophenone

4.3 Optimisation of Reaction Conditions

Initial attempts focussed on using the imino(pyridine)phosphinite iron catalyst **54** developed by Haung. Following the reported conditions, it was found that 2'-allylacetophenone **325** was converted to the racemic indane product **347** (5-membered ring) and to a linear alkene hydrosilylation product **348** in a 1:1 ratio (Scheme 4.5). There was no observed decanil product (6-membered ring) or ketone hydrosilylation product.

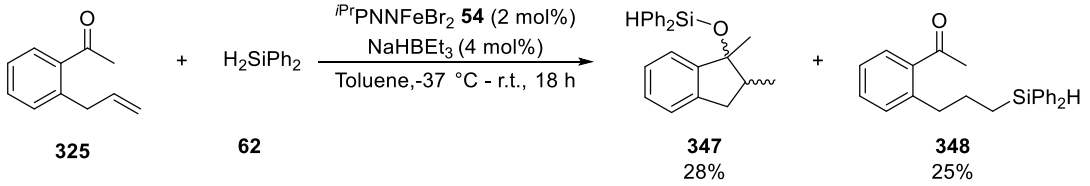

Scheme 4.5 Reductive cyclisation of 2'allylacetophenone using Huang's catalyst **54**.

Attempts to optimise this methodology further were largely unsuccessful. Phenyl silane, triethoxysilane and triethylsilane were all unreactive when trialled. Several different substrates were synthesised and trialled. Using 2'-vinylacetophenone **349** the hydrometallation product is likely to be a secondary organometallic intermediate which could then undergo a 4-*exo*-*trig* reductive cyclisation to form a cyclobutene **350** (Scheme 4.6). However, neither hydrosilylation or reductive cyclisation product was observed - Huang's original manuscript did not include styrene derivatives bearing ortho-substituents and styrene derivatives bearing electron-withdrawing groups led to reduced yields.[96] Using 1-(2-Allylphenyl)propan-2-one **346** gave a 31% yield of the linear hydrosilylation product **351** (Scheme 4.6). The carbonyl had additional conformational flexibility and therefore reductive cyclisation was less likely to occur.

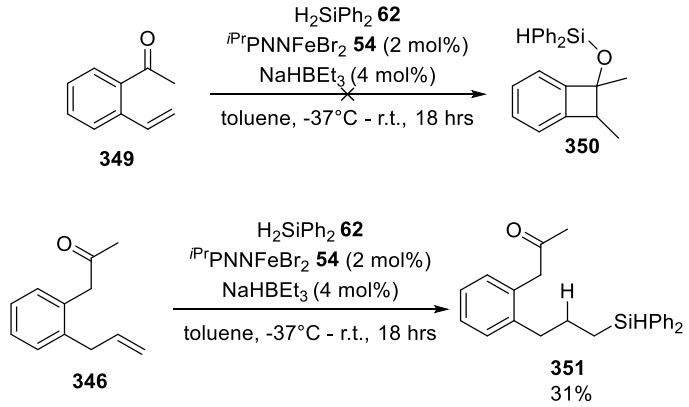

Scheme 4.6 Attempts towards the reductive cyclisation of 2'-vinylacetophenone and 1-(2-allylphenyl)propan-2-one.

We found the activation procedure ($NaHBEt_3$ at -37 °C) to be unreliable and the limited substrate scope and poor selectivity led us to trial other catalyst systems. A range of bis(imino)pyridine iron(II) complexes were screened with the substituents of the *N*-aryl substituents being changed. $^{DIPP}BIPFeBr_2$ **354** displayed no catalytic activity as it was insoluble in tetrahydrofuran (Table 4.1, entry 1). $^{Mes}BIPFeBr_2$ **355** gave a small yield but only the linear hydrosilylation product was observed (entry 2). $^{Et}BIPFeBr_2$ **356** and $^{Me}BIPFeBr_2$ **357** both gave reasonable conversion of starting material which was distributed equally between the linear silane and the reductive cyclisation product (entries 3 and 4). Generally, the catalysts bearing smaller *N*-aryl substituents were more active (i.e. less remaining starting material) and more likely to give the cyclised product.

Table 4.1 Effect of *N*-aryl substituent of the bis(imino)pyridine ligand on reductive cyclisation.

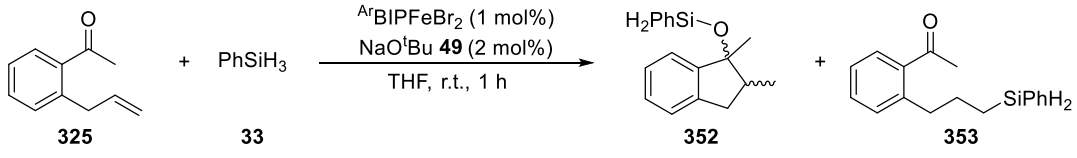

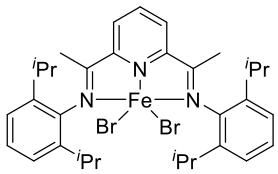

DIPPBIPFeBr2 354

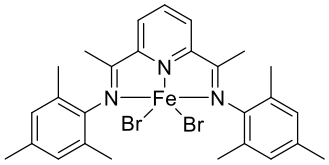

MesBIPFeBr2 355

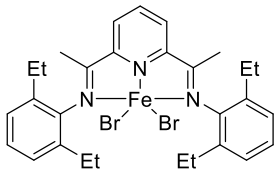

EtBIPFeBr2 356

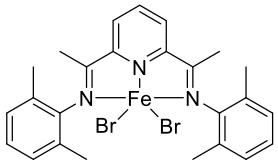

MeBIPFeBr2 357

Entry	Catalyst	Remaining Starting Material (%)[a]	Hydrosilylation (%)[a]	Reductive Cyclisation (%)[a]
1	^{DIPP}BIPFeBr$_2$ **354**	>95	0	0
2	^{Mes}BIPFeBr$_2$ **355**	41	13	trace
3	^{Et}BIPFeBr$_2$ **356**	35	21	21
4	^{Me}BIPFeBr$_2$ **357**	28	26	27

Reaction conditions: Enone (0.5 mmol), $HSiR_3$ (0.5 mmol), catalyst (0.005 mmol), reductant (0.01 mmol), THF (0.5 mL), r.t., 1 h. a) Yield determined by ^{1}H NMR of the crude reaction mixture.

Additional attempts at optimising the bis(imino)pyridine iron(II)dibromide complex were unsuccessful. Investigations at high temperatures showed increases in a presumed polymerisation side-product. Replacing a silane with pinacolborane led to decreased activity with only trace amounts of hydroboration and reductive cyclisation products observed.

Finally screening was attempted using the $Fe(OTf)_2$-catalysed method (Scheme 4.3A).[215] 2'-Allylacetophenone **325** underwent ketone and alkene reduction in a 65% yield (Scheme 4.7). Additionally, a 33% yield of the isomerised alkene product was observed. This suggests whilst an iron-hydride is inserting into the alkene, it is incapable of reductive cyclisation. 2'-Allylbenzonitrile **344** underwent chemoselective alkene hydrogenation in a 41% yield (Scheme 4.7).

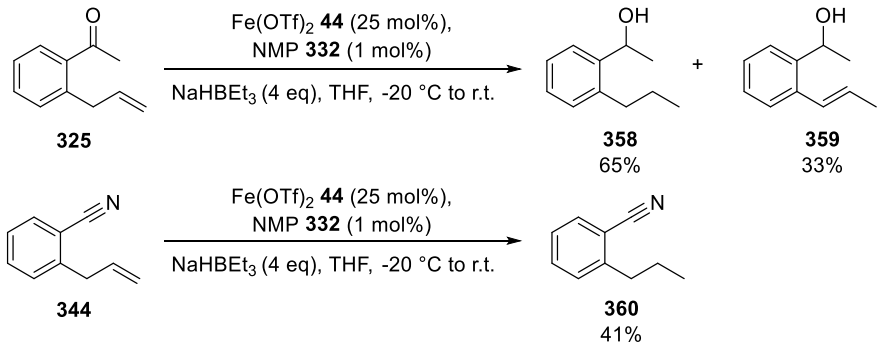

Scheme 4.7 Attempts at reductive cyclisation using iron(II) triflate as a catalyst.

4.4 Conclusions and Future Work

Conditions for the iron-catalysed reductive cyclisation of alkenes of enones have been discovered (Scheme 4.8). However, the conditions are only moderately active (~50% conversion to products) and display poor selectivity as an equal distribution of linear hydrosilylation and reductive cyclisation product are formed.

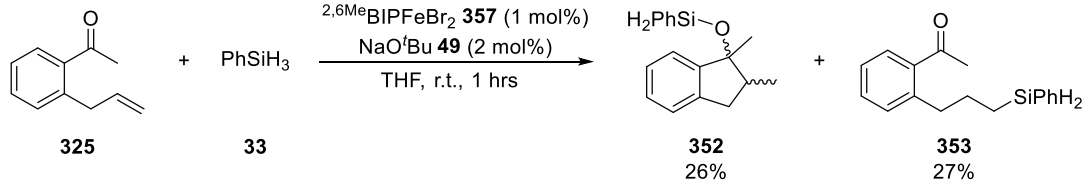

Scheme 4.8 Best developed conditions for the iron-catalysed reductive cyclisation of enones using a bis(imino)pyridine ligand.

To develop this work into a useful methodology, greater activity and control of selectivity needs to be achieved. Bis(imino)pyridine has been shown to be a more flexible ligand than the imino(pyridine)phosphinite ligand (i.e. more tolerant of silanes and substrates for instance ortho-substituted styrenes). Therefore, they are the most promising candidate for optimisation. Most notably, the sterically least demanding bis(imino)pyridine ligand (phenyl *N*-aryl group) was not tested here. It has previously been shown to be the most chemoselective iron-catalyst for alkene hydrosilylation.[96] The smaller size might also help slow reductive elimination and therefore increase selectivity for the reductive cyclisation product.[217,218] Thorough optimisation of all conditions including the silane, the reaction temperature, the solvent and the activation methodology could all help to improve this reaction further.

To attempt to control the selectivity, the rate of carbon–silicon reductive elimination would need to be slowed. Changing to an octahedral catalyst would have the potential to slow reductive elimination.[219] Using a silane with electron-donating substituents could slow reductive elimination by making the metal more electron-rich but this is unlikely to be a significant factor.[220] Another way to potentially control the selectivity of substrates bearing longer chains would be to use a substrate containing a heteroatom to coordinate the metal and keep the conformational rigidity needed to favour reductive cyclisation.

Since the conclusion of this project, there have been reports coupling between alkenes and compounds with carbonyl functional groups. Baran and co-workers have extensively demonstrated the coupling of highly-substituted alkenes with enones (amongst other

electron deficient alkenes), through hydrogen atom transfer (HAT) (Scheme 4.9A). Additionally, Zheng *et. al.* demonstrated the iron(III)bromide catalysed coupling of aldehydes with alkenes (Scheme 4.9B). These methodologies do not exhibit the selectivity problems in our developed methodology and the radical nature of the reaction means that any potential ring-closing reaction would be reliable and predictable.

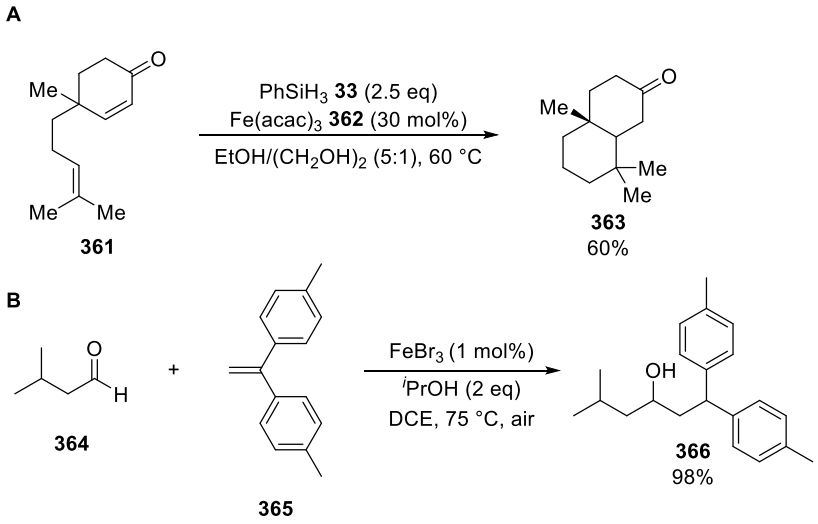

Scheme 4.9 A) Coupling of alkenes and enones catalysed by $Fe(acac)_3$. B) Couping of an aldehyde with a 1,1-disubstituted alkene.

5. Conclusions and Outlooks

At the outset of this project there were no detailed reports of the manganese catalysed-hydrofunctionalisation of alkenes. There were several detailed investigations into manganese-catalysed carbonyl hydrosilylation but the hydrosilylation of alkenes is a more important application in industry. The few reports of manganese-catalysed alkene hydrosilylation were limited to one hydrocarbon substrate (e.g. pentene, octene).

The aim of this project was to develop a general method for the manganese-catalysed hydrosilylation of alkenes. In addition, we aimed to use this methodology as an entry point to manganese-catalysis and use the results and mechanistic insight generated to inspire further research in manganese-catalysis.

The foundation in the discovery of the manganese-catalysed hydrosilylation is the use of NaO^{t}Bu as an activator for a range of bis(imino)pyridine manganese(II) halide complexes. These complexes have previously been synthesised but were found to be inactive in a range of transformations. The new activation methodology was demonstrated to be essential in order to generate an active catalyst. Whilst the activated catalyst remains undefined there is evidence to suggest that *in situ* formation of a siliconate species is responsible for catalyst activation.

The discovered method was extensively optimised and then applied to a range of substrates. Aliphatic, terminal alkenes underwent hydrosilylation in good to excellent yields and excellent regioselectivity. Styrene derivatives gave significantly lower yields and the presence of carbonyl functional groups generally gave chemoselective reduction of the carbonyl group.

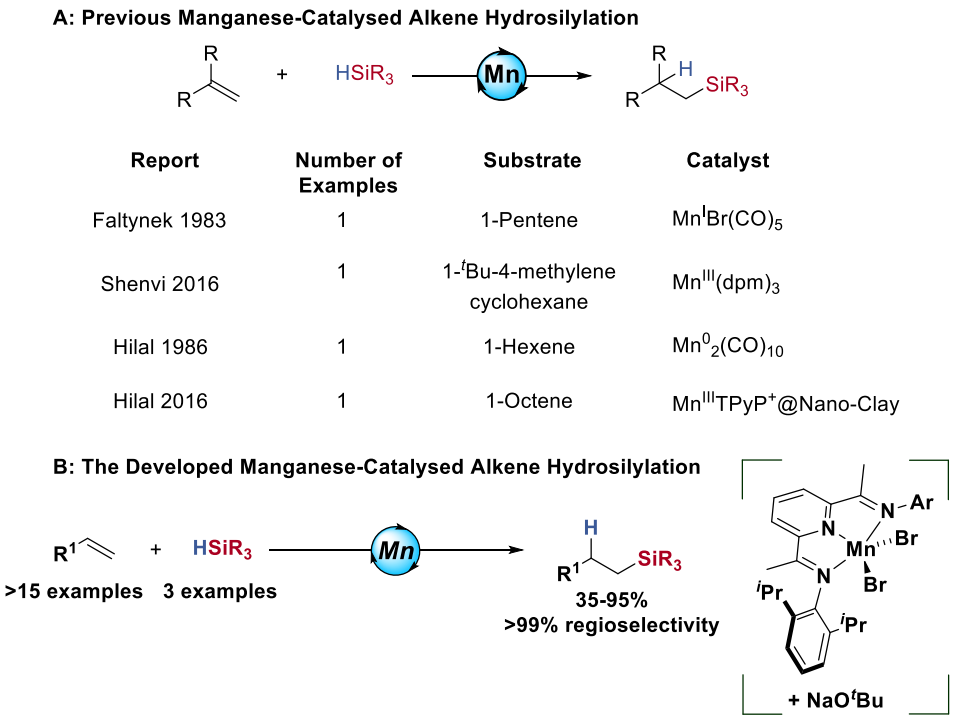

Report	Number of Examples	Substrate	Catalyst
Faltynek 1983	1	1-Pentene	$Mn^{I}Br(CO)_5$
Shenvi 2016	1	1-^{t}Bu-4-methylene cyclohexane	$Mn^{III}(dpm)_3$
Hilal 1986	1	1-Hexene	$Mn^{0}{}_2(CO)_{10}$
Hilal 2016	1	1-Octene	$Mn^{III}TPyP^{+}$@Nano-Clay

Scheme 5.1 A) State-of-the-art manganese-catalysed alkene hydrosilylation methods at the outset of the project. B) The developed manganese-catalysed hydrosilylation methodology.

The catalyst/activator manifold was then applied to the manganese-catalysed hydroboration of alkenes. In the early stages of developing this methodology, a report demonstrating the manganese-catalysed hydroboration of alkenes was published. Our method differed from this report by displaying consistent *anti*-Markovnikov regioselectivity over a range of substrates whilst the published method showed Markovnikov selectivity for the hydroboration of styrene derivatives.

The application of this catalyst/activator platform to the manganese catalysed: hydrogenation of alkenes, hydrovinylation and [2π+2π] alkene cyclisation reactions is a natural progression of this methodology, as these reactions have been demonstrated with iron and cobalt bis(imino)pyridine catalysts. To gain more detailed mechanistic insight, characterisation of the activated manganese species would be an ideal starting point.

Since the publication of our manganese-catalysed hydrofunctionalisation method, there has been a further report investigating the manganese-catalysed hydrosilylation of alkenes using a β-diketimine manganese catalyst.[221] The continued exploration of different manganese species is crucial to the further development of manganese-

catalysis. Mechanistic insight into earth-abundant metal catalysis has proved difficult but detailed mechanistic investigations carried out by Trovitch[145] and Gade[222] into manganese-catalysed carbonyl hydrofunctionalisation reactions are valuable contributions to the field. There are multiple examples of manganese catalysts comparing favourably to more established cobalt and iron analogues, especially in the fields of carbonyl hydrofunctionalisation and hydrogenation.[146,223,224] However the development of methodologies unique to manganese should remain the ultimate ambition in the field.

6. Experimental Details

6.1 General Experimental Information

Reaction Setup: All reactions were performed in oven (180 °C) dried glassware under an atmosphere of argon, unless otherwise indicated. All air- and moisture sensitive reactions were carried out using standard vacuum line and Schlenk techniques, or in a glovebox with a purified argon atmosphere. All glassware was cleaned using base (KOH, ^{i}PrOH) and acid (HCl_{aq}) baths. All reported reaction temperatures correspond to external bath temperatures. Room temperature (r.t) was approximately 20 °C. "Brine" refers to a saturated solution of sodium chloride in H_2O. For the hydrosilylation of olefins, the reactions were typically carried out in a glass vial (10 ml, Fisher Scientific, product code 11563680), under an inert atmosphere of argon, unless otherwise stated.

NMR Spectroscopy: ^{1}H, ^{11}B, ^{13}C, ^{19}F and ^{29}Si NMR spectra were recorded on BrukerAvance III 400 and 500 MHz; Bruker AVI 400 MHz; BrukerAvance I 600 MHz spectrometers. Chemical shifts are reported in parts per million (ppm). ^{1}H and ^{13}C NMR spectra were referenced to the residual deuterated solvent peak ($CHCl_3$: 7.27 ppm, 77.00 ppm; CH_2Cl_2: 5.32 ppm, 54.00 ppm; d_8-THF: 1.73 ppm, 25.37 ppm; CD_3CN: 1.94 ppm, 1.39 ppm). Multiplicities are indicated by app. (apparent), br. (broad), s (singlet), d (doublet), t (triplet), q (quartet), quin. (quintet), sext. (sextet), sept. (septet), non. (nonet). Coupling constants, *J*, are reported in Hertz and rounded to the nearest 0.1 Hz. Integration is provided.

Infrared Spectroscopy: Infra-red (IR) spectra were recorded on a Perkin-Elmer Spectrum One FT-IR, or Shimadzu IRAffinity-1 spectrometer (serial no. A213749). Peaks are reported in cm^{-1} with indicated relative intensities: s (strong, 0–33% T); m (medium, 34–66% T), w (weak, 67–100% T), and br. (broad).

Mass Spectrometry: Mass spectrometry (MS) was performed by the University of Edinburgh, School of Chemistry Mass Spectrometry Laboratory. High resolution mass spectra were recorded on a VG autospec, or Thermo/Finnigan MAT 900, mass spectrometer. Data are reported in the form of m/z (intensity relative to the base peak = 100).

X-ray Crystallography: X-ray crystallography was performed by the University

of Edinburgh, X-ray Crystallography Service. Crystals suitable for X-ray crystallography were mounted on a MITIGEN holder in Paratone oil and spectra were obtained on either an Agilent Technologies SuperNova diffractometer or a Bruker SMART APEXII diffractometer. Crystals were kept at T = 120.0 K during data collection. Using **Olex2**[2] the structure was solved with either: the SIR2008 structure solution program, using the Direct Methods solution method; or the **ShelXS**[3] structure solution program, using the Patterson solution method. The model was refined with version of **ShelXL**[2] using Least Squares minimisation.

Melting Points: Melting points (mp) were determined on a Stuart Scientific SMP10, or Griffin Gallankamp melting point apparatus in capillary tubes and are uncorrected.

Chromatography: Analytical thin-layer chromatography was performed on aluminium-backed silica plates (Merck 60 F_{254}). Pet. ether refers to petroleum ether 40-60. Product spots were visualised by UV light at 254 nm, and subsequently developed using potassium permanganate solution if appropriate. Flash column chromatography was performed on silica gel (Merck Kielselgel 60, 40-63 μm).

Solvents: All solvents for air- and moisture sensitive techniques were obtained from an anhydrous solvent system (Innovative Technology). Anhydrous d_8-tetrahydrofuran was distilled from sodium/benzophenone. Reaction solvents tetrahydrofuran (THF) (Fisher, HPLC grade), ether (Et_2O) (Fisher, BHT stabilized ACS grade), and dichloromethane (CH_2Cl_2) (Fisher, unstabilised HPLC grade) were dried by percolation through two columns packed with neutral alumina under a positive pressure of argon. Toluene (ACS grade) was dried by percolation through a column packed with neutral alumina and a column packed with Q5 reactant (supported copper catalyst for scavenging oxygen) under a positive pressure of argon. Solvents for filtration, transfers, chromatography, and recrystallization were dichloromethane (CH_2Cl_2) (ACS grade), ether (Et_2O) (Fisher, BHT stabilised ACS grade), ethyl acetate (EtOAc) (Fisher, ACS grade), hexane (Optima), methanol (MeOH) (ACS grade), pentane (ACS grade), and petroleum ether (40–60°C, ACS grade).

Chemicals: All reagents were purchased from Sigma Aldrich, Alfa Aesar, Acros Organics, Tokyo Chemical Industries UK, Fluorochem, Fisher Scientific UK and Apollo Scientific or synthesised within the laboratory. Manganese(II) Bromide 98% (Product

Number 223646) was purchased from Sigma Aldrich. Sodium *tert*-butoxide (97%) was purchased from Sigma Aldrich.

6.2 General Procedures

General Procedure A: Formation of $MnLX_2$ species

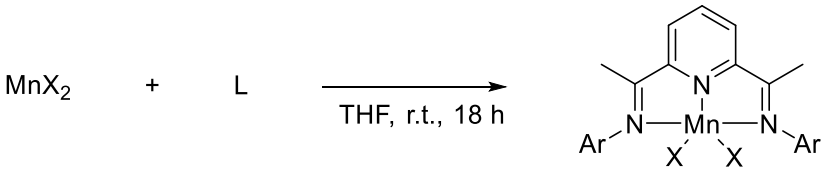

MnX_2·$(THF)_2$ (5.84 mmol) and ligand (6.24 mmol, 1.1 eq.) were stirred in anhydrous tetrahydrofuran for 18 hours and then filtered and washed with Et_2O (3 x 20 mL). The resulting orange solid was then dissolved in boiling dichloromethane and filtered before being concentrated *in vacuo* to give an orange solid.

General Procedure B: Hydrosilylation of alkenes

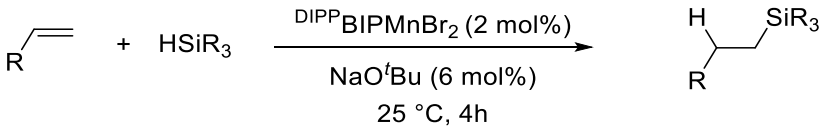

Triethoxysilane (230 µL, 1.25 mmol 1.25 eq.) was added to $^{DIPP}BIPMnBr_2$ (14 mg, 20 µmol, 2 mol%) and NaO^tBu (5.8 mg, 60 µmol, 6 mol%) followed by addition of alkene (1.0 mmol, 1.0 eq.) and the reaction mixture left to stir for 4 hours at 25 °C. ***Caution! Silane addition produces a highly exothermic reaction and may result in the formation of SiH_4. Perform the reaction carefully.*** The reaction was then quenched by the addition of an aqueous solution of HCl (2M, 1 mL). The crude reaction yield was determined by the addition of trimethoxybenzene (16.8 mg, 0.2 mmol, 0.2 eq.), dissolved in diethyl ether (1 mL), as an internal standard. The product was purified by vacuum distillation.

General Procedure C: Hydroboration of alkenes

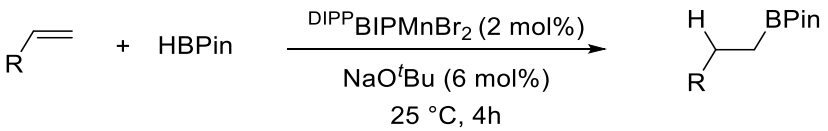

Pinacolborane (220 μL, 1.5 mmol 1.5 eq.) was added to ^{DIPP}BIPMnBr$_2$ (14mg, 20 μmol, 2 mol%) and NaO^{t}Bu (5.8 mg, 60 μmol, 6 mol%) followed by addition of alkene (1.0 mmol, 1.0 eq.) and the reaction mixture left to stir for 18 hours at 60 °C. The reaction was then quenched by the addition of an aqueous solution of HCl (2M, 1 mL). The crude reaction yield was determined by the addition of trimethoxybenzene (16.8 mg, 0.2 mmol, 0.2 eq.), dissolved in diethyl ether (1 mL), as an internal standard. The product was purified by flash column chromatography.

Gram- Scale Hydrosilylation of Octene

In an argon atmosphere glove-box, triethoxysilane (2.03 mL, 11 mmol, 1.25 eq.) was added to NaO^{t}Bu (13 mg, 0.13 mmol, 1.5 mol%) and ^{DIPP}BIPMnBr$_2$ (31.38 mg, 0.445 mmol, 0.5 mol%) in a Schlenk tube (15 mL). ***Caution! Silane addition produces a highly exothermic reaction and may result in the formation of SiH_4. Perform the reaction carefully.*** 1-Octene (1.4 mL, 8.9 mmol, 1 eq.) was quickly added and the reaction left to stir for 4 hours. The reaction was then quenched by the addition of an aqueous solution of HCl (2M, 10 mL) and extracted with diethyl ether (3 x 10 mL). The product was purified by vacuum distillation ($8x10^{-2}$ mbar, 80°C) to give triethoxy(octyl)silane as a colourless oil (2.34 g, 95%).

6.3 Ligand Synthesis

2,6-Bis{1-[(2,6-di*iso*propylphenyl)imino]ethyl}pyridine

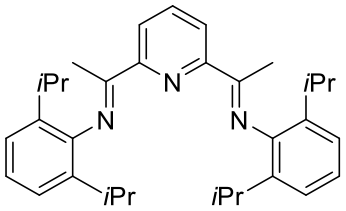

2,6-Di*iso*propylaniline (3.6 mL, 19.3 mmol) was added to a stirred suspension of 2,6-diacetylpyridine (1.45 g. 8.8 mmol) and *para*-toluenesulfonic acid mono-hydrate (101 mg, 0.53 mmol) in toluene (30 mL). The resulting mixture was heated at reflux under Dean-Stark conditions for 20 hours. After cooling to room temperature, the solvent was removed *in vacuo* and the solid recrystallised from dichloromethane (20 mL) to give 2,6-bis{1-[(2,6-di*iso*propylphenyl)imino]ethyl}pyridine (6 crops, 2.8 g, 66%) as yellow needles.

m.p: 298°C-299°C Lit: 298°C-299°C[225]

^{1}H NMR: (601 MHz, $CDCl_3$)

δ 8.51 (d, J = 7.8 Hz, 2H, ArH), 7.96 (t, J = 7.8 Hz, 1H, ArH), 7.22 – 7.19 (m, 4H, ArH), 7.16 – 7.11 (m, 2H, ArH), 2.80 (hept, J = 6.9 Hz, 4H, ArCH), 2.30 (s, 6H, CCH_3), 1.19 (d, J = 6.9 Hz, 24H, CH(CH_3)$_2$).

^{13}C NMR: (151 MHz, $CDCl_3$)

δ 167.0 (C), 155.2 (C), 146.5 (C), 136.9 (CH), 135.8 (CH), 123.6 (CH), 123.0 (CH), 122.2 (CH), 28.31 (CH), 23.24 (CH_3), 22.92 (CH_3), 17.15 (CH_3).

The spectroscopic data were consistent with those reported.[226]

2,6-Bis{1-[(2,6-diethyl propylphenyl)imino]ethyl}pyridine

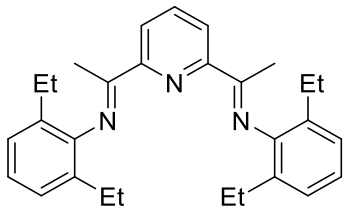

2,6-Diethylaniline (4.5 mL, 27 mmol) was added to a stirred suspension of 2,6-diacetylpyridine (2 g. 12.3 mmol) and *para*-toluenesulfonic acid mono-hydrate (105 mg, 0.6 mmol) in toluene (40 mL). The resulting mixture was heated at reflux under Dean-Stark conditions for 20 hours. After cooling to room temperature, the solvent was removed *in vacuo* and the solid recrystallised from dichloromethane (20 mL) to give 2,6-bis{1-[(2,6-diethylphenyl)imino]ethyl}pyridine (5 crops, 3.9 g, 75%) as yellow needles.

m.p: 182°C-184°C Lit:[90] 185°C-186°C

^{1}H NMR: (500 MHz, $CDCl_3$) δ 8.50 (d, J = 7.8 Hz, 2H, ArH), 7.95 (t, J = 7.8 Hz, 1H, ArH), 7.17 – 7.13 (m, 4H, ArH), 7.09 – 7.04 (m, 2H, ArH), 2.51 – 2.34 (m, 8H, $ArCH_2$), 2.28 (s, 6H, $C\mathit{CH_3}$), 1.18 (t, J = 7.5 Hz, 12H, $CH_2\mathit{CH_3}$).

^{13}C NMR: (126 MHz, $CDCl_3$)

δ 166.9 (C), 155.2 (C), 147.8 (C), 136.9 (CH), 131.2 (C), 126.0 (CH), 123.3 (CH), 122.2 (CH), 24.6 (CH_2), 16.8 (CH_3), 13.7 (CH_3).

The spectroscopic data were consistent with those reported.[174]

2,6-Bis{1-[(2,4,6-trimethylphenyl)imino]ethyl}pyridine

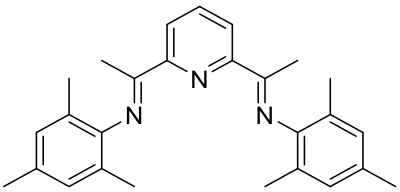

2,4,6-Trimethyllaniline (3.8 mL, 27 mmol) was added to a stirred suspension of 2,6-diacetylpyridine (2 g. 12.3 mmol) and *para*-toluenesulfonic acid mono-hydrate (172 mg, 0.62 mmol) in toluene (40 mL). The resulting mixture was heated at reflux under Dean-Stark conditions for 20 hours. After cooling to room temperature, the solvent was removed *in vacuo* and the solid recrystallised from dichloromethane (25 mL) to give 2,6-bis{1-[(2,4,6-trimethylphenyl)imino]ethyl}pyridine (4 crops, 3.3 g, 68%) as yellow needles.

m.p: 164°C-166°C Lit:[227] 164°C-165°C

^{1}H NMR: (500 MHz, $CDCl_3$)

δ 8.48 (d, J = 7.8 Hz, 2H, ArH), 7.92 (t, J = 7.8 Hz, 1H, ArH), 6.95 – 6.87 (m, 4H, ArH), 2.32 (s, 6H, C*CH*$_3$), 2.26 (s, 6H, $ArCH_3$), 2.04 (s, 12H, $ArCH_3$).

^{13}C NMR: (126 MHz, $CDCl_3$)

δ 167.4 (C), 155.3 (C), 146.3 (C), 136.8 (CH), 132.2 (C), 128.6 (C), 125.3 (CH), 122.2 (CH), 20.7 (CH_3), 17.9 (CH_3), 16.4 (CH_3).

The spectroscopic data were consistent with those reported.[228]

2,6-Bis{1-[(phenyl)imino]ethyl}pyridine

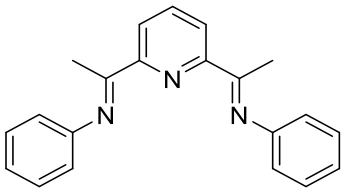

Aniline (2.5 mL, 27 mmol) was added to a stirred suspension of 2,6-diacetylpyridine (2 g. 12.3 mmol) and *para*-toluenesulfonic acid mono-hydrate (105 mg, 0.62 mmol) in toluene (40 mL). The resulting mixture was heated at reflux under Dean-Stark conditions for 20 hours. After cooling to room temperature, the solvent was removed *in vacuo* and the solid recrystallised from dichloromethane (25 mL) to give 2,6-bis{1-[(phenyl)imino]ethyl}pyridine (2 crops, 2.1 g, 54%) as yellow needles.

m.p: 157°C-158°C

^{1}H NMR: (400 MHz, $CDCl_3$)

δ 8.38 (d, J = 7.9 Hz, 2H, ArH), 7.90 (t, J = 7.7 Hz, 1H, ArH), 7.43 (t, J = 7.5 Hz, 4H, ArH), 7.18 (t, J = 7.2 Hz, 2H, ArH), 6.87 (d, J = 7.9 Hz, 4H, ArH), 2.44 (s, 6H, CCH_3).

^{13}C NMR: (101 MHz, $CDCl_3$)

δ 167.4 (C), 155.5 (C), 151.3 (C), 136.8 (CH), 129.0 (CH), 123.6 (CH), 122.3 (CH), 119.3 (CH), 16.2 (CH_3).

The spectroscopic data were consistent with those reported.[229]

6.4 Catalyst Synthesis

2,6-Bis[1-(2,6-di*iso*propylphenylimino)ethyl]pyridine manganese(II) bromide

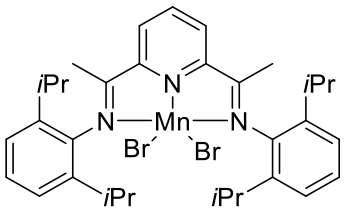

According to a modified version of General Procedure A, $MnBr_2 \cdot (THF)_2$ (2.06 g, 5.84 mmol) and 2,6-bis{1-[(2,6-di*iso*propylphenyl)imino]ethyl}pyridine (3.00 g, 6.24 mmol) were stirred in anhydrous tetrahydrofuran for 18 hours, the solution quickly became orange. The solution was then filtered and washed with diethylether (3 x 20 mL). The resulting powder was then dissolved in dichloromethane and filtered before being concentrated *in vacuo* to give an amorphous orange solid (2.92 g, 4.2 mmol, 72%). Crystals were grown at −40 °C from a saturated solution in anhydrous dichloromethane to give orange needles.

MS: (HRMS - EI+)

Found 694.11961 ($C_{33}H_{43}N_3Br_2Mn$), requires 694.11987

IR: 2961 (m), 2924 (w), 2866 (w), 1622 (m), 1582 (s), 1464 (m), 1445 (m), 1369 (s), 1254 (s), 1202 (s), 1103 (w), 1018 (m), 935 (w), 818 (s), 795 (s), 775 (s).

2,6-Bis[1-(2,6-diethylphenylimino)ethyl]pyridine manganese(II) bromide

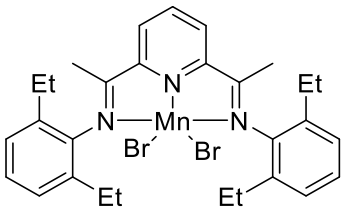

Following a modified version of General Procedure A, $MnBr_2 \cdot (THF)_2$ (2.06 g, 5.84 mmol) and 2,6-bis{1-[(2,6-diethylphenyl)imino]ethyl}pyridine (3.00 g, 6.24 mmol) were stirred in anhydrous tetrahydrofuran for 18 hours, the solution quickly became orange. The solution was then filtered and washed with diethylether (3 x 20 mL). The resulting powder was then dissolved in dichloromethane and filtered before being concentrated *in vacuo* to give an amorphous orange solid (2.92 g, 4.2 mmol, 72%). Crystals were grown at −40 °C from a saturated solution in anhydrous dichloromethane to give orange needles.

IR: ν_{max}(neat)
2970 (m), 1630 (m), 1584 (m), 1462 (m), 1443 (m), 1375 (m), 1260 (s), 1206 (s), 1107 (w), 1016 (m), 866 (w), 810 (s), 779 (s), 768 (m), 739 (m).

2,6-Bis{1-[(2,4,6-trimethylphenyl)imino]ethyl}pyridine manganese(II) bromide

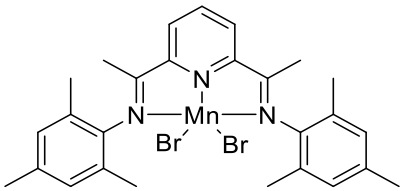

Following a modified version of General Procedure A, $MnBr_2 \cdot (THF)_2$ (400 mg, 1.12 mmol) and 2,6-bis{1-[(2,4,6-trimesitylphenyl)imino]ethyl}pyridine (477 mg, 1.2 mmol) were stirred in anhydrous tetrahydrofuran (24 mL) for 18 hours, the solution quickly became orange. The solution was then filtered and washed with diethylether (3 x 20 mL). The resulting powder was then dissolved in dichloromethane and filtered before being concentrated *in vacuo* to give an amorphous orange solid (624 mg, 1.1 mmol, 91%).

MS: (HRMS - EI+)

Found 610.02231 ($C_{27}H_{31}N_3Br_2Mn$), requires 610.02597

IR: ν_{max}(neat)

2970 (w), 2951 (w), 2913 (w), 2857 (w), 1636 (w), 1585 (m), 1475 (m), 1431 (w), 1369 (m), 1369 (m), 1267 (s), 1258 (s), 1219 (s), 1159 (w), 1062, 1016 (m), 856 (s), 812 (s), 740 (m), 565 (m).

The data were consistent with those reported.[230]

Synthesis of other bis(imino)pyridine manganese catalysts

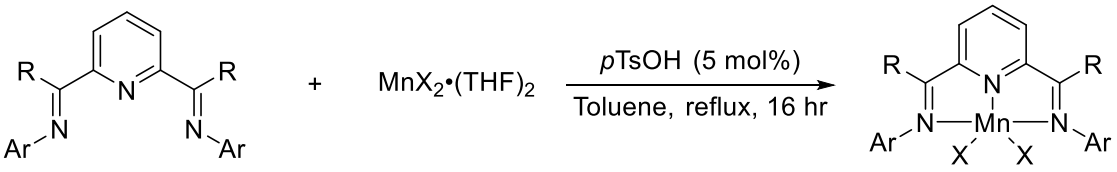

Entry	Ar	R	X	Yield (%)
1	2,6-Me	CH_3	Br	65
2	Ph	CH_3	Br	82
3	DIPP	CH_3	Cl	81
4	Mes	CH_3	Cl	48
5	Ph	CH_3	Cl	40
6	DIPP	CH_3	I	41
7	Mes	CH_3	I	56
8	DIPP	CH_3	OTf	23
9	DIPP	Ph	Br	74

All catalysts were synthesized according to General Procedure A except for entry 7 which was synthesized by salt metathesis.

2,2':6,',2"-Terpyridine manganese(II) bromide

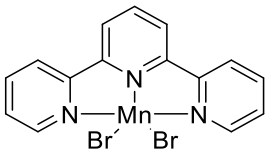

$MnBr_2 \cdot (THF)_2$ (300 mg, 0.86 mmol) and terpyridine (200 mg, 0.86 mmol) were stirred in anhydrous tetrahydrofuran for 18 hours. The solution was then filtered and washed with diethylether (3 x 20 mL). The resulting amorphous solid was then dissolved in dichloromethane and filtered before being concentrated *in vacuo* to give a yellow solid (155 mg, 0.34 mmol, 80%).

MS: (HRMS - EI+)

Found 366.95202 ($C_{15}H_{11}N_3{}^{79}Br^{55}Mn_1$) requires 366.95202

IR: 3043.67 (w), 1593.20 (m), 1573.91 (w), 1562.34 (w), 1475.54 (w), 1452.40 (m), 1317.38 (m), 1298.09 (w), 1253.73 (m), 1159.22 (w), 1014.56 (m), 775.38 (s), 651.94 (m), 638.44 (m).

The data were consistent with those reported.[231]

2,2':6,',2"-Terpyridine manganese(II) chloride

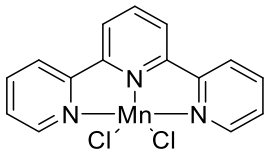

$MnCl_2 \cdot (THF)_2$ (115 mg, 0.43 mmol) and terpyridine (100 mg, 0.43 mmol) were stirred in anhydrous tetrahydrofuran (10 mL) for 18 hours. The solution was then filtered and washed with diethylether (3 x 20 mL). The resulting amorphous solid was then dissolved in dichloromethane and filtered before being concentrated *in vacuo* to give a yellow solid (155 mg, 0.34 mmol, 80%).

MS: (HRMS - EI+)

Found 357.97127 ($C_{15}H_{11}N_3{}^{35}Cl_2{}^{55}Mn_1$) requires 357.97050

IR: 3053.32 (w), 1593.20 (m), 1575.84 (w), 1560.41 (w), 1473.62 (w), 1436.97 (m), 1313.52 (m), 1294.24 (w), 1247.94 (m), 1159.22 (w), 1014.56 (m), 775.38 (s), 657.73 (m), 638.44 (m).

The data were consistent with those reported.[231]

6.5 Substrate Synthesis

1-Fluoro-4-(3-butenyl)-benzene

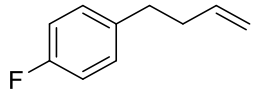

Allylmagnesium bromide (31.0 mL, 1 M in diethylether, 31.0 mmol) was added to a solution of 4-fluorobenzyl bromide (5.00 g, 26.5 mmol) in anhydrous tetrahydrofuran (20 mL) at 0 °C under a nitrogen atmosphere. The reaction was allowed to warm to room temperature over 18 hours. Aqueous sulfate buffer solution (10 mL) was added and the aqueous phase extracted with diethyl ether (3 x 30 mL). The combined organic extracts were washed with water and brine, dried ($MgSO_4$) and concentrated *in vacuo* to give 1-fluoro-4-(3-butenyl)-benzene as a colourless oil (3.40 g, 22.6 mmol, 85%).

^{1}H NMR: (400 MHz, $CDCl_3$)

δ 7.19 – 7.12 (m, 2H, ArH), 7.03 – 6.94 (m, 2H, ArH), 5.86 (ddt, J = 16.9, 10.2, 6.6 Hz, 1H, *HC*=CH_2), 5.12 – 4.92 (m, 2H, HC=*CH_2*), 2.75-2.66 (m, 2H, $ArCH_2$), 2.42-2.32 (m, 2H, CH_2).

^{13}C NMR: (126 MHz, $CDCl_3$)

δ 161.3 (d, J = 242.9 Hz, C), 137.8 (CH), 137.4 (d, J = 3.1 Hz, C), 129.7 (d, J = 7.7 Hz, CH), 115.1 (d, J = 8.0 Hz, CH), 114.9 (CH_2), 35.6 (CH_2), 34.5 (CH_2).

^{19}F NMR: (471 MHz, $CDCl_3$)

δ -117.9.

The spectroscopic data were consistent with those reported.[174]

1-Chloro-4-(3-butenyl)-benzene

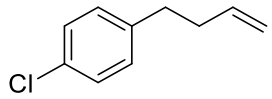

Allylmagnesium bromide (5.85 mL, 2 M in tetrahydrofuran, 11.7 mmol) was added to a solution of 4-chlorobenzyl bromide (2 g, 9.75 mmol) in anhydrous tetrahydrofuran (15 mL) at 0 °C under a nitrogen atmosphere. The reaction was allowed to warm to room temperature over 3 hours. Aqueous sulfate buffer solution (10 mL) was added and the aqueous phase extracted with diethyl ether (3 x 30 mL). The combined organic extracts were washed with water and brine, dried ($MgSO_4$) and concentrated *in vacuo* to give 1-chloro-4-(3-butenyl)-benzene as a colourless oil (1.48 g, 8.88 mmol, 91%).

^{1}H NMR: (400 MHz, $CDCl_3$)

δ 7.28 – 7.23 (m, 2H, ArH), 7.16 – 7.11 (m, 2H, ArH), 5.85 (ddt, J = 16.9, 10.2, 6.6 Hz, 1H, *HC*=CH_2), 5.11 – 4.94 (m, 2H, HC=*CH_2*), 2.75 – 2.66 (m, 2H, $ArCH_2$), 2.43 – 2.31 (m, 2H, CH_2).

^{13}C NMR: (101 MHz, $CDCl_3$)

δ 140.3 (C), 137.6 (CH), 131.5 (C), 129.8 (CH), 128.4 (CH), 115.3 (CH_2), 35.4 (CH_2), 34.7 (CH_2).

The spectroscopic data were consistent with those reported.[174]

1-Bromo-4-(3-butenyl)-benzene

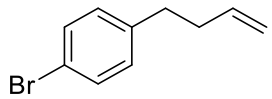

Allylmagnesium bromide (30 mL, 1 M in diethylether, 30.0 mmol) was added to a solution of 4-bromobenzyl bromide (6.32 g, 25.0 mmol) in anhydrous tetrahydrofuran (15 mL) at 0 °C under a nitrogen atmosphere. The reaction was allowed to warm to room temperature over 3 hours. Aqueous sulfate buffer solution (10 mL) was added and the aqueous phase extracted with diethyl ether (3 x 30 mL). The combined organic extracts were washed with water and brine, dried ($MgSO_4$) and concentrated *in vacuo* to give 1-bromo-4-(3-butenyl)-benzene as a colourless oil (4.91 g, 23.2 mmol, 93%).

^{1}H NMR: (500 MHz, $CDCl_3$)

δ 7.39 (m, 2H, ArH), 7.08 – 7.02 (m, 2H, ArH), 5.82 (ddt, J = 16.9, 10.2, 6.6 Hz, 1H, CH), 5.07 – 4.91 (m, 2H, CHCH_2), 2.71-2.63z (m, 2H, ArCH_2), 2.38-2.31 (m, 2H, CH_2CH_2).

^{13}C NMR: (101 MHz, $CDCl_3$)

δ 140.8 (C), 137.6 (CH), 131.3 (CH), 130.2 (CH), 119.6 (C), 115.3 (CH_2), 35.3 (CH_2), 34.8 (CH_2).

The spectroscopic data were consistent with those reported.[174]

4-(3-Butenyl)-benzoic acid

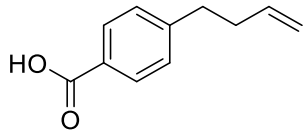

1-Bromo-4-(3-butenyl)-benzene (0.35 g, 16.6 mmol) was added to magnesium turnings (0.81 g, 33 mmol) in anhydrous tetrahydrofuran (30 mL) under a nitrogen atmosphere. This was followed by the addition of a single iodine crystal to initiate the reaction. When the reaction temperature increased, the remaining 1-bromo-4-(3-butenyl)-benzene (3.2 g, 15 mmol) was added periodically over 15 minutes. The reaction was left for 2 hours and then excess solid carbon dioxide was added. After a further 1 hour of reaction time, the solution was quenched with sodium hydrogen carbonate solution (aq, 10 mL) and the aqueous phase washed with ether (3 x 10 mL). Conc. HCl was added to the aqueous phase and extracted with diethyl ether (3 x 30 mL). The organic phase was dried ($MgSO_4$) and concentrated *in vacuo* to give 4-(3-butenyl)-benzoic acid as a colourless amorphous solid (2.41 g, 13.6 mmol, 82%).

^{1}H NMR: (500 MHz, $CDCl_3$)

δ 8.05 – 7.97 (m, 2H, ArH), 7.32 – 7.28 (m, 2H, ArH), 5.84 (ddt, J = 16.9, 10.2, 6.6 Hz, 1H, CH), 5.12 – 4.97 (m, 2H, CHCH_2), 2.86 – 2.70 (m, 2H, ArCH_2), 2.50 – 2.31 (m, 2H, CH_2CH_2).

^{13}C NMR: (101 MHz, $CDCl_3$)

δ 171.7 (CO_2H), 148.4 (C), 137.4 (CH), 130.3 (CH), 128.7 (CH), 127.0 (C), 115.5 (CH_2), 35.5 (CH_2), 35.0 (CH_2).

The spectroscopic data were consistent with those reported.[174]

4-(3-Butenyl)-benzoic acid methyl ester

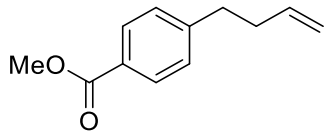

Sulfuric acid (conc., 30 drops) was added to 4-(3-butenyl)-benzoic acid (1.5 g, 8.5 mmol) in anhydrous methanol (60 mL) and left to stir at reflux at 18 hours. The reaction was then allowed to cool to room temperature and then quenched by addition of sodium hydrogen carbonate solution (aq, 50 mL). The aqueous phase washed with ethyl acetate (3 x 10 mL) and the combined organic phase was dried ($MgSO_4$) and concentrated *in vacuo* to give 4-(3-butenyl)-benzoic acid methyl ester as a yellow oil (1.51 g, 7.9 mmol, 93%).

^{1}H NMR: (500 MHz, $CDCl_3$)

δ 8.00 – 7.96 (m, 2H, ArH), 7.30 – 7.25 (m, 2H, ArH), 5.85 (ddt, J = 16.9, 10.2, 6.6 Hz, 1H, CH), 5.15 – 4.89 (m, 2H, CHCH_2), 3.92 (s, 3H, OCH_3), 2.85 – 2.75 (m, 2H, $ArCH_2$), 2.49 – 2.33 (m, 2H, CH_2CH_2).

^{13}C NMR: (101 MHz, $CDCl_3$)

δ 167.1 (C=O), 147.4 (C), 137.5 (CH), 129.7 (CH), 128.5 (CH), 127.9 (C), 115.4 (CH_2), 52.0 (OCH_3), 35.4 (CH_2), 35.1 (CH_2).

The spectroscopic data were consistent with those reported.[174]

d_1-4-Phenyl-1-butyne

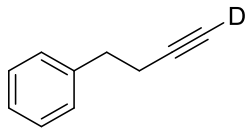

tert-Butyllithium (10.8 mL, 1.7 M in diethylether, 18.4 mmol) was added to a solution of 4-phenyl-1-butyne (2 mL, 15.4 mmol) in anhydrous tetrahydrofuran (20 mL) at -78 °C under a nitrogen atmosphere. The reaction was stirred for 1 hour before the dropwise addition of d_1-methanol (1 mL) over 15 minutes. The reaction was allowed to warm to room temperature before HCl (aq, 5 mL, 2M) was added. The aqueous phase was extracted with diethyl ether (3 x 15 mL). The combined organic extracts were dried ($MgSO_4$) and concentrated *in vacuo* to give d_1-4-phenyl-1-butyne as a yellow oil (1.66 g, 12.6 mmol, 82%). The product was used without further purification.

^{1}H NMR: (500 MHz, $CDCl_3$)

δ 7.36 – 7.30 (m, 2H, ArH), 7.27 – 7.22 (m, 3H, ArH), 2.88 (t, J = 7.6 Hz, 2H, $ArCH_2$), 2.51 (t, J = 7.6 Hz, 2H, CH_2CH_2).

^{2}H NMR: (77 MHz, $CHCl_3$)

δ 1.98 (s, 1D, CD)

The spectroscopic data were consistent with those reported.[232]

d_3-4-Phenyl-1-butene

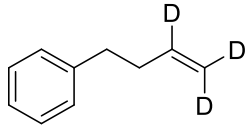

d_1-4-Phenyl-1-butyne (1.6 g, 12.6 mmol) was added to a stirred solution of Lindlar's catalyst (532 mg, 0.25 mmol of Pd) in DCM/Methanol (1:1 v/v, 20 mL) at room temperature under a deuterium atmosphere (1 atm). After 16 hours, HCl (aq, 2M) was added and the aqueous phase extracted with DCM (3 x 20 mL). The organic phase was dried ($MgSO_4$) and concentrated concentrated *in vacuo*. The off-white oil was then purified by vacuum distillation (2 x10^{-1}, 60 °C) to give d_3-4-phenyl-1-butene as a clear oil (320 mg, 2.3 mmol, 18%). There was also some over-reduction product d_5-4-phenyl-1-butane which could not be removed from the crude product.

^{1}H NMR: (400 MHz, $CDCl_3$)

δ 7.34 – 7.29 (m, 2H, ArH), 7.25 – 7.18 (m, 3H, ArH), 2.74 (t, J = 7.5 Hz, 2H, $ArCH_2$), 2.44 – 2.35 (m, 2H, CH_2CH_2).

^{2}H NMR: (77 MHz, $CHCl_3$)

δ 5.9 (s, 1H, CD), 5.0 (br, 2H, CD_2).

^{13}C NMR: (101 MHz, $CDCl_3$)

δ 141.9 (C), 137.6 (t, J = 23.4 Hz, CD), 128.5 (CH), 128.3 (CH), 125.9 (CH), 114.3 (p, J = 23.8 Hz, CD_2), 35.4 (CH_2), 35.3 (CH_2).

MS: (HRMS - EI^+)

Found 135.11107 ($C_{10}H_9D_3$) requires 135.11218

6.6 Hydrosilylation Products

1-(Triethoxysilyl)octane

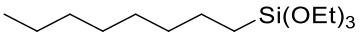

The title compound was produced according to General Procedure B. Triethoxysilane (230 µL, 1.25 mmol 1.25 eq.) was added to ^{DIPP}BIPMnBr$_2$ (14 mg, 20 µmol, 2 mol%) and NaO^{t}Bu (5.8 mg, 60 µmol, 6 mol%) followed by addition of octene (156 µl 1.0 mmol, 1.0 eq.) and the reaction mixture left to stir for 4 hours at 25 °C. The yellow oil was then purified by distillation ($8x10^{-2}$ mbar, 80°C) to give 1-(triethoxysilyl)octane as a colourless oil (235 mg, 85%).

^{1}H NMR: (500 MHz, $CDCl_3$)

δ 3.84 (q, *J* = 7.0 Hz, 6H, OCH_2), 1.46 – 1.23 (m, 21H, $6xCH_2$+$3xCH_3$), 0.90 (t, *J* = 6.9 Hz, 3H, CH_3), 0.72 – 0.61 (m, 2H, $SiCH_2$).

^{13}C NMR: (101 MHz, $CDCl_3$)

δ 58.3 (CH_2), 33.2 (CH_2), 31.9 (CH_2), 29.2 (CH_2) (2 resonances), 22.8 (CH_2), 22.7 (CH_2), 18.3 (CH_3), 14.1 (CH_3), 10.4 (CH_2).

^{29}Si NMR: (99 MHz, $CDCl_3$)

δ −44.5.

HRMS: (HRMS - EI^+)

Found 276.2143 ($C_{14}H_{32}O_3Si$), requires 276.2115.

The spectroscopic data were consistent with those reported.[48]

Octylsilylbenzene

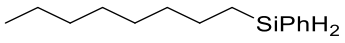

The title compound was produced according to General Procedure B. Phenylsilane (168 µL, 1.25 mmol 1.25 eq.) was added to ^{Et}BIPMnBr$_2$ (12.8 mg, 20 µmol, 2 mol%) and NaO^{t}Bu (5.8 mg, 60 µmol, 6 mol%) followed by addition of octene (156 µl 1.0 mmol, 1.0 eq.) and the reaction mixture left to stir for 4 hours at 25 °C. The yellow oil was then purified by distillation (2.5 x 10 $^{-1}$ mbar, 80 °C) to give octylsilylbenzene as a yellow oil (193 mg, 88%).

^{1}H NMR: (500 MHz, $CDCl_3$)

δ 7.63 – 7.56 (m, 2H, ArH), 7.45 – 7.35 (m, 3H, ArH), 4.31 (t, *J* = 3.7 Hz, 2H, Si*H*$_2$Ph), 1.52 – 1.43 (m, 2H, CH_2), 1.42 – 1.34 (m, 2H, CH_2), 1.30 – 1.17 (m, 8H, CH_2), 1.00 – 0.93 (m, 2H, $SiCH_2$), 0.90 (t, *J* = 6.9 Hz, 2H, CH_2*CH*$_3$).

^{13}C NMR: (126 MHz, $CDCl_3$)

δ 135.2 (CH), 132.9 (C), 129.5 (CH), 127.9 (CH), 32.8 (CH_2), 31.9 (CH_2), 29.5 (CH_2), 29.3 (CH_2), 29.2 (CH_2), 25.1 (CH_2), 22.7 (CH_2), 14.1 (CH_3), 10.0 (CH_2).

^{29}Si NMR: (99 MHz, $CDCl_3$)

δ −30.8.

HRMS: (HRMS - EI$^+$)

Found 220.1632 ($C_{14}H_{24}Si$), requires 220.1641.

The spectroscopic data were consistent with those reported.[233]

1-[(Diethoxy)methylsilyl]octane

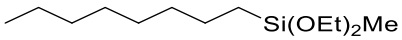

The title compound was produced according to General Procedure B. Diethoxy(methyl)silane (160.2 µL, 1.25 mmol 1.25 eq.) was added to ^{Et}BIPMnBr$_2$ (12.8 mg, 20 µmol, 2 mol%) and NaO^{t}Bu (5.8 mg, 60 µmol, 6 mol%) followed by addition of octene (156 µl 1.0 mmol, 1.0 eq.) and the reaction mixture left to stir for 4 hours at 25 °C. The yellow oil was then purified by distillation (2.5 x 10 $^{-1}$ mbar, 80 °C) to give 1-[(diethoxy)methylsilyl]octane as a yellow oil (210 mg, 85%).

^{1}H NMR: (500 MHz, $CDCl_3$)

δ 3.78 (q, *J* = 7.0 Hz, 4H, $SiOCH_2$), 1.42 – 1.27 (m, 12H, CH_2), 1.24 (t, *J* = 7.0 Hz, 6H, CH_3), 0.94 – 0.87 (m, 3H, CH_3), 0.67 – 0.60 (m, 2H, CH_2), 0.13 (s, 3H, $SiCH_3$).

^{13}C NMR: (126 MHz, $CDCl_3$)

δ 58.0 (OCH_2), 33.3 (CH_2), 31.9 (CH_2), 29.2 (CH_2), 22.8 (CH_2), 22.7 (CH_2), 18.4 (CH_3), 14.1 (CH_2), 13.9 (CH_2), -4.9 (CH_3).

^{29}Si NMR: (99 MHz, $CDCl_3$)

δ −4.2.

The spectroscopic data were consistent with those reported.[48]

1-Phenyl-4-(triethoxysilyl)butane

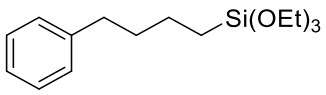

The title compound was produced according to General Procedure B. Triethoxysilane (230 µL, 1.25 mmol 1.25 eq.) was added to ^{DIPP}BIPMnBr$_2$ (14 mg, 20 µmol, 2 mol%) and NaO^{t}Bu (5.8 mg, 60 µmol, 6 mol%) followed by addition of 4-phenyl-1-butene (156 µl 1.0 mmol, 1.0 eq.) and the reaction mixture left to stir for 4 hours at 25 °C. The yellow oil was then purified by distillation (1.6 x 10 $^{-1}$ mbar, 100 °C) to give 1-phenyl-4-(triethoxysilyl)butane as a colourless oil (254 mg, 86%).

^{1}H NMR: (600 MHz, $CDCl_3$)

δ 7.32 – 7.25 (m, 2H, ArH), 7.22 – 7.16 (m, 3H, ArH), 3.83 (q, *J* = 7.0 Hz, 6H, $SiOCH_2$), 2.63 (t, *J* = 7.0 Hz, 2H, Ar*CH*$_2$), 1.74 – 1.65 (m, 2H, CH_2), 1.54 – 1.45 (m, 2H, CH_2), 1.24 (t, *J* = 7.0, 9H, CH_3), 0.77 – 0.65 (m, 2H, $SiCH_2$).

^{13}C NMR: (151 MHz, $CDCl_3$)

δ 142.7 (C), 128.4 (CH), 128.2 (CH), 125.6 (CH), 58.3 (CH_2), 35.6 (CH_2), 34.9 (CH_2), 22.5 (CH_2), 18.3 (CH_3), 10.3 (CH_2).

^{29}Si NMR: (99 MHz, $CDCl_3$)

δ −45.0.

HRMS: (HRMS - EI$^+$)

Found 296.1804 ($C_{16}H_{28}O_3Si$), requires 296.1802.

IR: ν_{max}(neat)

2972 (w), 2926 (w), 2884 (w), 2862 (w), 1454 (w, 1443 (w), 1389 (w), 1294 (w), 1165 (w), 1101 (s), 1074 (s), 1030 (w), 999 (w), 953 (s), 849 (w), 779 (s), 745 (s), 698 (s), 635 (w)

The spectroscopic data were consistent with those reported.[48]

1,3-Bis(triethoxysilyl)propane

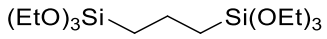

The title compound was produced according to General Procedure B. Triethoxysilane (230 µL, 1.25 mmol 1.25 eq.) was added to ^{DIPP}BIPMnBr$_2$ (14 mg, 20 µmol, 2 mol%) and NaO^{t}Bu (5.8 mg, 60 µmol, 6 mol%) followed by addition of allyltriethoxysilane (228 µl 1.0 mmol, 1.0 eq.) and the reaction mixture left to stir for 4 hours at 25 °C. The yellow oil was then purified by distillation (2 x 10^{-1} mbar, 80°C) to give 1,3-bis(triethoxysilyl)propane as a yellow oil (287 mg, 78%)

^{1}H NMR: (400 MHz, $CDCl_3$)

3.82 (q, *J* = 7.0 Hz, 12H, OCH_2), 1.64 – 1.53 (m, 2H, CH_2), 1.23 (t, *J* = 7.0 Hz, 18H, CH_3), 0.78 – 0.70 (m, 4H $SiCH_2$).

^{13}C NMR: (126 MHz, $CDCl_3$)

δ 58.3 (CH_2), 18.3 (CH_3), 16.5 (CH_2), 14.3 (CH_2).

^{29}Si NMR: (99 MHz, $CDCl_3$)

δ −45.3.

The spectroscopic data were consistent with those reported.[234]

3-Phenylpropyltriethoxysilane

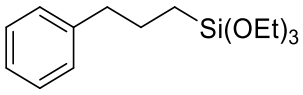

The title compound was produced according to General Procedure B. Triethoxysilane (230 µL, 1.25 mmol 1.25 eq.) was added to ^{DIPP}BIPMnBr$_2$ (14 mg, 20 µmol, 2 mol%) and NaO^{t}Bu (5.8 mg, 60 µmol, 6 mol%) followed by addition of allylbenzene (132 µl 1.0 mmol, 1.0 eq.) and the reaction mixture left to stir for 4 hours at 25 °C. The yellow oil was then purified by distillation (2.5 x 10 $^{-1}$ mbar, 120 °C) to give 3-phenylpropyltriethoxysilane as a colourless oil (230.1 mg, 81%).

^{1}H NMR: (600 MHz, $CDCl_3$)

δ 7.31 – 7.26 (m, 2H, ArH), 7.23 – 7.16 (m, 3H, ArH), 3.83 (q, *J* = 7.0, 1.0 Hz, 6H, OCH_2), 2.67 (t, *J* = 7.6 Hz, 2H, $ArCH_2$), 1.84 – 1.70 (m, 2H, CH_2), 1.24 (t, *J* = 7.0, 1.0 Hz, 9H, CH_3), 0.79 – 0.61 (m, 2H, $SiCH_2$).

^{13}C NMR: (126 MHz, $CDCl_3$)

δ 142.4 (C), 128.5 (CH), 128.2 (CH), 125.7 (CH), 58.3 (CH_2), 39.2 (CH_2), 24.8 (CH_2), 18.3 (CH_3), 10.2 (CH_2).

^{29}Si NMR: (99 MHz, $CDCl_3$)

δ −45.2.

The spectroscopic data were consistent with those reported.[235]

4-(2-Triethoxysilyl)ethylcyclohexene

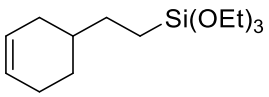

The title compound was produced by General Procedure B. Triethoxysilane (230 µL, 1.25 mmol 1.25 eq.) was added to ^{DIPP}BIPMnBr$_2$ (14 mg, 20 µmol, 2 mol%) and NaO^{t}Bu (5.8 mg, 60 µmol, 6 mol%) followed by addition of 4-vinylcyclohexene (130 µl 1.0 mmol, 1.0 eq.) and the reaction mixture left to stir for 4 hours at 25 °C. The yellow oil was then purified by distillation (8 x 10 $^{-2}$ mbar, 80 °C) to give 4-(2-triethoxysilyl)ethylcyclohexene as a colourless oil (214 mg, 77%).

^{1}H NMR: (600 MHz, $CDCl_3$)

δ 5.74 – 5.61 (m, 2H, HC=CH), 3.84 (q, *J* = 7.0, 6H, OCH_2), 2.18 – 2.10 (m, 1H, CH), 2.10 – 1.99 (m, 2H, CH_2), 1.82 – 1.73 (m, 1H, CH_2), 1.69 – 1.61 (m, 1H, CH_2), 1.55 – 1.44 (m, 1H, CH_2), 1.43 – 1.37 (m, 2H, CH_2), 1.26 (t, *J* = 7.0 Hz, 9H, CH_3), 1.22 – 1.11 (m, 1H, CH) 0.71 – 0.64 (m, 2H, CH_2).

^{13}C NMR: (151 MHz, $CDCl_3$)

δ 127.1 (CH), 126.6 (CH), 58.4 (OCH_2), 36.3 (CH), 31.5 (CH_2), 29.4, 28.4, 25.3, 18.3, 7.5.

^{29}Si NMR: (99 MHz, $CDCl_3$)

δ –44.4.

The spectroscopic data were consistent with those reported.[48]

1-(Triethoxysilyl)-4-butylmorpholine

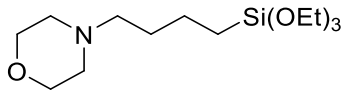

The title compound was produced according to General Procedure B. Triethoxysilane (230 µL, 1.25 mmol 1.25 eq.) was added to ^{DIPP}BIPMnBr$_2$ (14 mg, 20 µmol, 2 mol%) and NaO^{t}Bu (5.8 mg, 60 µmol, 6 mol%) followed by addition of 4-(3-buten-1-yl)morpholine (141 mg, 1.0 mmol, 1.0 eq.) and the reaction mixture left to stir for 4 hours at 25 °C. The yellow oil was then purified by distillation (2 x 10 $^{-1}$ mbar, 120 °C) to give *1-(triethoxysilyl)-4-butylmorpholine* as a yellow oil (183 mg, 60%).

^{1}H NMR: (500 MHz, $CDCl_3$)

δ 3.84 (q, *J* = 7.0 Hz, 6H, OCH_2), 3.73 (t, *J* = 7.0 Hz, 4H, OCH_2), 2.52 – 2.40 (m, 4H, NCH_2), 2.35 (t, *J* = 7.0 Hz, 2H, NCH_2), 1.59 – 1.42 (m, 4H, CH_2), 1.27 – 1.23 (t, *J* = 7.0 Hz, 9H, CH_3), 0.71 – 0.65 (m, 2H, $SiCH_2$).

^{13}C NMR: (126 MHz, $CDCl_3$)

δ 67.0 (CH_2), 58.7(CH_2), 58.3 (CH_2), 53.8 (CH_2), 29.8 (CH_2), 20.8 (CH_2), 18.3 (CH_3), 10.4 (CH_2).

^{29}Si NMR: (99 MHz, $CDCl_3$)

δ −45.2.

HRMS: (HRMS - EI+)

Found 305.20273 ($C_{14}H_{31}O_4NSi$), requires 305.20169.

IR: ν_{max} (neat)

2970 (w), 2928 (w), 2886 (w), 2859 (w), 2806 (w), 1389 (w), 1200 (w), 1165 (w), 1101 (s), 1072 (s), 1036 (w), 1007 (w), 953 (w), 916 (w), 872 (w), 860 (w), 779 (s), 741 (w), 677 (w), 627 (w).

1-(Triethoxysilyl)-4-(4-trifluoromethylphenyl)butane

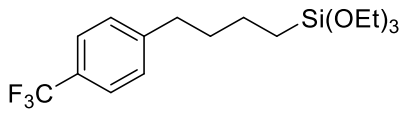

The title compound was produced according to General Procedure B. Triethoxysilane (230 µL, 1.25 mmol 1.25 eq.) was added to ^{DIPP}BIPMnBr$_2$ (14 mg, 20 µmol, 2 mol%) and NaO^{t}Bu (5.8 mg, 60 µmol, 6 mol%) followed by addition of 4-(4-trifluoromethyphenyl)-1-butene (200 mg, 1.0 mmol, 1.0 eq.) and the reaction mixture left to stir for 4 hours at 25 °C. The yellow oil was then purified by distillation (2 x 10 $^{-1}$ mbar, 120 °C) to give *1-(triethoxysilyl)-4-(4-trifluoromethylphenyl)butane* as a yellow oil (218 mg, 60%).

^{1}H NMR: (500 MHz, $CDCl_3$)

δ 7.54 (d, *J* = 7.6 Hz, 2H, ArCH), 7.30 (d, *J* = 8.0 Hz, 2H, ArCH), 3.83 (q, *J* = 7.0 Hz, 6H, OCH_2), 2.69 (t, *J* = 7.7 Hz, 2H, $ArCH_2$), 1.75 – 1.64 (m, 2H, CH_2), 1.54 – 1.44 (m, 2H, CH_2), 1.24 (t, *J* = 7.0 Hz, 9H, CH_3), 0.74 – 0.64 (m, 2H, $SiCH_2$).

^{13}C NMR: (126 MHz, $CDCl_3$)

δ 146.8 (C), 128.7 (CH_2), 128.0 (q, J = 32.2 Hz, C), 125.1 (q, J = 3.8 Hz, CH)

124.4 (q, J = 271.5, CF_3), 58.3 (CH_2), 35.4 (CH_2), 34.4 (CH_2), 22.4 (CH_2),

18.3 (CH_3), 10.2 (CH_2).

^{29}Si NMR: (99 MHz, $CDCl_3$)

δ −45.2.

^{19}F NMR: (471 MHz, $CDCl_3$)

δ −62.29.

HRMS: (HRMS - EI$^+$)

Found 364.16755 ($C_{17}H_{27}O_3F_3Si$), requires 364.16761.

IR: ν_{max} (neat)

2976 (w), 2928 (w), 2887 (w), 1618 (w), 1443 (w), 1391 (s), 1325 (s), 1300 (w), 1163 (s), 1099 (w), 1067 (s), 1018 (s), 1003 (w), 955 (s), 843 (w), 789 (s), 689 (w), 631 (w), 598 (w).

1-(Triethoxysilyl)-4-(4-fluoromethylphenyl)butane

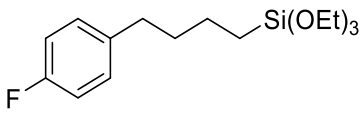

The title compound was produced according to General Procedure B. Triethoxysilane (230 µL, 1.25 mmol 1.25 eq.) was added to ^{DIPP}BIPMnBr$_2$ (14 mg, 20 µmol, 2 mol%) and NaO^{t}Bu (5.8 mg, 60 µmol, 6 mol%) followed by addition of 1-fluoro-4-(3-butenyl)-benzene (150 mg, 1.0 mmol, 1.0 eq.) and the reaction mixture left to stir for 4 hours at 25 °C. The yellow oil was then purified by distillation (2 x 10 $^{-1}$ mbar, 100 °C) to give *1-(triethoxysilyl)-4-(4-fluoromethylphenyl)butane* as a yellow oil (245 mg, 78%).

^{1}H NMR: (500 MHz, $CDCl_3$)

δ 7.17 – 7.11 (m, 2H, ArH), 7.01 – 6.89 (m, 2H, ArH), 3.83 (q, *J* = 7.0 Hz, 6H, OCH_2), 2.60 (t, *J* = 7.0 Hz, 2H, $ArCH_2$), 1.72 – 1.62 (m, 2H, CH_2), 1.51 – 1.44 (m, 2H, CH_2), 1.24 (t, *J* = 7.0 Hz, 9H, CH_3), 0.71 – 0.65 (m, 2H, $SiCH_2$).

^{13}C NMR: (126 MHz, $CDCl_3$)

δ 161.2 (d, J = 242.8 Hz, CF), 138.3 (C), 129.6 (d, J = 7.84 Hz, CH), 114.9 (d, J = 21.0 Hz, CH), 58.3 (CH_2), 35.0 (CH_2), 34.7 (CH_2), 22.4 (CH_2), 18.3 (CH_3), 10.3 (CH_2).

^{29}Si NMR: (99 MHz, $CDCl_3$)

δ -45.1.

^{19}F NMR: (471 MHz, $CDCl_3$)

δ -118.32.

MS: (HRMS - EI$^+$)

Found 314.1707 ($C_{16}H_{27}O_3FSi$), requires 314.1708

IR: ν_{max}(neat)

2974 (w), 2928 (w), 2886 (w), 2864 (w), 1508 (m), 1389 (w), 1221 (m), 1157 (s), 1101 (s), 1074 (s), 1001 (w), 953 (m), 847 (w), 779 (m), 756 (m), 702 (w), 677 (w).

1-(Triethoxysilyl)-4-(4-chlorophenyl)butane

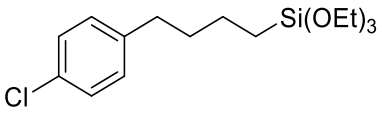

The title compound was produced according to General Procedure B. Triethoxysilane (230 µL, 1.25 mmol 1.25 eq.) was added to ^{DIPP}BIPMnBr$_2$ (14 mg, 20 µmol, 2 mol%) and NaO^{t}Bu (5.8 mg, 60 µmol, 6 mol%) followed by addition of 1-bromo-4-(3-butenyl)-benzene (211 mg, 1.0 mmol, 1.0 eq.) and the reaction mixture left to stir for 4 hours at 25 °C. The yellow oil was then purified by distillation (2 x 10 $^{-1}$ mbar, 100 °C) to give *1-(triethoxysilyl)-4-(4-chlorophenyl)butane* as a yellow oil (139 mg, 65%).

^{1}H NMR: (500 MHz, $CDCl_3$)

δ 7.27 – 7.22 (m, 2H, ArH), 7.14 – 7.10 (m, 2H, ArH), 3.83 (q, J = 7.0 Hz, 6H, OCH_2), 2.62 – 2.57 (m, 2H, $ArCH_2$), 1.70 – 1.61 (m, 2H, CH_2), 1.52 – 1.43 (m, 2H, CH_2), 1.24 (t, J = 7.0 Hz, 9H, CH_3), 0.71 – 0.65 (m, 2H, CH_2Si).

^{13}C NMR: (126 MHz, $CDCl_3$)

δ 141.1 (C), 131.3 (C), 129.7 (CH), 128.3 (CH), 58.3 (CH_2), 34.9 (CH_2), 34.7 (CH_2), 22.4 (CH_2), 18.3 (CH_3), 10.3 (CH_2).

^{29}Si NMR: (99 MHz, $CDCl_3$)

δ -45.2.

HRMS: (HRMS - EI$^+$)

Found 330.1419 ($C_{16}H_{27}O_3ClSi$), requires 330.1413.

IR: ν_{max} (neat)
2974 (w), 2926 (w), 2855 (w), 1490 (m), 1388 (w), 1165 (m), 1101 (s), 1074 (s), 1101 (m), 1002 (m), 954 (m), 856 (w), 833 (m), 779 (s), 738 (s), 704 (m), 659 (m), 628 (w)

1-(Triethoxysilyl)-4-(4-bromophenyl)butane

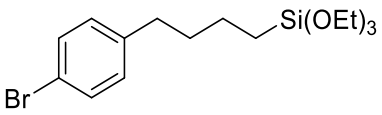

The title compound was produced according to General Procedure B. Triethoxysilane (230 µL, 1.25 mmol 1.25 eq.) was added to ^{DIPP}BIPMnBr$_2$ (14 mg, 20 µmol, 2 mol%) and NaO^{t}Bu (5.8 mg, 60 µmol, 6 mol%) followed by addition of 1-bromo-4-(3-butenyl)-benzene (211 mg, 1.0 mmol, 1.0 eq.) and the reaction mixture left to stir for 4 hours at 25 °C. The yellow oil was then purified by distillation (2 x 10 $^{-1}$ mbar, 100 °C) to give *1-(triethoxysilyl)-4-(4-bromophenyl)butane* as a yellow oil (139 mg, 37%).

^{1}H NMR: (601 MHz, $CDCl_3$)

δ 7.40 (d, *J* = 8.4 Hz, 2H, ArH), 7.06 (d, *J* = 8.4 Hz, 2H, ArH), 3.83 (q, *J* = 7.0 Hz, 6H, $SiCH_2$), 2.57 (m, 2H, CH_2), 1.70 – 1.60 (m, 2H, CH_2), 1.52 – 1.44 (m, 2H, CH_2), 1.24 (t, *J* = 7.0 Hz, 9H, CH_3), 0.70 – 0.65 (m, 2H, CH_2).

^{13}C NMR: (126 MHz, $CDCl_3$)

δ 141.7 (C) , 131.3 (CH), 130.2 (CH), 119.3 (C), 58.3 (CH_2), 35.00 (CH_2), 34.6 (CH_2), 22.4 (CH_2), 18.3 (CH_3), 10.3 (CH_2).

^{29}Si NMR: (99 MHz, $CDCl_3$)

δ −45.1.

HRMS: (HRMS - EI$^+$)

Found 374.0906 ($C_{16}H_{27}O_3BrSi$), requires 374.0907.

IR: ν_{max}(neat)
2972 (w), 2926 (w), 2884 (w), 1487 (m), 1389 (w), 1165 (m), 1101 (s), 1070 (s), 1011 (m), 955 (m), 856 (w), 777 (m), 631 (w), 602 (w).

1-(Triethoxysilyl)-5-(triethoxysilylether)hexane

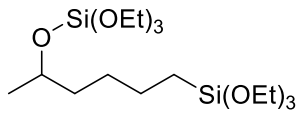

The title compound was produced according to General Procedure B. Triethoxysilane (552 µL, 3 mmol 3 eq.) was added to ^{DIPP}BIPMnBr$_2$ (14 mg, 20 µmol, 2 mol%) and NaO^{t}Bu (5.8 mg, 60 µmol, 6 mol%) followed by addition of 5-hexen-2-one (117 µl, 1.0 mmol, 1.0 eq.) and the reaction mixture left to stir for 4 hours at 25 °C. The yellow oil was then purified by distillation (2 x 10 $^{-1}$ mbar, 100 °C) to give *1-(Triethoxysilyl)-5-(triethoxysilylether)hexane* as a yellow oil (345 mg, 81%).

^{1}H NMR: (500 MHz, $CDCl_3$)

δ 4.09 – 4.02 (m, 1H, OCH), 3.88 – 3.81 (m, 12H, OCH_2), 1.49 – 1.30 (m, 6H, CH_2), 1.28 – 1.23 (m, 18H, CH_3), 1.22 (d, *J* = 6.1 Hz, 3H, CH*CH_3*), 0.69 – 0.63 (m, 2H, $SiCH_2$).

^{13}C NMR: (126 MHz, $CDCl_3$)

δ 69.6 (CH), 59.1 (CH_2), 58.3 (CH_2), 38.9 (CH_2), 29.1 (CH_2), 23.2 (CH_2), 22.9, 18.3 (CH_3), 18.1 (CH_3), 10.5 (CH_2).

^{29}SI NMR: (99 MHz, $CDCl_3$)

δ −44.9 ($RSi(OEt)_3$), −82.9 ($Si(OR)_4$).

MS: (HRMS - EI^+)

Found 426.2464 ($C_{18}H_{42}O_7Si_2$), requires 426.2464.

IR: ν_{max}(neat)

2974 (w), 2928 (w, 2886 (w), 1391 (w), 1167 (w), 1102 (w), 1075 (s), 957 (s), 851 (w), 785 (s), 737 (w), 677 (w)

2-[4-(*tert*-Butyl)phenyl]-(triethoxysilyl)ethane

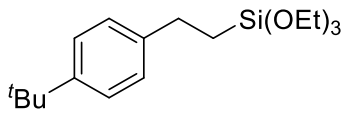

The title compound was produced according to General Procedure B. Triethoxysilane (230 µL, 1.25 mmol 1.25 eq.) was added to $^{DIPP}BIPMnBr_2$ (14 mg, 20 µmol, 2 mol%) and NaO^{t}Bu (5.8 mg, 60 µmol, 6 mol%) followed by addition of 4-*tert*-butylstyrene (184 µl, 1.0 mmol, 1.0 eq.) and the reaction mixture left to stir for 4 hours at 25 °C. The yellow oil was then purified by distillation (2 x 10^{-1} mbar, 100 °C) to give 2-(4-(*tert*-butyl)phenyl-(triethoxysilyl)ethane as a yellow oil (97 mg, 30%, as a 94:6 mixture of linear:branched regioisomers).

^{1}H NMR: (500 MHz, $CDCl_3$)

δ 7.35 – 7.31 (m, 2H, ArH), 7.20 – 7.16 (m, 2H, ArH), 3.84 (q, J = 7.0 Hz, 6H, OCH_2), 2.78 – 2.70 (m, 2H, $ArCH_2$), 1.33 (s, 9H, CH_3), 1.25 (t, J = 7.0 Hz, 9H, CH_3), 1.06 – 0.99 (m, 2H, $SiCH_2$).

^{13}C NMR: (101 MHz, $CDCl_3$)

δ 148.43 (C), 141.51 (C), 127.44 (CH), 125.18 (CH), 58.38 (CH_2), 34.33 (CH_2), 31.42 (C), 28.25 (CH_3), 18.30 (CH_3), 12.34 (CH_2).

^{29}Si NMR: (99 MHz, $CDCl_3$)

δ -45.8

IR: ν_{max}(neat)

3707 (w), 3680 (w), 3665 (w), 2972 (m), 2924 (w), 2876 (w), 2845 (w), 1454 (w), 1389 (w), 1165 (m), 1099 (s), 1072 (s), 1034 (s), 955 (m), 775 (m), 741 w), 698 (m).

2-[4-(Methoxy)phenyl]-(triethoxysilyl)ethane

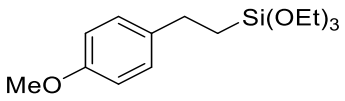

The title compound was produced according to General Procedure B. Triethoxysilane (230 µL, 1.25 mmol 1.25 eq.) was added to ^{DIPP}BIPMnBr$_2$ (14 mg, 20 µmol, 2 mol%) and NaO^{t}Bu (5.8 mg, 60 µmol, 6 mol%) followed by addition of 4-methoxystyrene (133 µl, 1.0 mmol, 1.0 eq.) and the reaction mixture left to stir for 4 hours at 25 °C. The yellow oil was then purified by distillation (2 x 10 $^{-1}$ mbar, 100 °C) to give 2-(4-(methoxy)phenyl-(triethoxysilyl)ethane as a yellow oil (97 mg, 30%, as a 94:6 mixture of linear: branched regioisomers).

^{1}H NMR: (500 MHz, $CDCl_3$)

δ 7.15 (d, *J* = 8.6 Hz, 2H, ArH), 6.85 (d, *J* = 8.6 Hz, 2H, ArH), 3.85 (q, *J* = 7.0 Hz, 6H, OCH_2), 3.81 (s, 3H, OCH_3), 2.74 – 2.67 (m, 2H, $ArCH_2$), 1.26 (t, *J* = 7.0 Hz, 9H, CH_3), 1.03 – 0.92 (m, 2H, $SiCH_2$).

^{13}C NMR: (126 MHz, $CDCl_3$)

δ 157.7 (C), 136.8 (C), 128.7 (CH), 113.7 (CH), 58.4 (CH_2), 55.3 (CH_3), 28.0 (CH_2), 18.3 (CH_3), 12.8 (CH_2).

^{29}Si NMR: (99 MHz, $CDCl_3$)

δ −45.9.

The spectroscopic data were consistent with those reported.[236]

Phenyl-2-(triethoxysilyl)ethane

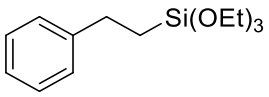

The title compound was produced according to General Procedure B. Triethoxysilane (230 µL, 1.25 mmol 1.25 eq.) was added to ^{DIPP}BIPMnBr$_2$ (14 mg, 20 µmol, 2 mol%) and NaO^{t}Bu (5.8 mg, 60 µmol, 6 mol%) followed by addition of styrene (115 µl, 1.0 mmol, 1.0 eq.) and the reaction mixture left to stir for 4 hours at 25 °C. The yellow oil was then purified by distillation (1 x 10 $^{-2}$ mbar, 100 °C) to give phenyl-2-(triethoxysilyl)ethane as a yellow oil (89 mg, 33%, 80:20 L:B).

Phenyl-2-(triethoxysilyl)ethane

^{1}H NMR: (601 MHz, $CDCl_3$)
δ 7.33 – 7.17 (m, 5H, ArH), 3.85 (q, *J* = 7.0 Hz, 6H, OCH_2), 2.79 – 2.74 (m, 2H, $ArCH_2$), 1.26 (t, *J* = 7.0 Hz, 9H), 1.05 – 0.98 (m, 2H, CH_2).

^{13}C NMR: (151MHz, $CDCl_3$)
δ 144.6 (C), 128.3 (CH), 127.8 (CH), 125.6 (CH), 58.4 (CH_2), 28.9 (CH_2), 18.3 (CH_3), 12.5 (CH_2).

Phenyl-1-(triethoxysilyl)ethane

^{1}H NMR: (601 MHz, $CDCl_3$)
δ 7.33 – 7.17 (m, 5H, ArH), δ 3.75 (q, *J* = 7.0 Hz, 6H, OCH_2), 2.37 – 2.30 (q, J= 7.4 Hz, 1H, ArCH), 1.46 – 1.42 (d, J = 7.6 Hz, 3H, CH_3), 1.17 (t, *J* = 7.0 Hz, 9H, CH_3).

^{13}C NMR: (151MHz, $CDCl_3$)
δ 144.1 (C), 128.0 (CH), 127.9 (CH), 124.8 (CH), 58.8 (CH_2), 26.2 (CH), 18.2 (CH_3), 15.6 (CH_3).

The spectroscopic data were consistent with those reported.[233]

***d*$_3$-Phenyl-4-(triethoxysilyl)butane**

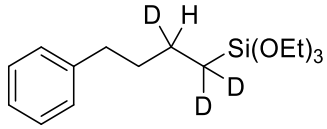

The title compound was produced according to General Procedure B. Triethoxysilane (115 µL, 0.625 mmol, 1.25 eq.) was added to ^{DIPP}BIPMnBr$_2$ (7 mg, 10 µmol, 2 mol%) and NaO^{t}Bu (2.9 mg, 30 µmol, 6 mol%) followed by addition of d$_3$-4-phenyl-1-butene (67 mg, 0.5 mmol, 1.0 eq.) and the reaction mixture left to stir for 4 hours at 25 °C. T rimethoxybenzene (16.8 mg, 0.2 mmol) dissolved in diethylether (1 mL) was added to the reaction. The volatiles were removed *in vacuo* and an NMR taken. The predominant product is *d$_3$-phenyl-4-(triethoxysilyl)butane.*

^{1}H NMR: (600 MHz, $CDCl_3$)

δ 7.33 – 7.26 (m, 2H, ArH), 7.24 – 7.16 (m, 3H, ArH), 3.83 (q, *J* = 7.0 Hz, 6H, $SiCH_2$), 2.63 (t, *J* = 7.0 Hz, 2H, Ar*CH$_2$*), 1.74 – 1.65 (m, 2H, CH_2), 1.54 – 1.45 (m, 2H, CDH), 1.24 (t, *J* = 7.0, 9H, CH_3), 0.77 – 0.65 (m, 2H, $SiCD_2$).

^{2}H NMR: (77 MHz, $CHCl_3$)

δ 1.51 (CD_2), 0.71 (CDH).

^{13}C NMR: (151 MHz, $CDCl_3$)

δ 142.7 (C), 128.4 (CH), 128.2 (CH), 125.6 (CH), 58.3 (CH_2), 35.6 (CH_2), 34.7 (CH_2), 22.0 (t, J = 18.9 Hz, CHD), 18.3 (CH_3), 9.4 (p, J = 18.0 Hz, CD_2).

^{29}Si NMR: (99 MHz, $CDCl_3$)

δ –45.1.

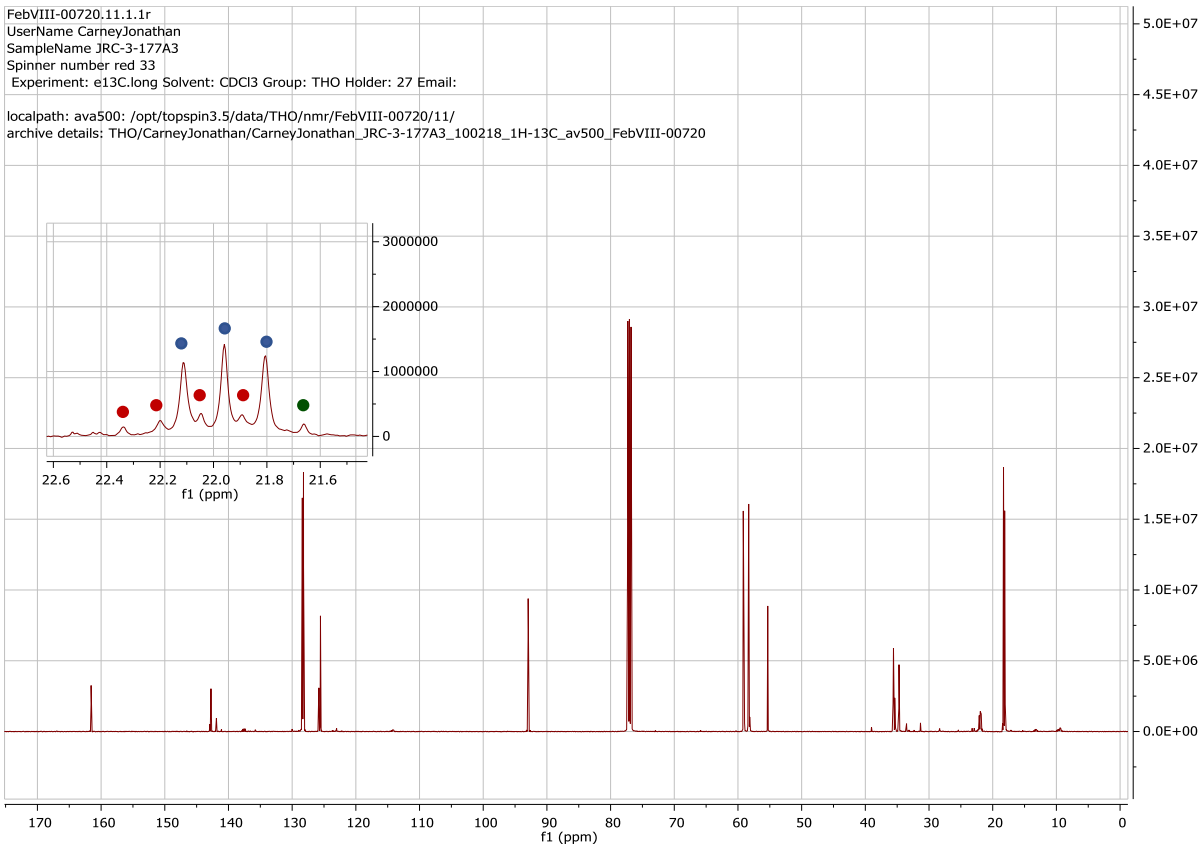

^{13}C NMR of hydrosilylation of d_3-4-phenyl-1-butene with peak at ~22.0 expanded to show multiple hydrosilylation products corresponding to the following products:

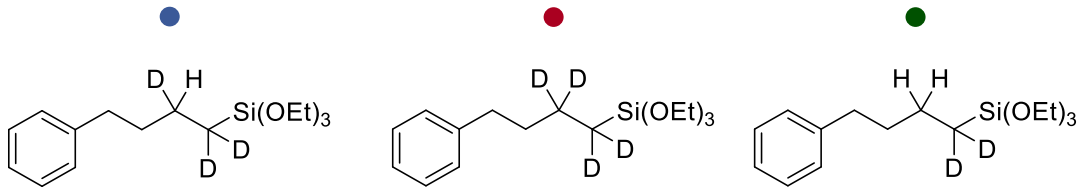

6.7 Hydroboration Products

2-[4-(*tert*-Butyl)phenethyl]-4,4,5,5-tetramethyl]-1,3,2-dioxaborolane

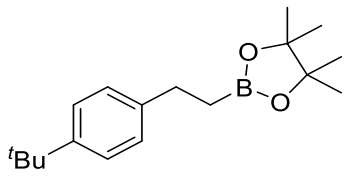

The title compound was produced according to General Procedure C. Pinacolborane (220 µL, 1.5 mmol 1.5 eq.) was added to ^{DIPP}BIPMnBr$_2$ (14 mg, 20 µmol, 2 mol%) and NaO^{t}Bu (5.8 mg, 60 µmol, 6 mol%) followed by addition of 4-*tert*-butylstyrene (184 µl, 1.0 mmol, 1.0 eq.) and the reaction mixture left to stir for 18 hours at 60 °C. The yellow oil was then purified by flash column chromatography (40 g SiO_2, 30 mm Ø, wet loaded, 9:1 pentane:EtOAc, *ca*. 5 mL fractions) to give 2-[4-(*tert*-butyl)phenethyl]-4,4,5,5-tetramethyl-1,3,2-dioxaborolane as a yellow oil (276 mg, 96%, as a 90:10 mixture of linear:branched regioisomers).

^{1}H NMR: (500 MHz, $CDCl_3$)

δ 7.34 – 7.29 (m, 2H, ArH), 7.20 – 7.15 (m, 2H, ArH), 2.77 – 2.71 (m, 2H, $ArCH_2$), 1.32 (s, 9H, C(CH_3)$_3$), 1.24 (s, 12H, C(CH_3)$_2$), 1.19 – 1.13 (m, 2H, CH_2).

^{13}C NMR: (126 MHz, $CDCl_3$)

δ 148.3 (C), 141.4 (C), 127.6 (CH), 125.1 (CH), 83.1 (C), 34.3 (C), 31.4 (CH_3), 29.4 (CH_2), 24.8 (CH_3). Missing CH_2 peak (CH_2–B) due to quadrupole effect.

^{11}B NMR: (160 MHz, $CDCl_3$)

δ 34.0.

The spectroscopic data were consistent with those reported.[237]

2-[4-(Trifluoromethyl)phenethyl]-4,4,5,5-tetramethyl-1,3,2-dioxaborolane

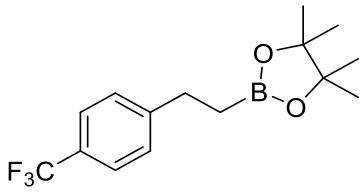

The title compound was produced according to General Procedure C. Pinacolborane (220 µL, 1.5 mmol 1.5 eq.) was added to ^{DIPP}BIPMnBr$_2$ (14 mg, 20 µmol, 2 mol%) and NaO^{t}Bu (5.8 mg, 60 µmol, 6 mol%) followed by addition of 4-(trifluoromethyl)styrene (130 µl, 1.0 mmol, 1.0 eq.) and the reaction mixture left to stir for 18 hours at 60 °C. The yellow oil was then purified by flash column chromatography (40 g SiO_2, 30 mm Ø, wet loaded, 9:1 pentane:EtOAc, *ca*. 5 mL fractions) to give 2-[4-(trifluoromethyl)phenethyl]-4,4,5,5-tetramethyl-1,3,2-dioxaborolane as a yellow oil (216 mg, 72%, as a 89:11 mixture of linear:branched regioisomers).

2-[4-(trifluoromethyl)phenethyl]-4,4,5,5-tetramethyl-1,3,2-dioxaborolane

^{1}H NMR: (500 MHz, $CDCl_3$)

δ 7.53 (d, *J* = 7.8 Hz, 2H, ArH), 7.34 (d, *J* = 7.9 Hz, 2H, ArH), 2.82 (t, *J* = 8.1 Hz, 2H, $ArCH_2$), 1.24 (s, 12H, CH_3), 1.20 – 1.14 (m, 2H, BCH_2)

^{13}C NMR: (126 MHz, $CDCl_3$)

δ 148.5 (C), 128.3 (CH), 128.0 (CH), 127.9 (q, *J* = 32.2 Hz, C), 125.1 (q, *J* = 4.0 Hz, CH)), 124.5 (q, *J* = 271.7 Hz, CF_3), 83.3 (C), 29.8 (CH_2), 24.8 (CH_3). Missing CH_2 peak (CH_2–B) due to quadrupole effect.

^{11}B NMR: (160 MHz, $CDCl_3$)

δ 33.8

1-[4-(trifluoromethyl)phenethyl]-4,4,5,5-tetramethyl-1,3,2-dioxaborolane

^{1}H NMR: (500 MHz, $CDCl_3$)

δ 7.53 (d, *J* = 7.8 Hz, 2H, ArH), 7.34 (d, *J* = 7.9 Hz, 2H, ArH), 2.53 (q, *J* = 7.5 Hz, 1H, ArCH), 1.37 (d, *J* = 7.5 Hz, 3H, CH_3), 1.24 (s, 12H, C(CH_3)$_3$).

^{13}C NMR: (126 MHz, $CDCl_3$)

δ 149.3 (C), 128.0 (CH), 125.1 (m, overlapped by linear product), 83.6 (C), 24.6 (CH_3), 24.6 (CH_3), 16.7 (CH_3). Peaks at 127.4 (q, J = 32.5 Hz, CH), 124.5 (q, J = 271.6 Hz) not observed because of the C-F coupling and the dominance of the linear product in the sample. Missing CH_2 peak (CH_2–B) due to quadrupole effect.

^{11}B NMR: (160 MHz, $CDCl_3$)

δ 33.8

The spectroscopic data were consistent with those reported.[237]

2-[4-(Fluoro)phenethyl]-4,4,5,5-tetramethyl-1,3,2-dioxaborolane

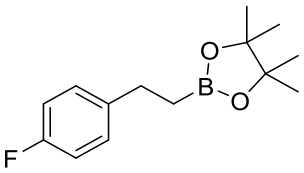

The title compound was produced according to General Procedure C. Pinacolborane (220 µL, 1.5 mmol 1.5 eq.) was added to ^{DIPP}BIPMnBr$_2$ (14 mg, 20 µmol, 2 mol%) and NaO^{t}Bu (5.8 mg, 60 µmol, 6 mol%) followed by addition of 4-fluorostyrene (120 µl, 1.0 mmol, 1.0 eq.) and the reaction mixture left to stir for 18 hours at 60 °C. The yellow oil was then purified by flash column chromatography (30 g SiO_2, 30 mm Ø, wet loaded, 3:1 pentane:EtOAc, *ca*. 5 mL fractions) to give 2-[4-(fluoro)phenethyl]-4,4,5,5-tetramethyl-1,3,2-dioxaborolane as a yellow oil (185 mg, 74%, as a 93:7 mixture of linear:branched regioisomers).

2-[4-(fluoro)phenethyl]-4,4,5,5-tetramethyl-1,3,2-dioxaborolane

^{1}H NMR: (400 MHz, $CDCl_3$)

δ 7.21 – 7.15 (m, 2H, ArH), 7.00 – 6.91 (m, 2H, ArH), 2.74 (t, *J* = 8.1 Hz, 2H, $ArCH_2$), 1.23 (s, 12H, CH_3), 1.17 – 1.11 (t, *J* = 8.2 Hz, 2H, BCH_2).

^{13}C NMR: (151 MHz, $CDCl_3$)

δ 161.1 (d, *J* = 238 Hz), 140.0 (d, *J* = 3.1 Hz), 129.3 (d, *J* = 7.9 Hz), 114.8 (d, *J* = 21.3 Hz), 83.2, 29.2, 24.8. Missing CH_2 peak (CH_2–B) due to quadrupole effect.

^{11}B NMR: (128 MHz, $CDCl_3$)

34.4.

^{19}F NMR: (376 MHz, $CDCl_3$)

δ −118.41.

1-[4-(fluoro)phenethyl]-4,4,5,5-tetramethyl-1,3,2-dioxaborolane

^{1}H NMR: (400 MHz, $CDCl_3$)

δ 7.21 – 7.15 (m, 2H, ArH), 7.00 – 6.91 (m, 2H, ArH), 2.43 (q, *J* = 7.3 Hz, 1H, ArCH), 1.33 (d, *J* = 7.5 Hz, 3H, CH*CH*$_3$), 1.23 (s, 12H, C(*CH*$_3$)$_2$).

^{13}C NMR: (151 MHz, $CDCl_3$)

δ 160.9 (d, *J* = 242 Hz), 140.5 (d, *J* = 3.0 Hz), 129.0 (d, J =7.7 Hz), 115.0 (d, *J* = 21.9 Hz), 83.4, 24.6, 24.6, 17.2. Missing CH_2 peak (CH_2–B) due to quadrupole effect.

^{11}B NMR: (128 MHz, $CDCl_3$)

34.4.

^{19}F NMR: (376 MHz, $CDCl_3$)

δ –119.02.

The spectroscopic data were consistent with those reported.[237]

2-[4-(Bromo)phenethyl]-4,4,5,5-tetramethyl-1,3,2-dioxaborolane

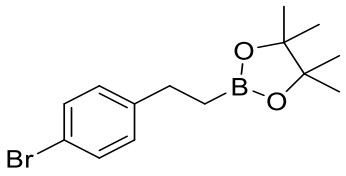

The title compound was produced according to General Procedure C. Pinacolborane (220 µL, 1.5 mmol 1.5 eq.) was added to ^{DIPP}BIPMnBr$_2$ (14 mg, 20 µmol, 2 mol%) and NaO^{t}Bu (5.8 mg, 60 µmol, 6 mol%) followed by addition of 4-bromostyrene (131 µl, 1.0 mmol, 1.0 eq.) and the reaction mixture left to stir for 18 hours at 60 °C. The yellow oil was then purified by flash column chromatography (40 g SiO_2, 30 mm Ø, wet loaded, 9:1 pentane:EtOAc, *ca*. 5 mL fractions) to give 2-[4-(bromo)phenethyl]-4,4,5,5-tetramethyl-1,3,2-dioxaborolane as a yellow oil (198 mg, 64%, as a 91:9 mixture of linear:branched regioisomers).

^{1}H NMR: (500 MHz, $CDCl_3$)

δ 7.42 – 7.36 (m, 2H, ArH), 7.13 – 7.08 (m, 2H, ArH), 2.72 (t, *J* = 8.1 Hz, 2H, $ArCH_2$), 1.24 (s, 12H, CH_3) 1.16 – 1.10 (m, 2H, CH_2).

^{13}C NMR: (126 MHz, $CDCl_3$)

δ 143.4 (C), 131.2 (CH), 129.8 (CH), 119.2 (C), 83.5 (C), 29.4 (CH_2), 24.8 (CH_3). Missing CH_2 peak (CH_2–B) due to quadrupole effect.

^{11}B NMR: (160 MHz, $CDCl_3$)

δ 33.8.

The spectroscopic data were consistent with those reported.[237]

2-[3-(Methoxy)phenethyl]-4,4,5,5-tetramethyl-1,3,2-dioxaborolane

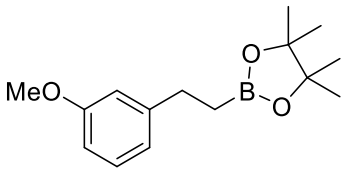

The title compound was produced according to General Procedure C. Pinacolborane (220 µL, 1.5 mmol 1.5 eq.) was added to ^{DIPP}BIPMnBr$_2$ (14 mg, 20 µmol, 2 mol%) and NaO^{t}Bu (5.8 mg, 60 µmol, 6 mol%) followed by addition of 3-vinylanisole (139 µl, 1.0 mmol, 1.0 eq.) and the reaction mixture left to stir for 18 hours at 60 °C. The yellow oil was then purified by flash column chromatography (40 g SiO_2, 30 mm Ø, wet loaded, 9:1 pentane:EtOAc, *ca*. 5 mL fractions) to give 2-[3-(methoxy)phenethyl]-4,4,5,5-tetramethyl-1,3,2-dioxaborolane as a yellow oil (274 mg, 99%, (as a 93:7 mixture of linear:branched regioisomers).

^{1}H NMR: (500 MHz, $CDCl_3$)

δ 7.23 – 7.16 (m, 1H, ArH), 6.83 (ddt, *J* = 7.5, 1.6, 0.8 Hz, 1H, ArH), 6.82 – 6.78 (m, 1H, ArH), 6.73 (ddd, *J* = 8.2, 2.7, 1.0 Hz, 1H, ArH), 3.81 (s, 3H, OCH_3), 2.79 – 2.71 (m, 2H, $ArCH_2$), 1.25 (s, 12H, $C(CH_3)_2$), 1.18 – 1.14 (m, 2H, BCH_2).

^{13}C NMR: (126 MHz, $CDCl_3$)

δ 159.6 (C), 146.1 (C), 129.1 (CH), 120.4 (CH), 113.6 (CH), 111.0 (CH), 83.1 (CH_3), 55.1 (CH_2), 30.0 (CH_2), 24.8 (CH_3). Missing CH_2 peak (CH_2–B) due to quadrupole effect.

^{11}B NMR: (160 MHz, $CDCl_3$)

δ 33.9.

MS: (HRMS - EI^+)

Found 262.17478 ($C_{15}H_{23}O_3B$), requires 262.17348.

IR: ν_{max}(neat)

2976 (w), 2934 (w), 2835 (w), 1601 (w), 1584 (w), 1489 (w), 1454 (w), 1369 (s), 1315 (m), 1260 (s), 1213 (w), 1163 (m), 1142 (s), 1107 (w), 1045 (m), 966 (m), 847 (m), 777 (m), 694 (m), 673 (w).

2-(2,4,6-Trimethylphenethyl)-4,4,5,5-tetramethyl-1,3,2-dioxaborolane

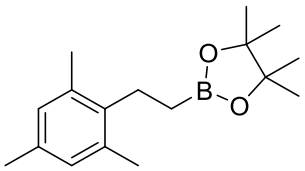

The title compound was produced according to General Procedure C. Pinacolborane (220 µL, 1.5 mmol 1.5 eq.) was added to ^{DIPP}BIPMnBr$_2$ (14 mg, 20 µmol, 2 mol%) and NaO^{t}Bu (5.8 mg, 60 µmol, 6 mol%) followed by addition of 2,4,6-trimethylstyrene (161 µl, 1.0 mmol, 1.0 eq.) and the reaction mixture left to stir for 18 hours at 60 °C. The yellow oil was then purified by flash column chromatography (40 g SiO_2, 30 mm Ø, wet loaded, 9:1 pentane:EtOAc, *ca*. 5 mL fractions) to give 2-(2,4,6-trimethylphenethyl)-4,4,5,5-tetramethyl-1,3,2-dioxaborolane as a yellow oil (104 mg, 31%, as a 97:3 mixture of linear:branched regioisomers).

^{1}H NMR: (601 MHz, $CDCl_3$)

δ 6.83 (s, 2H, ArH), 2.72 – 2.67 (m, 2H, $ArCH_2$), 2.32 (s, 6H $ArCH_3$), 2.26 (s, 3H, $ArCH_3$), 1.29 (s, 12H, CH_3), 1.02 – 0.95 (m, 2H, BCH_2).

^{13}C NMR: (126 MHz, $CDCl_3$)

δ 138.5 (C), 135.6 (CH), 134.6 (C), 128.9 (C), 83.1 (C), 24.9 (CH_3), 23.3 (CH_3), 20.8 (CH_3), 19.7 (CH_3). Missing CH_2 peak (CH_2–B) due to quadrupole effect.

^{11}B NMR: (160 MHz, $CDCl_3$)

δ 34.0.

MS: (HRMS - EI$^+$)

Found 274.20986 ($C_{17}H_{27}O_2B$), requires 274.21060.

IR: ν_{max}(neat)
2976 (w), 2916 (w), 2870 (w), 1612 (w), 1481 (w), 1466 (w), 1447 (w), 1369 (s), 1312 (s), 1271 (w), 1213 (w), 1165 (m), 1144 (s), 1109 (w), 1074 (w), 1028 (w), 1007 (w), 966 (m), 885 (w), 847 (s), 741 (w), 673 (w).

2-(2-Phenyl-2-methylethyl)-4,4,5,5-tetramethyl-1,3,2-dioxaborolane

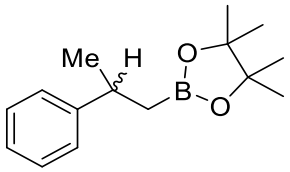

The title compound was produced according to General Procedure C. Pinacolborane (220 µL, 1.5 mmol 1.5 eq.) was added to ^{DIPP}BIPMnBr$_2$ (14 mg, 20 µmol, 2 mol%) and NaO^{t}Bu (5.8 mg, 60 µmol, 6 mol%) followed by addition of α-methylstyrene (130 µl, 1.0 mmol, 1.0 eq.) and the reaction mixture left to stir for 18 hours at 60 °C. The yellow oil was then purified by flash column chromatography (40 g SiO_2, 30 mm Ø, wet loaded, 9:1 pentane:EtOAc, *ca*. 5 mL fractions) to give 2-(2-phenyl-2-methylethyl)-4,4,5,5-tetramethyl-1,3,2-dioxaborolane as a yellow oil (81 mg, 33%, >99:1 linear:branched).

^{1}H NMR: (500 MHz, $CDCl_3$)

δ 7.32 – 7.23 (m, 4H, ArH), 7.19 – 7.14 (m, 1H, ArH), 3.05 (app. sextet , *J* = 7.1 Hz, 1H, ArCH), 1.30 (d, *J* = 6.9 Hz, 3H CH*CH$_3$*), 1.23-1.12 (m, 2H, BCH_2), 1.18 (s, 12H, $C(CH_3)_2$).

^{13}C NMR: (126 MHz, $CDCl_3$)

δ 149.2 (C), 128.2 (CH), 126.6 (CH), 125.7 (CH), 83.0 (C), 35.8 (CH), 24.9 (CH_3), 24.8 (CH_3), 24.7 (CH_3). Missing CH_2 peak (CH_2–B) due to quadrupole effect.

^{11}B NMR: (160 MHz, $CDCl_3$)

δ 33.7.

The spectroscopic data were consistent with those reported.[174]

Octyl-4,4,5,5-tetramethyl-1,3,2-dioxaborolane

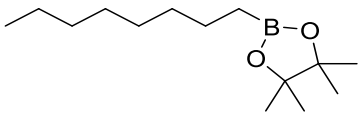

The title compound was produced according to General Procedure C. Pinacolborane (220 µL, 1.5 mmol 1.5 eq.) was added to ^{DIPP}BIPMnBr$_2$ (14 mg, 20 µmol, 2 mol%) and NaO^{t}Bu (5.8 mg, 60 µmol, 6 mol%) followed by addition octene (156 µl, 1.0 mmol, 1.0 eq.) and the reaction mixture left to stir for 18 hours at 60 °C. The yellow oil was then purified by flash column chromatography (40 g SiO_2, 30 mm Ø, wet loaded, 4:1 pentane:EtOAc, *ca*. 5 mL fractions) to give Octyl-4,4,5,5-tetramethyl-1,3,2-dioxaborolane as a yellow oil (225 mg, 94%, >99:1 linear:branched).

^{1}H NMR: (500 MHz, $CDCl_3$)

δ 1.47 – 1.37 (m, 2H, CH_2), 1.27-1.23 (m, 22H, CH_2/C(CH_3)$_2$), 0.90 (d, *J* = 7.1 Hz, 3H, CH_3), 0.79 (t, *J* = 7.8 Hz, 2H, BCH_2).

^{13}C NMR: (126 MHz, $CDCl_3$)

δ 82.8 (C), 32.4 (CH_2), 31.9 (CH_2), 29.4 (CH_2), 29.3 (CH_2), 24.8 (CH_3), 24.0 (CH_3), 22.7 (CH_2), 14.1 (CH_3). Missing CH_2 peak (CH_2–B) due to quadrupole effect.

^{11}B NMR: (160 MHz, $CDCl_3$)

δ 34.1.

The spectroscopic data were consistent with those reported.[238]

4,4,5,5-Tetramethyl-2-(4-phenylbutyl)-1,3,2-dioxaborolane

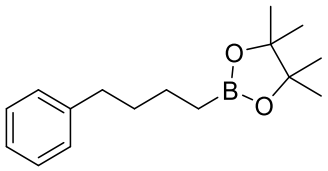

The title compound was produced according to General Procedure C. Pinacolborane (220 µL, 1.5 mmol 1.5 eq.) was added to ^{DIPP}BIPMnBr$_2$ (14 mg, 20 µmol, 2 mol%) and NaO^{t}Bu (5.8 mg, 60 µmol, 6 mol%) followed by addition of 4-phenyl-1-butene (130 µl, 1.0 mmol, 1.0 eq.) and the reaction mixture left to stir for 18 hours at 60 °C. The yellow oil was then purified by flash column chromatography (40 g SiO_2, 30 mm Ø, wet loaded, 9:1 pentane:EtOAc, *ca*. 5 mL fractions) to give 4,4,5,5-tetramethyl-2-(4-phenylbutyl)-1,3,2-dioxaborolane as a yellow oil (242 mg, 93%, >99:1 linear:branched).

^{1}H NMR: (400 MHz, $CDCl_3$)

δ 7.32 – 7.24 (m, 2H, ArH), 7.22 – 7.14 (m, 3H, ArH), 2.70 – 2.55 (t, *J* = 7.7 Hz, 2H, $ArCH_2$), 1.71 – 1.61 (m, 2H, CH_2), 1.54 – 1.45 (m, 2H, CH_2), 1.26 (s, 12H, CH_3), 0.84 (t, *J* = 7.8 Hz, 2H, BCH_2).

^{13}C NMR: (101 MHz, $CDCl_3$)

δ 142.9 (C), 128.4 (CH), 128.2 (CH), 125.5 (C), 82.9 (C), 35.8 (CH_2), 34.2 (CH_2), 24.8 (CH_3), 23.8 (CH_2). Missing CH_2 peak (CH_2–B) due to quadrupole effect.

^{11}B NMR: (128 MHz, $CDCl_3$)

34.6.

The spectroscopic data were consistent with those reported.[174]

4,4,5,5-Tetramethyl-2-(3-triethoxysilylpropyl)-1,3,2-dioxaborolane

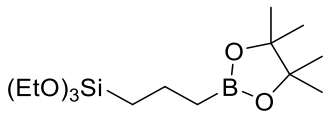

The title compound was produced according to General Procedure C. Pinacolborane (220 µL, 1.5 mmol 1.5 eq.) was added to ^{DIPP}BIPMnBr$_2$ (14 mg, 20 µmol, 2 mol%) and NaO^{t}Bu (5.8 mg, 60 µmol, 6 mol%) followed by addition of allyltriethoxysilane (130 µl, 1.0 mmol, 1.0 eq.) and the reaction mixture left to stir for 18 hours at 60 °C. The yellow oil was then purified by flash column chromatography (30 g SiO_2, 30 mm Ø, wet loaded,4:1 pentane:EtOAc, *ca*. 5 mL fractions) to give 4,4,5,5-tetramethyl-2-(3-triethoxysilylpropyl)-1,3,2-dioxaborolane as a colourless oil (279 mg, 84%, (>99:1 linear:branched).

^{1}H NMR: (500 MHz, $CDCl_3$)

δ 3.82 (q, *J* = 7.0 Hz, 6H, OCH_2), 1.60 – 1.52 (m, 2H, CH_2), 1.28 – 1.17 (m, 21H, $C(CH_3)_2/CH_3$), 0.86 (t, *J* = 7.6 Hz, 2H, BCH_2), 0.73 – 0.64 (m, 2H, $SiCH_2$).

^{13}C NMR: (126 MHz, $CDCl_3$)

δ 82.8 (C), 58.2 (CH_2), 24.8 (CH_3), 18.3 (CH_2), 17.5 (CH_2), 13.4 (CH_2). Missing CH_2 peak (CH_2–B) due to quadrupole effect.

^{11}B NMR: (160 MHz, $CDCl_3$)

δ 34.0.

IR: ν_{max}(neat)

2978 (w), 2930 (w), 2882 (w), 1371 (s), 1333 (m), 1312 (s), 1273 (w), 1219 (m), 1142 (s) 1105 (s), 1074 (s), 1026 (s), 968 (m), 885 (w), 866 (m), 847 (m), 760 (m), 675 (m).

6.8 Reductive Cyclisation Substrates and Products

1-(2-allylphenyl)ethanone

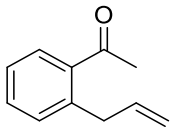

To a solution of LiCl (2.13 g, 50.3 mmol) and $Pd(PPh_3)_4$ (0.58 g, 0.500 mmol) in anhydrous tetrahydrofuran (50 mL) was added 2'bromoacetophenone (2.00 g, 1.40 ml, 10.0 mmol) and allyltributyltin (3.99 g, 3.73 ml, 12.1 mmol). The reaction was heated to reflux and left to stir for 18 hours. After this time, the reaction mixture was cooled and then diluted with 100ml of water. The aqueous phase was extracted with ethyl acetate (3 x 100ml) and the combined organic phase dried over $MgSO_4$. The crude oil was then purified by flash column chromotogaphy (SiO_2/K_sCO_3 9:1, wet loaded, 19:1 petroleum ether:EtOAc) to give 1-(2-allylphenyl)ethanone as a colourless oil (1.17 g, 7.2 mmol, 72%).

OR

2-[(1',1'-ethylenedioxy)ethyl]bromobenzene (1.08 g, 4.44 mmol) was added to a stirred solution of magnesium (129 mg, 5.33 mmol) and THF (5 mL). Initially 10% was added and the remainder added over 10 minutes after activation of Mg (by addition of I_2 crystal and heating) had occurred. After stirring for 1 hour, allyl bromide was added (1.27 g, 6.66 mmol) and the reaction stirred at room temperature. After 2 hours the reaction was poured onto NH_4Cl (50 mL), dried with $MgSO_4$, filtered and concentrated *in vacuo*. Without further purification, the product was added to a stirred suspension of $FeCl_3{\cdot}6H_2O$ (3.04 g, 13.8 mmol) in CH_2Cl_2 (45 ml). The reaction was stirred for an hour and then sat. $NaHCO_3$ (75 mL) was added and the reaction stirred for 5 minutes. The aqueous layer was extracted with DCM (3 x 30 mL) and dried with Na_2SO_4. The organic layer was then concentrated *in vacuo* and purified by flash chromatography (95:5 pet ether-ethyl acetate) to give 1-(2-allylphenyl)ethanone (604 mg, 85% over two steps) as a yellow oil.

^{1}H NMR: (500 MHz, $CDCl_3$)

δ 7.68 (dd, J = 8.1, 1.4 Hz, 1H, ArH), 7.46 – 7.41 (m, 2H, ArH), 7.34 – 7.30 (m, 1H, ArH), 6.01 (ddt, J = 16.6, 10.1, 6.5 Hz, 1H, CH), 5.08 – 4.99 (m, 2H, C2=CH_2), 3.68 (d, J = 6.5 Hz, 1H, CH_2), 2.60 (s, 3H, CH_3).

^{13}C NMR: (126 MHz, $CDCl_3$)

δ 202.1 (C=O), 139.7 (C), 138.1 (C), 137.5 (CH), 131.5 (CH), 131.2 (CH), 129.0 (CH), 126.2 (CH), 115.7 (CH_2), 38.0 (CH_3), 29.8 (CH_2).

The spectroscopic data were consistent with those reported.[239]

2-[(1',1'-ethylenedioxy)ethyl]bromobenzene

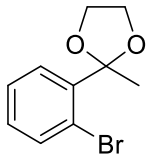

2'-bromoacetophenone (3.00 g, 15.1 mmol), glycol ether (1.87 g, 30.1 mmol), tosic acid (57.1 mg, 0.30 mmol) and toluene (9 ml) are stirred under reflux. After 18 hours, the reaction was allowed to cool then $NaHCO_3$ (20 mL) was added. The aqueous layer was extracted with diethyl ether (3 x 20 mL). The combined organic extracts were then dried over Na_2SO_4, filtered and concentrated *in vacuo*. The crude oil was then purified by flash chromatography (96:4 pet ether:ethyl acetate) to give the 2-[(1',1'-ethylenedioxy)ethyl]bromobenzene (1.1 g, 31%) as an oil.

^{1}H NMR: (601 MHz, $CDCl_3$)

δ 7.69 (dd, J = 7.8, 1.8 Hz, 1H, ArH), 7.62 (dd, J = 7.9, 1.3 Hz, 1H, ArH), 7.31 (td, J = 7.6, 1.3 Hz, 1H, ArH), 7.16 (ddd, J = 8.0, 7.3, 1.8 Hz, 1H, ArH), 4.10 – 4.07 (m, 2H, CH_2), 3.80 – 3.77 (m, 2H, CH_2), 1.84 (s, 3H, CH_3).

^{13}C NMR: (151 MHz, $CDCl_3$)

δ 141.1 (C), 135.0 (CH), 129.5 (CH), 127.9 (CH), 127.1 (CH), 120.6 (C), 108.8 (OCO), 64.3 (OC), 25.3 (CH_3).

The spectroscopic data were consistent with those reported.[240]

2-Allylbenzaldehyde

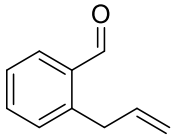

To a solution of LiCl (0.58 g, 13.7 mmol) and $Pd(PPh_3)_4$ (0.16 g, 0.137 mmol) in anhydrous tetrahydrofuran (20 mL) was added 2-bromobenzaldehyde (0.51 g, 0.32 ml, 2.74 mmol) and allyltributyltin (0.73 g, 0.68 ml, 3.3 mmol). The reaction was heated to reflux and left to stir for 18 hours. After this time, the reaction mixture was cooled and then diluted with 100ml of water. The aqueous phase was extracted with ethyl acetate (3 x 100ml) and the combined organic phase dried over $MgSO_4$. The crude oil was then purified by flash column chromotogaphy (SiO_2/K_sCO_3 9:1, wet loaded, 19:1 petroleum ether:EtOAc) to give 2-allylbenzaldehyde as a colourless oil (0.32 g, 2.2 mmol, 80%).

^{1}H NMR: (601 MHz, $CDCl_3$) JRC-1-70

δ 10.28 (s, 1H, COH), 7.87 (dd, J = 7.7, 1.5 Hz, 1H, ArH), 7.55 (td, J = 7.5, 1.5 Hz, 1H, ArH), 7.46 – 7.39 (m, 1H, ArH), 7.35 – 7.30 (m, 1H, ArH), 6.06 (ddt, J = 17.1, 10.1, 6.2 Hz, 1H, CH), 5.18 – 4.93 (m, 2H, CH_2), 3.88 – 3.81 (m, 2H, $ArCH_2$).

^{13}C NMR: (151 MHz, $CDCl_3$)

δ 192.3 (C=O), 142.3 (C), 137.0 (CH), 134.0 (CH), 133.9 (C), 131.6 (CH), 131.1 (CH), 126.9 (CH), 116.4 (CH_2), 36.5 (CH_2).

The spectroscopic data were consistent with those reported.[242]

2-Allylbenzonitrile

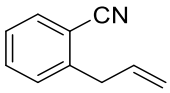

To a solution of LiCl (0.58 g, 13.7 mmol) and $Pd(PPh_3)_4$ (0.16 g, 0.137 mmol) in anhydrous tetrahydrofuran (10 mL) was added 2-bromobenzonitrile (0.5 g, 2.74 mmol) and allyltributyltin (0.73 g, 0.68 ml, 3.30 mmol). The reaction was heated to reflux and left to stir for 18 hours. After this time, the reaction mixture was cooled and then diluted with 25 mL of water. The aqueous phase was extracted with ethyl acetate (3 x 20 mL) and the combined organic phase dried over $MgSO_4$. The crude oil was then purified by flash column chromotogaphy (SiO_2/K_sCO_3 9:1, wet loaded, 19:1 petroleum ether:EtOAc) to give 1-(2-allylphenyl)ethanone as a colourless oil (0.282 g, 1.92 mmol, 72%).

^{1}H NMR: (601 MHz, $CDCl_3$)

δ 7.65 (dd, J = 7.7, 1.4 Hz, 1H), 7.55 (td, J = 7.7, 1.4 Hz, 1H), 7.38 – 7.31 (m, 2H), 5.98 (ddt, J = 16.8, 10.1, 6.6 Hz, 1H), 5.21 – 5.12 (m, 2H), 3.64 (d, J = 6.6, 2H).

^{13}C NMR: (151 MHz, $CDCl_3$)

δ 201.3 (CN), 141.5 (C), 133.9 (CH), 133.7 (C), 131.8 (CH), 128.9 (CH), 127.5 (CH), 118.9 (CH_2), 30.3 (CH_2).

The spectroscopic data were consistent with those reported.[239]

1-(2-Allylphenyl)propan-2-one

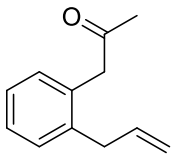

To a solution of LiCl (0.30 g, 7.05 mmol) anzd $Pd(PPh_3)_4$ (0.008 g, 0.007 mmol) in anhydrous tetrahydrofuran (5 mL) was added 1-(2-bromophenyl)propane-2-one (0.30 g, 0.32 mL, 1.41 mmol) and allyltributyltin (0.56 g, 0.53 mL, 1.7 mmol). The reaction was heated to reflux and left to stir for 18 hours. After this time, the reaction mixture was cooled and then diluted with 10 mL of water. The aqueous phase was extracted with ethyl acetate (3 x 15 mL) and the combined organic phase dried over $MgSO_4$. The crude oil was then purified by flash column chromotogaphy (SiO_2/K_sCO_3 9:1, wet loaded, 19:1 petroleum ether:EtOAc) to give 1-(2-allylphenyl)propan-2-one as a yellow oil (0.21 g, 1.2 mmol, 84%).

^{1}H NMR: (500 MHz, $CDCl_3$)

δ 7.28 – 7.14 (m, 4H, ArH), 5.94 (ddt, J = 17.1, 10.1, 6.2 Hz, 1H, CH), 5.16 – 4.87 (m, 2H, CHCH_2), 3.76 (s, 2H, ArCH_2CO), 3.49 – 3.32 (m, 2H, ArCH_2), 2.17 (s, 3H, CH_3).

^{13}C NMR: (126 MHz, CDCl3)

δ 206.5 (C=O), 138.4 (C), 136.6 (CH), 133.0 (C), 130.8 (CH), 130.1 (CH), 127.6 (CH), 126.8 (CH), 116.1 (CH_2), 48.5 (CH_2), 37.5 (CH_2), 29.4 (CH_3).

The spectroscopic data were consistent with those reported.[243]

1,2-Dimethyl-2,3-dihydroindene-diphenylsilyl ether

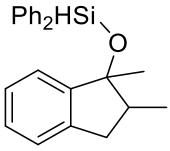

A Schlenk tube was charged with complex **18** (3.26 mg, 6 μmol), diphenyl silane (110 mg, 0.6mmol), and dry toluene (1 mL). The reaction mixture was cooled to -34°C (Acetonitrile/$CO_{2(s)}$) and $NaHBEt_3$ (12 μl, 12μmol) was then added to the mixture. After 2 minutes, the carbonyl-substituted alkene (**21**) (96.12 mg, .6 mmol) was added to the solution. The reaction mixture was stirred at room temperature for 1 hr and then 1M HCl (aq, 5 ml) was added. The organic product was extracted with diethyl ether (3x10ml) and dried with $MgSO_4$. The racemic product was obtained by flash chromatography on silica gel with an eluent of pet ether:ethyl acetate (95:5).

^{1}H NMR: (601 MHz, $CDCl_3$)
δ 7.56 – 7.52 (m, 2H, ArH), 7.44 – 7.29 (m, 6H, ArH), 7.27 – 7.09 (m, 6H, ArH), 5.11 (s, 1H, SiH), 2.84 (dd, J = 15.3, 7.3 Hz, 1H, ArCH), 2.62 (dd, J = 15.3, 9.9 Hz, 1H, ArCH), 2.25 – 2.13 (m, 1H, CH), 1.68 (s, 3H, CCH_3), 1.27 (d, J = 6.8 Hz, 3H, CHCH_3).

^{13}C NMR: (126 MHz, $CDCl_3$)
δ 148.1, 142.7, 136.1, 135.7, 135.0, 134.5, 130.2, 129.8, 128.3, 128.0, 125.8, 80.8, 47.0, 38.1, 24.8, 12.8.

The spectroscopic data were consistent with those reported.[244]

6.9 X-Ray Crystallography Data

Compound	**^{Et}BipMnBr$_2$ (196)**	**^{Dipp}BIPMnBr$_2$ (197)**
Formula	$C_{30}H_{37}Br_2Cl_2MnN_3$	$C_{36}H_{49}Br_2Cl_6MnN_3$
$D_{calc.}$/ g cm^{-3}	1.521	1.492
□/mm^{-1}	8.071	8.447
Formula Weight	725.28	951.24
Colour	pale brown	dark orange
Shape	cylinder	needle
Size/mm^3	0.53×0.05×0.05	0.81×0.12×0.06
T/K	120.0	120.0
Crystal System	orthorhombic	triclinic
Space Group	Pbca	P-1
a/Å	14.95995(14)	9.9404(3)
b/Å	16.39558(12)	10.6641(4)
c/Å	25.8321(2)	20.5595(6)
□/°	90	83.404(3)
□/°	90	78.033(3)
□/°	90	87.267(3)
V/Å^3	6336.02(9)	2117.30(12)
Z	8	2
Z'	1	1
Wavelength/Å	1.54184	1.54184
Radiation type	CuK□	Cu K□
□$_{min}$/°	4.352	4.175
□$_{max}$/°	76.693	76.568
Measured Refl.	124047	43439
Independent Refl.	6619	8803
Reflections Used	6090	7253
R_{int}	0.1159	0.0937
Parameters	350	444
Restraints	0	0
Largest Peak	1.107	0.832
Deepest Hole	-1.007	-0.911
GooF	1.135	1.032
wR_2 (all data)	0.1877	0.1426
wR_2	0.1850	0.1314
R_1 (all data)	0.0688	0.0639
R_1	0.0652	0.0514

^{Et}**BIPMnBr$_2$ (196)** – Ellipsoid Plot

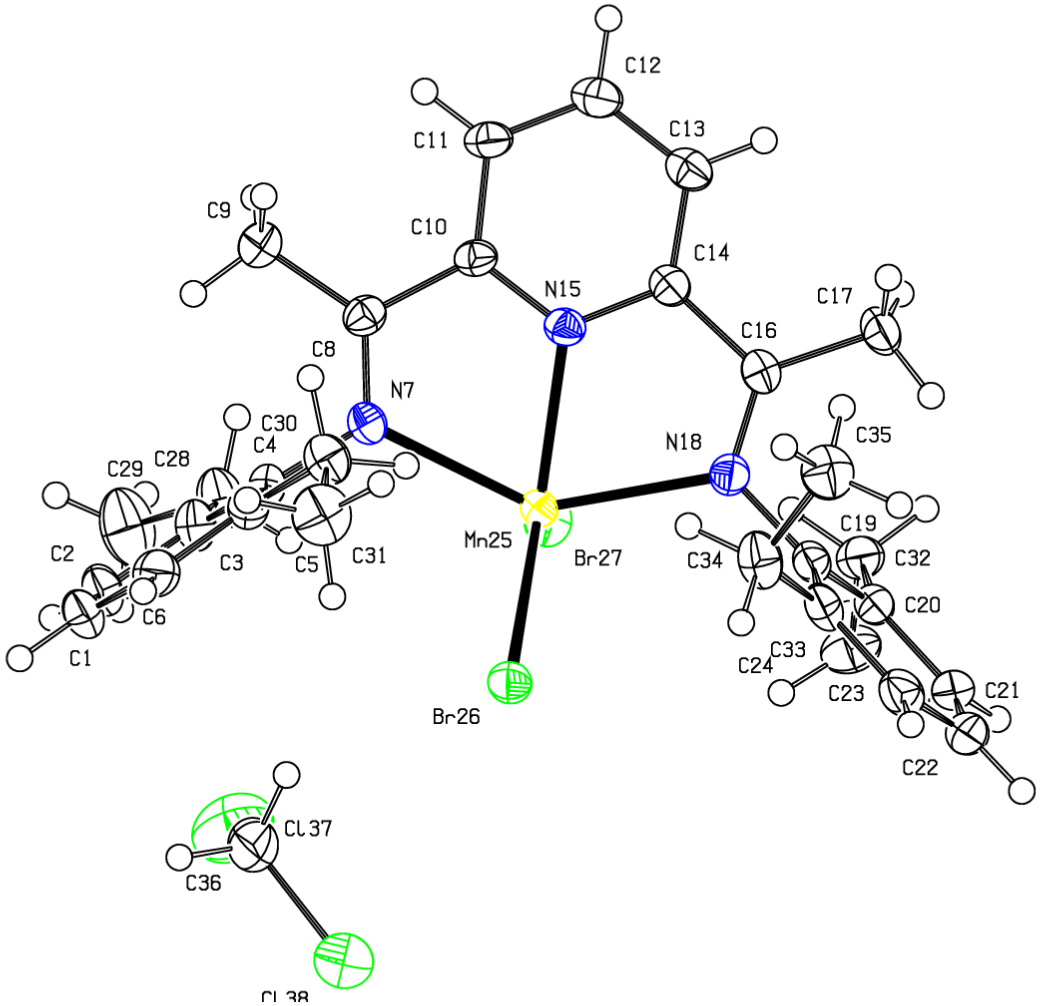

^{DIPP}**BIPMnBr$_2$ (197)** – Ellipsoid Plot

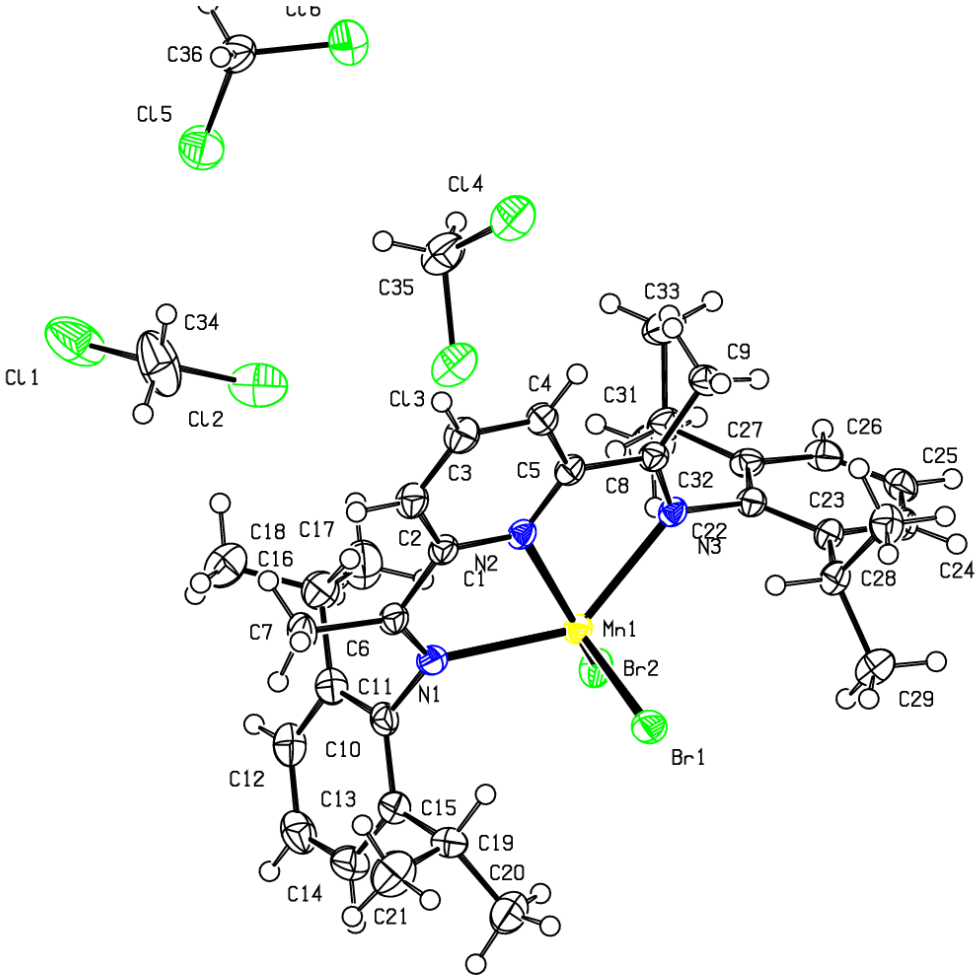

7. References

1 P. T. Anastas and J. C. Warner, *Green Chemistry: Theory and Practice*, Oxford University Press, 1998.
2 The Nobel Prize in Chemistry 2010, http://www.nobelprize.org/nobel_prizes/chemistry/laureates/2010.
3 The Nobel Prize in Chemistry 2005.
4 R. Franke, D. Selent and A. Börner, *Chem. Rev.*, 2012, **112**, 5675–5732.
5 H. M. Bogdan Marciniec, *Hydrosilylation A Comprehensive Review of Recent Advances*, Springer, New York, 2009.
6 D. Troegel and J. Stohrer, *Coord. Chem. Rev.*, 2011, **255**, 1440–1459.
7 L. Bini, C. Müller, J. Wilting, L. von Chrzanowski, A. L. Spek and D. Vogt, *J. Am. Chem. Soc.*, 2007, **129**, 12622–12623.
8 C. A. Tolman, R. J. McKinney, W. C. Seidel, J. D. Druliner and W. R. Stevens, in *Advances in Catalysis*, eds. D. D. Eley, H. Pines and P. B. Weisz, Academic Press, 1985, vol. 33, pp. 1–46.
9 5166298, 1992.
10 R. Lorant and N. GUILLIER, 2013.
11 D. Candau and C. Gombert, 2005.
12 J. V. Obligacion and P. J. Chirik, *Nat. Rev. Chem.*, 2018, **2**, 15–34.
13 A. J. Holwell, *Platinum Metals Review*, 2008, **52**, 243–246.
14 J. L. Speier, J. A. Webster and G. H. Barnes, *J. Am. Chem. Soc.*, 1957, **79**, 974–979.
15 3775452, .
16 Y. Nakajima and S. Shimada, *RSC Adv.*, 2015, **5**, 20603–20616.
17 A. J. Chalk and J. F. Harrod, *J. Am. Chem. Soc.*, 1965, **87**, 16–21.
18 S. Sakaki, N. Mizoe and M. Sugimoto, *Organometallics*, 1998, **17**, 2510–2523.
19 M. A. Schroeder and M. S. Wrighton, *J. Organomet. Chem.*, 1977, **128**, 345–358.
20 US2637738A, 1953.
21 1962.
22 US3220972A, .
23 Hitchcock Peter B., Lappert Michael F. and Warhurst Nicholas J. W., *Angew. Chem. Int. Ed.*, 1991, **30**, 438–440.
24 J. Stein, L. N. Lewis, Y. Gao and R. A. Scott, *J. Am. Chem. Soc.*, 1999, **121**, 3693–3703.
25 I. E. Markó, S. Stérin, O. Buisine, G. Mignani, P. Branlard, B. Tinant and J.-P. Declercq, *Science*, 2002, **298**, 204.
26 T. K. Meister, K. Riener, P. Gigler, J. Stohrer, W. A. Herrmann and F. E. Kühn, *ACS Catal.*, 2016, **6**, 1274–1284.
27 Steffanut Pascal, Osborn John A., DeCian Andre and Fisher Jean, *Chem. Eur. J.*, 1998, **4**, 2008–2017.
28 T. J. Brown, C. E. Wrighton, N. E. Idoine, E. R. Raycraft, R. A. Shaw, E. A. Deady, J. Rippingale and T. Bide, *World Mineral Production 2010-14*, British Geological Survey: Keyworth, Nottingham, 2016.
29 *Risk List 2015*, British Geological Survey, 2015.
30 N. N. Greenwood and A. Earnshaw, *Chemistry Of The Elements*, Pergamon, 1989.
31 W. W. Fischer, J. Hemp and J. E. Johnson, *Origins of Life and Evolution of Biospheres*, 2015, **45**, 351–357.
32 N. Abbaspour, R. Hurrell and R. Kelishadi, *J. Res. Med. Sci.*, 2014, **19**, 164–174.
33 F. Naud, F. Spindler, C. J. Rueggeberg, A. T. Schmidt and H.-U. Blaser, *Org. Process Res. Dev.*, 2007, **11**, 519–523.
34 V. B. Phapale and D. J. Cardenas, *Chem. Soc. Rev.*, 2009, **38**, 1598–1607.

35 B. M. Rosen, K. W. Quasdorf, D. A. Wilson, N. Zhang, A.-M. Resmerita, N. K. Garg and V. Percec, *Chem. Rev.*, 2011, **111**, 1346–1416.
36 F.-S. Han, *Chem. Soc. Rev.*, 2013, **42**, 5270–5298.
37 S. Z. Tasker, E. A. Standley and T. F. Jamison, *Nature*, 2014, **509**, 299.
38 V. P. Ananikov, *ACS Catal.*, 2015, **5**, 1964–1971.
39 Pospech Jola, Fleischer Ivana, Franke Robert, Buchholz Stefan and Beller Matthias, *Angew. Chem. Int. Ed.*, 2013, **52**, 2852–2872.
40 J. Sun and L. Deng, *ACS Catal.*, 2016, **6**, 290–300.
41 C. Wang, W. J. Teo and S. Ge, *ACS Catal.*, 2017, **7**, 855–863.
42 J. H. Docherty, J. Peng, A. P. Dominey and S. P. Thomas, *Nat. Chem.*, 2017, **9**, 595–600.
43 M. Brookhart and B. E. Grant, *J. Am. Chem. Soc.*, 1993, **115**, 2151–2156.
44 Mo Zhenbo, Liu Yang and Deng Liang, *Angew. Chem. Int. Ed.*, 2013, **52**, 10845–10849.
45 C. Chen, M. B. Hecht, A. Kavara, W. W. Brennessel, B. Q. Mercado, D. J. Weix and P. L. Holland, *J. Am. Chem. Soc.*, 2015, **137**, 13244–13247.
46 C. H. Schuster, T. Diao, I. Pappas and P. J. Chirik, *ACS Catal.*, 2016, **6**, 2632–2636.
47 B. Raya, S. Jing, V. Balasanthiran and T. V. RajanBabu, *ACS Catal.*, 2017, **7**, 2275–2283.
48 Y. Liu and L. Deng, *J. Am. Chem. Soc.*, 2017, **139**, 1798–1801.
49 J. Peng, J. H. Docherty, A. P. Dominey and S. P. Thomas, *Chem. Commun.*, 2017, **53**, 4726–4729.
50 H. L. Sang, S. Yu and S. Ge, *Chem. Sci.*, 2018, **9**, 973–978.
51 Xiaoyong Du, Yanlu Zhang, Dongjie Peng and Zheng Huang, *Angew. Chem. Int. Ed.*, 2016, **55**, 6671–6675.
52 B. Cheng, W. Liu and Z. Lu, *J. Am. Chem. Soc.*, 2018, **140**, 5014–5017.
53 C. C. H. Atienza, T. Diao, K. J. Weller, S. A. Nye, K. M. Lewis, J. G. P. Delis, J. L. Boyer, A. K. Roy and P. J. Chirik, *J. Am. Chem. Soc.*, 2014, **136**, 12108–12118.
54 Z. Mo, J. Xiao, Y. Gao and L. Deng, *J. Am. Chem. Soc.*, 2014, **136**, 17414–17417.
55 C. Wu, W. J. Teo and S. Ge, *ACS Catal.*, 2018, 5896–5900.
56 Teo Wei Jie, Wang Chao, Tan Ye Wei and Ge Shaozhong, *Angew. Chem. Int. Ed.*, 2017, **56**, 4328–4332.
57 X. Du, W. Hou, Y. Zhang and Z. Huang, *Org. Chem. Front.*, 2017, **4**, 1517–1521.
58 Z. Ziqing, Y. Ji and H. Zheng, *Angew. Chem. Int. Ed.*, **55**, 10839–10843.
59 Guo Jun, Shen Xuzhong and Lu Zhan, *Angew. Chem. Int. Ed.*, 2016, **56**, 615–618.
60 A. Kuznetsov and V. Gevorgyan, *Org. Lett.*, 2012, **14**, 914–917.
61 M. I. Lipschutz and T. D. Tilley, *Chem. Commun.*, 2012, **48**, 7146–7148.
62 V. Srinivas, Y. Nakajima, W. Ando, K. Sato and S. Shimada, *Catal. Sci. Technol.*, 2015, **5**, 2081–2084.
63 T. J. Steiman and C. Uyeda, *J. Am. Chem. Soc.*, 2015, **137**, 6104–6110.
64 I. Buslov, S. C. Keller and X. Hu, *Org. Lett.*, 2016, **18**, 1928–1931.
65 Buslov Ivan, Becouse Jeanne, Mazza Simona, Montandon-Clerc Mickael and Hu Xile, *Angew. Chem. Int. Ed.*, 2015, **54**, 14523–14526.
66 Buslov Ivan, Song Fang and Hu Xile, *Angew. Chem. Int. Ed.*, 2016, **55**, 12295–12299.
67 I. Pappas, S. Treacy and P. J. Chirik, *ACS Catal.*, 2016, **6**, 4105–4109.
68 Y. Chen, C. Sui-Seng, S. Boucher and D. Zargarian, *Organometallics*, 2005, **24**, 149–155.
69 L. Benítez Junquera, M. C. Puerta and P. Valerga, *Organometallics*, 2012, **31**, 2175–2183.
70 H. Maciejewski, B. Marciniec and I. Kownacki, *J. Organomet. Chem.*, 2000, **597**, 175–181.
71 K. S. Egorova and V. P. Ananikov, *Angew. Chem. Int. Ed.*, 2016, **55**, 12150–12162.
72 K. S. Egorova and V. P. Ananikov, *Organometallics*, 2017, **36**, 4071–4090.
73 C. Bolm, J. Legros, J. Le Paih and L. Zani, *Chem. Rev.*, 2004, **104**, 6217–6254.
74 I. Bauer and H.-J. Knölker, *Chem. Rev.*, 2015, **115**, 3170–3387.

75 A. N. Nesmeyanov, R. K. Freidlina, E. C. Chukovskaya, R. G. Petrova and A. B. Belyavsky, *Tetrahedron*, 1962, **17**, 61–68.
76 W. A. G. Graham and W. Jetz, *Inorg. Chem.*, 1971, **10**, 4–9.
77 M. A. Schroeder and M. S. Wrighton, *J. Organomet. Chem.*, 1977, **128**, 345–358.
78 C. L. Randolph and M. S. Wrighton, *J. Am. Chem. Soc.*, 1986, **108**, 3366–3374.
79 C. L. Reichel and M. S. Wrighton, *Inorg. Chem.*, 1980, **19**, 3858–3860.
80 Seitz Friedrich and Wrighton Mark S., *Angew. Chem. Int. Ed.*, 1988, **27**, 289–291.
81 F. Kakiuchi, Y. Tanaka, N. Chatani and S. Murai, *J. Organomet. Chem.*, 1993, **456**, 45–47.
82 R. N. Naumov, M. Itazaki, M. Kamitani and H. Nakazawa, *J. Am. Chem. Soc.*, 2012, **134**, 804–807.
83 Y. Sunada, H. Tsutsumi, K. Shigeta, R. Yoshida, T. Hashimoto and H. Nagashima, *Dalton Trans.*, 2013, **42**, 16687–16692.
84 S. C. Bart, E. Lobkovsky and P. J. Chirik, *J. Am. Chem. Soc.*, 2004, **126**, 13794–13807.
85 P. J. Chirik and K. Wieghardt, *Science*, 2010, **327**, 794.
86 M. W. Bouwkamp, A. C. Bowman, E. Lobkovsky and P. J. Chirik, *J. Am. Chem. Soc.*, 2006, **128**, 13340–13341.
87 R. J. Trovitch, E. Lobkovsky and P. J. Chirik, *Inorg. Chem.*, 2006, **45**, 7252–7260.
88 S. K. Russell, J. M. Darmon, E. Lobkovsky and P. J. Chirik, *Inorg. Chem.*, 2010, **49**, 2782–2792.
89 A. M. Tondreau, C. C. H. Atienza, K. J. Weller, S. A. Nye, K. M. Lewis, J. G. P. Delis and P. J. Chirik, *Science*, 2012, **335**, 567–570.
90 M. D. Greenhalgh, D. J. Frank and S. P. Thomas, *Adv. Synth. Cat*, 2014, **356**, 584–590.
91 M. Greenhalgh, *Iron-Catalysed Hydrofunctionalisation of Alkenes and Alkynes*, Springer Theses, 2016.
92 Challinor Amy J., Calin Marc, Nichol Gary S., Carter Neil B. and Thomas Stephen P., *Adv. Synth. Cat*, 2016, **358**, 2404–2409.
93 Y. C. Lam, R. J. Nielsen, W. A. Goddard and A. K. Dash, *Dalton Trans.*, 2017, **46**, 12507–12515.
94 K. Kamata, A. Suzuki, Y. Nakai and H. Nakazawa, *Organometallics*, 2012, **31**, 3825–3828.
95 A. M. Tondreau, C. C. H. Atienza, J. M. Darmon, C. Milsmann, H. M. Hoyt, K. J. Weller, S. A. Nye, K. M. Lewis, J. Boyer, J. G. P. Delis, E. Lobkovsky and P. J. Chirik, *Organometallics*, 2012, **31**, 4886–4893.
96 D. Peng, Y. Zhang, X. Du, L. Zhang, X. Leng, M. D. Walter and Z. Huang, *J. Am. Chem. Soc.*, 2013, **135**, 19154–19166.
97 A. M. Tondreau, E. Lobkovsky and P. J. Chirik, *Org. Lett.*, 2008, **10**, 2789–2792.
98 Y. Jian and T. T. Don, *Angew. Chem. Int. Ed.*, **49**, 10186–10188.
99 Chen Jianhui, Cheng Biao, Cao Minyi and Lu Zhan, *Angew. Chem. Int. Ed.*, 2015, **54**, 4661–4664.
100 M.-Y. Hu, Q. He, S.-J. Fan, Z.-C. Wang, L.-Y. Liu, Y.-J. Mu, Q. Peng and S.-F. Zhu, *Nat. Comm.*, 2018, **9**, 221.
101 J. Y. Wu, B. N. Stanzl and T. Ritter, *J. Am. Chem. Soc.*, 2010, **132**, 13214–13216.
102 D. Noda, A. Tahara, Y. Sunada and H. Nagashima, *J. Am. Chem. Soc.*, 2016, **138**, 2480–2483.
103 Y. Sunada, D. Noda, H. Soejima, H. Tsutsumi and H. Nagashima, *Organometallics*, 2015, **34**, 2896–2906.
104 E. Chalmin, M. Menu and C. Vignaud, *Analysis of rock art painting and technology of Paleolithic painters*, 2003, vol. 14.
105 R. A. Layfield, *Chem. Soc. Rev.*, 2008, **37**, 1098–1107.
106 K. Oshima, *J. Organomet. Chem.*, 1999, **575**, 1–20.
107 R. J. K. Taylor, M. Reid, J. Foot and S. A. Raw, *Acc. Chem. Res.*, 2005, **38**, 851–869.

108 R. C. D. Brown and J. F. Keily, *Angew. Chem. Int. Ed.*, 2001, **40**, 4496–4498.
109 W. Zhang, J. L. Loebach, S. R. Wilson and E. N. Jacobsen, *J. Am. Chem. Soc.*, 1990, **112**, 2801–2803.
110 R. Irie, K. Noda, Y. Ito, N. Matsumoto and T. Katsuki, *Tetrahedron: Asymmetry*, 1991, **2**, 481–494.
111 J. T. Groves, W. J. Kruper and R. C. Haushalter, *J. Am. Chem. Soc.*, 1980, **102**, 6375–6377.
112 W. Liu and J. T. Groves, *J. Am. Chem. Soc.*, 2010, **132**, 12847–12849.
113 W. Liu, X. Huang, M.-J. Cheng, R. J. Nielsen, W. A. Goddard and J. T. Groves, *Science*, 2012, **337**, 1322–1325.
114 X. Huang, T. M. Bergsten and J. T. Groves, *J. Am. Chem. Soc.*, 2015, **137**, 5300–5303.
115 W. Liu and J. T. Groves, *Acc. Chem. Res.*, 2015, **48**, 1727–1735.
116 Kallmeier Fabian and Kempe Rhett, *Angew. Chem. Int. Ed.*, 2017, **57**, 46–60.
117 Garbe Marcel, Junge Kathrin and Beller Matthias, *Eur. J. Org. Chem*, 2017, **2017**, 4344–4362.
118 S. Elangovan, C. Topf, S. Fischer, H. Jiao, A. Spannenberg, W. Baumann, R. Ludwig, K. Junge and M. Beller, *J. Am. Chem. Soc.*, 2016, **138**, 8809–8814.
119 Kallmeier Fabian, Irrgang Torsten, Dietel Thomas and Kempe Rhett, *Angew. Chem. Int. Ed.*, 2016, **55**, 11806–11809.
120 A. Bruneau-Voisine, D. Wang, T. Roisnel, C. Darcel and J.-B. Sortais, *Catalysis Communications*, 2017, **92**, 1–4.
121 Elangovan Saravanakumar, Garbe Marcel, Jiao Haijun, Spannenberg Anke, Junge Kathrin and Beller Matthias, *Angew. Chem. Int. Ed.*, 2016, **55**, 15364–15368.
122 Widegren Magnus B., Harkness Gavin J., Slawin Alexandra M. Z., Cordes David B. and Clarke Matthew L., *Angew. Chem. Int. Ed.*, 2017, **56**, 5825–5828.
123 M. B. Widegren and M. L. Clarke, *Org. Lett.*, 2018, **20**, 2654–2658.
124 Espinosa-Jalapa Noel Angel, Nerush Alexander, Shimon Linda J. W., Leitus Gregory, Avram Liat, Ben-David Yehoshoa and Milstein David, *Chem. Eur. J.*, 2016, **23**, 5934–5938.
125 R. van Putten, E. A. Uslamin, M. Garbe, C. Liu, A. Gonzalez-de-Castro, M. Lutz, K. Junge, E. J. M. Hensen, M. Beller, L. Lefort and E. A. Pidko, *Angew. Chem. Int. Ed.*, 2017, **56**, 7531–7534.
126 M. Mastalir, M. Glatz, E. Pittenauer, G. Allmaier and K. Kirchner, *J. Am. Chem. Soc.*, 2016, **138**, 15543–15546.
127 Deibl Nicklas and Kempe Rhett, *Angew. Chem. Int. Ed.*, 2017, **56**, 1663–1666.
128 Kallmeier Fabian, Dudziec Beata, Irrgang Torsten and Kempe Rhett, *Angew. Chem. Int. Ed.*, 2017, **56**, 7261–7265.
129 M. Mastalir, E. Pittenauer, G. Allmaier and K. Kirchner, *J. Am. Chem. Soc.*, 2017, **139**, 8812–8815.
130 S. Elangovan, J. Neumann, J.-B. Sortais, K. Junge, C. Darcel and M. Beller, *Nat. Comm.*, 2016, **7**, 12641.
131 Neumann Jacob, Elangovan Saravanakumar, Spannenberg Anke, Junge Kathrin and Beller Matthias, *Chem. Eur. J.*, 2017, **23**, 5410–5413.
132 A. Bruneau-Voisine, D. Wang, V. Dorcet, T. Roisnel, C. Darcel and J.-B. Sortais, *J. Catal.*, 2017, **347**, 57–62.
133 Peña-López Miguel, Piehl Patrick, Elangovan Saravanakumar, Neumann Helfried and Beller Matthias, *Angew. Chem. Int. Ed.*, 2016, **55**, 14967–14971.
134 R. Ren, H. Zhao, L. Huan and C. Zhu, *Angew. Chem. Int. Ed.*, 2015, **54**, 12692–12696.
135 J. A. Gladysz, *Acc. Chem. Res.*, 1984, **17**, 326–332.
136 B. T. Gregg, P. K. Hanna, E. J. Crawford and A. R. Cutler, *J. Am. Chem. Soc.*, 1991, **113**, 384–385.

137 M. DiBiase Cavanaugh, B. T. Gregg and A. R. Cutler, *Organometallics*, 1996, **15**, 2764–2769.
138 J. Zheng, S. Elangovan, D. A. Valyaev, R. Brousses, V. César, J.-B. Sortais, C. Darcel, N. Lugan and G. Lavigne, *Adv. Synth. Cat*, 2014, **356**, 1093–1097.
139 R. Arias-Ugarte, H. K. Sharma, A. L. C. Morris and K. H. Pannell, *J. Am. Chem. Soc.*, 2012, **134**, 848–851.
140 M. Igarashi and T. Fuchikami, *Tetrahedron Lett.*, 2001, **42**, 1945–1947.
141 J. Zheng, S. Chevance, C. Darcel and J.-B. Sortais, *Chem. Commun.*, 2013, **49**, 10010–10012.
142 S. U. Son, S.-J. Paik, I. S. Lee, Y.-A. Lee, Y. K. Chung, W. K. Seok and H. N. Lee, *Organometallics*, 1999, **18**, 4114–4118.
143 V. K. Chidara and G. Du, *Organometallics*, 2013, **32**, 5034–5037.
144 T. K. Mukhopadhyay, M. Flores, T. L. Groy and R. J. Trovitch, *J. Am. Chem. Soc.*, 2014, **136**, 882–885.
145 T. K. Mukhopadhyay, C. L. Rock, M. Hong, D. C. Ashley, T. L. Groy, M.-H. Baik and R. J. Trovitch, *J. Am. Chem. Soc.*, 2017, **139**, 4901–4915.
146 R. J. Trovitch, *Synlett*, 2014, **25**, 1638–1642.
147 R. J. Trovitch, *Acc. Chem. Res.*, 2017, **50**, 2842–2852.
148 C. M. Kelly, R. McDonald, O. L. Sydora, M. Stradiotto and L. Turculet, *Angew. Chem. Int. Ed.*, 2017, **56**, 15901–15904.
149 X. Ma, Z. Zuo, G. Liu and Z. Huang, *ACS Omega*, 2017, **2**, 4688–4692.
150 S. L. Pratt and R. A. Faltynek, *J. Organomet. Chem.*, 1983, **258**, C5–C8.
151 H. S. Hilal, M. Abu-Eid, M. Al-Subu and S. Khalaf, *J. Mol. Catal.*, 1987, **39**, 1–11.
152 H. Hilal, M. Suleiman, W. Jondi, S. Khalaf and M. Masoud, *Poly(siloxane)-supported decacarbonyldimanganese(0) catalyst for terminal olefin hydrosilylation reactions: The effect of the support on the catalyst selectivity, activity and stability*, 1999, vol. 144.
153 W. Jondi, A. Zyoud, W. Mansour, A. Q. Hussein and H. S. Hilal, *React Chem. Eng.*, 2016, **1**, 194–203.
154 C. Obradors, R. M. Martinez and R. A. Shenvi, *J. Am. Chem. Soc.*, 2016, **138**, 4962–4971.
155 V. C. Gibson, C. Redshaw and G. A. Solan, *Chem. Rev.*, 2007, **107**, 1745–1776.
156 B. A. F. Le Bailly and S. P. Thomas, *RSC Adv.*, 2011, **1**, 1435–1445.
157 X. Du and Z. Huang, *ACS Catal.*, 2017, **7**, 1227–1243.
158 H. Sugiyama, I. Korobkov, S. Gambarotta, A. Möller and P. H. M. Budzelaar, *Inorg. Chem.*, 2004, **43**, 5771–5779.
159 S. C. Bart, K. Chłopek, E. Bill, M. W. Bouwkamp, E. Lobkovsky, F. Neese, K. Wieghardt and P. J. Chirik, *J. Am. Chem. Soc.*, 2006, **128**, 13901–13912.
160 D. A. Edwards, M. F. Mahon, W. R. Martin, K. C. Molloy, P. E. Fanwick and R. A. Walton, *J. Chem. Soc., Dalton Trans.*, 1990, 3161–3168.
161 B. de Bruin, E. Bill, E. Bothe, T. Weyhermüller and K. Wieghardt, *Inorg. Chem.*, 2000, **39**, 2936–2947.
162 D. Reardon, G. Aharonian, S. Gambarotta and G. P. A. Yap, *Organometallics*, 2002, **21**, 786–788.
163 G. J. P. Britovsek, M. Bruce, V. C. Gibson, B. S. Kimberley, P. J. Maddox, S. Mastroianni, S. J. McTavish, C. Redshaw, G. A. Solan, S. Strömberg, A. J. P. White and D. J. Williams, *J. Am. Chem. Soc.*, 1999, **121**, 8728–8740.
164 G. J. P. Britovsek, V. C. Gibson, S. J. McTavish, G. A. Solan, A. J. P. White, D. J. Williams, G. J. P. Britovsek, B. S. Kimberley and P. J. Maddox, *Chem. Commun.*, 1998, 849–850.
165 B. L. Small, M. Brookhart and A. M. A. Bennett, *J. Am. Chem. Soc.*, 1998, **120**, 4049–4050.
166 G. J. P. Britovsek, J. England, S. K. Spitzmesser, A. J. P. White and D. J. Williams, *Dalton Trans.*, 2005, 945–955.

167 S. K. Russell, A. C. Bowman, E. Lobkovsky, K. Wieghardt and P. J. Chirik, *Eur. J. Inorg. Chem.*, 2012, **2012**, 535–545.
168 S. K. Russell, Cornell University, 2011.
169 R. J. Trovitch, E. Lobkovsky, E. Bill and P. J. Chirik, *Organometallics*, 2008, **27**, 1470–1478.
170 S. Monfette, Z. R. Turner, S. P. Semproni and P. J. Chirik, *J. Am. Chem. Soc.*, 2012, **134**, 4561–4564.
171 V. A. Schmidt, J. M. Hoyt, G. W. Margulieux and P. J. Chirik, *J. Am. Chem. Soc.*, 2015, **137**, 7903–7914.
172 A. Sood, M. T. Räisänen, E. Aitola, A. Sibaouih, E. Colacio, M. Ahlgren, M. Nieger, T. Repo and M. Leskelä, *Polyhedron*, 2013, **56**, 221–229.
173 G. Zhang, H. Zeng, J. Wu, Z. Yin, S. Zheng and J. C. Fettinger, *Angew. Chem. Int. Ed.*, 2016, **55**, 14369–14372.
174 M. D. Greenhalgh and S. P. Thomas, *Chem. Commun.*, 2013, **49**, 11230–11232.
175 A. A. Toutov, W.-B. Liu, K. N. Betz, A. Fedorov, B. M. Stoltz and R. H. Grubbs, *Nature*, 2015, **518**, 80.
176 S. Banerjee, Y.-F. Yang, I. D. Jenkins, Y. Liang, A. A. Toutov, W.-B. Liu, D. P. Schuman, R. H. Grubbs, B. M. Stoltz, E. H. Krenske, K. N. Houk and R. N. Zare, *J. Am. Chem. Soc.*, 2017, **139**, 6880–6887.
177 W.-B. Liu, D. P. Schuman, Y.-F. Yang, A. A. Toutov, Y. Liang, H. F. T. Klare, N. Nesnas, M. Oestreich, D. G. Blackmond, S. C. Virgil, S. Banerjee, R. N. Zare, R. H. Grubbs, K. N. Houk and B. M. Stoltz, *J. Am. Chem. Soc.*, 2017, **139**, 6867–6879.
178 S. L. Buchwald, *Chem. Eng. News*, 1993, **71**, 2.
179 W. Duczmal, B. Maciejewska, E. Śliwińska and B. Marciniec, *Transition Metal Chemistry*, 1995, **20**, 162–165.
180 T. Yoshida, L. Ilies and E. Nakamura, *Org. Lett.*, 2018, **20**, 2844–2847.
181 J. Boyer, R. J. P. Corriu, R. Perz and C. Reye, *Tetrahedron*, 1981, **37**, 2165–2171.
182 A. Hosomi, H. Hayashida, S. Kohra and Y. Tominaga, *J. Chem. Soc., Chem. Commun.*, 1986, 1411–1412.
183 C. Chuit, R. J. P. Corriu, C. Reye and J. C. Young, *Chem. Rev.*, 1993, **93**, 1371–1448.
184 R. J. P. Corriu, C. Guerin, B. Henner and Q. Wang, *Organometallics*, 1991, **10**, 2297–2303.
185 S. Kohra, H. Hayashida, Y. Tominaga and A. Hosomi, *Tetrahedron Lett.*, 1988, **29**, 89–92.
186 S. Kondo, K. Tokuhashi, H. Nagai, M. Iwasaka and M. Kaise, *Combustion and Flame*, 1995, **101**, 170–174.
187 H. Sugiyama, G. Aharonian, S. Gambarotta, G. P. A. Yap and P. H. M. Budzelaar, *J. Am. Chem. Soc.*, 2002, **124**, 12268–12274.
188 A. C. Albéniz, P. Espinet, R. López-Fernández and A. Sen, *J. Am. Chem. Soc.*, 2002, **124**, 11278–11279.
189 D. R. Anton and R. H. Crabtree, *Organometallics*, 1983, **2**, 855–859.
190 Chakraborty Uttam, Reyes-Rodriguez Efrain, Demeshko Serhiy, Meyer Franc and Jacobi von Wangelin Axel, *Angew. Chem. Int. Ed.*, 2018, **57**, 4970–4975.
191 T. N. Gieshoff, M. Villa, A. Welther, M. Plois, U. Chakraborty, R. Wolf and A. Jacobi von Wangelin, *Green. Chem.*, 2015, **17**, 1408–1413.
192 M. D. Greenhalgh, A. Kolodziej, F. Sinclair and S. P. Thomas, *Organometallics*, 2014, **33**, 5811–5819.
193 D. A. Straus, C. Zhang and T. D. Tilley, *J. Organomet. Chem.*, 1989, **369**, C13–C17.
194 S. R. Bahr and P. Boudjouk, *J. Org. Chem.*, 1992, **57**, 5545–5547.
195 Männig Detlef and Nöth Heinrich, *Angew. Chem. Int. Ed.*, 1985, **24**, 878–879.
196 S. Pereira and M. Srebnik, *Tetrahedron Lett.*, 1996, **37**, 3283–3286.
197 D. A. Evans, G. C. Fu and A. H. Hoveyda, *J. Am. Chem. Soc.*, 1992, **114**, 6671–6679.

198 D. A. Evans, G. C. Fu and B. A. Anderson, *J. Am. Chem. Soc.*, 1992, **114**, 6679–6685.
199 C. Widauer, H. Grützmacher and T. Ziegler, *Organometallics*, 2000, **19**, 2097–2107.
200 D. G. Musaev, A. M. Mebel and K. Morokuma, *J. Am. Chem. Soc.*, 1994, **116**, 10693–10702.
201 Dorigo Andrea E. and von Ragué Schleyer Paul, *Angew. Chem. Int. Ed.*, 1995, **34**, 115–118.
202 Crudden Cathleen M. and Edwards David, *Eur. J. Org. Chem*, 2003, **2003**, 4695–4712.
203 J. R. Smith, B. S. L. Collins, M. J. Hesse, M. A. Graham, E. L. Myers and V. K. Aggarwal, *J. Am. Chem. Soc.*, 2017, **139**, 9148–9151.
204 M. D. Greenhalgh, A. S. Jones and S. P. Thomas, *ChemCatChem*, 2015, **7**, 190–222.
205 A. Bismuto, M. J. Cowley and S. P. Thomas, *ACS Catal.*, 2018, **8**, 2001–2005.
206 P. Eisenberger, A. M. Bailey and C. M. Crudden, *J. Am. Chem. Soc.*, 2012, **134**, 17384–17387.
207 J. S. McGough, S. M. Butler, I. A. Cade and M. J. Ingleson, *Chem. Sci.*, 2016, **7**, 3384–3389.
208 Bismuto Alessandro, Thomas Stephen P. and Cowley Michael J., *Angew. Chem. Int. Ed.*, 2016, **55**, 15356–15359.
209 M. Fleige, J. Möbus, T. vom Stein, F. Glorius and D. W. Stephan, *Chem. Commun.*, 2016, **52**, 10830–10833.
210 Yin Qin, Kemper Sebastian, Klare Hendrik F. T. and Oestreich Martin, *Chem. Eur. J.*, 2016, **22**, 13840–13844.
211 Lawson James R., Wilkins Lewis C. and Melen Rebecca L., *Chem. Eur. J.*, 2017, **23**, 10997–11000.
212 Yang Zhi, Zhong Mingdong, Ma Xiaoli, De Susmita, Anusha Chakkittakandiyil, Parameswaran Pattiyil and Roesky Herbert W., *Angew. Chem. Int. Ed.*, 2015, **54**, 10225–10229.
213 N. W. J. Ang, C. S. Buettner, S. Docherty, A. Bismuto, J. R. Carney and J. H. Docherty, *Synthesis*, 2018, **50**, 803–808.
214 P. J. Chirik, *Acc. Chem. Res.*, 2015, **48**, 1687–1695.
215 T. S. Carter, L. Guiet, D. J. Frank, J. West and S. P. Thomas, *Adv. Synth. Cat*, 2013, **355**, 880–884.
216 D. C. Harrowven, D. P. Curran, S. L. Kostiuk, I. L. Wallis-Guy, S. Whiting, K. J. Stenning, B. Tang, E. Packard and L. Nanson, *Chem. Commun.*, 2010, **46**, 6335–6337.
217 G. Mann, Q. Shelby, A. H. Roy and J. F. Hartwig, *Organometallics*, 2003, **22**, 2775–2789.
218 U. Schubert, *Angew. Chem. Int. Ed.*, 1994, **33**, 419–421.
219 D. M. Crumpton-Bregel and K. I. Goldberg, *J. Am. Chem. Soc.*, 2003, **125**, 9442–9456.
220 F. Kakiuchi and S. Murai, *Acc. Chem. Res.*, 2002, **35**, 826–834.
221 T. K. Mukhopadhyay, M. Flores, T. L. Groy and R. J. Trovitch, *Chem. Sci.*, , DOI:10.1039/C8SC02768D.
222 V. Vasilenko, C. K. Blasius and L. H. Gade, *J. Am. Chem. Soc.*, 2018, **140**, 9244–9254.
223 Kallmeier Fabian and Kempe Rhett, *Angew. Chem. Int. Ed.*, 2017, **57**, 46–60.
224 V. Vasilenko, C. K. Blasius, H. Wadepohl and L. H. Gade, *Angewandte Chemie International Edition*, 2017, **56**, 8393–8397.
225 M. D. Greenhalgh and S. P. Thomas, *J. Am. Chem. Soc.*, 2012, **134**, 11900–11903.
226 B. L. Small, M. Brookhart and A. M. A. Bennett, *J. Am. Chem. Soc.*, 1998, **120**, 4049–4050.
227 T. Yang, X. Fan, X. Zhao and W. Yu, *Org. Lett.*, 2018, **20**, 1875–1879.
228 B. Butschke, K. L. Fillman, T. Bendikov, L. J. W. Shimon, Y. Diskin-Posner, G. Leitus, S. I. Gorelsky, M. L. Neidig and D. Milstein, *Inorg. Chem.*, 2015, **54**, 4909–4926.
229 S. T. Babik and G. Fink, *J. Organomet. Chem.*, 2003, **683**, 209–219.
230 V. C. Gibson, S. McTavish, C. Redshaw, G. A. Solan, A. J. P. White and D. J. Williams, *Dalton Trans.*, 2003, 221–226.

231 C. Mantel, C. Baffert, I. Romero, A. Deronzier, J. Pécaut, M.-N. Collomb and C. Duboc, *Inorg. Chem.*, 2004, **43**, 6455–6463.
232 C. Weatherly, J. M. Alderson, J. F. Berry, J. E. Hein and J. M. Schomaker, *Organometallics*, 2017, **36**, 1649–1661.
233 Du Xiaoyong, Zhang Yanlu, Peng Dongjie and Huang Zheng, *Angew. Chem. Int. Ed.*, 2016, **55**, 6671–6675.
234 D. A. Loy, J. P. Carpenter, T. M. Alam, R. Shaltout, P. K. Dorhout, J. Greaves, J. H. Small and K. J. Shea, *J. Am. Chem. Soc.*, 1999, **121**, 5413–5425.
235 R. Hu, W. Hao and M. Cai, *Chinese Journal of Chemistry*, 2011, **29**, 1629–1634.
236 J. Li, C. Niu, J. Peng, Y. Deng, G. Zhang, Y. Bai, C. Ma, W. Xiao and G. Lai, *Applied Organometallic Chemistry*, 2014, **28**, 454–460.
237 K. Yang and Q. Song, *Green Chem.*, 2016, **18**, 932–936.
238 J. V. Obligacion and P. J. Chirik, *Org. Lett.*, 2013, **15**, 2680–2683.
239 M. O. Akram, P. S. Mali and N. T. Patil, *Org. Lett.*, 2017, **19**, 3075–3078.
240 B. S. Pilgrim, A. E. Gatland, C. T. McTernan, P. A. Procopiou and T. J. Donohoe, *Org. Lett.*, 2013, **15**, 6190–6193.
241 S. Xing, W. Pan, C. Liu, J. Ren and Z. Wang, *Angew. Chem. Int. Ed.*, 2010, **49**, 3215–3218.
242 I. D. G. Watson, S. Ritter and F. D. Toste, *J. Am. Chem. Soc.*, 2009, **131**, 2056–2057.
243 T. Azemi, M. Kitamura and K. Narasaka, *Tetrahedron*, 2004, **60**, 1339–1344.
244 N. M. Kablaoui and S. L. Buchwald, *J. Am. Chem. Soc.*, 1995, **117**, 6785–6786.

8. Appendix: Publications

Journal Publications (Chronological Order):

1. Recent Advances of Manganese Catalysis for Organic Synthesis

   Carney, J. R.; Dillon, B. R.; Thomas, S.P. *Eur. J. Org. Chem.* **2016,** 3912-3929

2. Borane-Catalysed Hydroboration of Alkynes and Alkenes

   N. W. J. Ang, C. S. Buettner, S. Docherty, A. Bismuto, J. R. Carney and J. H. Docherty, *Synthesis*, 2018, **50**, 803–808

3. Manganese-Catalyzed Hydrofunctionalization of Alkenes

   Carney, J. R.; Dillon, B. R.; Campbell, L.; Thomas, S.P. *Angew. Chem. Int. Ed.* **2018**, *57*, 10620-10624